GEOLOGICAL SURVEY OF CANADA
OPEN FILE 2122

Mechanical Properties of Ice and Frozen Soil

Thurber Consultants Ltd.
for
Geological Survey of Canada

September 1989

Energy, Mines and Resources Canada
Énergie, Mines et Ressources Canada

This document was produced
by scanning the original publication.

Ce document est le produit d'une
numérisation par balayage
de la publication originale.

Canada

FOREWORD

This Open File reports on a literature review on the mechanical properties of frozen soil and ground ice relevant to the design of energy transportation developments in permafrost regions. The study was conducted by T.E. Hoeve, P.Eng., and L.B. Smith, P.Eng., of Thurber Consultants Ltd., Calgary, as a research contract for the Geological Survey of Canada, Department of Energy, Mines and Resources, and Supply and Services Canada.

The report has not been edited in any way by the Geological Survey of Canada, and statements contained herein do not necessarily reflect the views or policies of the Government of Canada.

Funds to support this contract were provided by the Panel on Energy Research and Development, under Task 6, Oil, Gas and Electricity; Program 6.1.2, Permafrost and Gas Hydrates Geoscientific Research and Development. This support is gratefully acknowledged.

J.A. Heginbottom
Scientific Authority

MECHANICAL PROPERTIES OF ICE AND FROZEN SOIL

Report Submitted

to

SUPPLY AND SERVICES CANADA
HULL, QUEBEC
(DSS File NO. 63SS.23233-7-1126)

Thurber Consultants Ltd.
Calgary, Alberta

PERMIT TO PRACTICE
THURBER CONSULTANTS LTD.
Signature
Date 30 JUNE 1988
PERMIT NUMBER: P 355
The Association of Professional Engineers, Geologists and Geophysicists of Alberta

June, 1988
File: 16-5-43

T.E. Hoeve, P.Eng.
Project Engineer

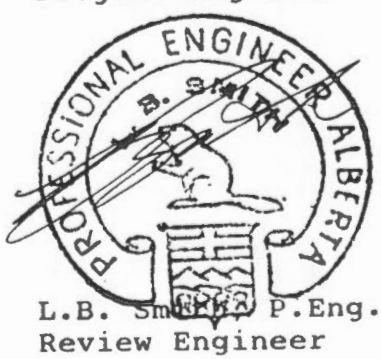

L.B. Smith, P.Eng.
Review Engineer

EXECUTIVE SUMMARY

Introduction

This report presents the results of a literature review with respect to the mechanical properties of ice and frozen soil which are relevant to the design of energy transportation projects in permafrost regions.

The mechanical behaviour of ice and frozen soil is discussed within the framework of the following theories:

- Nonlinear elasticity,
- Primary creep,
- Secondary creep,
- Strength,
- Adfreeze strength,
- Thaw consolidation,
- Frost heave,
- Dynamic response, and
- Electrical response.

Each of the foregoing aspects is discussed in a section of the report. The most widely accepted behavioural theory is briefly outlined together with a brief discussion of the range of design applications and the more significant limitations. The behaviour of the soil in response to variables such as stress, time, temperature, soil type, ice content, and unfrozen water content are discussed within the context of the relevant theory. Each section provides summaries of relevant data pertinent to the theoretical relationships, in a form which should be a convenient reference source for practising geotechnical engineers. Key references are cited and a list of references is presented at the end of each section for the convenience of those readers requiring further detail.

Research Priorities

The review has identified a number of areas in which further research should be considered, as described in the respective sections of the report. The more noteworthy areas in which research should be considered are briefly outlined below. No attempt has been made here to establish priorities for research. Research priorities can change very rapidly, either as a result of developments arising out of ongoing research (and often in disciplines other than civil engineering) or because new design problems arise or new construction techniques are developed. In order to ensure that the efforts of the geotechnical

THURBER

engineering research community are directed in the most productive areas, it is essential that a close relationship be maintained between researchers and practising engineers. Collaboration between the two parties has been undertaken in the past and often with spectacular success. It is recommended that an effort be made to establish more positive means by which closer communication and dialogue between researchers and practising engineers can be promoted and developed.

Saline Soils

Recent information has shown that saline soils are far more widespread in Northern Canada than had been expected in the past. Further research into the geologic origin and distribution of saline soils appears worthwhile. The relationships between pore fluid salinity, soil type, temperature and unfrozen water content have been established for some soils and this work should be extended to other soil types. Quantitative data concerning the effect which pore fluid salinity has on the mechanical properties of frozen soils is currently very limited. Further laboratory investigations should be considered.

Creep and Strength

One of the major difficulties in interpreting the strength data available in the literature is that researchers have not always clearly differentiated between brittle failure (which occurs at high strain rates and for which discrete fracture planes appear in the material) and ductile failure (which occurs at low strain rates and for which the material behaves as a continium). A consistent relationship between brittle strength and ductile strength has never been established and may not exist. This is an area in which further research may be of value.

Brittle strength is generally relatively high in ice and frozen soil whereas, ductile strength is lower than brittle strength in the short term and very much lower than brittle strength in the long term. Ductile strength therefore governs in most design situations and is therefore of most concern to designers.

Recent research into creep processes in pure ice have provided considerable new insight into the relationship between creep and ductile strength of this material. For example, it has been established that accelerating strain rates (failure) will occur once total strain reaches 1 or 2 percent, irrespective of stress level. This finding has significant implications for designers, particularly if

THURBER

similar behaviour occurs in frozen soils. In the past, the objective of defining the creep properties of a material was to ensure that total strains would not exceed some tolerable level for the proposed structure. In light of recent research, the primary reason for establishing the creep properties is to establish the time at which the failure strain will be reached.

There are a number of areas in which further research into the process of creep in ice and soils should be worthwhile. Consideration should be given to undertaking systematic studies to establish whether a limiting (failure) strain exists for ice poor soils. This work should be carried out over a broad range of soil types and temperatures.

At very low stress levels, the small changes in strain rate make it difficult to establish the point at which failure occurs. In addition, the increase in strain rate at failure may be so small that it can be safely ignored, in which case total allowable deformations may govern the design. Furthermore, under very slow strain rates, recrystallization or other healing processes may occur such that strain rates continue to decelerate, so that failure never occurs. These are all areas in which further research appears worthwhile.

The factors which control the creep behaviour of non-homogeneous frozen soils and frozen soils which contain segregated ice are poorly understood. Recent research has demonstrated that the measurement of creep properties of such soil is difficult and may not result in values for creep parameters which are representative of field conditions. This is an area in which further research may be warranted.

Adfreeze Strength

Adfreeze strength appears, in many cases, to govern the capacity of adfreeze piles installed in ice and frozen soils, and is therefore of significant concern in design practice. The available data with respect to short term adfreeze strengths of ice and non-saline frozen soils is considered adequate. The data available with respect to the short term adfreeze strength of saline soils is almost non-existent and further laboratory and field investigations should be considered.

The quantitative data available with respect to long term adfreeze strengths of ice, or saline and non-saline frozen soils is very limited. A number of theoretical relationships between short term adfreeze strength and long

THURBER

term adfreeze strength have been suggested, however, none of these relationships have been adequately substantiated. As might be imagined, there are great difficulties in establishing long term adfreeze strength because of the long period of time over which observations must be made. Despite this, further research into the time dependent behaviour of adfreeze strength should be considered.

Recent research has demonstrated that a number of methods for increasing the capacity of adfreeze piles may have merit, including the use of lugs, flanges, pile surface treatments, and special backfill materials such as cement grout. There is, unfortunately, virtually no design data available on which the cost benefits of these techniques can be established. This is an area in which further laboratory and field testing should be productive.

Thaw Consolidation

Total settlements which will occur as frozen soils thaw can be estimated to a satisfactory degree of accuracy if the total water content (prior to thawing) and the water content after thaw consolidation are known. Useful correlations between total water content and thaw strain for the most common soil types are currently available. While these correlations exhibit considerable scatter the information is considered adequate for most applications in view of the unpredictable and random distribution of ground ice in natural deposits. The correlation between total water content and thaw strain should be extended as opportunities arise. Field observation should be made in order to establish empirical correction factors which will account for non-homogeneous field conditions.

An excellent theoretical framework within which the physical process of thaw consolidation can be interpreted has been developed by Nixon and Morgenstern. Their model can be used to predict water pressures at the thaw front, and therefore the stability of the thawing soils can be established. The theory also provides a framework within which remedial measures can be evaluated. This latter aspect is of particular concern where warm oil pipelines are to be placed in ice rich permafrost.

The essential validity of the thaw consolidation theory has been established for both reconstituted and natural soils in the laboratory. Field observations of the thaw consolidation process have found behaviour which is consistent with the theory. No further fundamental research into the process of thaw consolidation appears to be warranted at this time, however field studies related to thaw consolidation would be of great value, if opportunities arise.

THURBER

Frost Heave

The effect of frost heave on structures is a serious concern in both permafrost and non-permafrost areas. Frost heave represents one of the most critical geotechnical problems related to the construction of chilled gas pipelines in Northern Canada. The process of frost heave is relatively complex and has been the subject of intense research over the past 50 years.

Konrad and Morgenstern have proposed a behavioural model for frost heave which is currently the only model suitable for use by designers. The model appears to incorporate all of the significant variables affecting frost heave and can be used to provide a reasonable estimate of frost heave under design conditions. The model also shows great promise as a means of identifying frost susceptible soils and for evaluating the relative merits of alternative schemes for reducing heave.

The Konrad and Morgenstern model has been used to successfully match observed heave in laboratory tests and heave of chilled pipelines at the Calgary and Caen test facilities. However, many researchers are not convinced that the model will predict frost heave under all conditions, or that it will predict heave to a level of accuracy adequate for design purposes. Research into the process of frost heave is continuing and it can be expected that the validity and limitations of the current model will be further refined based on the results.

The process of frost heave below a chilled pipeline was monitored for a period of over 7 years at the Calgary test facility and the behaviour during that period conformed to that predicted by the Konrad-Morgenstern theory. A number of researchers have expressed concern that other processes (such as secondary heave) may begin to dominate heave over the long term. Consideration should be given to interpreting the behaviour of naturally occurring palsas, pingos and hydrolaccoliths with the framework of the Konrad and Morgenstern theory. Some of these landforms have existed for many decades.

Some researchers are concerned that the segregation potential (a key variable in the frost heave model) is so sensitive to soil density, structure and grain size, that it is not possible to obtain consistent results, nor to reliably predict field performance due to the inhomogeneity of natural deposits. These are valid concerns, and difficult to completely resolve. Additional field observations

THURBER

of frost heave may be of value in this regard. This could include observations of frost heave under natural freezing conditions as well as small scale insitu frost heave tests using artificial freezing.

A number of other areas with respect to the process of frost heave have been identified for which research may be of value and these are outlined in the appropriate section of the report.

Subsurface Exploration Techniques

Subsurface investigations in Northern Canada are expensive, primarily because of the large distances and the fact that most locations are accessible only by air.

A review of current exploration techniques was beyond the scope of this study. It is clear, however, that there is a requirement to develop more portable drilling and sampling equipment and more reliable geophysical techniques which can be used for subsurface explorations particularly as they relate to geotechnical engineering practice.

THURBER

ACKNOWLEDGEMENTS

This review was undertaken by two geotechnical engineers, both of whom have practical experience in permafrost regions and a reasonably good working knowledge of the behaviour of ice and frozen soil.

The nonhomogeneous composition of natural soils will always require that the design process involve some judgement. Engineering judgement can only be fully developed, however, within the context of sound behavioural theories. We would therefore like to acknowledge the valuable contribution which has been made over the past few decades by a relatively small number of scientists and engineers who have developed a number of very useful theories with respect to the mechanical behaviour of ice and frozen soil. These brilliant minds have an exceptional ability to evaluate the apparent random and chaotic behaviour of permafrost and explain their observations within the framework of a consistent set of physical laws.

We would like to acknowledge the Government of the Northwest Territories, Department of Public Works and Highways and the Department of National Defence, No. 1 Construction Engineering Unit, for their kind permission to include, in this report, valuable field and laboratory data from a variety of projects carried out in recent years.

We would like to thank Mr. Tony Sartorelli of Geo-Physi-Con Ltd. for his careful review of the sections on dynamic stress-strain behaviour and electrical properties of permafrost.

This review could not have been completed without the guidance and advice of the following external review consultants. Dr. Branko Ladanyi of Ecole Polytechnique initiated the study and with great patience and tolerance, reviewed draft versions of the report and provided valuable criticism and suggestions.

Dr. Dave Sego of the University of Alberta provided continuous assistance in explaining current theory and in the interpretation of data. He made himself available for discussions at all hours and patiently explained a variety of research papers and answered numerous questions.

THURBER

Dr. Wayne Savigny of the University of British Columbia provided valuable insight and comments with respect to the deformation behaviour of natural soils, particularly with respect to the effects of non-homogeneity on the mechanical behaviour of permafrost.

We would like to acknowledge Dr. Nordie Morgenstern for his critical review of the draft report and his overall guidance, suggestions, and above all his encouragement, throughout the course of the work.

We appreciated the careful review of the draft report, undertaken by Scott Dallimore and Paul Kurfurst, of the Geological Survey of Canada, both of whom provided valuable comments and criticisms aimed at improving the final report.

We would particularly like to thank Mr. Alan Heginbottom of the Geological Survey of Canada for his great patience throughout the course of the work and his helpful criticisms and comments of the various draft versions.

If this study has achieved its objectives, the credit must go primarily to the foregoing reviewers. The work could not have been accomplished without them. The reviewers should not, however, be held responsible for any errors or deficiencies in the report.

We would like to thank Linda Covert, who typed numerous draft versions of the report and Val Vasic who prepared the drawings. We would also like to thank Georgina Griffin who proofread the report and helped prepare the drawings. All of these hard working ladies now qualify as experts in permafrost engineering.

Bruce Smith
Ed Hoeve
June, 1988, Calgary

THURBER

TABLE OF CONTENTS

THURBER

TABLE OF CONTENTS
(continued)

THURBER

TABLE OF CONTENTS
(continued)

71-1

THURBER

SECTION 1

INTRODUCTION

SECTION 1

INTRODUCTION

1.1 General

This report presents the results of a literature review with respect to the mechanical properties of ice and frozen soil which are relevant to the design of energy transportation projects in permafrost regions. The review was carried out at the request of Mr. J.A. Heginbottom of the Terrain Sciences Division of the Geological Survey of Canada, Department of Energy Mines and Resources.

The scope of the review was outlined in a proposal from Thurber Consultants Ltd. dated October, 1987. Authorization to proceed with the work was received on November 23, 1987. The work was completed under DSS File Number: 63SS.23233-7-1126.

1.2 Project Background

The Geological Survey of Canada, as part of its contribution to the Energy Research and Development Program, has a mandate to carry out and promote research into various environmental constraints which affect energy transportation in Northern Canada. A component of this research includes an interest in the mechanical properties of ice and frozen soil.

A significant research effort has been made in recent years by a number of government and private organizations in order to establish the mechanical properties of frozen, thawing and freezing soils. These properties are required for use in the design of a wide variety of projects being undertaken or planned in permafrost regions. The Terrain Sciences Division identified a requirement to critically review the available data in order to establish those areas where future research should be concentrated.

1.3 Objectives

The work carried out under the terms of reference of this study had the following objectives:

1) To briefly outline the most relevant and widely accepted theories concerning the mechanical behaviour of ice and frozen soil.

2) To compile and summarize relevant data concerning the mechanical properties of ice and frozen soil in a form which would be a convenient reference source for practising design engineers.

3) To identify those areas where the mechanical behaviour of ice and frozen soils is not adequately defined within the context of available theory.

4) To identify those areas where existing information concerning the mechanical properties of ice and frozen soil is scarce or non-existent.

5) To identify and priorize key areas where further research should be considered in order develop or refine theoretical behaviour models and to provide the data necessary for design.

1.4 Scope of Work

For purposes of this report, the mechanical properties of ice and frozen soil have been reviewed and discussed within the framework of the following behavioural theories:

1) Non-linear Elasticity,
2) Creep,
3) Strength,
4) Adfreeze Strength,
5) Thaw Consolidation,
6) Frost Heave,
7) Dynamic Response, and
8) Electric Response.

The behavioural response of ice and frozen soil to the following variables is reviewed and discussed in the report, as appropriate:

1) Stress State,
2) Rate and Duration of Loading,
3) Temperature,
4) Soil Type,
5) Ice Content, and
6) Unfrozen Water Content.

An additional very important aspect concerns the thermal response and properties of ice and frozen soil. This aspect was not included in this review because it is the subject of a review currently being prepared by others.

THURBER

The only two geophysical properties discussed in this report are dynamic (seismic) properties and electrical properties. Other geophysical properties (such as nuclear and gravimetric response) have not been generally used in civil engineering applications in permafrost regions and have therefore not been discussed.

Variables such as density, degree of saturation and void ratio are controlled primarily by soil type and ice content, and are discussed under those headings. In some cases, additional variables which are pertinent to specific mechanical properties have been identified and discussed where appropriate. A more comprehensive discussion of the variables included in the study is presented in Section 2.

1.5 Limitations

The scope of this review was limited to the mechanical properties of ice and frozen soil which are relevant to the design of energy transportation facilities in permafrost regions of Northern Canada. These facilities include pipelines, and related ancillary structures such as compressor stations and control buildings, as well as related infrastructure, including access roads, airstrips and temporary and permanent accommodations.

The scope of work did not include offshore production and gathering systems, although some of the data may be applicable to these facilities.

The subject matter covered in this review is extremely broad, however the work had to be accomplished within a fixed budget and a relatively fixed schedule. In order to achieve the primary objectives, it has not been possible to review all of the literature available with respect to each aspect of permafrost behaviour. The approach has therefore been to review and discuss what are believed to be key papers related to the various topics. The emphasis has been to outline, in simple terms, the most applicable current theory, and to present and discuss the most representative data found within the context of that theory. The result is intended for use by geotechnical designers with a reasonable background of experience in permafrost engineering. A list of references has been presented at the end of each section, as well as at the end of the report, in order to assist the reader who wishes to investigate specific subjects in further detail.

THURBER

1.6 Methodology

The study involved the following major tasks:

1) Literature Search,
2) Review of Current Theory,
3) Review and Summary of Relevant Data, and the
4) Identification of Research Requirements.

1.6.1 Literature Search

This task involved a search of the literature to identify the key sources of information concerning current theories and available data.

The literature search included a review of the available data sources as listed in the CRREL (Cold Regions Research and Engineering Laboratory, New Hampshire) Bibliography which were current to about 1985, at the time of the search. Additional sources of information published since 1985 were reviewed where key papers could be identified. A comprehensive search of all sources of information published since 1985 has not been undertaken.

The Arctic Institute of North America at the University of Calgary carries the CRREL Bibliographies as well as all other CRREL publications. Publications from all sources, including external sources such as the Canadian Geotechnical Journal, are indexed and abstracted in the CRREL Bibliographies. The subject index was used to identify relevant literature. In addition the University of Alberta reference lists (as prepared by the Department of Civil Engineering) and the reference lists of some key review articles were used to identify important papers.

An attempt was made to conduct a comprehensive and thorough search of the literature through the use of a number of electronic data bases, including Compendex, NTIS, NRCPUBS, GEOREF and others. Unfortunately, this search could not be successfully completed because it was not possible to restrict the computer search to the point where a manageable volume of citations was achieved, and at the same time ensure that key publications were not overlooked. No key publications were identified in the initial computer generated reference lists which had not been identified in earlier literature searches. The computer based literature search was therefore abandoned since it did not appear to be a feasible approach within the limitations of this study.

THURBER

Literature was acquired from the following sources:

1) Arctic Institute of North America, Calgary
2) University of Calgary Library
3) Corporate and personal libraries at Thurber Consultants Ltd.
4) Personal libraries of Drs. Ladanyi, Sego and Morgenstern.

There is substantial literature, much of it in German, dealing with the behaviour of frozen soil adjacent to deep shafts. This literature has not been reviewed, because of the difficulty in translation.

1.6.2 Review of Current Theory

This task involved a review of current theories with respect to the various aspects of the mechanical behaviour of ice and frozen soil. A brief description of the most widely accepted theories was then prepared for inclusion in the report.

1.6.3 Review and Summary of Relevant Data

The data found in the literature search with respect to the mechanical properties of ice and frozen soil was compiled and reviewed concurrently with the review of the available theories. The data was evaluated within the framework of the applicable theory and relevant data was summarized in a form which would be a convenient reference by design engineers.

1.6.4 Identification of Research Priorities

An evaluation of the available data was undertaken. This evaluation was carried out with the assistance of the external reviewers. Those areas where the mechanical response of ice and frozen soils is not adequately defined by current theory, or where the available data was felt to be insufficient for design, were identified.

1.7 Definition of Terms

The conventional definition of permafrost in geotechnical engineering practice is that it is any ice, soil or rock which remains at a temperature of less than 0°C for a period of more than 1 year. This definition applies throughout this report.

In addition, the term "frozen soil", as used in this report, refers to any soil which has a temperature which is less than 0°C. In addition to soils which are frozen in the conventional sense, the term "frozen soil" as used here, also includes soils which have a high unfrozen water content (due to high pore water salinity or high clay content) and which would not normally be regarded in conventional terms as frozen. The definition used in this report is simply a matter of convenience.

1.8 Non-Homogeneity

A fundamental assumption of all of the behavioural theories is that permafrost is essentially a homogeneous, material. In addition, laboratory testing is often carried out on reconstituted, homogeneous samples, particularly where the validity of a particular theory is being tested.

The unfortunate fact is that most natural earth materials are not homogeneous. The geotechnical engineer must evaluate the degree of non-homogeneity expected to occur in the field and establish the degree to which it will affect theoretical predictions. This process, which requires considerable judgement and experience, represents one of the greatest challenges in design.

In many instances, the use of sophisticated and precise methods of analysis cannot be justified because of the highly variable nature of permafrost. On the other hand, such theoretical analyses, if carried out in the form of parametric studies, can be extremely enlightening and of great assistance to engineering judgement.

Provided the limitations of the various theories are understood and provided the effects of non-homogeneity are recognized and accounted for, it is possible to predict the behaviour of natural permafrost to an accuracy which is acceptable for the majority of design problems.

THURBER

SECTION 2

DISCUSSION OF VARIABLES

SECTION 2

DISCUSSION OF VARIABLES

2.1 General

As indicated in Figure 2.1, the distribution of permafrost in Canada is widespread. The composition of the permafrost in this area covers the entire range of earth materials encountered in geotechnical engineering practice and includes most igneous, metamorphic and sedimentary rocks, as well as most soils including boulders, cobbles, gravels, sands, silts and clays. Ground ice is widespread throughout the area.

The behaviour of frozen and thawed rock and of boulders and cobbles has generally been of less concern to geotechnical engineers since these materials are relatively strong and stable when thawed. The majority of geotechnical engineering problems in permafrost regions are concerned with the behaviour of gravels, sands, silts and clays. Of these, the behaviour of sands, silts and clays is of most concern and consequently much of the available research has been carried out on these materials, as well as on the behaviour of pure ice.

This report is therefore concerned with the response of ice and frozen soils to the effects of the following variables:

1) Stress State,
2) Rate and Duration of Loading,
3) Temperature,
4) Soil Type,
5) Ice Content, and
6) Unfrozen Water Content.

A brief description of each of these variables, together with an assessment of the range of values which are commonly encountered in Northern Canada, is presented in the following sections.

2.2 Stress State

Some aspects of the mechanical behaviour of ice and frozen soil are a function of stress path (the sequence in which the material is loaded or unloaded) as well as the

THURBER

final stress state. Stress state must therefore be evaluated by the designer in assigning material properties used in predicting the response of the material to the design conditions.

In conventional soil mechanics testing, it is convenient to separate the stresses which act on a material into two components:

1) Confining stress, and
2) Deviator stress.

The confining stress is an all-around, uniform stress which results in volumetric compression (or expansion) of the soil, but which results in no shear strains. The deviator stress (that is the stress which deviates from the uniform stress) is that stress which induces shear strains and volume changes (dilation) associated with shear.

In the laboratory, both stress components can be controlled, in homogeneous materials, through the geometry of the test set up and the loading arrangement. In the field, loading conditions can be complex and the distribution of stress and the separation of stress into its two components can be difficult. These difficulties are usually overcome by making simplifying assumptions concerning the geometry, sequence of loading and homogeneity which will occur in the field.

Where mechanical properties are established from laboratory test data, it is important that the loading conditions used in the laboratory simulate the expected field conditions as closely as possible, both in terms of stress path and stress magnitude. Most engineering problems which will be encountered in energy transportation projects will involve excavation, fill placement or foundation construction at relatively shallow depths. For the vast majority of problems, the confining stresses will range from 0 to 500 kPa. Deviator stresses can be expected to range from 0 to about 15,000 kPa depending on the design problem.

2.3 Rate and Duration of Loading

The deformation response of ice and frozen soil is time dependent and is therefore a function of the rate and duration of loading.

The rate of loading imposed by dynamic loads, or seismic events is much more rapid than that generally encountered in open excavations or in the application of structural loads on foundations. The short term deformation and

THURBER

strength properties of ice and frozen soil are often determined in laboratory tests in which the strain rate imposed on the sample is held constant. A rate of strain for such tests must be selected which will be consistent with the rate of loading expected to occur in the field.

Load durations which occur in the field may range from fractions of a second (for example due to dynamic loading, blasting effects and seismic events) to several days or weeks (in the case of short term live loads, temporary excavations etc.). The duration of loading can range from several decades (in the case of dead loads on building foundations), to several hundred years (in the case of highway fills and deep excavations). It is important, that the duration of loading used in laboratory tests to determine the deformation and strength parameters be reconciled with the duration of loading expected to occur in the field.

2.4 Temperature

As might be expected, the behaviour of ice and frozen soil is a function of temperature.

Ground temperatures vary with depth, as well as with location. An idealized ground temperature profile in a continuous permafrost area is shown in Figure 2.2. As indicated on the figure, large variations in ground temperature occur in the near surface 1 or 2 metres, due primarily to changes in air temperature. Other factors which affect the near surface ground temperatures include near surface water content, the presence or absence of vegetation, albedo (reflectivity), ground surface aspect, the reflection of long wave radiation from the ground surface to the atmosphere and back to the ground surface (the greenhouse effect) and the presence of snow, its depth and properties.

Fluctuations in near surface ground temperatures attenuate with depth. Ground temperatures at depths of 6 to 8 metres commonly fluctuate within 1 or 2 degrees above and below the mean temperature at that depth.

Ground temperature measurements as a function of depth and time are not normally available to the designer, however, an approximate indication of ground temperatures can be derived from air temperature data. The mean annual ground temperature can be calculated from the following equation:

$$T_m = (TI-FI)/365 \qquad (2.1)$$

THURBER

where

T_m denotes the mean annual ground temperature,

TI denotes the absolute value of the ground surface thawing index, and

FI denotes the absolute value of the ground surface freezing index.

The freezing and thawing indices for air can be established from the information presented on Figures 2.3 and 2.4 respectively. It is preferable, however, to use actual meterological data where it is available. The air freezing and thawing indices must be converted to ground surface freezing and thawing indices by multiplying by an appropriate factor to account for surface effects such as albedo, snow depth, etc. A list of the factors used to convert air freezing and thawing indices to ground surface freezing and thawing indices is presented in Figure 2.5.

The seasonal variation in ground surface temperature can be approximated for many problems by a sine curve as shown in Figure 2.6. A graph is presented in Figure 2.6 which provides a convenient method for determining the mean and amplitude of a sinusoidal variation when the freezing and thawing indices are given (Harlan and Nixon, 1978). A more accurate approach is to use a computer program that will fit a sine curve to air temperature data.

The foregoing method for estimating ground surface temperatures in permafrost regions has limited accuracy. Whenever possible, the designer should compare the ground temperature data estimated from air temperature data with field temperature measurements where they are available. Active layer depths are often known for many locations and the ground surface temperature variation should be checked to ensure that it is consistent with observed active layer depths.

Ground temperatures at various depths have been compiled for a number of communities in the Northwest Territories and the results are summarized on Figure 2.7 (Hoeve, 1988). The data indicate that permafrost temperatures at depths of 6 to 8 m range from 0 to -12°C. Temperatures in the near surface 1 or 2 m normally range from -20°C to + 10°C.

Ground temperatures at depth can vary significantly within short distances in some instances. For example the ground temperature at a depth of 6 m was found to be

THURBER

-9.2°C at a school site in the community of Pond Inlet, N.W.T. in late August. Ground temperatures at a location about 5 km from the community were found to range from -2 to -4°C at a depth of 6 m in early September. These observations indicate that in critical design situations, it may be essential to obtain actual field temperature data rather than rely on estimates made from air temperature observations.

2.5 Soil Type

The behaviour of frozen soils will be affected by the composition of the soil which includes the grain size distribution and the mineralogical composition of the soil particles.

Permafrost soils are normally classified using the Unified Soils Classification system. A modified version of this system is presented in Figure 2.8. The grain size distribution of frozen soils ranges from gravels, sands, silts and clays, to organic silts, organic clays and peat. In general, thick peat deposits, fine grained alluvial and lacustrine deposits, and silty clay till deposits are common in the vicinity of the Mackenzie River in the Western Arctic. These fine grained soils occur in an area where ground temperatures are relatively warm or where permafrost is sporadic, and can be particularly troublesome.

In the Arctic Archipelago, the Keewatin and Baffin Regions, fine grained soils such as clay and organic deposits are not as common. In these areas the near surface soils often consist of sands and gravels underlain by silty sand till, which contains cobbles and boulders derived from the underlying bedrock. The bedrock in these areas generally consists of various igneous and metamorphic rocks, as well as some of the harder sedimentary rocks such as limestones and dolomites.

Most behavioural theories assume that the soil has a homogeneous texture and density throughout. In addition, artificially prepared samples, which are often tested in the laboratory to determine the mechanical properties of frozen soils, are of necessity homogeneous, in order to obtain a consistent set of test data. Natural soils (particularly glacial tills) are highly non-homogeneous. This non-homogeneity can have a significant effect on the behaviour of the material in the field. For this reason, it is important that, wherever practical, laboratory test data be supplemented with actual field observations.

THURBER

2.6 Ice Content

Ice occurs in frozen soils either as pore (interstitial) ice or as segregated ice which is present as virtually pure ice in the form of irregularly shaped lenses or bands. The segregated ice varies greatly in width and orientation and is derived from a variety of geological processes, some of which are not completely understood. In most locations, the excess ice content, which is present as segregated ice, decreases with depth. Segregated ice is common at depths down to about 3 m and much less common below depths of 5 to 10 m.

Most behavioural theories assume that the ice in frozen soils is uniformly distributed throughout the material. Where excess ice is present in natural ice rich permafrost, it most often exists as segregated ice, which has different mechanical properties than the surrounding soil matrix. The random and often unpredictable presence and orientation of segregated ice constitutes one of the most significant challenges in predicting the behaviour of permafrost.

A number of systems for describing ground ice have been suggested by various authors. The most widely used is the NRC ice classification system, which is reproduced in Figure 2.9.

The ice content of frozen soil is one of the most important variables which influences the behaviour of the soil. The ice content controls the strength and deformation behaviour, the rate and amount of thaw settlement as well as the rate of thaw (since the latent heat of ice has a major influence on the rate of thaw).

The ice content, combined with a knowledge of grain size distribution and mineralogical composition can be used to calculate soil density and void ratio, provided the degree of ice saturation is known or can be estimated. The vast majority of frozen soils and in particular those soils which pose the most significant problems to the geotechnical engineer, are ice saturated. It is fortunate that the ice content of frozen soils can be established simply and inexpensively from tests on disturbed or undisturbed samples.

The relationships between water content, void ratio, porosity, degree of saturation and density are summarized on Figures 2.10 and 2.11. Typical ranges in water contents, void ratios, porosities, and densities of frozen soils are presented on Figure 2.12.

THURBER

2.7 Unfrozen Water Content

Unfrozen water is usually present even though the soil temperature is lower than the freezing point of water (0°C). The presence of unfrozen water can have a very significant effect on the mechanical response of frozen soils.

A number of methods for determining the relationship between unfrozen water content and the temperature of frozen soils have been used in the past. These methods are described by Anderson and Morgenstern (1973). Recently, the technique of time domain reflectometry (TDR) has been developed as a means of measuring unfrozen water content. The use of this convenient technique is becoming more common. The method is described by Patterson and Smith, (1981).

Typical unfrozen water contents as a function of temperature for a variety of soils are presented in Figures 2.14 and 2.15. Based on these results, Anderson and Morgenstern (1973) suggested that unfrozen water content can be conveniently represented by a simple power relationship as:

$$w_u = m\ \theta^n \qquad (2.1)$$

where

w_u denotes the unfrozen water content (gms of water/gms of soil).

θ denotes the absolute temperature below freezing (°C), and

m, n are characteristic soil parameters.

Anderson, Tice and McKim (1973) have reported the following values for the parameters m and n from experimental data.

Soil	m	n
Manchester fine sand	0.0346	-0.048
Fairbanks silt	0.0481	-0.326
Kaolinite	0.2380	-0.360
Suffield silty clay	0.1392	-0.315
Hawaiian clay	0.3242	-0.243
Umiat bentonite	0.6755	-0.343

THURBER

As indicated on Figures 2.13 and 2.14, the unfrozen water content is a function of the grain size distribution of the soil. Fine grained soils (such as silts and clays) have significantly higher unfrozen water contents, at a given temperature, than coarse grained soils such as sands and gravels.

Another important factor which affects the unfrozen water content-temperature relationship, is the concentration of soluble salts in the pore water (salinity), which tends to depress the freezing point of water, increasing the unfrozen water content in the frozen soil.

Patterson and Smith (1983, 1985) have used the TDR technique to establish the relationship between unfrozen water content and temperature for a number of soil types. Their results are presented on Figures 2.15 and 2.16.

The freezing process in saline soils is poorly understood and may be relatively complex because water soluble salts are pushed ahead of the freezing front as pore ice forms. The distribution of saline pore water (and consequently the distribution of unfrozen water) will therefore depend on the rate and direction of freezing. This phenomenon can have a significant effect on the properties of saline soils as measured in the laboratory. It is essential that the freezing process for reconstituted saline soils prepared in the laboratory be carefully controlled in order to achieve a uniform and representative distribution of pore water salinity throughout the sample.

The presence of saline soils in permafrost, and the possible effects which pore fluid salinity have on unfrozen water contents and the mechanical properties of frozen soils, has only recently been identified as a significant problem. Researchers and practising engineers began routinely measuring the salinity of the pore water in frozen soils in the early 1980's. Some of the available data has been compiled by Hoeve (1988). This data indicates that saline soils are far more widespread in permafrost regions than had been expected. Values for pore fluid salinity as measured in soil samples taken from various communities in the Northwest Territories are summarized on Figure 2.17.

The distribution of saline soils, its effect on unfrozen water content and its effect on the mechanical properties of frozen soils are all areas which have been identified as worthy of further investigation by a number of researchers.

DISCUSSION OF VARIABLES

LIST OF REFERENCES

Andersland, O.B. and Anderson, D.M., 1978. Geotechnical Engineering for Cold Regions. McGraw-Hill, New York, 566 p.

Anderson, D.M. and Morgenstern, N.R., 1973. Physics, chemistry, and mechanics of frozen ground: a review. PERMAFROST: The North American Contribution to the Second International Conference on Permafrost, Yakutsk, National Academy Science, Washington, D.C., pp. 257-288.

Anderson, D.M., Pusch,R., and Penner, E., 1978. Chapter 2, Physical and Thermal Properties of Frozen Ground in Geotechnical Engineering for Cold Regions (Andersland and Anderson, 1978).

Anderson, D.M., Tice, A.R. and McKim, H.L., 1973. The unfrozen water and the apparent specific heat capacity of frozen soils. Proc. 2nd International Conference on Permafrost, Yakutsk, U.S.S.R., North American Contribution, U.S. National Academy of Sciences, pp. 289-295.

Boyd, D.W., 1976. Normal freezing and thawing degree days from normal monthly temperatures. Can. Geot. Journ., 13, pp. 176-180.

Brown, R.J.E., 1970. Permafrost in Canada, Its influence on Northern Development. University of Toronto Press, 207 p.

Brown, R.J., Johnston, G.H., MacKay, J.R., Morgenstern, N.R., and Shilts, W.W., Chapter 2, Permafrost distribution and terrain characteristics. In Permafrost Engineering Design and Construction, (Johnston, 1981).

Goodrich, L.E., and Gold, L.W., 1981. Chapter 4, Ground Thermal Analysis, in Permafrost. Engineering Design and Construction, Johnson, G.H., 1981.

Harlan, R.L., and Nixon, J.F., 1978. Chapter 3, Ground Thermal Regime. in Geotechnical Engineering for Cold Regions, (Andersland and Anderson, 1978).

Hoeve, T.E., 1988. The distribution of saline soils in the Northwest Territories. M.Eng. Project, University of Alberta (in preparation).

THURBER

LIST OF REFERENCES
(continued)

Holtz, R.D. and Kovacs, W.D., 1981. An Introduction to Geotechnical Engineering. Prentice-Hall, Englewood Cliffs, N.J. 733 p.

Johnston, G.H., (Ed.), 1981. Permafrost Engineering Design and Construction. John Wiley & Sons, Toronto, 540 p.

Johnston, G.H., Ladanyi, B., Morgenstern, N.R., and Penner, E., 1981. Chapter 3, Engineering Characteristics of Frozen and thawing soils. in Permafrost, Engineering Design and Construction, (Johnston, 1981).

Patterson, D.E. and Smith, M.W., 1981. The measurement of unfrozen water content by time domain reflectometry: results from laboratory tests. Can. Geot. Journ., 18, pp. 131-144.

Patterson, D.E. and Smith, M.W., 1983. Measurements of unfrozen water content in saline permafrost using time-domain reflectometry. PERMAFROST: Fourth International Conference, Proceedings, Fairbanks, national Academy Science, Washington, D.C., 1, pp. 968-972.

Patterson, D.E. and Smith, M.W., 1985. Unfrozen water content in saline soils: results using time-domain reflectometry. Can. Geot. Journ., 22, pp. 95-101.

Pihlainen, J.A. and Johnston, G.H., 1963. Guide to a Field Description of Permafrost for Engineering Purposes. Technical memorandum 79, NRC 7576, published by the National Research Council of Canada.

THURBER

LIST OF FIGURES

THURBER

2.16 Unfrozen water content data for soils with various pore fluid salinities (Patterson and Smith, 1983).

2.17 Unfrozen water content data for a silty clay at various salinities (Patterson and Smith, 1985).

2.18 Pore fluid salinity data for selected communities in the Northwest Territories.

THURBER

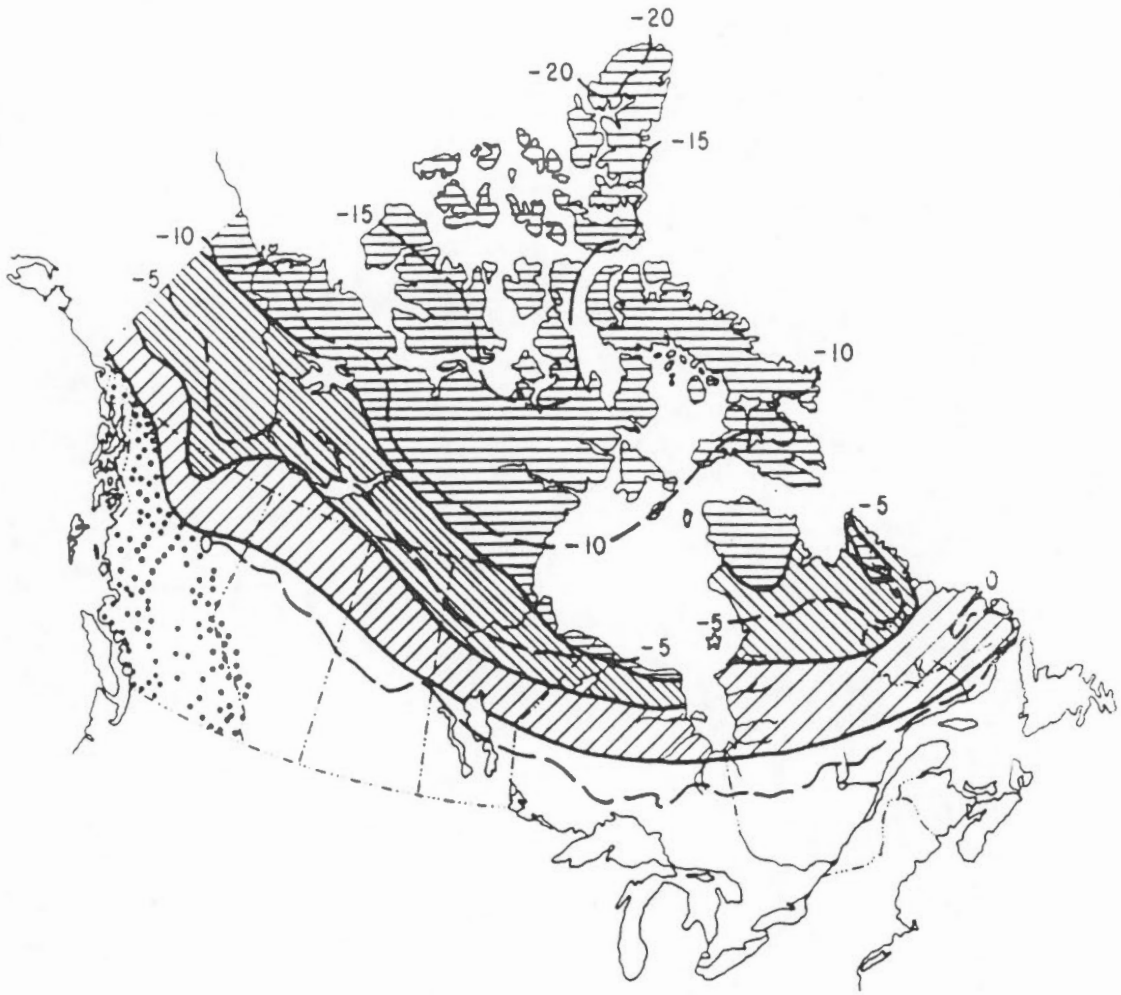

The distribution of permafrost in Canada (Johnston, 1981).

FIGURE 2.1

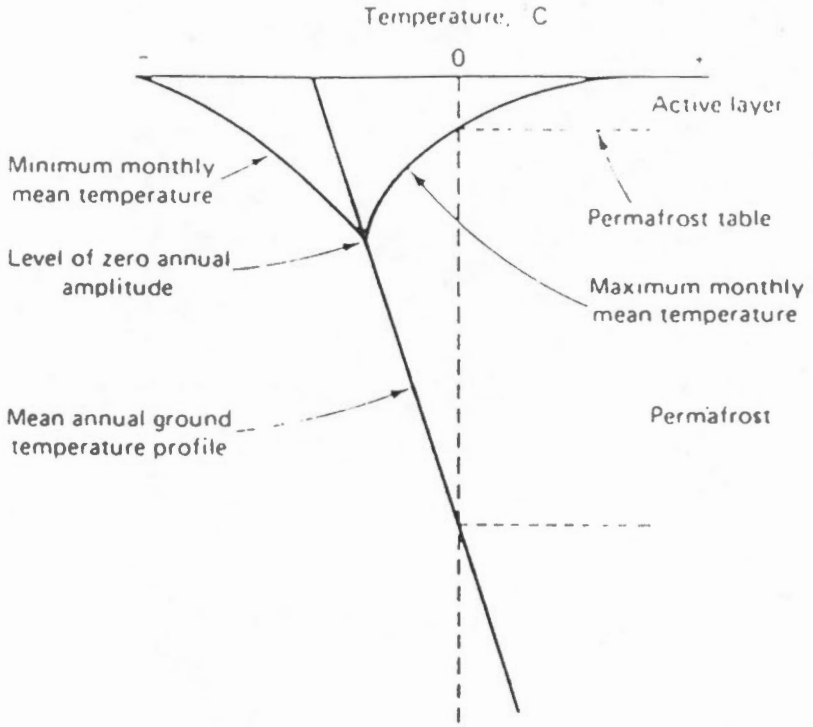

Idealized ground temperature profile in permafrost (Harlan and Nixon, 1978).

FIGURE 2.2

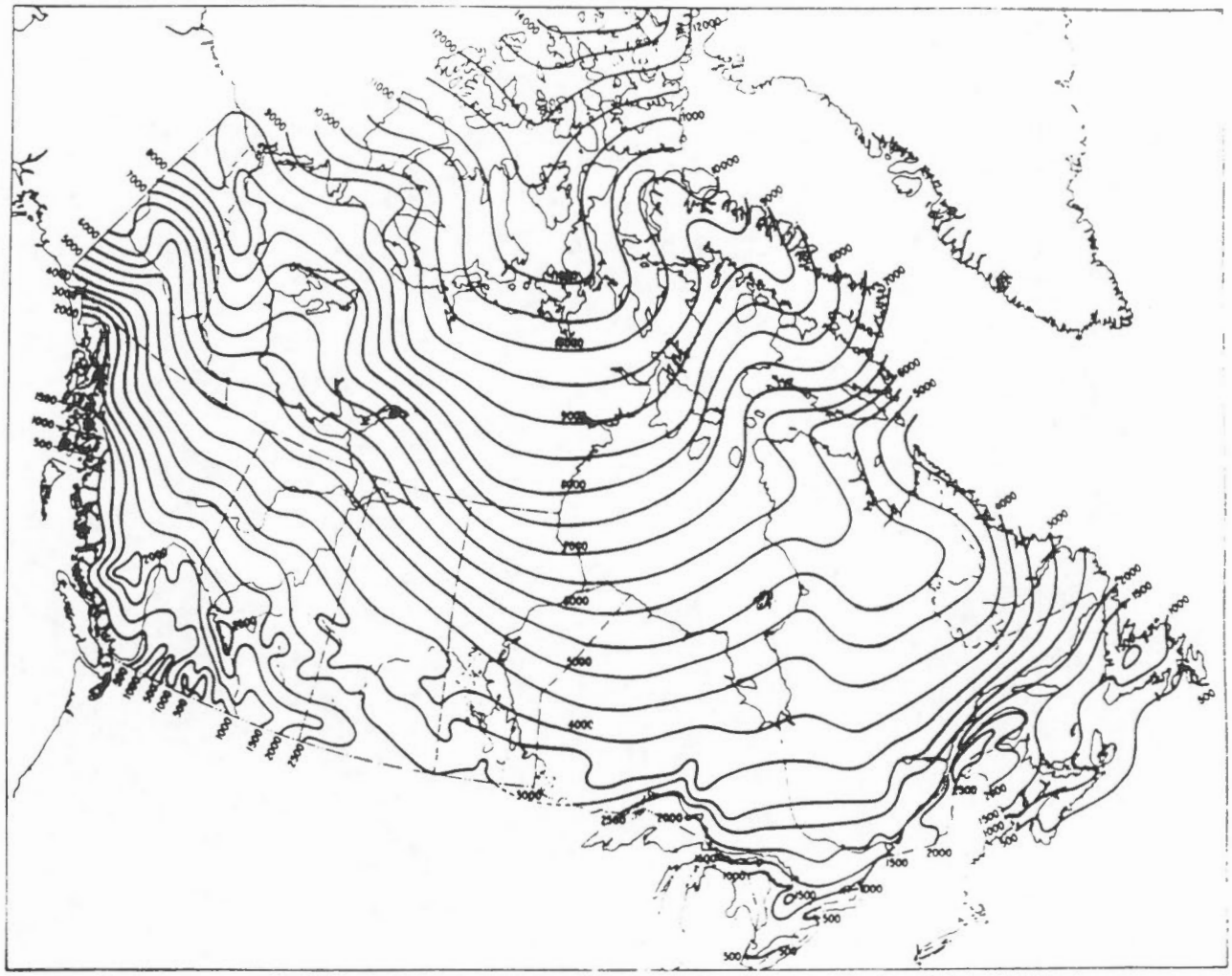

Distribution of mean air freezing index in Fahrenheit degree days (Boyd, 1976).

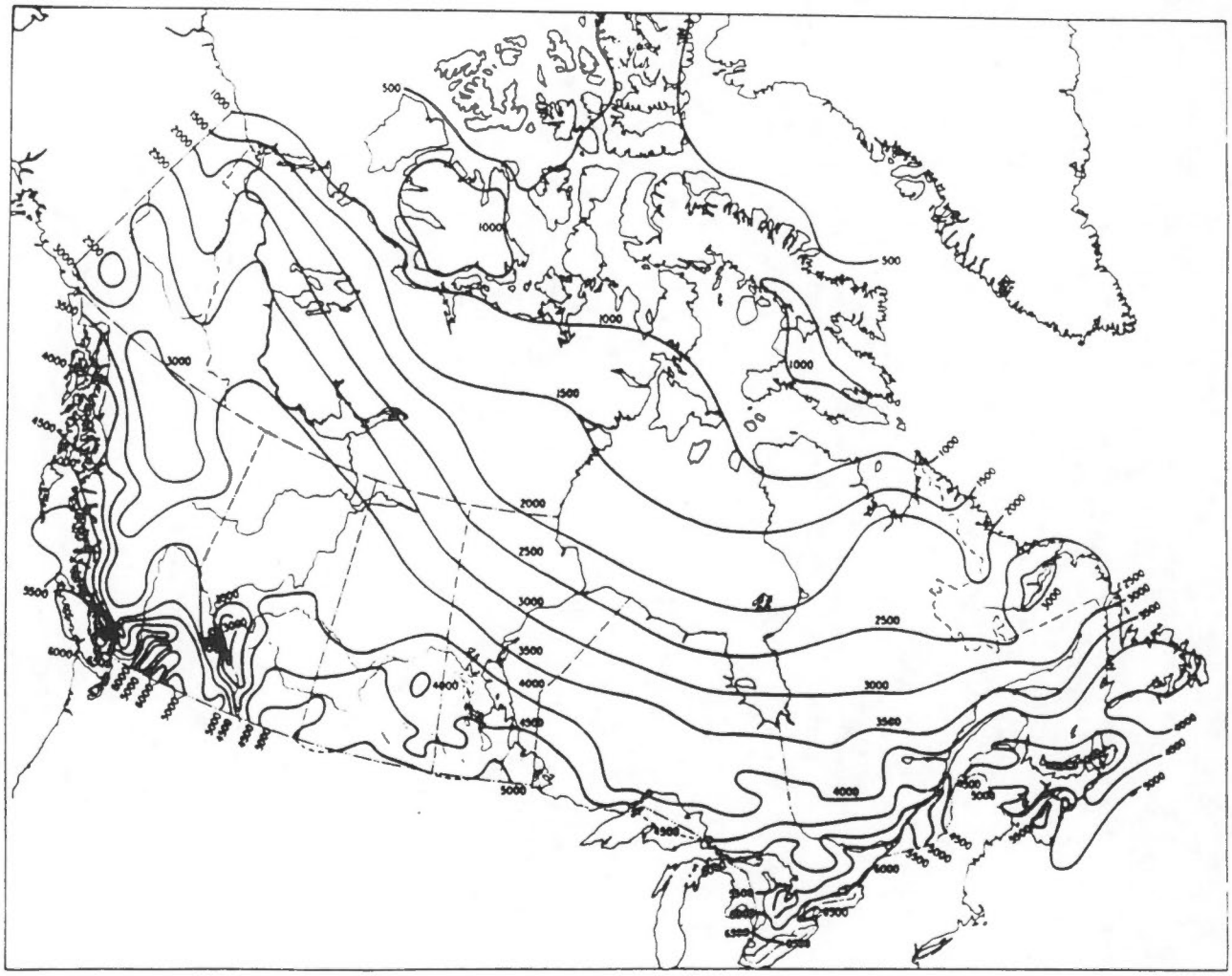

Distribution of mean air thawing index in Fahrenheit degree days (Boyd, 1976).

Values of n-factors for Different Surfaces
(After Lunardini 1978)

Surface Type	Freezing-n_f	Thawing-n_t
Spruce trees, brush, moss over peat—soil surface	0.29 (under snow)	0.37
As above with trees cleared—soil surface	0.25 (under snow)	0.73
Turf	0.5 (under snow)	1.0
Snow	1.0	—
Gravel	0.6 – 1.0	1.3 – 2
(probable range for northern conditions)	(0.9 – 0.95)	
Asphalt pavement	0.29 – 1.0 or greater	1.4 – 2.3
(probable range for northern conditions)	(0.9 – 0.95)	
Concrete pavement	0.25 – 0.95	1.3 – 2.1
(probable range for northern conditions)	(0.7 – 0.9)	

Empirical factors to convert air temperatures to ground surface temperatures (Goodrich and Gold, 1981).

THURBER

FIGURE 2.5

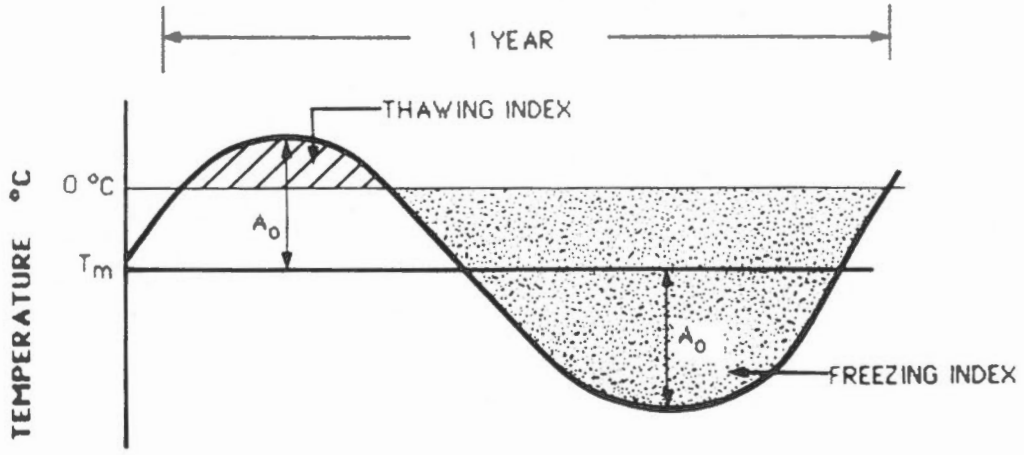

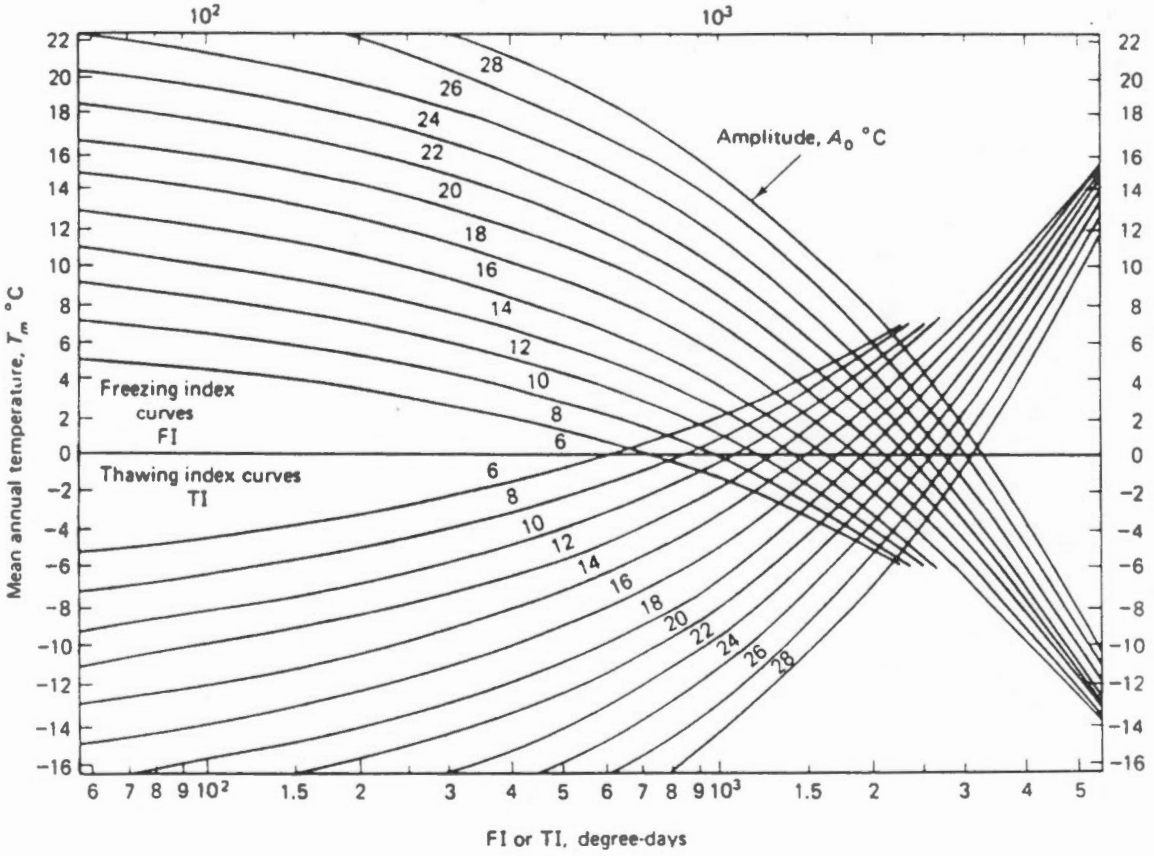

Chart for determining the mean and amplitude of a sinusoidal temperature variation from the freezing and thawing indices (Harlan and Nixon, 1978).

FIGURE 2.6

COMMUNITY	PROJECT	MEASURED TEMPERATURE (°C)	DEPTH (m)	DATE	MEAN ANNUAL AIR TEMPERATURE (°C)
ARCTIC BAY	SCHOOL	-9.7	6.0	3 OCT 83	-13.8
ARCTIC BAY	SCHOOL	-9.8	6.0	12 OCT 83	-13.8
ARCTIC BAY	SCHOOL	-9.5	6.0	28 OCT 83	-13.8
ARCTIC BAY	SCHOOL	-9.5	6.0	24 NOV 83	-13.8
ARCTIC RED RIVER	GYMNASIUM	-4.1	6.0	16 OCT 86	- 8.2
ARCTIC RED RIVER	FIREHALL	-3.9	6.0	16 OCT 86	- 8.2
BROUGHTON ISLAND	POWER HOUSE	-8.7	5.5	5 JUN 88	-11.1
CAPE DORSET	RECREATION COMPLEX	-3.7	5.8	8 DEC 86	- 9.1
CAPE DORSET	SCHOOL	-5.6	6.1	4 AUG 87	- 9.1
CLYDE RIVER	SCHOOL	-8.7	6.0	3 OCT 82	-12.2
CLYDE RIVER	SCHOOL	-8.8	6.0	17 OCT 82	-12.2
CLYDE RIVER	SCHOOL	-9.2	6.0	26 OCT 82	-12.2
ESKIMO POINT	SCHOOL	-5.3	5.6	29 OCT 85	- 9.4
FORT MCPHERSON	RECREATION COMPLEX	-3.8	6.0	15 OCT 86	- 8.5
FORT SIMPSON	NAKEHKO KOE DENEPLEX	-0.2	6.1	12 MAR 87	- 3.3
HOLMAN	HAMLET OFFICES	-9.3	5.8	15 NOV 85	-12.2
IQALUIT	ARCTIC COLLEGE	-0.9	6.1	13 OCT 86	- 9.1
IQALUIT	ARCTIC COLLEGE	-1.4	6.1	20 OCT 86	- 9.1
IQALUIT	ARCTIC COLLEGE	-2.5	6.1	28 OCT 86	- 9.1
IQALUIT	YOUNG OFFENDERS SECURE FACILITY	-3.0	6.1	24 NOV 87	- 9.1
IQALUIT	DISCOVERY LODGE EXPANSION	-6.4	6.0	19 JUL 87	- 9.1
PANGNIRTUNG	PRIMARY-ELEMENTARY SCHOOL	-6.4	6.0	2 DEC 86	-10.3
PANGNIRTUNG	RECREATION COMPLEX	-6.8	6.0	4 DEC 86	-10.3
POND INLET	PRIMARY SCHOOL	-9.2	6.0	26 AUG 86	-14.3
POND INLET	SUBDIVISION	-13.8	6.0	13 JUN 86	-14.3
POND INLET	WATER SUPPLY	-6.0	6.0	15 JUN 87	-14.3
RANKIN INLET	KEEWATIN REGIONAL EDUCATION CENTRE	-9.2	5.7	31 JUL 87	-10.8
RANKIN INLET	KEEWATER REGIONAL EDUCATION CENTRE	-7.4	5.8	1 AUG 86	-10.8
RANKIN INLET	FISH PROCESSING PLANT	-5.7	6.1	9 MAY 87	-10.8
TUKTOYAKTUK	STORAGE FACILITY	-4.6	6.0	11 FEB 87	-10.7

NOTE:

1) The mean annual air temperature (MAAT) was calculated by subtracting the Thawing Index from the Freezing Index and dividing by 365.

Measured ground temperatures in selected communities in the Northwest Territories (Hoeve, 1988).

TABLE 5.33
UNIFIED SOIL CLASSIFICATION SYSTEM (ASTM D-2487) [After USAWES (1967)[30a]]

Major Divisions			Group Symbols	Typical Names	Laboratory Classification Criteria	
Coarse-grained soils (More than half of material is larger than No. 200 sieve size)	Gravels (More than half of coarse fraction is larger than No. 4 sieve size)	Clean gravels (Little or no fines)	GW	Well-graded gravels, gravel-sand mixtures, little or no fines	$C_u = \frac{D_{60}}{D_{10}}$ greater than 4; $C_c = \frac{(D_{30})^2}{D_{10} \times D_{60}}$ between 1 and 3	
			GP	Poorly graded gravels, gravel-sand mixtures, little or no fines	Not meeting all gradation requirements for GW	
		Gravels with fines (Appreciable amount of fines)	GM[a] d / u	Silty gravels, gravel-sand-silt mixtures	Atterberg limits below "A" line or P.I. less than 4	Above "A" line with P.I. between 4 and 7 are *borderline* cases requiring use of dual symbols
			GC	Clayey gravels, gravel-sand-clay mixtures	Atterberg limits below "A" line with P.I. greater than 7	
	Sands (More than half of coarse fraction is smaller than No. 4 sieve size)	Clean sands (Little or no fines)	SW	Well-graded sands, gravelly sands, little or no fines	$C_u = \frac{D_{60}}{D_{10}}$ greater than 6; $C_c = \frac{(D_{30})^2}{D_{10} \times D_{60}}$ between 1 and 3	
			SP	Poorly graded sands, gravelly sands, little or no fines	Not meeting all gradation requirements for SW	
		Sands with fines (Appreciable amount of fines)	SM[a] d / u	Silty sands, sand-silt mixtures	Atterberg limits above "A" line or P.I. less than 4	Limits plotting in hatched zone with P.I. between 4 and 7 are *borderline* cases requiring use of dual symbols
			SC	Clayey sands, sand-clay mixtures	Atterberg limits above "A" line with P.I. greater than 7	
Fine-grained soils (More than half material is smaller than No. 200 sieve)	Silts and clays (Liquid limit less than 50)		ML	Inorganic silts and very fine sands, rock flour, silty or clayey fine sands, or clayey silts with slight plasticity		
			CL	Inorganic clays of low to medium plasticity, gravelly clays, sandy clays, silty clays, lean clays		
			OL	Organic silts and organic silty clays of low plasticity		
	Silts and clays (Liquid limit greater than 50)		MH	Inorganic silts, micaceous or diatomaceous fine sandy or silty soils, elastic silts		
			CH	Inorganic clays of high plasticity, fat clays		
			OH	Organic clays of medium to high plasticity, organic silts		
	Highly organic soils		Pt	Peat and other highly organic soils		

Determine percentages of sand and gravel from grain-size curve. Depending on percentage of fines (fraction smaller than No. 200 sieve size), coarse-grained soils are classified as follows:
Less than 5 per cent — GW, GP, SW, SP
More than 12 per cent — GM, GC, SM, SC
5 to 12 per cent — *Borderline* cases requiring dual symbols[b]

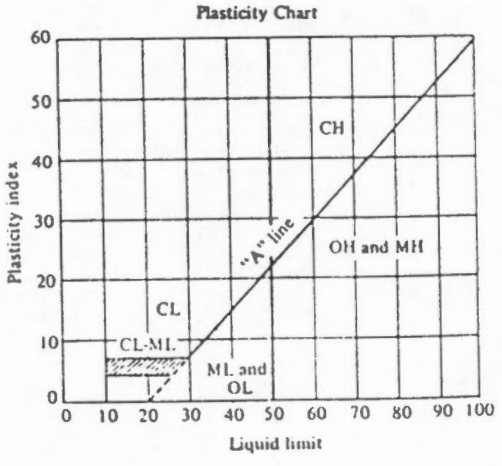

[a] Division of GM and SM groups into subdivisions of d and u are for roads and airfields only. Subdivision is based on Atterberg limits; suffix d used when L.L. is 28 or less and the P.I. is 6 or less; the suffix u used when L.L. is greater than 28.
[b] Borderline classifications, used for soils possessing characteristics of two groups, are designated by combinations of group symbols. For example: GW-GC, well-graded gravel-sand mixture with clay binder.

The Unified Soil Classification system.

FIGURE 2.8

THURBER

ICE NOT VISIBLE

GROUP SYMBOL	SUBGROUP		
	SYMBOLS	DESCRIPTION	
N	Nf	Poorly bonded or friable	
	Nbn	No excess ice, well bonded	
	Nbe	Excess ice, well bonded	

VISIBLE ICE LESS THAN 50% BY VOLUME

V	Vx	Individual ice crystals or inclusions	
	Vc	Ice coatings on particles	
	Vr	Random or irregularly oriented ice formations	
	Vs	Stratified or distinctly oriented ice formations	

VISIBLE ICE GREATER THAN 50% BY VOLUME

ICE	ICE + soil type	Ice with soil inclusions	
	ICE	Ice without soil inclusions (greater than 25mm (1 in.) thick)	

LEGEND · SOIL ICE

The NRC system for describing permafrost (Pihlainen and Johnston, 1963).

VOID RATIO e

$$e = \frac{V_v}{V_s}$$

POROSITY n

$$n = \frac{e}{1 + e}$$

DEGREE OF SATURATION S

$$S = \frac{V_w}{V_v}$$

WATER CONTENT w

$$w = \frac{W_w}{W_s} = \frac{Se}{G_s}$$

V_v volume of voids
V_s volume of soil solids
V_w volume of water

W_w weight of water
W_s weight of dry soil
S degree of saturation
e void ratio
G_s specific gravity of soil solids

Definitions of void ratio, porosity, degree of saturation and water content of soils.

THURBER

BULK DENSITY γ_t

$$\gamma_t = \frac{W}{V} = \frac{(G_s + Se)_w}{1 + e}$$

DRY DENSITY γ_d

$$\gamma_d = \frac{\gamma_t}{(1 + w)}$$

EFFECTIVE (SUBMERGED OR BUOYANT) DENSITY

$$\gamma' = \gamma_t - \gamma_w$$

W	weight of soil and water
V	volume of soil and water
G_s	specific gravity of soil solids
S	degree of saturation
e	void ratio
w	water content

Definitions of Density (by weight) for soils.

Soil	Void Ratio e	Porosity n	Water Content w (%)
Peat	>5	>85	>500
Mud	3-6	75-85	150-300
Clay, soft	1-3	50-75	40-100
Stiff	0.3-0.8	25-45	10-40
Silt	0.3-1.4	25-60	10-50
Sand, poorly graded	0.5-0.9	35-45	10-35
Well graded	0.15-0.4	15-30	
Till	0.1-0.3	10-25	5-10

Characteristic void ratios, porosities and water contents for various soils (after Anderson et al, 1978).

Soil Type	Total Density kN/m^3	Dry Density kN/m^3	Submerged Density kN/m^3
Sands and Gravels	18-24	15-23	10-13
Silts and Clays	14-21	6-18	4-11
Glacial Tills	21-24	17-23	11-14
Crushed Rock	18-22	15-20	9-12
Peats	10-11	1-3	0-1
Organic Silts and Clays	12-18	5-15	3-8

Typical values for different densities of some common soils (after Holtz and Kovacs, 1981).

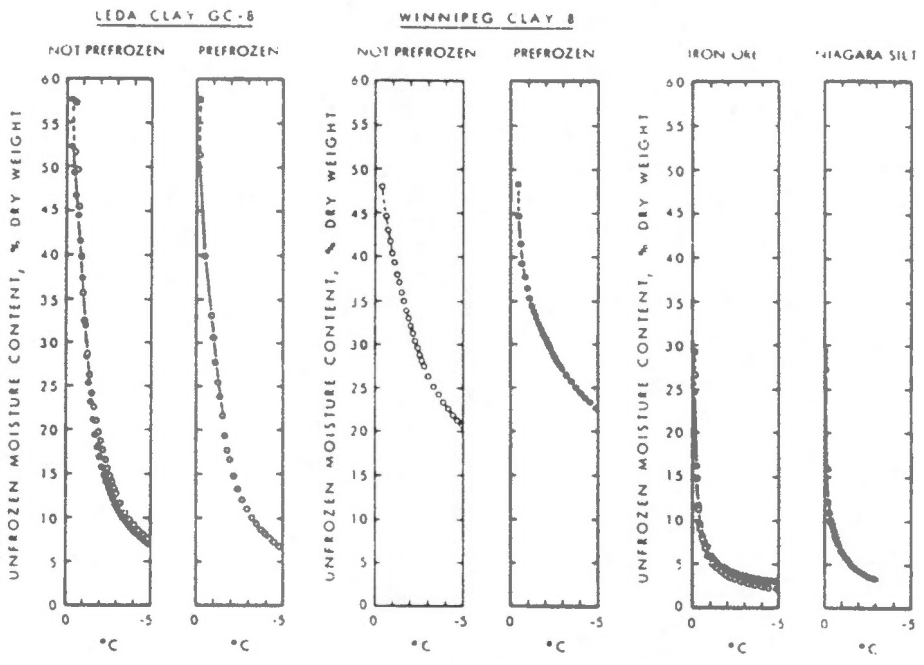

Variation of unfrozen water content data for four different soils (after Williams, 1967 in Johnson et al, 1981).

THURBER

FIGURE 2.14

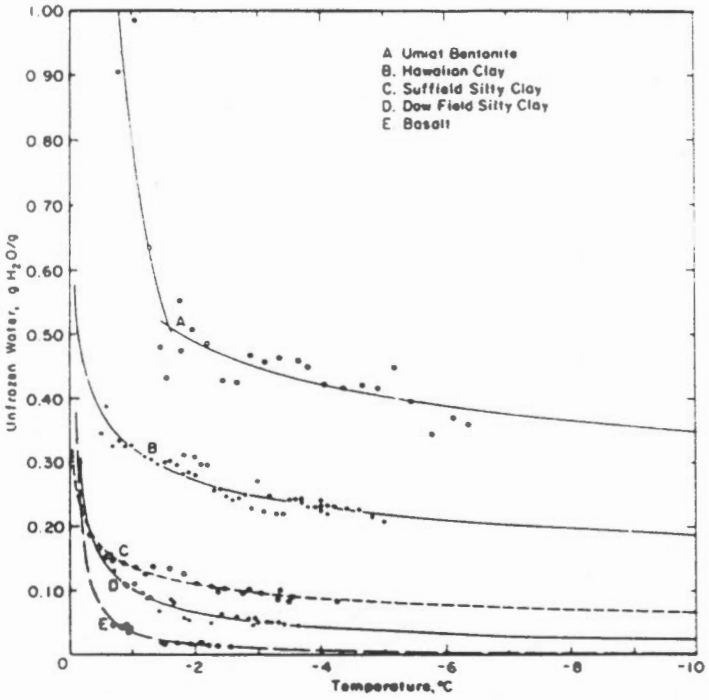

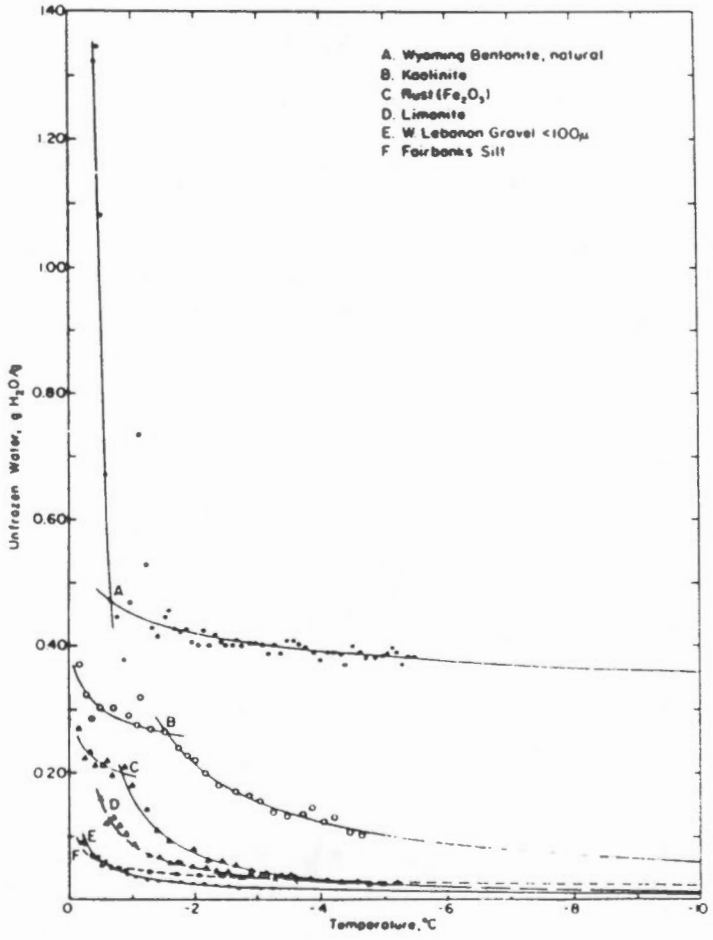

Unfrozen water content data for various soils (Anderson and Morgenstern, 1973).

FIGURE 2.15

THURBER

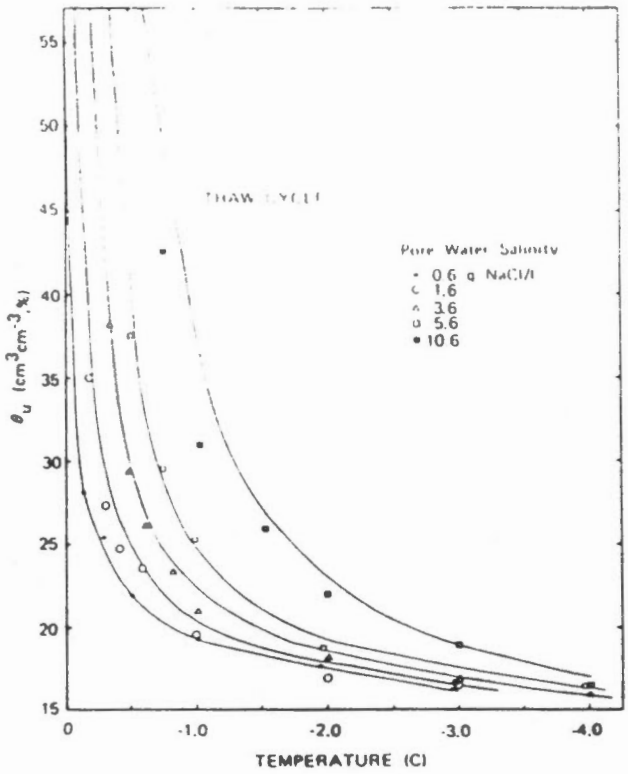

Freezing characteristic data for
Allendale silty clay at various salinities.

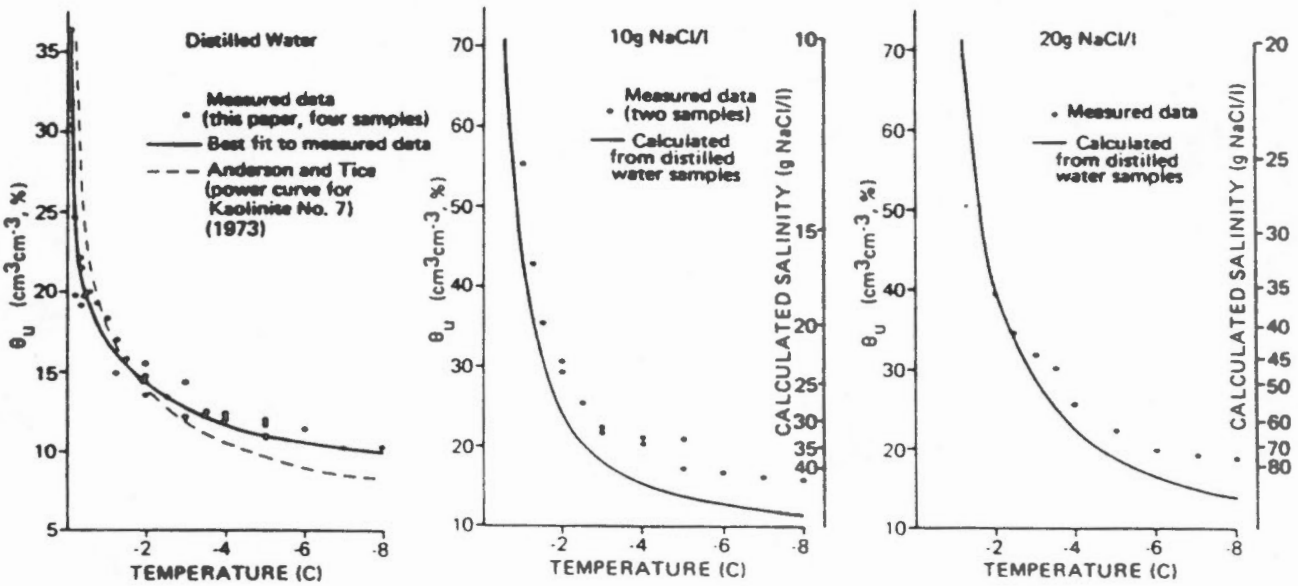

Freezing characteristic data for Kaolinite #3 at various salinities.

Unfrozen water content data for soils with various pore fluid salinities (Patterson and Smith, 1983).

THURBER

FIGURE 2.16

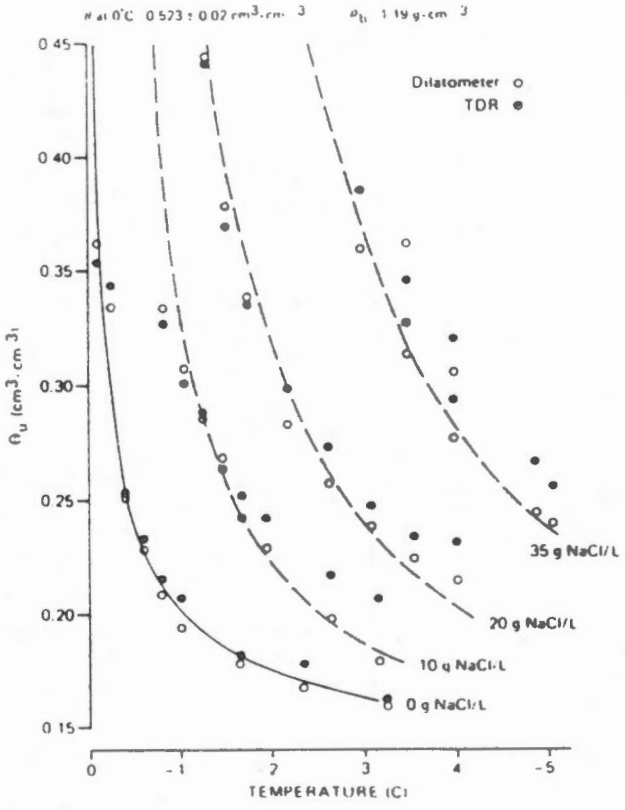

Unfrozen water content data for a silty clay at various salinities (Patterson and Smith, 1985).

FIGURE 2.17

COMMUNITY	NUMBER OF TESTS	RANGE IN SALINITY (ppt)	AVERAGE SALINITY (ppt)	SOIL TYPE
ARCTIC BAY	26	1.0 - 32.0	12.5	SHALE-LIMESTONE
ARCTIC RED RIVER	20	1.2 - 41.3	11.3	CI-SHALE
BAKER LAKE	3	0.1 - 16.3	7.9	SP-SM
CAPE DORSET	13	0.5 - 25.2	8.6	GP-ML
CLYDE RIVER	101	0.5 - 45.1	13.0	SM
CORAL HARBOUR	3	1.3 - 2.9	1.9	?
ESKIMO POINT	11	1.4 - 38.3	8.5	SM
FORT GOOD HOPE	2	0.7 - 2.4	1.6	SM-CI
FORT MCPHERSON	9	0.4 - 22.7	8.5	SM-CI-SHALE
FORT SIMPSON	6	0.5 - 0.9	0.7	SM
GJOA HAVEN	1	0.2 - 0.2	0.2	SM
HOLMAN	4	3.0 - 5.7	4.3	GM
IQALUIT	71	0.1 - 14.8	2.0	SM-GP-GRANITE
PANGNIRTUNG	24	0.1 - 31.3	14.8	SM-ML
PELLY BAY	4	12.0 - 33.7	22.5	?
POND INLET	30	0.2 - 23.4	6.4	SM
RANKIN INLET	32	3.0 - 28.9	14.9	ML-SM-GM
REPULSE BAY	8	0.5 - 10.4	2.4	SP-GRANITE
TUKTOYAKTUK	19	0.0 - 2.7	0.3	ICE-SM
WHALE COVE	6	0.3 - 0.9	0.5	SM-SW

Pore fluid salinity data for selected communities in the Northwest Territories (Hoeve, 1988)

SECTION 3

DEFORMATION BEHAVIOUR

SECTION 3

DEFORMATION BEHAVIOUR OF FROZEN SOILS

3.1 General

The deformation response of ice and frozen soils to applied loads is time dependent. This time dependent behaviour is often established in uniaxial or triaxial tests on frozen cylinders, as illustrated in Figure 3.1. If the sample is subjected to a constant deviator stress $(\sigma_1-\sigma_3)$ it will deform with time. As indicated in Figure 3.1, the time-dependent deformation curve can be considered to consist of four components.

The initial response to load application is some elastic, instantaneous deformation, ϵ_i, as indicated on the figure.

Strain continues after the initial elastic deformation, as shown, except at a decreasing rate. This phase is termed primary creep, ϵ_p.

The rate of strain will continue to decrease until an inflection point is reached at point B, after which the rate of strain will begin to increase. The minimum strain rate will occur at B. For soils under low stress levels (relative to their long term strength) the change in strain rate between points A and C will be small and this portion of the deformation curve can be approximated by a straight line. This straight line portion of the curve is referred to as secondary (or steady state) creep, ϵ_s. For ice or frozen soil which is subjected to a high deviator stress, the secondary creep portion of the curve may be short or non-existent.

At some point in time, the rate of strain will begin to increase dramatically (Point C on the curve) and the sample will enter the tertiary creep phase.

If deformations after the onset of tertiary creep are ignored, the total strain at any time will be:

$$\epsilon_t = \epsilon_i + \epsilon_p + \epsilon_s \qquad (3.1)$$

where

THURBER

ϵ_t denotes the total strain,

ϵ_i denotes the strain due to elastic, (instantaneous) deformations,

ϵ_p denotes the strain due to primary creep, and

ϵ_s denotes the strain due to secondary creep.

3.2 Elastic Deformations

In situations where the applied stress is very low, relative to the strength of the frozen soil or where the duration of the applied load is short (say less than 1 day), creep may not be significant. Deformations may be dominated by the elastic response of the frozen soil, as indicated by Curve 1 on Figure 3.2. The elastic response of ice and frozen soil to applied stress is discussed in Section 4 of the report.

3.3 Primary Creep

If the applied deviator stress is significant, but less than the thawed strength of the frozen soil, then deformations may be dominated by primary creep. Deformations in ice poor soils (which have no excess ice but have some thawed strength) will, in most cases be governed by primary creep. That is, the rate of creep will tend to decrease with time, at least during reasonable durations of load application. This behaviour is represented by Curve 2 on Figure 3.2, and is discussed in more detail in Section 5.

3.4 Secondary Creep

If the applied stress is greater than the long term strength of the frozen soil but less than the short term strength, then total deformations may be dominated by secondary creep. This situation occurs in ice and ice rich soils for which the long term (thawed strength) is zero. Curve 3 on Figure 3.2 illustrates a deformation curve where secondary creep is dominant. Secondary creep is discussed in Section 6.

3.5 Strength

Curve 4 on Figure 3.2 illustrates typical deformation behaviour of ice or frozen soil in which the long term

THURBER

strength is exceeded and tertiary creep occurs. The factors which control the strength of ice and frozen soils are discussed in Section 7 of the report.

3.6 Interpretation of Deformation Response

While it is convenient to discuss the deformation behaviour of ice and frozen soil within the context of elastic deformations, primary creep and secondary creep, it should be understood that the deformation behaviour of these materials actually involves a gradual transition from one stage to the next. In addition, there is no fixed definition for "short term", "long term" or "very long term", nor for "very dense", "ice poor" and "ice rich" soils. These vaguely defined terms can lead to misunderstanding and disagreement between researchers as to the most appropriate method of interpreting test data or predicting the response of ice and frozen soils. It is important, therefore, that the designer understand the time dependent behaviour of ice and frozen soil and apply a consistent deformation model and data set to his particular problem.

Creep testing of frozen soils is difficult and time consuming. Long periods of time may elapse before primary creep ends and secondary creep begins. This was recognized by Roggensack (1977) and supported by Sego and Morgenstern (1983) who found that when low stresses were applied to pure ice, primary creep continued over a period of more than 1.5 years. Both temperature and stresses must be carefully controlled throughout primary and secondary creep in order to obtain meaningful results.

Deformations due to processes not strictly associated with creep can complicate the interpretation of laboratory test data. Deformations may be due to consolidation (particularly in soils with significant unfrozen water content) or due to shear strains along discontinuities within the material.

The deformation theories outlined in the following sections assume that the ice or frozen soil is homogeneous and isotopic. They also assume that excess ice is uniformly distributed throughout the frozen soil. Most natural permafrost does not, of course meet these assumptions. Soil composition, temperature, ice content and density can all vary significantly over short distances. Excess ice is usually presented in the form of segregated ice lenses which are randomly oriented. All of these factors must be accounted for by the designer in assessing the deformation response of the soils.

THURBER

DEFORMATION BEHAVIOUR OF FROZEN SOILS

LIST OF FIGURES

THURBER

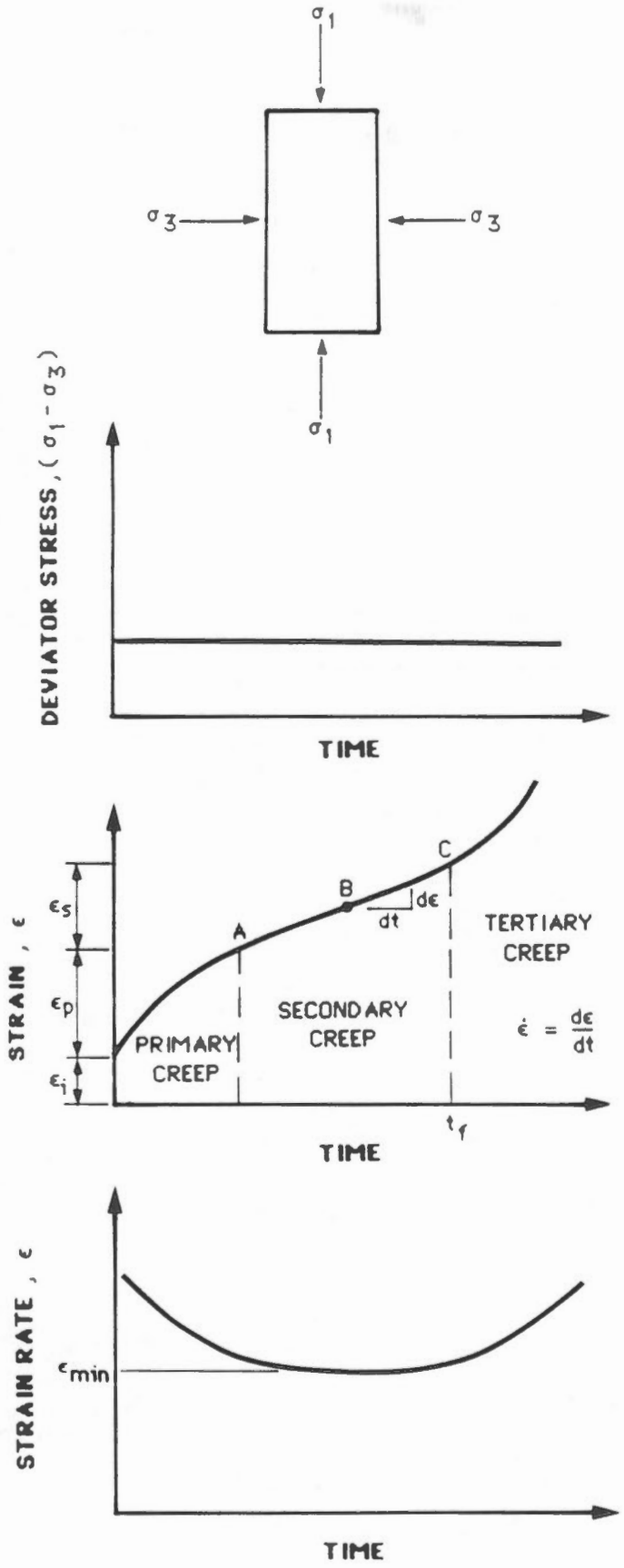

Idealized time dependent deformation behaviour of ice and frozen soils.

FIGURE 3.1

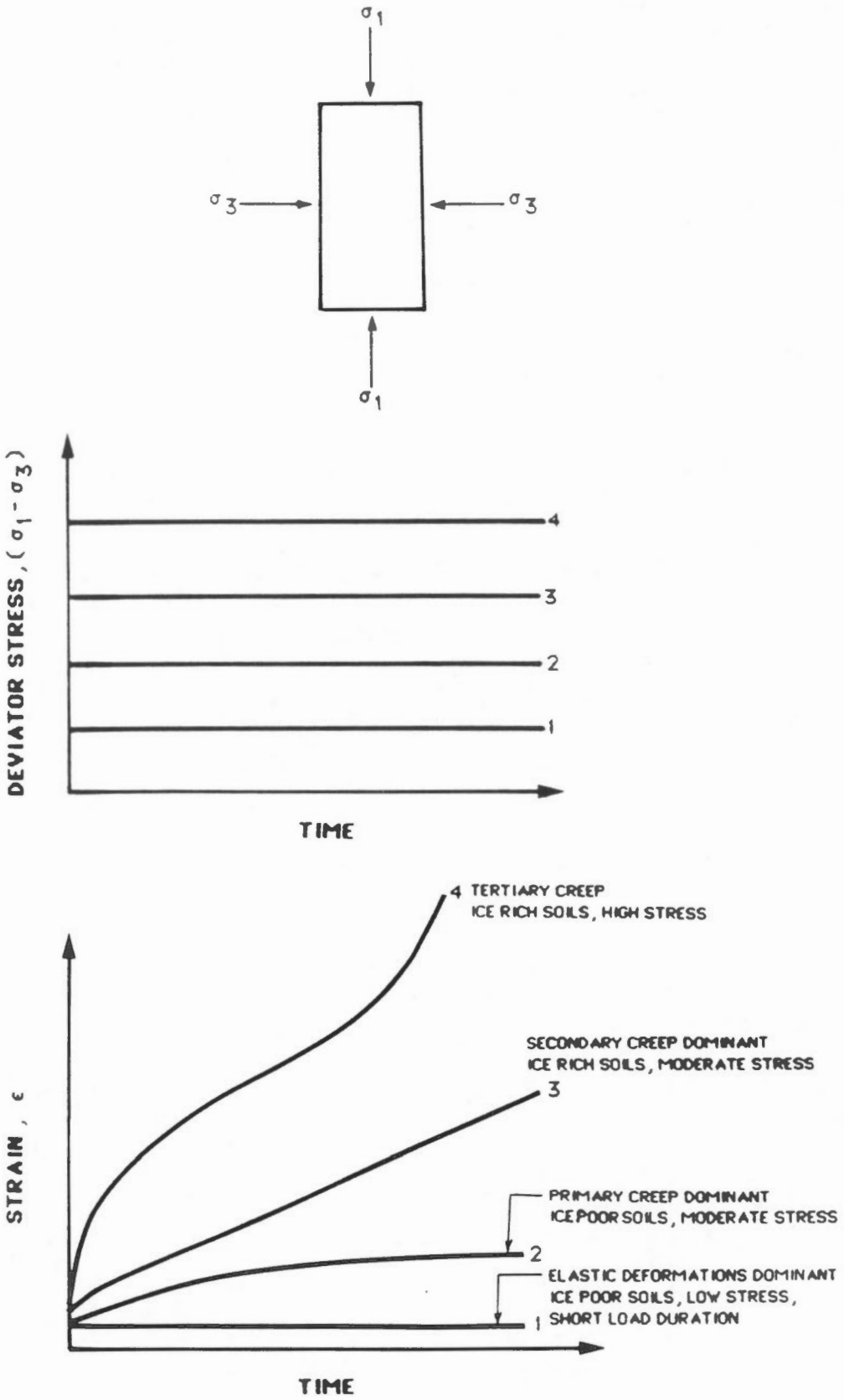

Effect of stress level on the time dependent deformation behaviour of ice and frozen soils.

FIGURE 3.2

SECTION 4

ELASTIC DEFORMATIONS

SECTION 4

ELASTIC DEFORMATIONS

4.1 General

As mentioned in Section 3, elastic deformations will often dominate total deformations in situations where the applied stress is low, relative to the strength of the ice or frozen soil, or where the duration of the applied load is not more than several days.

For some design applications, therefore, it is reasonable to assume that the frozen soil behaves as a nonlinear elastic material, and hence its deformation behaviour can be interpreted within the framework of conventional nonlinear elastic theory.

The elastic properties of frozen soils are usually established in the laboratory through uniaxial or triaxial tests on frozen cylinders. A sketch of a typical triaxial test configuration is shown in Figure 4.1. The sample is loaded, at a constant rate of displacement, and the load response is measured. The rate of displacement is selected such that the sample fails in a period of several minutes or hours. The deviator stress is plotted as a function of strain as shown on the figure.

Young's Modulus is defined as the slope of the stress-strain curve as follows:

$$E = \frac{\sigma_1 - \sigma_3}{\epsilon_z} \qquad (4.1)$$

where

E denotes Young's Modulus

$\sigma_1 - \sigma_3$ denotes the deviator stress, and

ϵ_z denotes the strain in the direction of the applied stress.

It should be noted that for unfrozen soils, the stresses would normally be expressed as effective stresses (total stress minus the pore pressure). In frozen soils and ice the stresses would normally be expressed in terms of total stresses since there is no pore fluid. However, where significant unfrozen water is present within the

THURBER

frozen soil (such as for soils with saline pore water or nonsaline soils at temperatures between about 0 and -2°C) it might be appropriate to consider the effect of pore water pressures and interpret the test results in terms of effective stress.

The volume change response of a material to the applied stresses can be determined from a uniaxial or triaxial compression test, through Poisson's Ratio, which is defined as follows:

$$\mu = - \frac{\epsilon_r}{\epsilon_a} \qquad (4.2)$$

where

μ denotes Poisson's Ratio, and

ϵ_r denotes radial strain.

For materials which are perfectly incompressible (no volume change when deviator stress is applied) Poisson's Ratio will have a value of 0.5. For materials which are perfectly compressible, Poisson's Ratio will be 0. Most solids have values which lie within this range.

Uniaxial or triaxial compression induces both shear and volumetric strains in an elastic material. The shear strain is due to the shear stress while the volumetric strain is due to the mean normal stress. For some types of analyses it is more convenient to express the elastic properties of the material in terms of the shear modulus, G (which is the ratio of the shear stress to the shear strain) and the bulk modulus, B (which is the ratio of the mean normal stress to the volumetric strain). The theoretical relationship between G, B, E and μ for elastic materials is given by the following equations:

$$G = \frac{E}{2(1+\mu)} \qquad (4.3)$$

$$B = \frac{E}{3(1-2\mu)} \qquad (4.4)$$

For most soils, the elastic properties are determined by carrying out compression tests. However, for materials

THURBER

which exhibit significant tensile strength (such as frozen soils or ice) the elastic properties can also be determined from uniaxial tension tests.

The range in Young's Modulus and Poisson's Ratio for selected materials are indicated on Figure 4.2. Young's Modulus for frozen soil is seen to be in the same order of magnitude as sandstone or shale.

The elastic properties of frozen soils are known to be a function of the following variables:

- Strain magnitude,
- Strain rate,
- Confining stress,
- Temperature,
- Soil type,
- Ice content, and
- Unfrozen water content.

The effect which these variables have on Young's Modulus are discussed in the following sections. Only limited data with respect to Poisson's Ratio was found in the literature. Data reported by Tsytovich (1975) is presented in Figure 4.3. The effect which the variables listed above have on Poisson's Ratio are discussed only where data is available with respect to the effect of the variable on Poisson's Ratio.

4.2 Strain Magnitude

As shown in Figure 4.4, the stress-strain curve for most materials is nonlinear. That is, the modulus of elasticity (the slope of the stress-strain curve) tends to decrease as the magnitude of the strain increases and the peak deviator stress is approached.

As indicated on Figure 4.4, Young's Modulus can be defined in a number of ways. The initial tangent modulus, E_i is the slope of the initial portion of the stress strain curve. The secant modulus, E_s is the slope to any inside point on the curve, and the tangent modulus, E_t is the slope of the stress strain curve at any level of stress (or strain).

Two other types of modulus are occasionally encountered in the literature. The 50% strength modulus, E_{50}, is defined as the tangent modulus at 50% of the maximum deviator stress. This modulus is useful because it can be established more reliably from stress-strain data than the

THURBER

initial tangent modulus and it can be empirically correlated to the initial tangent modulus (Yuanlin and Carbee, 1983). The unloading modulus, E_u, can be calculated from the slope of an unloading curve. It tends to be higher than the initial tangent modulus and eliminates inaccuracies due to seating.

The elastic moduli as measured on laboratory specimens is often lower than that observed in the field, as a result of sample disturbance. A common method of overcoming this problem and obtaining representative field values for Young's Modulus for use in design is to apply a cyclic load to the sample until a constant value of the modulus is obtained over the stress range expected to be encountered in the field. As illustrated on Figure 4.5, the modulus values obtained from cyclic load tests will be higher than values obtained from the primary stress-strain curve.

Very high values of Young's Modulus will be obtained from acoustic response tests of ice and frozen soil, because the strains applied in acoustic tests are very much smaller than those encountered in conventional uniaxial or triaxial compression testing.

All of the various elastic moduli provide an indication of the stiffness of the material, the higher the modulus, the stiffer the material. The different types of moduli are often referred to collectively as the stiffness or deformation moduli.

As indicated in the foregoing discussion, it is important that the modulus values selected for design be consistent with the sequence of loading and the range in stress changes which are expected to occur in the field.

4.3 Strain Rate

It has been found that for ice and frozen soils, if the rate of strain applied to the sample is increased, Young's Modulus will also increase. This effect is illustrated on Figure 4.6.

The effect of strain rate on the initial tangent modulus is summarized in Figure 4.7. The figure summarizes values for the initial tangent modulus over a range of strain rates, temperatures and soil types, as reported by a number of researchers as noted. The data indicates that the initial tangent modulus generally increases with increasing strain rate, however, the influence of strain rate is not significant in comparison with other variables such as soil type and temperature.

THURBER

Tests on frozen Fairbanks Silt by Yuanlin and Carbee (1983) provide some additional information regarding the effect of strain rate on elastic response. They report that while the initial tangent modulus is practically insensitive to strain rate, the 50% strength modulus was found to generally increase with increasing strain rate. Their test data are summarized on Figure 4.8, and while the trends discussed by these researchers are apparent, there is considerable scatter to the data.

4.4 Confining Stress

The influence of confining stress on the initial Young's Modulus can be evaluated from data on tests carried out by a number of researchers.

Sayles (1973) reported the results of a number of triaxial tests on samples of frozen Ottawa Sand at various confining stresses and at a constant temperature of -3.85°C. The results of tests carried out at a strain rate of 0.5/min are shown in the upper half of Figure 4.9. A second series of tests carried out at a much slower strain rate of 0.03/min are shown in the lower half of Figure 4.9. The initial tangent moduli have been calculated from the tests carried out at a strain rate of 0.5/min and are as follows:

Confining Pressure (kPa)	E_i (GN/m^2)
689	5.5
1380	5.3
2760	18
5510	13
8270	18

These results indicate that the initial tangent modulus generally increases as confining stress is increased. A similar trend is apparent in the second series of tests reported by Sayles, at the slower strain rate (0.03/min), as shown on Figure 4.9. It was not possible to calculate Young's Modulus accurately from most of these latter curves, however, because the strain scale is too small.

The confining stresses used in the tests carried out by Sayles are significantly higher (689 to 8270 kPa) than those normally encountered in geotechnical engineering

THURBER

practice (0 to 500 kPa). It is of interest, therefore to examine the effect of confining stress on Young's Modulus at lower levels of confining stress.

Tsytovich (1975) has reported the initial tangent modulus values from tests on sand (w = 16 to 20%) at two different confining pressures, 100 and 300 kPa, as follows:

Temperature °C	E_i at Confining Stress 100 kPa	300 kPa	Change %
-0.5	1.3 GN/m²	0.8 GN/m²	-40
-2.1	7.0 GN/m²	4.4 GN/m²	-37
-10.0	19.6 GN/m²	18.6 GN/m²	-5

The modulus values from Tsytovich are of the same order as those from Sayles but Tsytovich's data indicates that Young's Modulus for sand apparently decreases with increasing confining pressure. This trend does not appear reasonable and it is speculated that the apparent differences measured in these tests reflect small variations in sample density, which may override the effects of confining stress.

Parmeswaran and Jones (1981) reported the results of a series of triaxial compression tests on frozen Ottawa Sand at a temperature of about -10°C. The initial tangent modulus has been plotted as a function of confining stress as shown on Figure 4.10. It is clear from this data that for sand at this temperature, the initial tangent modulus is unaffected by confining stress.

The limited data reviewed here indicates that within the range of stresses normally encountered in civil engineering projects, and provided the soil does not contain a significant unfrozen water content, confining stress will not have a significant effect on Young's modulus.

4.5 Temperature

The effect of temperature on Young's Modulus for a variety of soil types is summarized on Figure 4.11. As indicated on the figure, Young's Modulus is influenced by both the soil type and strain rate. Values for Young's Modulus are highest for the confined cyclic tests, and generally decrease with decreasing strain rate as discussed earlier.

For all soil types, however, there is a clear trend of increasing Young's Modulus as temperature decreases.

THURBER

4.6 Soil Type

The results presented in Figure 4.7 and 4.11 indicate that the deformation modulus will be a function of soil type. For the same temperature or strain rate, Young's Modulus will be higher for coarse grained soils such as sands, as compared to fine grained soils such as clays.

The difference in the stress-strain response of sands and clays is dramatically illustrated in Figure 4.12 (Andersland et al, 1978). It will be noted, however, that in these tests, the initial tangent modulus, E_i, could be interpreted to be almost the same for both the sand and the clay.

Tsytovich (1975) summarizes the moduli for various soils as measured in confined cyclic tests as follows:

Soil	E_i (GN/m²)	T (°C)	σ_3 (kPa)	w (%)
Sand	3.7	-1.5	200	19
Silt	2.8	-1.5	200	30
Clay	0.7	-1.5	200	55
Ice	2.4	-1.5	200	100

The modulus for frozen clay is less than that of ice whereas the moduli for frozen sand and silt are greater than that for ice. The reduced stiffness of clays is primarily due to the high unfrozen water content in this soil type as compared to silts and sands. In addition, however, the soil skeleton in clays is generally less stiff than for silts and sands.

4.7 Ice Content

Alkire and Andersland (1973) carried out a series of tests on Ottawa Sand at different void ratios and at a temperature of -12.0°C. The stress-strain curves from these tests are shown in the lower half of Figure 4.13. The initial tangent moduli are seen to decrease as void ratio (ice content) increases. It would be of interest to compare the stress-strain curve of pure ice at the same temperature and strain rate as was used for these tests on sand, however such data is not reported.

Alkire, (1972) investigated the effect which the degree of ice saturation has on the stress-strain behaviour of frozen sand. These test results are presented in the upper

THURBER

half of Figure 4.13. In the two unconfined tests, the stress-strain curve is seen to be sensitive to the degree of ice saturation. In the two confined tests, the difference between the stress-strain curves is much less significant.

Yuanlin and Carbee (1983), carried out a series of unconfined compression tests on samples of Fairbanks Silt prepared at different dry densities. The 50% strength modulus is plotted as a function of strain rate and dry density on Figure 4.14. The results are of interest because the 50 percent strength modulus decreases as dry density increases, a result which does not seem reasonable. The authors do not discuss this unexpected trend in their paper. It is speculated that as the dry density increases, the proportion of unfrozen pore water in the frozen soil increases, resulting in decreased stiffness of the material. This hypothesis cannot be confirmed because the unfrozen water content - dry density relationship was not reported.

4.8 Unfrozen Water Content

It can be expected that as unfrozen water content increases, Young's Modulus will decrease in frozen soils. The unfrozen water content will increase as pore fluid salinity increases or as clay content increases.

As indicated on Figures 4.7, 4.11, and 4.12, the stiffness moduli of clay soils are generally much lower than the corresponding moduli for silts and sands. As mentioned earlier, the reduced stiffness of clay soils is primarily due to the presence of unfrozen water within the frozen soil. No quantitative data correlating unfrozen water content to the deformation modulus was found in the literature.

Baker and Kurfurst (1985) carried out a series of tests to establish the relationship between pore fluid salinity and the elastic behaviour of reconstituted samples of frozen sand. Young's Modulus and Poisson's Ratio were calculated from acoustic velocities measured on samples over a range of temperatures and pore fluid salinities. These results are presented in the lower half of Figure 4.15.

Young's Modulus is seen to decrease dramatically as pore fluid salinities increase from 0 to 5.0 parts per thousand (ppt). The decrease continues as salinity increases to 40 ppt, however the change in Young's Modulus with increasing salinity is not as significant. It should

THURBER

be noted that the relatively high values of Young's Modulus measured in these tests are due to the very low strain magnitudes achieved in acoustic tests.

The insensitivity of Poisson's Ratio to changes in pore fluid salinity is also indicated by the data shown on the upper half of Figure 4.15.

Sego et al (1982) reported the results of a series of unconfined compression tests (at various applied displacement rates) on reconstituted samples of sand in which pore fluid salinities were varied from 0 to 100 ppt. The secant Young's Modulus at failure was calculated from the data. The variation in secant Young's Modulus at failure with pore fluid salinity is shown on Figure 4.16. Pore fluid salinity (and by inference unfrozen water content) is seen to have a very significant effect on the secant Young's Modulus.

4.9 Summary

The significant factors which affect the short term deformation behaviour of frozen soils have been identified by researchers and a reasonable body of data is available in the literature concerning the elastic properties of ice and frozen soil.

The available information indicates that the elastic moduli of ice and frozen soils is affected significantly by strain magnitude, temperature, soil type and unfrozen water content. Strain rate, confining stress and ice content do not have a major influence on the elastic response of the materials.

The data currently available with respect to the elastic behaviour of ice and frozen soil is probably adequate for most design problems for a number of reasons. First of all, most frozen soils are considerably stiffer than unfrozen soils and hence the elastic response of frozen soils is of less concern for the range of loads commonly encountered in geotechnical engineering practice.

Secondly, for many geotechnical design problems, loads are imposed for periods of more than several days. It is therefore essential to incorporate the time dependent deformation behaviour of ice and frozen soils into the deformation analysis. Consequently, past research has, quite correctly, been concentrated on investigations into the time dependent deformations of ice and frozen soil, which are typically much greater than the short term (elastic) deformations.

ELASTIC DEFORMATIONS

LIST OF REFERENCES

AlNouri, I., 1969. Time-dependant strength behaviour of two soil types at lowered temperatures. Unpublished Ph.D. Thesis, Michigan State University, East Lansing.

Andersland, O.B., Sayles, F.H., and Ladanyi, B., 1978. Mechanical Properties of Frozen Ground. Chapter 5 in Andersland, O.B., and Anderson, D.M. Geotechnical Engineering for Cold Regions. McGraw-Hill, 566 p.

Baker, T.H.W., and Kurfurst, P.J., 1985. Acoustic and mechanical properties of frozen sand. Proceedings of the Fourth International Symposium on Ground Freezing. August 5-7, Sapporo, Japan. pp. 227-234.

Hawkes, I. and Mellor, M., 1972. Deformation and fracture of ice under uniaxial stress. Journal of Glaciology, Vol. 11 (61), pp. 103-131.

Haynes, F.D., 1978. Strength and deformation of frozen silt. Proceedings of the Third International Conference on Permafrost. July 10-13, Edmonton, Canada, pp. 656-661.

Hunt, R.E., 1984. Geotechnical Engineering Investigation Manual. McGraw-Hill, 983 p.

MacFarlane, I.C., 1968. Strength and deformation tests on frozen peat. Proceedings of the Third International Peat Congress. August 18-23, Quebec, Canada. pp. 143-149.

Parmeswaran, V.R., 1980. Deformation behaviour and strength of frozen sand. Canadian Geotechnical Journal, Vol. 17, pp. 74-88.

Parmeswaran, V.R., and Jones, S.J., 1981. Triaxial testing of frozen sand. Journal of Glaciology, Vol. 27 (95) pp. 147-156.

Parmeswaran, V.R., and Roy, M., 1982. Strength and deformation of frozen saturated sand at -30°C. Canadian Geotechnical Journal, Vol. 19, pp. 104-107.

THURBER

LIST OF REFERENCES
(continued)

Sayles, F.H., 1973. Triaxial and creep tests on frozen Ottawa Sand in Permafrost: The North American contribution to the Second International Conference on Permafrost. July 13-28, Yakutsk, U.S.S.R., pp. 384-391.

Sego, D.C., and Morgenstern, N.R., 1983. Deformation of ice under low stress. Canadian Geotechnical Journal, Vol. 20, pp. 587-602.

Sego, D.C., Shultz, T. and Banasch, R., 1982. Strength and deformation behaviour of frozen saline sand. Proceedings of the Third International Symposium on Ground Freezing, June 22-24, Hanover, U.S.A., pp. 11-18.

Togrol, E., and Ersoy, T., 1977. Stress-deformation characteristics of a frozen soil.

Tsytovich, N.A., 1973. The mechanics of frozen ground. McGraw-Hill, 426 p.

Yuanlin, Z. and Carbee, D.L., 1983. Uniaxial compressive strength of frozen soil under constant deformation rates. Cold Regions Science and Technology, Vol. 9, pp. 3-15.

Yuanlin, Z., and Carbee, D.L., 1985. Strain rate effect on the tensile strength of frozen silt. Proceedings of the Fourth International Symposium on Ground Freezing. August 5-7, Sapporo, Japan., pp. 153-157.

THURBER

LIST OF FIGURES

THURBER

LIST OF FIGURES
(continued)

THURBER

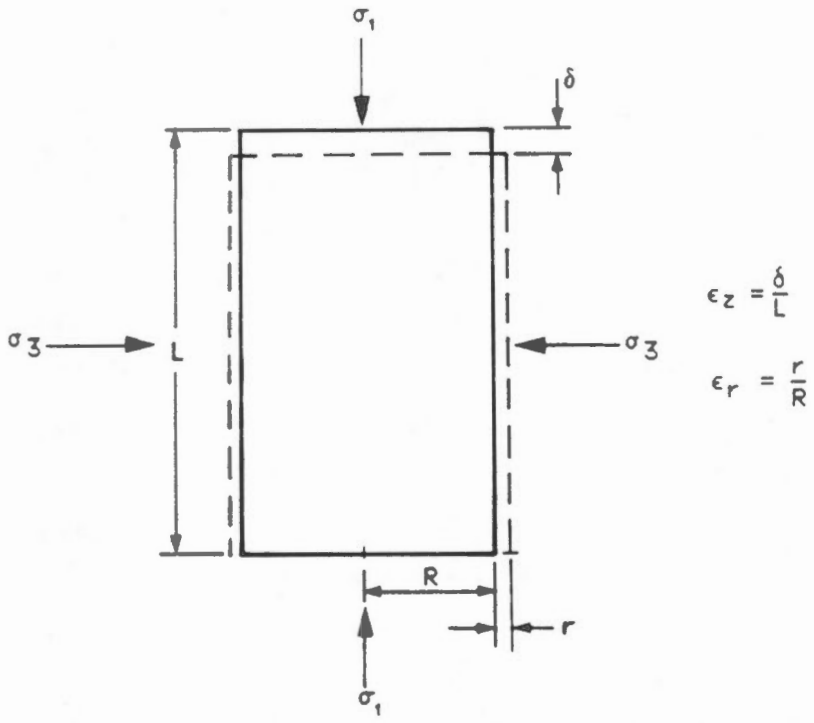

YOUNG'S MODULUS $E = \frac{(\sigma_1 - \sigma_3)}{\epsilon_z}$

POISSON'S RATIO $\mu = -\frac{\epsilon_r}{\epsilon_z}$

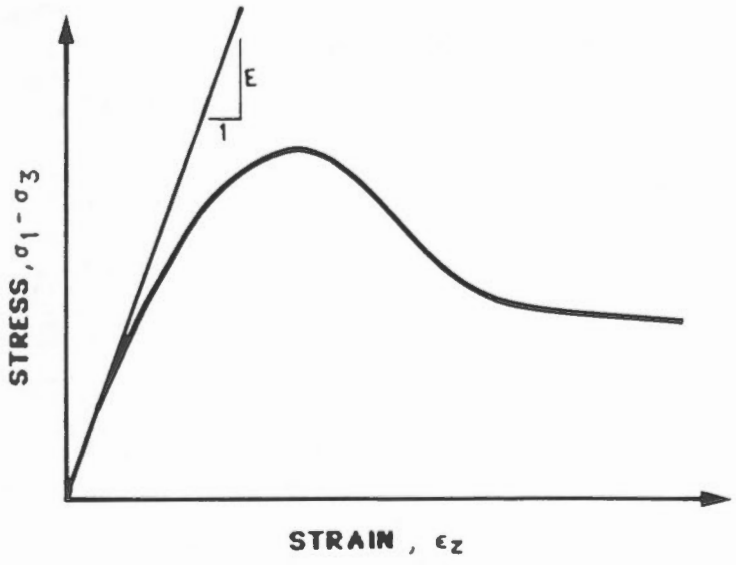

Idealized uniaxial compression.

FIGURE 4 1

Material	Young's Modulus, E (GN/m^2)	Poisson's Ratio, μ	Source
Steel	210	0.28 - 0.29	Table 3.33, Hunt (1984)
Concrete	20-30	0.15 - 0.25	Table 3.33, Hunt (1984)
Granite	27-48	0.25 - 0.33	Table 3.26, Hunt (1984)
Sandstone	7-20	0.25 - 0.33	Table 3.26, Hunt (1984)
Dense Sand	0.05-0.08	0.3 - 0.4	Table 3.33, Hunt (1984)
Loose Sand	0.01-0.03	0.2 - 0.35	Table 3.33, Hunt (1984)
Shale	3-14	0.25 - 0.30	Table 3.26, Hunt (1984)
Hard Clay	0.008-0.02	0.4 - 0.5	Table 3.33, Hunt (1984)
Soft Clay	0.002-0.004	0.4 - 0.5	Table 3.33, Hunt (1984)
Frozen Peat[2]	0.08-0.4	-	Figure 5, MacFarlane (1968)
Frozen Sand[1]	3	0.1 - 0.4	Figure 96, Tsytovich (1975)
Frozen Silt[1]	2	0.1 - 0.4	Figure 96, Tsytovich (1975)
Frozen Clay[1]	1	0.3 - 0.5	Figure 96, Tsytovich (1975)
Ice[1]	2.4	-	Page 187, Tsytovich (1975)

Notes: 1) Temperature = -1.5°C, σ_3 = 200 kPa

2) Temperature = -10°C, w = 700% - 1200%, σ_3 = 0

Range in Young's Modulus and Poisson's Ratio for selected materials.

Designation of soil	w,%	θ,°C	σ_3,kPa	Poisson's coefficient,μ
Frozen sand	19.0	-0.2	200	0.41
	19.0	-0.8	600	0.13
Frozen silty loam	28.0	-0.3	150	0.35
	28.0	-0.8	200	0.18
	25.3	-1.5	200	0.14
	28.7	-4.0	600	0.13
Frozen clay	50.1	-0.5	200	0.45
	53.4	-1.7	400	0.35
	54.8	-5.0	1200	0.26

Poisson's Ratio for various frozen soils (after Tsytovich, 1975).

THURBER

FIGURE 4.3

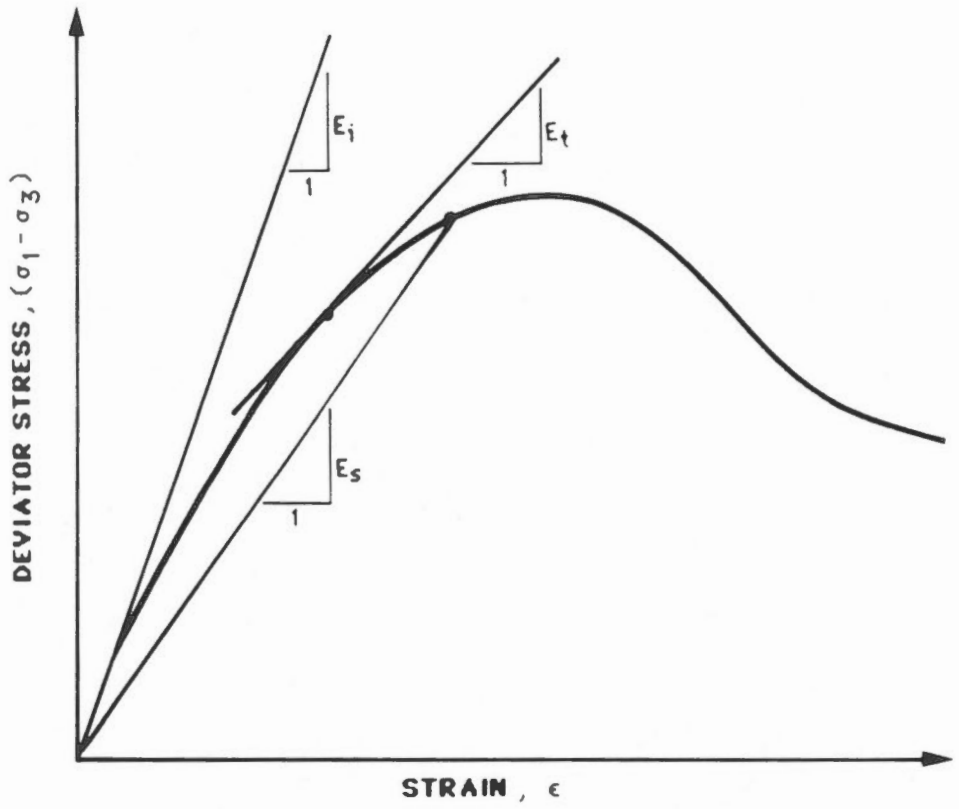

E_i INITIAL TANGENT MODULUS

E_s SECANT MODULUS AT ANY STRESS (OR STRAIN) MAGNITUDE

E_t TANGENT MODULUS AT ANY STRESS (OR STRAIN) MAGNITUDE

The effect of strain magnitude on Young's Modulus.

FIGURE 4 4

THURBER

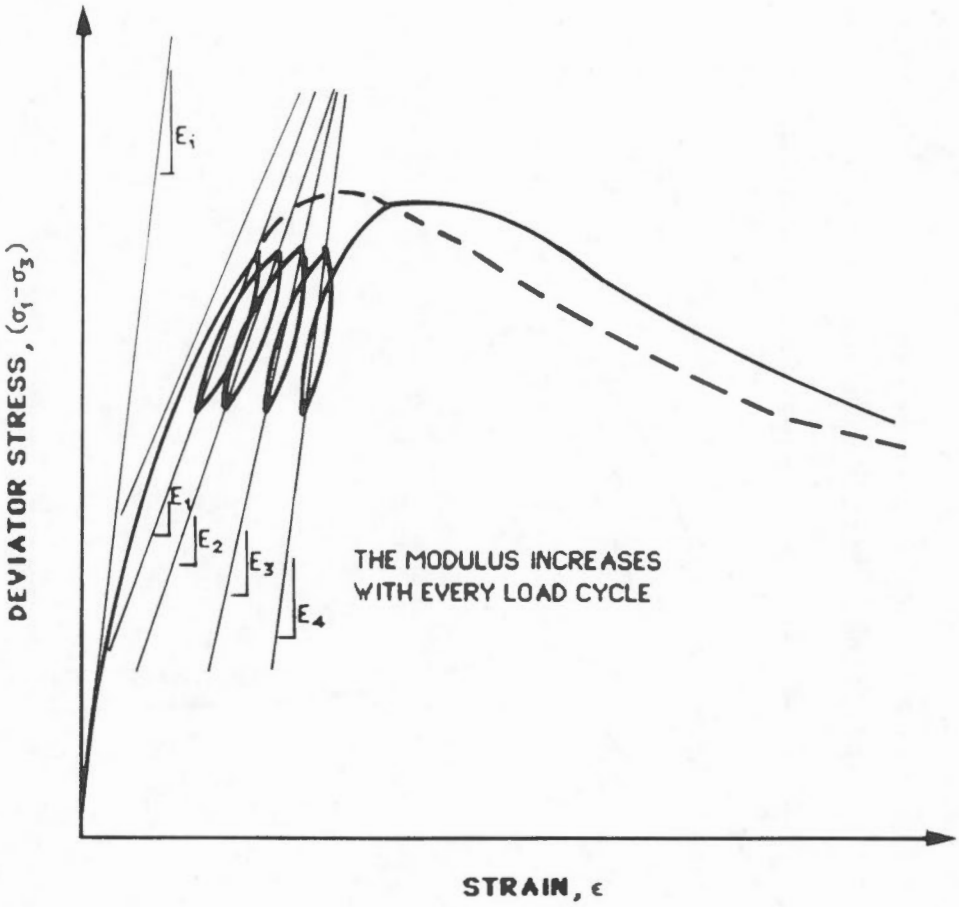

The effect of cyclic loading on Young's Modulus.

THURBER

FIGURE 4.5

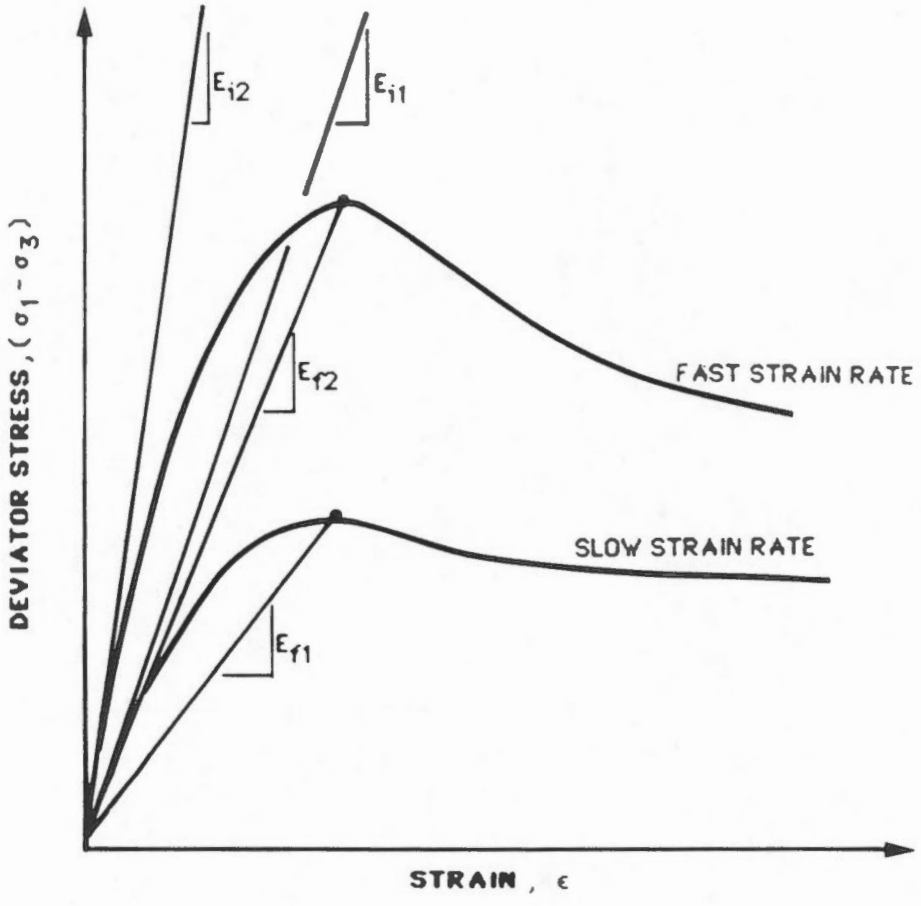

The effect of strain rate on Young's Modulus.

FIGURE 4.6

THURBER

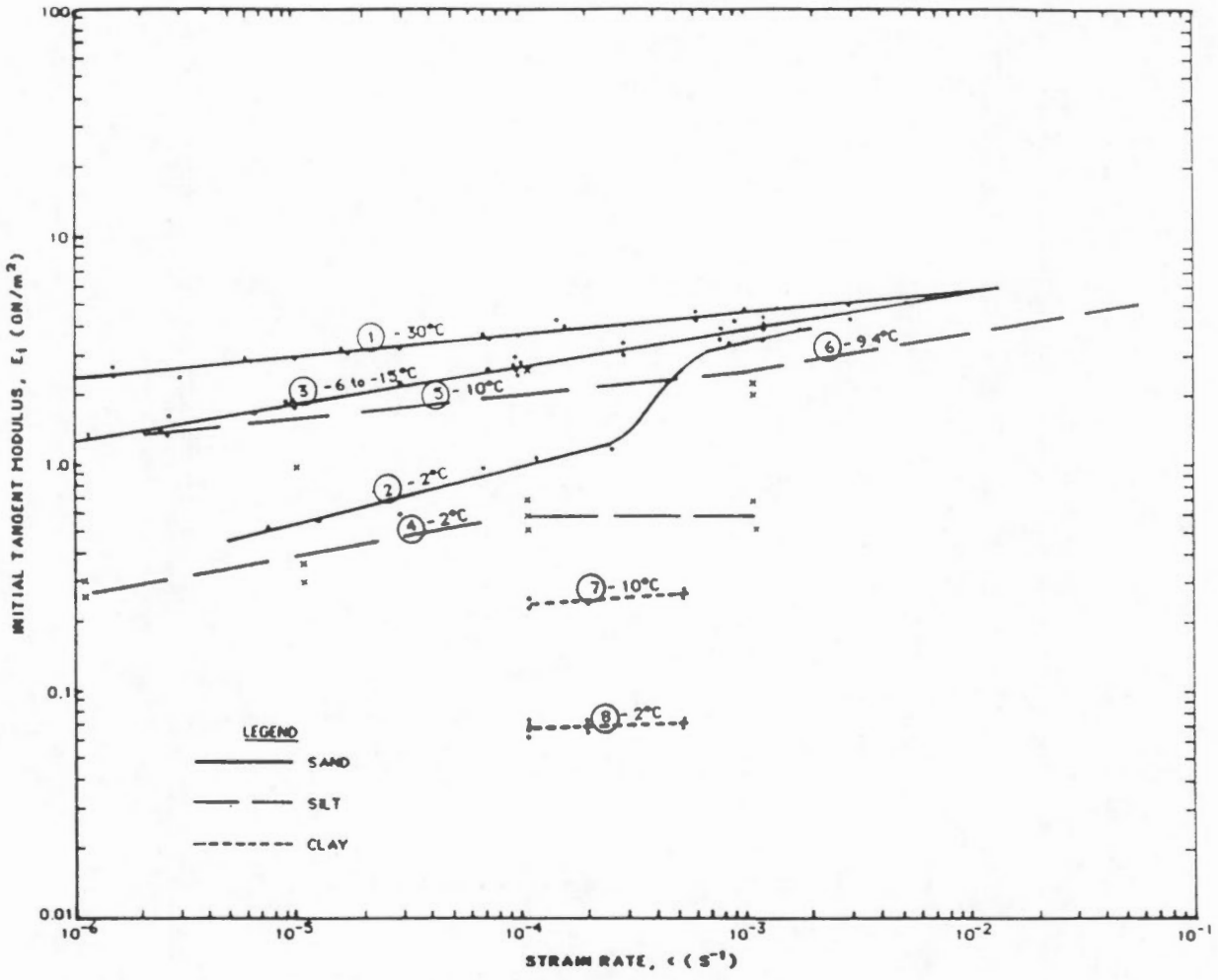

SUMMARY OF SOIL DATA

	SOIL	SOURCE	T (°C)	σ (kPa)	OTHER DATA
①	SAND (Ottawa)	Parmeswaran and Roy 1982	- 30	0	w = 20%
②	SAND1 (Ottawa)	Parmeswaran, 1980	- 2	0	w = 20%
③	SAND2 (Ottawa)	Parmeswaran, 1980	-6 to -15	0	w = 20%
④	SILT 1 (Fairbanks)	Yuanlin and Carbee, 1983	- 2	0	w = 42%, γ_d = 11 8 kN/m^3 LL = 38.4, PL = 34 2
⑤	SILT2 (Fairbanks)	Yuanlin and Carbee, 1983	- 10	0	w = 42%, γ_d = 11 8 kN/m^3 LL = 38.4, PL = 34.2
⑥	SILT	Haynes, 1978	- 9.4	0	w = 30%, e = 0.95, γ_d = 13.9 kN/m^3, γ_b = 18.0 kN/m^3, Tensile and Compression tests
⑦	CLAY1	Togrol and Ersoy, 1977	- 10	200	w = 19, LL = 40 2 , PL = 24 7 16 - 20% fines (< 0.002 mm)
⑧	CLAY 2	Togrol and Ersoy, 1977	- 2	200	w = 19, LL = 40.2 , PL = 24.7 16 - 20% fines (< 0 002 mm)

The effect of strain rate and soil type on the initial tangent modulus.

FIGURE 4.7

THURBER

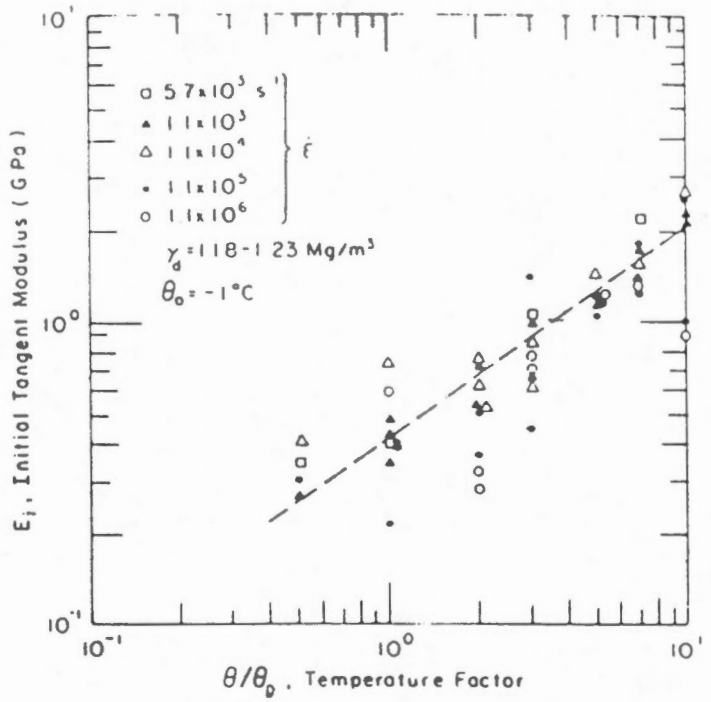

Initial tangent modulus vs. temperature factor in logarithm.

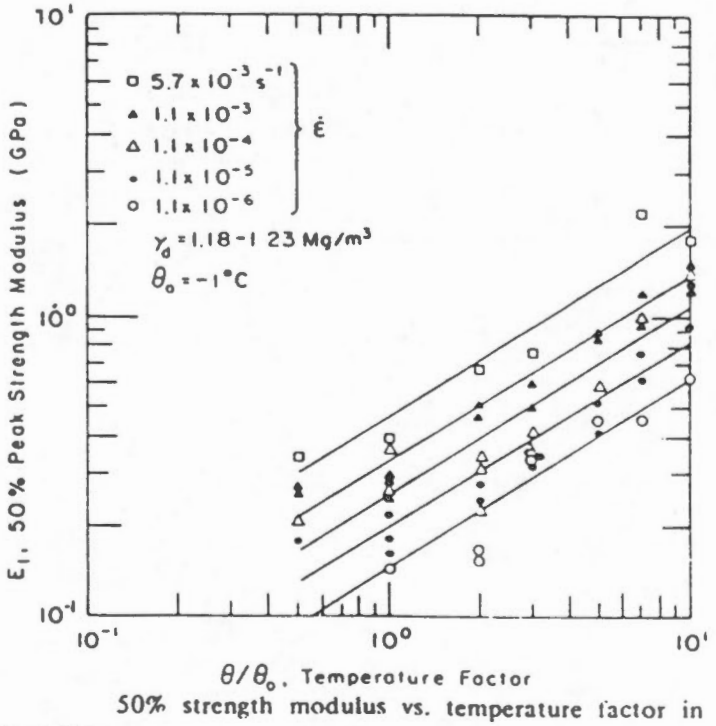

50% strength modulus vs. temperature factor in logarithm.

The effect of strain rate on the initial tangent modulus and the 50% strength modulus of Fairbanks silt (Yuanlin and Carbee, 1983).

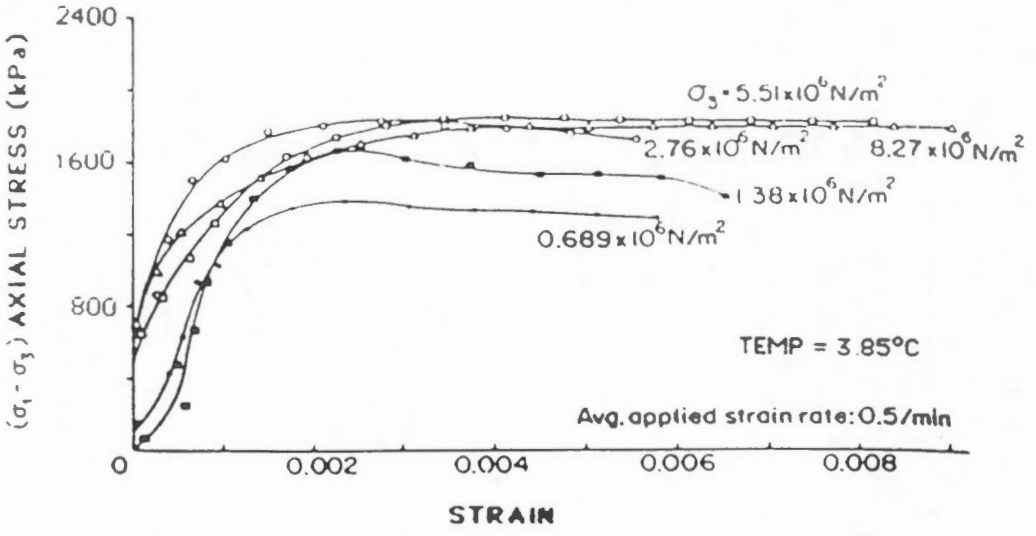

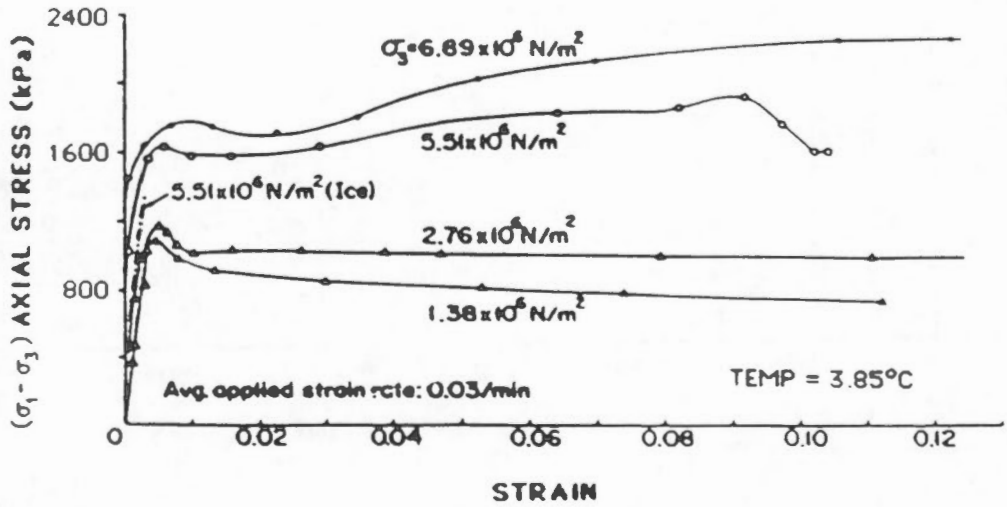

MATERIAL PROPERTIES

γ_d = 16.4 kN/m^3
S = 1
w = 22%
e = 0.59
n = 0.37

The effect of confining stress on the stress-strain behaviour of frozen Ottawa sand (Sayles, 1973).

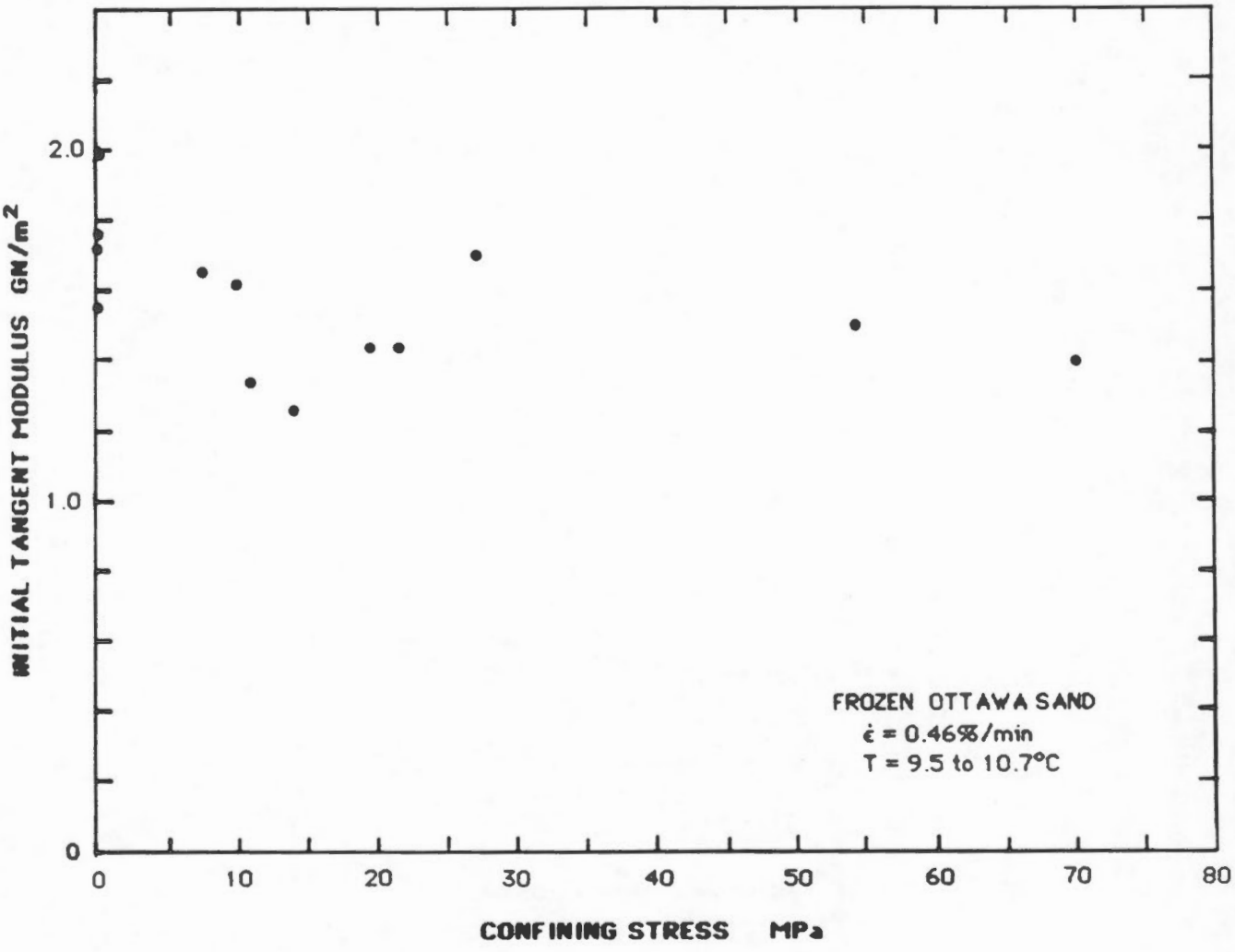

The effect of confining stress on the initial tangent modulus of frozen sand(after Parameswaran and Jones, 1981).

FIGURE 4.10

NO.	SOIL	SOURCE	σ_3 (kPa)	$\dot{\epsilon}$ (%/min)	OTHER DATA
1	SAND	Tystovich, 1975	200	(cyclic)	w = 17 - 19%, 93% > 0.25 mm, 1.4% < 0.05
2	SAND (Ottawa)	Parmeswaran, 1980	0	7.8	w = 20%
3	SILT	Tystovich, 1975	200	(cyclic)	w = 26 - 29%, 35.6% > 0.05 mm, 9.2% < 0.005 mm
4	SILT (Fairbanks)	Haynes, 1978	0	6.6	w = 30%, e = 0.95, γ_d = 13.9 kN/m^3, γ_b = 18.0 kN/m^3
5	SILT (Fairbanks)	Yuanlin and Carbee, 1983	0	6.6	w = 42%, γ_d = 11.8 kN/m^3, LL = 38.4, PL = 34.2
6	CLAY	Tystovich, 1975	200	(cyclic)	w = 47%, 50% < 0.005 mm
7	CLAY	Togrol and Ersoy, 1977	200	1.8	w = ?, LL = 40.2, PL = 24.7 16 - 20% < 0.002 mm

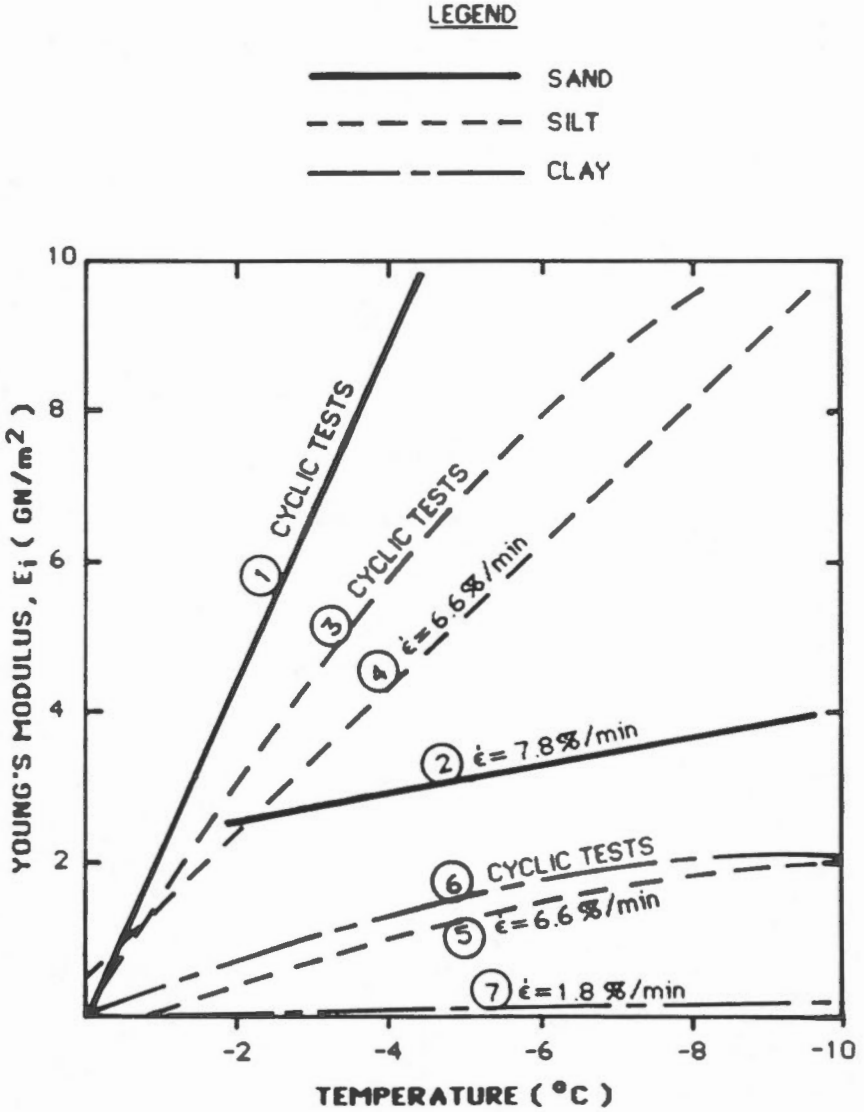

The effect of temperature, soil type and strain rate on Young's Modulus.

THURBER

FIGURE 4.11

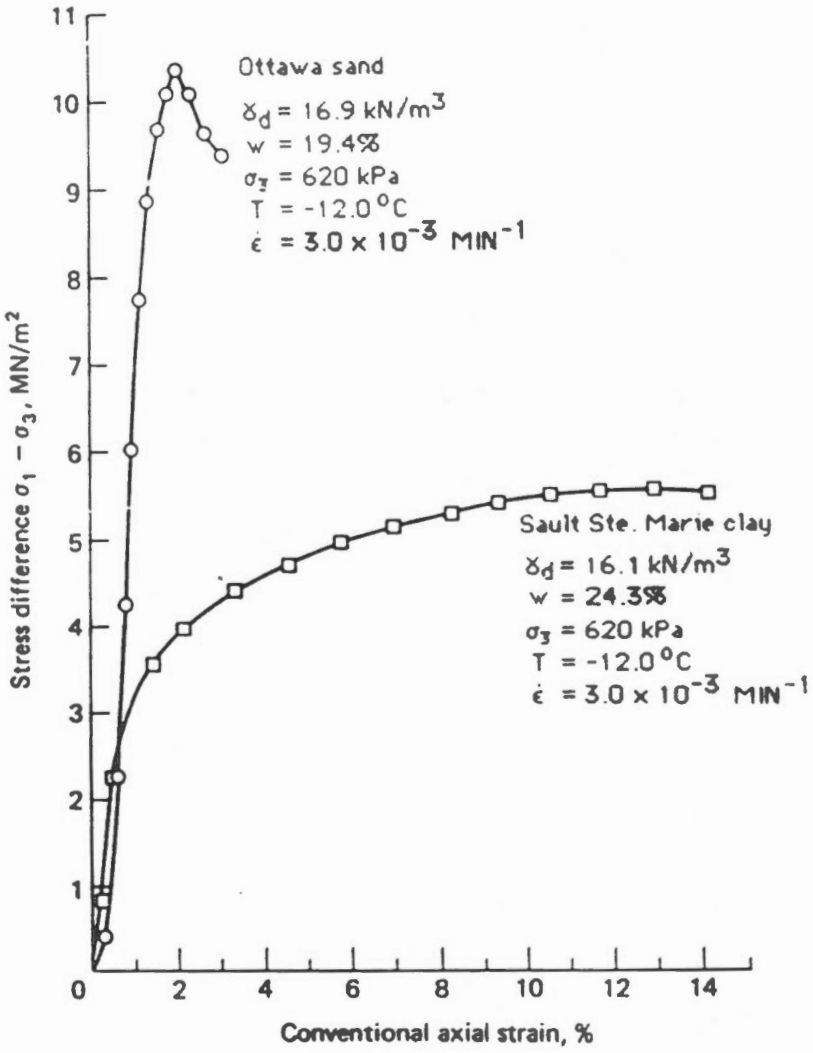

The effect of soil type on stress-strain behaviour (after Andersland et al, 1978).

FIGURE 4.12

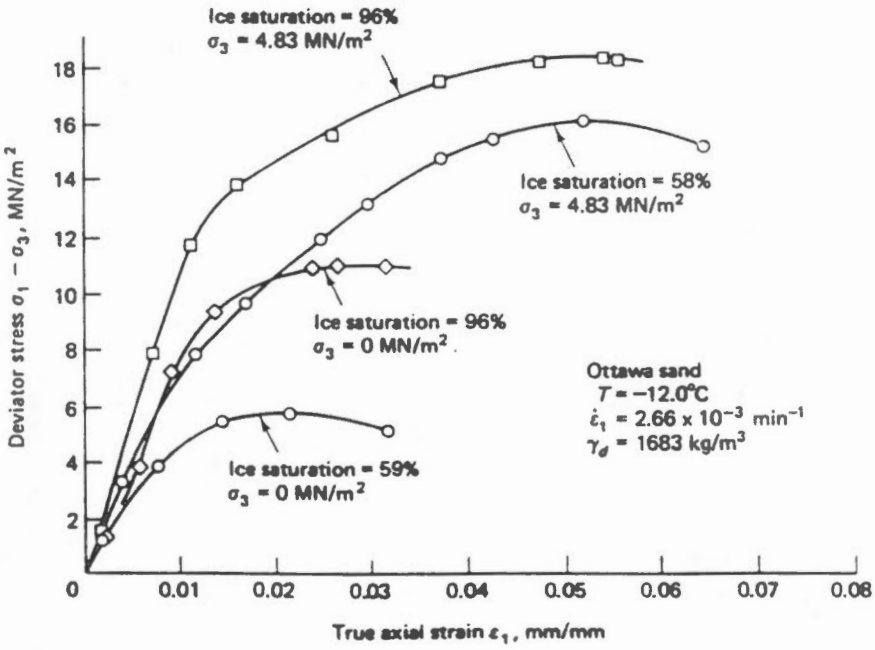

Stress-strain curves for two levels of ice saturation. (*Data from Alkire, 1972.*)

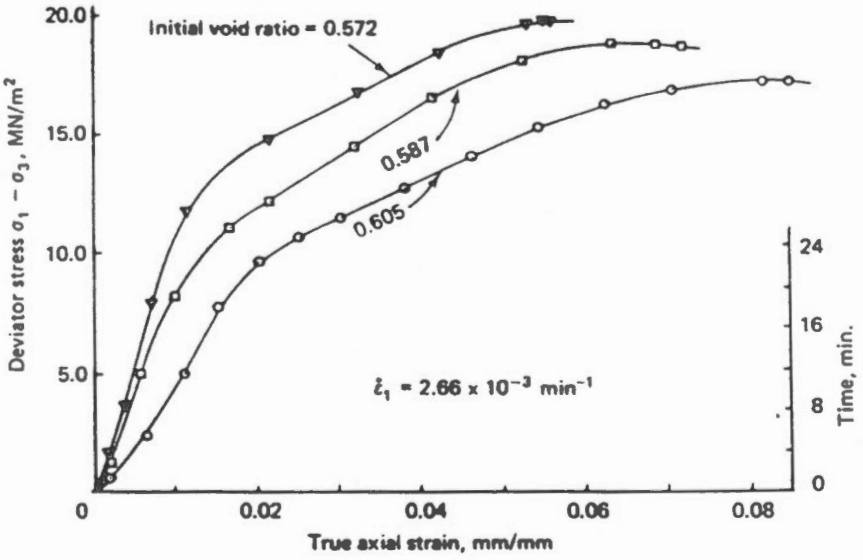

Influence of void ratio on the stress-strain behavior for Ottawa sand; ice saturation ≈97 percent, σ_3 = 4.83 MN/m², T = −12.0°C. (*After Alkire and Andersland, 1973, reproduced from the Journal of Glaciology by permission of the International Glaciological Society.*)

The effect of ice content and ice saturation on the stress-strain behaviour of Ottawa sand (Andersland et al, 1978).

FIGURE 4.13

THURBER

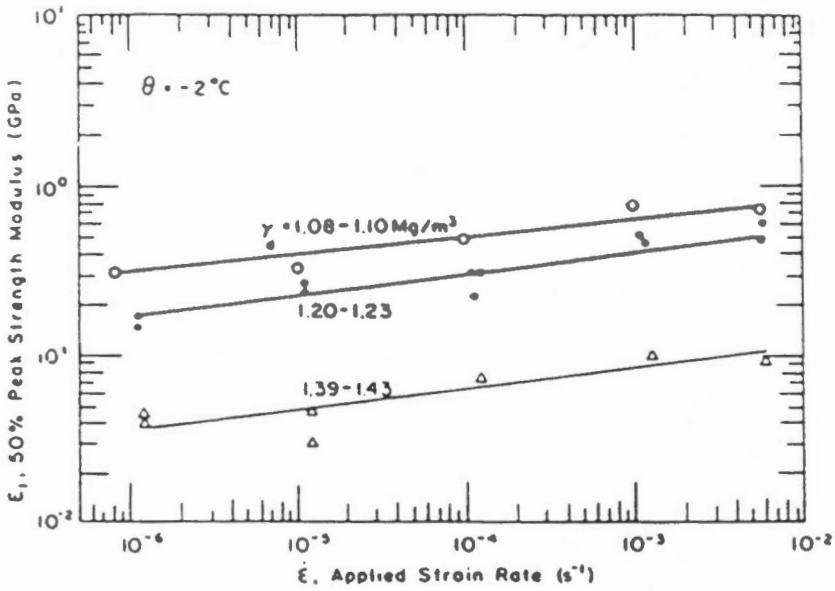

The effect of sample dry density on the 50% strength modulus of Fairbanks silt (Yuanlin and Carbee, 1983).

FIGURE 4.14

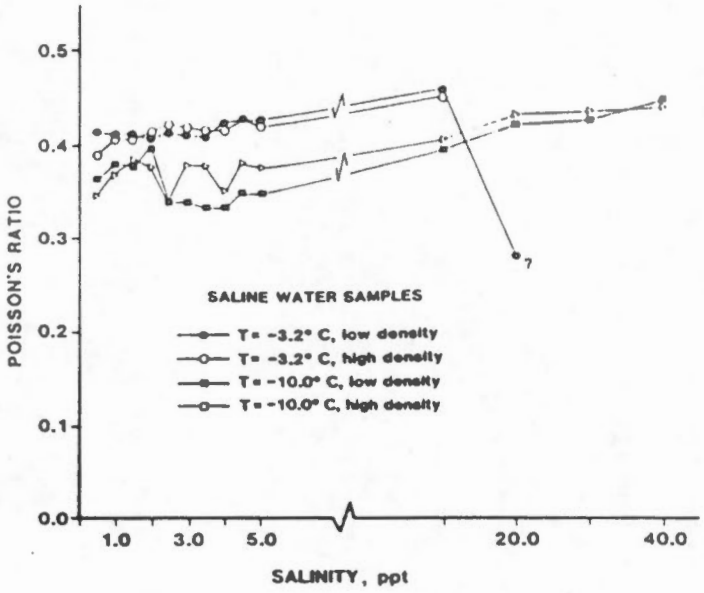

EFFECT OF CHANGING SALINITY ON POISSON'S RATIO

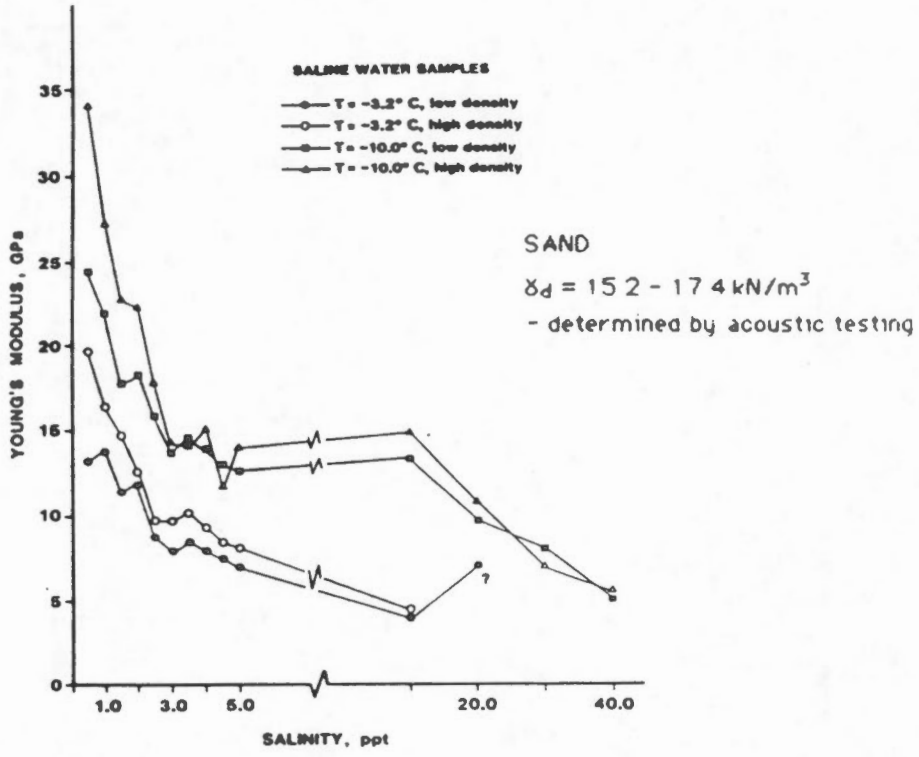

EFFECT OF CHANGING SALINITY ON YOUNG'S MODULUS

The effect of pore water salinity on Young's Modulus and Poisson's Ratio (Baker and Kurfurst, 1985).

THURBER

FIGURE 4.15

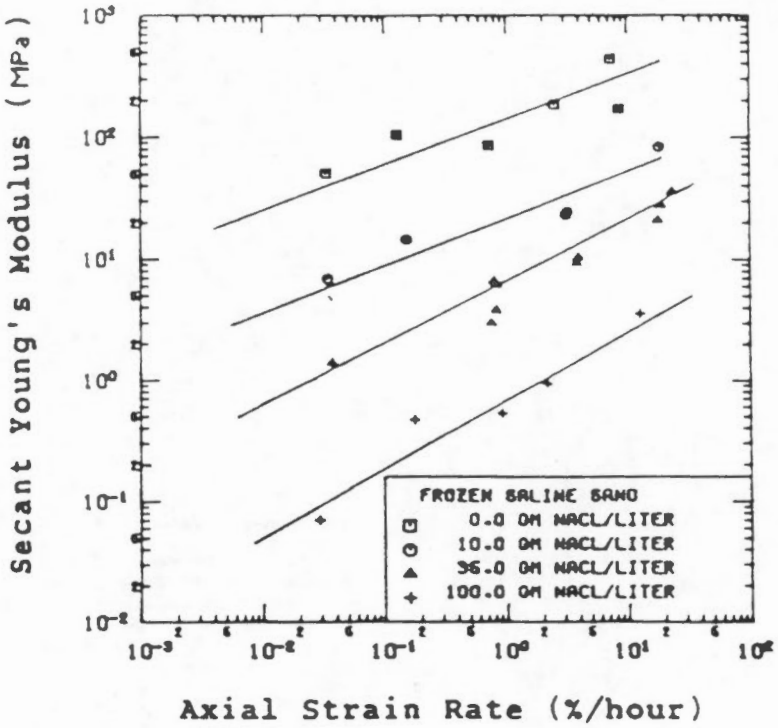

MORTAR SAND

T = -7°C
w = 30%
γ_b = 19.6 kN/m^3
σ_3 = 0
1 gm NaCl/ litre = 1 ppt

The effect of salinity and strain rate on the secant modulus at failure (after Sego et al, 1982).

THURBER

FIGURE 4.16

SECTION 5

PRIMARY CREEP

SECTION 5

PRIMARY CREEP

5.1 General

If the applied deviator stress is significant, but less than the thawed strength of the ice or frozen soil, or if the duration of loading is such that secondary creep is not reached, then deformations will often be dominated by primary creep. Many researchers believe that deformations in ice poor soils (which have no excess ice but have a relatively low thawed strength) will, in most cases be governed by primary creep.

Primary creep behaviour of ice and frozen soil is normally established in constant stress tests as shown on Figure 5.1. As indicated on the figure, primary creep is characterized by a decrease in the rate of strain with time.

Ladanyi (1972, 1983) has proposed the following equation for the calculation of deformations in soils where primary creep is dominant:

$$\epsilon_p = \left(\frac{\dot{\epsilon}_o}{b}\right)^b \left(\frac{\sigma}{\sigma_{oue}}\right)^n t^b \qquad (5.1)$$

where

ϵ_p denotes the strain due to primary creep,

σ_{oue} denotes a nominal unconfined proof stress at a particular temperature θ,

$\dot{\epsilon}_o$ denotes the strain rate at the proof stress,

σ denotes the applied stress,

t denotes time, and

b and n denote creep parameters.

THURBER

For convenience, Equation 5.1 can be simplified to:

$$\epsilon_p = Ct^b \qquad (5.2)$$

where $$C = \left(\frac{\dot{\epsilon}_o}{b}\right)^b \left(\frac{\sigma}{\sigma_{ouo}}\right)^n \qquad (5.3)$$

Two methods for deriving the primary creep parameters $\dot{\epsilon}_o$, σ_{ouo} , n and b from test data are described by Andersland et al (1978). The procedure will not be described here.

Weaver and Morgenstern (1981) first summarized the primary creep constants. Ladanyi (1988) revised the creep contents to conform with Equation 5.1. Ladanyi's summary is presented in Figure 5.2. A summary of pertinent properties for the soils on which the primary creep properties were established is presented in Figure 5.3.

The following variables can be expected to affect the primary creep behaviour of ice and frozen soil.

1) Confining stress,
2) Temperature,
3) Soil type,
4) Ice content, and
5) Unfrozen water content.

Unfortunately, only a limited amount of primary creep data was found in the literature, and as a result it was generally only possible to provide a qualitative assessment of the effects of the foregoing variables on primary creep.

5.2 Confining Stress

The effect which confining stress will have on creep will depend on the unfrozen water content of the frozen soil.

5.2.1 No Unfrozen Water

The effect which confining stress has on primary creep of soils which contain no unfrozen water content is illustrated in Figure 5.4. Where unfrozen water contents are low, Ladanyi (1972, 1983) has suggested the following modification to Equation 5.1:

THURBER

$$\epsilon_p = \left(\frac{\dot{\epsilon}_o}{b}\right)^b \left[\frac{\sigma_1 - \sigma_3}{\sigma_o}\right]^n t^b \qquad (5.4)$$

where

$$\sigma_o = \sigma_{ouo} + \sigma_3 (f_o - 1) \qquad (5.5)$$

and σ_{ouo} denotes the proof stress (at $\dot{\epsilon}_o$) from unconfined tests at a particular temperature, θ,

σ_3 denotes the confining stress, and

$$f_o = \frac{1 + \sin \phi_o}{1 - \sin \phi_o} \qquad (5.6)$$

where

ϕ_o is the apparent total angle of internal friction of the material. It will be a function of strain rate, as indicated on Figure 5.4.

In addition to being a function of temperature and the basic properties of the frozen soil, ϕ_o will also be a function of strain rate. It must be determined at the same value as $\dot{\epsilon}_o$ (the arbitrary proof strain rate) used in Equation 5.4. In general, ϕ_o can be expected to decrease as strain rate is decreased. In ice and ice rich soils, the limit for ϕ_o at very low strain rates will be zero, in which case, the creep, as found from Equation 5.4, will not be affected by confining stress. At higher strain rates, however, ϕ_o will have some finite value, in which case total strain will be reduced as confining stress is increased.

In ice poor soils, ϕ_o will also decrease as strain rate is decreased, except a limiting finite value will be reached, which is speculated to be close to the thawed effective angle of friction of the soil. Thus, for ice poor soils, even under low applied deviator stresses, confining stress is expected to reduce the rate of primary creep.

THURBER

5.2.2 High Unfrozen Water Content

In soils which have a significant unfrozen water content (due to high pore water salinity or high clay content) increases in confining stress may cause consolidation and a consequent decrease in the rate of creep. As indicated in Figure 5.5, for such soils, it is reasonable to assume that the angle of internal friction Ø will be independent of strain rate. Therefore, the primary creep equation may be written in the following form:

$$\epsilon = \left(\frac{\dot{\epsilon}_o}{b}\right)^b \left(\frac{\sigma_1 - f\sigma_3}{\sigma_{oct}}\right)^n t^b \qquad (5.7)$$

where

$$f = \frac{1 + \sin \emptyset}{1 - \sin \emptyset} \qquad (5.8)$$

and

Ø denotes the angle of internal friction of the soil which will be approximately equal to the thawed angle of friction of the soil.

Equation 5.8 predicts that primary creep will be reduced significantly in soils which have a major proportion of unfrozen water, a result which appears reasonable.

5.2.3 Data Review

While the theoretical relationship suggested by Ladanyi to account for the effects of confining stress on primary creep appear reasonable, they have never been confirmed by systematic laboratory tests.

Weaver and Morgenstern (1981) used an equation similar in form to Equation 5.8, to calculate a value for f which would fit the primary creep deformation curves for Ottawa Sand, as reported by Sayles (1973). The confining pressures in the triaxial tests carried out by Sayles ranged from 345 kPa to 2760 kPa.

Weaver and Morgenstern found that a reasonable fit of the data could be obtained for values of f between 1.0 and 1.3. These results indicate that primary creep

THURBER

rates will decrease as confining stress is increased, however, the effect does not appear to be significant within the range of stresses normally encountered in geotechnical engineering practice.

It may be desirable to carry out further research into the effect which confining stress has on primary creep deformations, particularly in ice poor soils with significant unfrozen water contents. The length of time for which confining stress is applied prior to applying the deviator stress must be accounted for in such tests.

5.3 Temperature

The information available with respect to the effect of temperature on the primary creep parameters is limited. In general, it is known that as the temperature decreases, the rate of primary creep also decreases for a given stress.

Ladanyi (1972) has suggested that the effect of temperature on primary and secondary creep can be accounted for, with a reasonable degree of accuracy through the following relationship:

$$\sigma_{cu\theta} = \sigma_{cu_0} (1 + \theta/\theta_0)^k \qquad (5.8)$$

where

σ_{cu_0} denotes the proof stress as determined in an unconfined creep test at any reasonable temperature and extrapolated back to 0°C,

θ denotes the absolute value of temperature below 0°C in degrees C.

θ_0 is an arbitrary temperature assigned an absolute value of 1°C, and

k denotes a temperature exponent which is determined from experimental data.

Ladanyi has calculated values for σ_{cu_0} and k from the available test data, and the results are presented in Figure 5.2. These results indicate that k has a value of slightly less than 1 for most soils, while the value for pure ice is about 0.4. The value for σ_{cu_0} varies significantly and is apparently a function of soil type as

THURBER

well as other unidentified factors. Additional creep testing may be worthwhile to confirm the validity of Equation 5.4 for a wider variety of soil types.

5.4 Soil Type

The effect which soil composition (clay, silt or sand) has on the primary creep parameters is indicated in Figure 5.2. There is considerable variation in the values for b and n and it is therefore not possible to draw general conclusions with respect to the effect which soil composition has on primary creep behaviour. In general, however, it can be expected that the rate of primary creep will decrease as clay content decreases.

5.5 Ice Content

Primary creep parameters for 'ice poor' soils and ice are shown on Figure 5.2. No studies have been carried out to establish the primary creep behaviour of 'ice poor' soils over a range of ice contents. It can be expected that where the void ratio (ice content) is very low, the time over which primary creep will dominate will be very long, and total deformations will be small. On the other hand, at high void ratios (ice contents) the primary creep will be completed fairly quickly and the material will progress into secondary creep.

5.6 Unfrozen Water Content

Nixon and Lem (1984) carried out an important series of constant load tests to establish the relationship between the secondary creep parameters, temperature and salinity. There is not sufficient data presented in their paper to derive the primary creep parameters, however the required data should be available on file. Consideration should be given to having the data interpreted in order to establish the primary creep parameters.

No other information concerning the effect which unfrozen water content has on the primary creep parameters was found in the literature.

5.7 Comparison with Field Data

Weaver and Morgenstern (1981) derived an equation governing pile deformations in ice poor soils, for which primary creep can be expected to dominate. The solution incorporates a constitutive relationship for primary creep in a form which is similar to that given in Equation 5.1.

THURBER

They obtained reasonably good agreement between predicted deformations and the limited number of field observations available in the literature. These results appear to confirm the validity of Equation 5.1 and the creep parameters presented in Figure 5.2. However, all of the available field observations were for ground temperatures which ranged between -0.15 to -0.9°C, a temperature range in which it is very difficult to assign reliable values for the creep parameters.

It would be desirable to confirm the validity of the constitutive equation and data for primary creep over a much broader temperature range. This is an aspect for which further field observations would be of great value.

5.8 Summary

The data available concerning creep deformations of ice poor soils (which at low stresses and temperatures is dominated by primary creep) is limited.

Additional laboratory tests into the effect of confining stress, ice content and unfrozen water content should be considered. The primary creep behaviour of sand (often used as backfill for piles) and saline soils (which appear to be widespread in Northern Canada) are areas in which the initial stages of research could be focused. In particular, there is very little data concerning the creep behaviour of ice poor soils at low temperatures (-5 to -10°C) and stresses (50 to 300 kPa).

There is a need for documentation and interpretation of field creep behaviour in ice poor soils in order to confirm primary creep deformation behaviour as observed in the laboratory, and as interpreted by present theory.

THURBER

LIST OF REFERENCES

The references for both primary and secondary creep are given at the end of Section 6.

PRIMARY CREEP

LIST OF FIGURES

THURBER

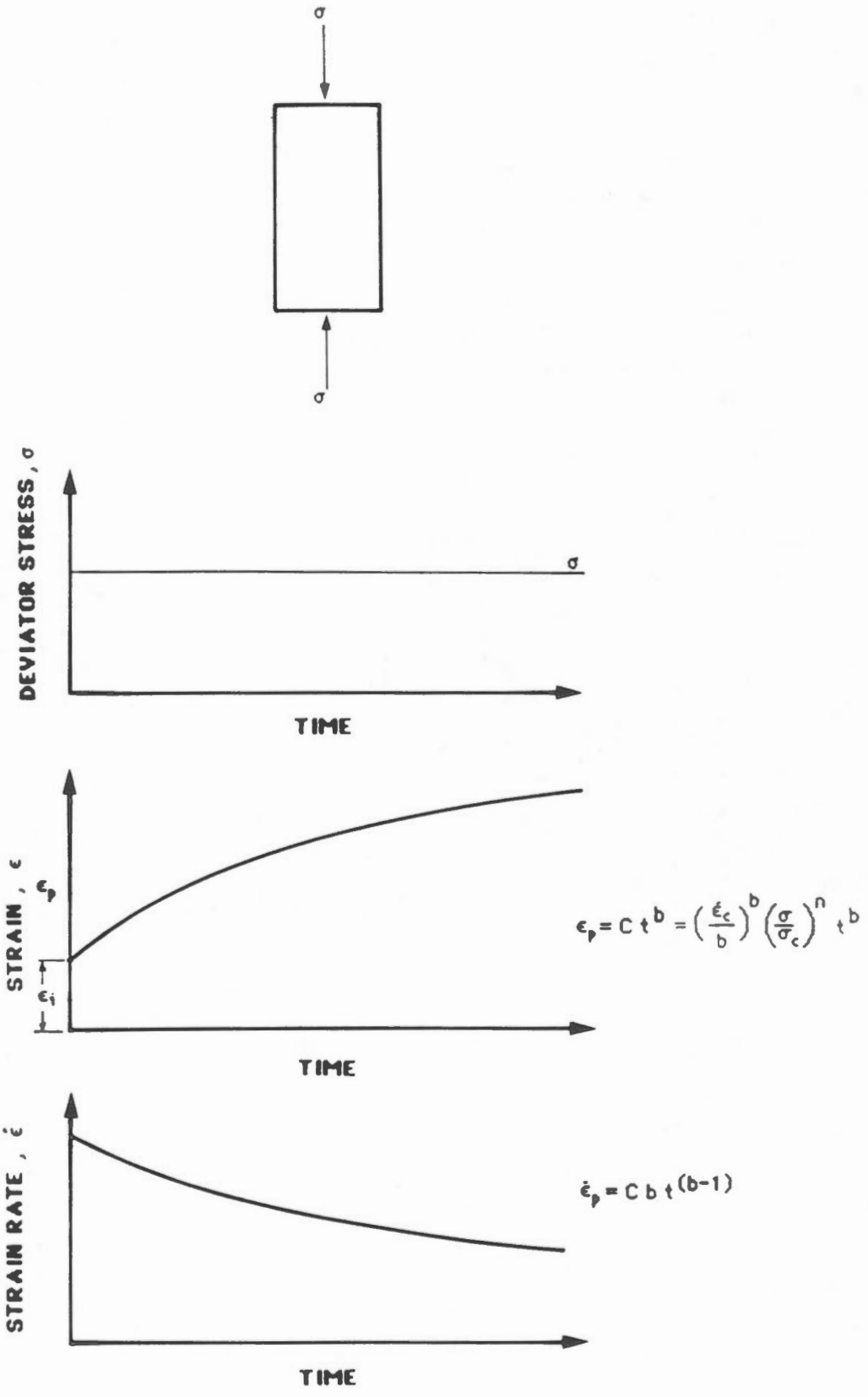

Idealized primary creep deformations in ice or frozen soil.

FIGURE 5.1

FROZEN SOIL TYPE	Reference	b	n	k	σ_{cuo}, MPa (At $\dot{\varepsilon} = 10^{-5} h^{-1}$)	Note
(1) CLAYS						
Suffield Clay	Sayles & Haines,1974	0.33	2.38	1.2	0.17	
Bat-Baioss Clay	Vyalov,1962	0.45	2.50	0.97	0.18	
(2) SILTS & LOAMS						
Hanover Silt	Sayles & Haines,1974	0.15	2.04	0.87	2.25	
Callovian Loam	Vyalov,1962	0.37	3.70	0.89	0.31	
Ice-Rich Silt, (undisturbed $(10^{-8} < \dot{\varepsilon} < 10^{-4} h^{-1})$	McRoberts et al.,1978	1.00	3.00	0.60	0.071	long term
(3) SANDS						
Ottawa Sand	Sayles,1968	0.45	1.28	1.00	1.05	
Manchester Fine Sand	"	0.63	2.63	1.00	0.16	
Karlsruhe Silty Sand	Meissner & Eckardt,1976	0.40	2.00	1.00	0.30	
(4) VERY ICE-RICH SOIL OR POLYCRYSTALLINE ICE (For: $\theta \leq 1^{\circ}C$, $10^{-7} < \dot{\varepsilon} < 10^{-2} h^{-1}$)	Morgenstern et al,,1980	1.00	3.00	0.37	0.103	long term

Primary creep parameters for selected materials (Weaver and Morgenstern, 1981; Ladanyi, 1988a).

FIGURE 5.2

THURBER

SOIL	% < 0.002 mm	% > 0.1 mm	% W_L	% W_p	G_s	% S	e	Mg/m^3 ρ_d	Mg/m^3 ρ
Suffield Clay	31	0	35	20	2.69	98.5	1.045	1.312	1.79
Bat-Baioss Clay[1]	30	10	51.2	23.6	2.73	?	0.59	1.72	2.06-2.15
Hanover Silt	2	18	-	-	2.74	99.5	0.923	1.42	1.86
Ice-Rich Silt[2]	20	6	33-60	25-50	?	100			1.2-1.45
Callovian Loam[3]	2	10	?	?	2.70		0.64--0.79	1.50--1.65	
Ottawa Sand	(20-30 mesh)		-	-	2.65	100	0.587	1.67	
Manchester Fine Sand	0	10	-	-	2.67	98.7	0.770	1.51	

1 w = 20 à 24%

2 w = 50 à 150%

3 w = 39 à 44%

Notation:

W_L, W_p	=	Atterberg Limits
G_s	=	Specific Gravity of Soil Grains
S	=	Degree of Saturation
e	=	Void Ratio
ρ_d	=	Dry Density
ρ	=	Bulk Density

Pertinent soil properties of the soils which primary creep parameters have been determined (Ladanyi, 1988b).

THURBER

FIGURE 5.3

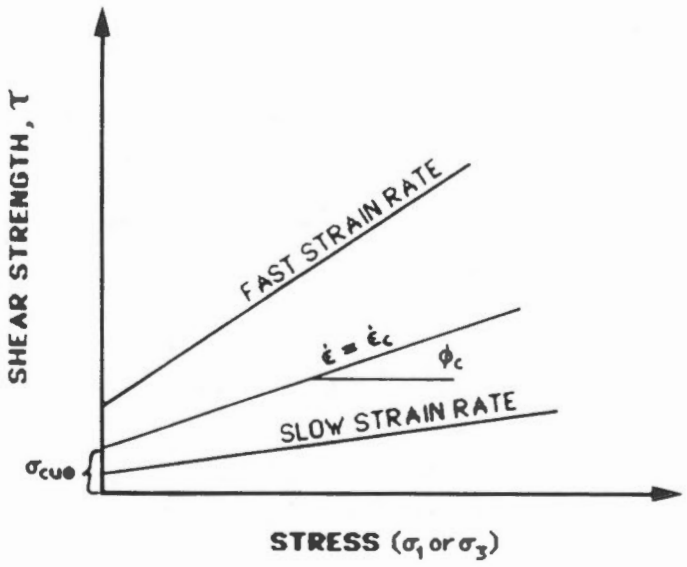

$$\epsilon = \left(\frac{\dot{\epsilon}_c}{b}\right)^b \left[\frac{\sigma_1 - \sigma_3}{\sigma_c}\right]^n t^b$$

$$\sigma_c = \sigma_{cu0} + \sigma_3 (f_c - 1)$$

$$f_c = \frac{1 + \sin \phi_c}{1 - \sin \phi_c}$$

Effect of confining stress on creep in soils with no unfrozen water (Ladanyi, 1983).

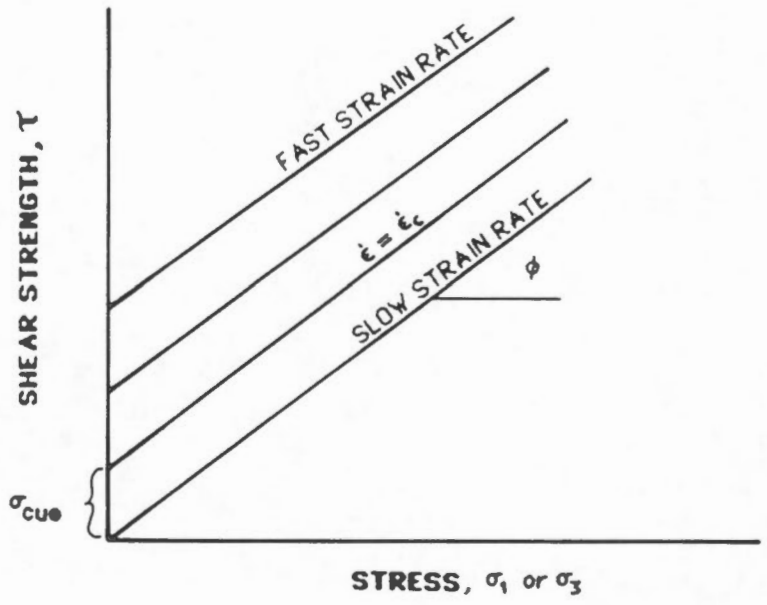

$$\epsilon = \left(\frac{\dot{\epsilon}_c}{b}\right)^b \left[\frac{\sigma_1 - f\sigma_3}{\sigma_{cuo}}\right]^n t^b$$

$$f = \frac{1 + \sin\phi}{1 - \sin\phi}$$

Effect of confining stress on creep in soils with high unfrozen water content (Ladanyi, 1983).

THURBER

FIGURE 5 .5

SECTION 6

SECONDARY CREEP

SECTION 6

SECONDARY CREEP

6.1 General

If the applied stress is greater than the long term strength of the frozen soil but less than the short term strength, or where loads are applied for an extended period of time, then total strain will be dominated by secondary creep. This situation occurs in ice and ice rich soils for which the long term (thawed) strength is zero. Ladanyi (1972) has suggested that strains due to secondary creep can be calculated from the following equation:

$$\epsilon_s = \dot{\epsilon}_o \left(\frac{\sigma}{\sigma_{cuo}} \right)^n t^b \qquad (6.1)$$

where

ϵ_s denotes the strain under secondary creep,

$\dot{\epsilon}_o$ denotes an arbitrary small secondary strain rate introduced to make the term dimensionless,

σ_{cuo} denotes the unconfined compressive stress at the arbitrary secondary strain rate at a temperature θ,

σ denotes the deviator stress,

n denotes the secondary creep exponent, and

t denotes time.

For convenience, Equation 6.1 can be simplified to:

$$\epsilon_s = B\sigma^n t \qquad (6.2)$$

where

$$B = \frac{\dot{\epsilon}_o}{\sigma_{cuo}^n} \qquad (6.3)$$

It should be noted that the values of $\dot{\epsilon}_o$ and σ_{cuo} for secondary creep will not have the same numerical value as $\dot{\epsilon}_o$ and σ_{cuo} for primary creep (Equation 5.1) even for the same soil tested under identical conditions.

THURBER

Under some conditions, both primary and secondary creep may be significant, in which case both must be calculated. It is often difficult to determine where primary creep ends and secondary creep begins, particularly at lower stress levels, where it is difficult to obtain reliable data because of the length of time required to reach secondary creep.

The secondary creep constants can be derived from a series of constant stress tests which are carried out under a specified temperature and confining stress. The tests must be carried out under stress conditions in which secondary creep occurs. The applied stresses are varied over a suitable range, as illustrated in Figure 6.1, and the rate of secondary strain under each stress level is established from the strain versus time plot. (In practise, it is usually more convenient to plot the log of the strain rate versus the log of time.) The log of the applied stresses are then plotted versus the log of the corresponding secondary strain rates. The creep parameters $\dot{\epsilon}_o$, σ_{ou} and n can then be derived from the plot as shown on Figure 6.1.

For convenience, the strains obtained in the test can be normalized by dividing by the value of which is arbitrarily chosen. The log of the normalized strain rate is then plotted against the applied deviator stress. The creep parameters are then established using essentially the same procedure shown on Figure 6.1.

Once the secondary creep parameters $\dot{\epsilon}_o$, σ_{ou} and n have been established for a given material under a specified confining stress they are inserted into Equation 6.1. The resulting equation is termed the 'flow law' for that material under the specified conditions.

Sego and Morgenstern (1983) have demonstrated that for pure ice, the secondary creep parameters $\dot{\epsilon}_o$, σ_{ou} and n can be derived from uniaxial or triaxial compression tests in which the sample is loaded at a constant rate of displacement, as shown on Figure 6.2. In the case of constant rate of displacement tests, the log of the rate of strain applied in the test is plotted against the log of the measured peak stress ($\sigma_1-\sigma_3$). The secondary creep parameters ϵ_o, σ_{ou} and n can then be derived from the plot in the same fashion as for data from constant load tests.

The flow law derived from Sego and Morgenstern's tests on pure ice are shown on Figure 6.3 and demonstrate that the same result will be obtained from constant rate of displacement tests as from constant stress test.

The significance of Sego and Morgenstern's result is that it is generally more convenient to carry out constant rate of displacement tests as compared to constant stress tests. It should be noted that it is not possible to derive the primary creep parameters from constant displacement rate tests.

In addition to time dependent effects, as discussed above, the following variables can be expected to affect secondary creep behaviour in ice and frozen soil:

1) Confining stress,
2) Temperature,
3) Soil type,
4) Ice content, and
5) Unfrozen water content.

6.2 Confining Stress

As was the case for primary creep, the effect which confining stress will have on secondary creep will depend on the unfrozen water content of the frozen soil.

6.2.1 No Unfrozen Water

Ladanyi (1972, 1983) has suggested that the influence of confining stress on secondary creep can be accounted for be modifying Equation 6.1 as follows:

$$\epsilon_s = \dot{\epsilon}_c \left(\frac{\sigma_1 - \sigma_3}{\sigma_c} \right)^n t \qquad (6.4)$$

where $\sigma_c = \sigma_{cuc} + \sigma_3(f_c - 1)$ (6.5)

and σ_{cuc} denotes the proof stress (at ϵ_c) from unconfined tests at a particular temperature θ,

σ_3 denotes the confining stress, and

$$f_c = \frac{1 + \sin \phi_c}{1 - \sin \phi_c} \qquad (6.6)$$

As discussed under primary creep, ϕ_c is the apparent angle of friction which decreases as strain rate decreases. In ice or ice rich soils the limiting value is $\phi_c = 0$, while in ice poor soils, the limiting value is speculated to be equal to the thawed angle of friction.

THURBER

Equation 6.4 predicts that for ice and ice rich soils, confining stress will have no effect on secondary creep, except at high rates of strain. In ice poor soils, confining stress may influence secondary creep, depending on the magnitude of the deviator stress and the thawed strength of the soil.

6.2.2 High Unfrozen Water Content

For soils which have a high unfrozen water content, Ladanyi (1972) has suggested that following equation will apply:

$$\epsilon_s = \dot{\epsilon}_o \left(\frac{\sigma_1 - f\sigma_3}{\sigma_{cuo}} \right)^n t \qquad (6.7)$$

where $$f = \frac{1 + \sin \phi}{1 - \sin \phi} \qquad (6.8)$$

where ϕ is the angle of internal friction of the frozen soil, which, if unfrozen water contents are high, will be independent of strain rate and approximately equal to the thawed angle of internal friction.

Equation 6.7 predicts that where unfrozen water contents are high, secondary creep rates will decrease as confining stress increases.

6.2.3 Data Review

Unfortunately, as was the case for primary creep, no systematic laboratory investigations were found in the literature to confirm the relationships proposed by Ladanyi.

McRoberts et al (1977) carried out creep tests on undisturbed ice-rich silt from Norman Wells, N.W.T. at temperatures ranging from -1 to -3°C. Of the 39 tests, 31 were carried out in unconfined compression and 8 were carried out at a confining pressure of 28 kPa. The confining pressure had no discernible effect on secondary creep rates.

Roggensack (1977) reported the results of a series of creep tests carried out on undisturbed clay samples from Mountain River and Fort Simpson, N.W.T. The tests were carried out at temperatures ranging from -0.75 to -1.40°C and the samples would be expected to contain

THURBER

a significant proportion of unfrozen water. In general, Roggensack found that for the same deviator stress, higher confining pressures appeared to result in a slight reduction in secondary creep rate, however the results were not entirely consistent or conclusive.

Caution must be exercised in assessing the effect which confining stress has on creep rates, where tests are carried out on natural samples which contain segregated ice. Savigny and Morgenstern (1986c) have reported the results of creep tests carried out on undisturbed samples of glaciolacustrine clay taken from near Fort Norman, N.W.T., and tested at temperatures ranging from -1.0 to -1.45°C. Confining pressures of 0 and 400 kPa were used. These samples contained significant quantities of segregated ice in various orientations and thicknesses. The creep tests carried out at the high confining pressures did not yield satisfactory creep data and most of the samples failed in much shorter times than had been expected on the basis of data from unconfined creep tests. The confined samples failed along the interfaces between he segregated ice and the soil. The times to failure were longer and more consistent data was obtained when unconfined creep tests were carried out on similar material. Savigny and Morgenstern have speculated that the application of high confining pressures caused stress-concentration at the interfaces between the soil and the segregated ice as a result of strain incompatability due to a significant difference between the stiffness of the segregated ice and the soil. The results illustrate that difficulties of obtaining representative creep parameters from tests carried out on natural materials.

In summary, the available laboratory data indicates that for ice and frozen soils which do not contain significant unfrozen water, confining stress will not have a significant effect on secondary creep rates, for the range of stresses commonly encountered in geotechnical engineering. However, confining stress can be expected to have a significant effect on creep rates in frozen soils which contain a high proportion of unfrozen water.

A systematic program of research to establish the effect of confining stress on primary and secondary creep, particularly in ice poor soils which have a high unfrozen water content, may be worthwhile.

THURBER

6.3 Temperature

As temperature decreases, the rate of secondary creep can be expected to decrease. Ladanyi (1972, 1983) has suggested the use of Equation 5.4 to account for the effect of temperature on primary and secondary creep.

Morgenstern et al (1980) carried out a review of available laboratory data with respect to the secondary creep behaviour of ice. The creep data was interpreted using the form of the secondary creep equation given in Equation 6.2. The authors found that a good fit of the available data could be achieved for a constant value of the creep exponent, n equal to 3.0. The creep parameter B was found to vary with temperature, as shown in Figure 6.4.

The use of the relationship shown in Figure 6.4 is not recommended for temperatures warmer than -1°C. The creep behaviour of ice and ice rich soils at temperatures warmer than -1°C are not normally of concern in geotechnical engineering practice, because, where such ground temperatures exist, there is a risk that permafrost degradation will occur. Therefore, measures are taken to either reduce ground temperatures, thaw the permafrost, or found the structure on a deeper, thaw stable stratum.

It appears from this literature review that no systematic studies have been carried out to determine the effects of temperature on the secondary creep parameters of ice poor soils for the range of temperatures and stresses commonly encountered in conventional geotechnical engineering practise. This is an area in which further research should be considered.

6.4 Soil Type

The secondary creep rates of frozen soil are controlled to a significant extent by the grain size distribution of the soil. In general, secondary creep rates in frozen fine grained soils such as clays can be expected to be significantly higher than creep rates in frozen sands and gravels. There are two reasons for this behaviour:

1) Unfrozen water content
2) Effective angle of friction

As mentioned earlier, fine grained soils such as silts and clays contain a significant proportion of unfrozen

THURBER

water, particularly in the temperature range between 0 and -5°C. The higher the proportion of unfrozen water, the weaker the strength of the interstitial ice with the result that creep rates increase.

An additional, but probably less important factor is that the resistance to deformations provided by the soil skeleton will be lower for clays, which have a lower angle of internal friction as compared to sands and gravels.

Savigny and Morgenstern (1986c) compiled secondary creep data from a variety of sources in order to establish the secondary creep parameters of an ice rich glaciolacustrine clay from the Mackenzie Valley N.W.T. The results are presented in Figure 6.5. It is apparent that there is considerable scatter to the data. The scatter is due to natural variability in the properties of the samples tested, differences in test procedures, differences in the interpretation of the test data and other factors. These results do indicate, however, that the flow law for pure ice provides a reasonable upper bound for secondary creep behaviour of ice rich clays, at temperatures colder than -1°C.

No systematic study has been undertaken to establish values for the secondary creep parameter B as a function of soil type and temperature. Consideration should be given to carrying out this work in the future.

6.5 Ice Content

As ice content is decreased, a point is reached where grain to grain contact of the soil particles occurs such that intergranular friction will contribute to the strength of the frozen material. Since intergranular friction is not time dependent, it can be expected that secondary creep rates will decrease as the ice content of the frozen soil decreases. As discussed earlier, in ice poor soils at low stresses, strain rates can be expected to continue to decrease with time for a very long period of time before the deformation behaviour can be approximated by a secondary creep model.

Hooke et al (1972) carried out a series of creep tests on reconstituted samples of ice and sand. The volume fraction of sand was varied and the secondary creep rate was established from the tests. The results of these tests are presented on Figure 6.6. The results demonstrate that a significant decrease in the secondary creep rate occurred as the volume fraction of sand increased. On the basis of these results, it would be expected that at water contents

THURBER

of about 10 percent, creep rates in sands would be negligible. It might be desirable to carry out a series of creep tests on dense frozen sands, silts and clays in order to confirm the behaviour of these materials at low ice contents.

It is of interest to note that ice which contains a very low proportion of soil may creep faster than pure ice, as indicated by the data shown in Figure 6.6. This somewhat surprising behaviour may occur because the soil particles provide areas of stress concentration which facilitates the initiation of cracks and failure of the ice. This is an area which deserves further research, because it has significant practical implications in that ground ice is not normally pure.

As mentioned earlier, Savigny and Morgenstern (1986c) carried out a series of triaxial tests on undisturbed samples of glaciolacustrine clay which contained significant quantities of segregated ice. The test results indicated that the creep behaviour of this material was dominated by the shear stresses which developed at the interfaces between the segregated ice and the soil. These test results demonstrate that the assumption that frozen soil behaves as a plastic continuum may not be adequate, at least where large quantities of segregated ice are present. The test results indicate that research into the fundamental physical processes by which creep occurs in ice rich soils may be of value.

No systematic studies have been undertaken in homogeneous soils to establish values for the creep parameters B and n as functions of ice content and temperature. This is an area in which a more comprehensive review of the literature, together with supplementary laboratory testing should be considered.

6.6 Unfrozen Water Content

As unfrozen water content increases, either due to increasing pore fluid salinity, or increasing clay content, the rate of secondary creep can be expected to increase.

Sego (1982) carried out a series of unconfined compression tests on sand samples which were tested at a constant rate of displacement. The tests were carried out over a range of pore fluid salinities at -7°C. The log of the peak deviator stress has been plotted against the log of axial strain rate on Figure 6.7. The creep parameters n and σ_{oo} (at a strain rate of 0.001% per hour) as determined from these tests are as follows:

THURBER

Pore Water Salinity (ppt)	Proof Stress σ_{oo} (kPa)	Creep Exponent n
0	1709.20	5.52
10	119.80	3.58
35	22.10	2.75
100	0.27	1.36

As indicated above, Sego found that the creep exponent n decreased as pore fluid salinity increased. As Sego points out, at very high salinities, unfrozen water contents approach 100% and the creep exponent will decrease to 0. That is, the strength of the (now unfrozen) sand will become independent of strain rate over a reasonable range of strain rates. (At very high rates of strain, pore fluid pressures will affect measured strength values.)

Nixon and Lem (1984) carried out a series of constant stress, unconfined compression tests on a sandy silt in which pore fluid salinity was varied from 0 to 35 parts per thousand (ppt). The secondary creep parameters as defined by Equation 6.2 were calculated from the data. The applied axial stresses were plotted against strain rate as shown on Figure 6.8. It was found that a value for the creep parameter n, of 3.0 provided a reasonably good fit to the data, irrespective of pore fluid salinity and temperatures. The variation of the creep parameter B (assuming a value for the creep exponent of 3.0) as a function of temperature and salinity is presented on Figure 6.9.

Because of the variation in the creep exponent n in Sego's tests, it is not possible to plot values for the creep parameter B as a function of pore water salinity from his data, in order to make a direct comparison with the data provided by Nixon and Lem in Figure 6.9.

Further investigation into the reasons for the difference in n values, in the range from 0 to 35 ppt, should be undertaken through a detailed review of data from both sources. The different trends found by these researchers may be due to testing inaccuracy, differences in data interpretation, or differences in test procedure. (Nixon and Lem's tests being stress controlled, whereas Sego's tests being displacement rate controlled.)

THURBER

Consideration should be given to carrying out additional creep tests in saline soils to establish creep parameters over a broader range of temperatures and soil types, particularly for ice poor saline soils. This additional data would also assist in evaluating the causes of the differences between these two sets of data.

6.7 Comparisons with Field Data

Savigny (1986b) measured creep of an ice rich slope in glaciolacustrine clay near Fort Norman, N.W.T. The equivalent creep properties were calculated using a computer based finite element analysis in order to determine the flow law for secondary creep which best represented the field observations. A value for the creep exponent of 3.0 was assumed, from which a value for B of 0.33×10^{-8} kPa^{-3} $year^{-1}$ was found to result in a good match between calculated and observed creep. However, in these ice rich soils, it would be reasonable to expect a value for the creep parameter B of about 2×10^{-8} kPa^{-3} $year^{-1}$. That is, the observed rate of creep in the field was much slower than expected.

The reasons for the much slower rate of creep observed in the field as compared to those which would be expected for ice rich soils are not known with certainty. The slower rate of creep observed in the field may be due to three dimensional effects which operate in the field. In addition, inhomogeneous field conditions may not have been adequately incorporated into the analysis. The laboratory tests were carried out under triaxial loading conditions, whereas in the field, plane strain conditions dominate. This may account for some of the discrepancy between the observed and predicted creep rates.

Thompson and Sayles (1972) reported the results of deformation monitoring of a room excavated in permafrost. Their observations are presented in Figure 6.10 and have been reviewed by Roggensack (1977). As discussed by Roggensack, a flow law for secondary creep was determined from a finite element analysis of the observed deformations, which indicated a strain rate in the field which was 3.3 times faster than the flow law for secondary creep measured on laboratory samples. Roggensack has suggested that the discrepancy between these results may be due to the dominance of primary creep deformations, (which would result in much faster rates of creep) during the period of monitoring. A definitive explanation for the difference between the field and laboratory results in this case has not been developed.

THURBER

Nixon and McRoberts (1976) derived a solution for pile deformations which incorporates the flow law for ice and ice rich soils as given in Equation 6.2. Morgenstern et al (1980) used the secondary creep parameters as given in Figure 6.2 in the Nixon and McRoberts equation and found good agreement between the predicted creep deformations and field observations of adfreeze piles in ice rich soils.

As indicated from the foregoing, these comparisons between field creep rates and laboratory creep rates have produced mixed results. The reasons for the discrepancies between laboratory test data and field observations are not clear. It is speculated that the differences may be due to a combination of sample disturbance (including stress unloading and thermal disturbance) and sample size effects. No investigations aimed at evaluating the effects of sample disturbance and sample size on the creep behaviour of frozen soils were found in this review. This is an area in which further research should be considered. It may be worthwhile to develop in situ techniques for measuring creep properties of natural soils.

6.8 Summary

This literature review indicates that a considerable amount of laboratory data is available concerning the secondary creep behaviour of ice. This information can be used to provide a good indication of the maximum creep rates which will occur in the field.

The creep behaviour of ice and frozen soils has not been investigated at low stress levels and temperatures, primarily because such testing is time consuming and consequently difficult. It is assumed by most researchers that secondary (and tertiary) creep will commence at the same strain levels at which they commence in tests at higher stress levels. This concept, although reasonable, has never been confirmed by appropriate laboratory tests. It is possible that under low stress levels and low rates of strain, other time dependent physical processes (such as strain hardening or healing) may operate, in which case strain may remain constant or decrease. This is an area in which further research should be considered.

The effect which the presence of segregated ice has on the creep behaviour of frozen soils is not completely understood. Research into the fundamental physical processes by which creep occurs in frozen soils may be of value.

THURBER

There is a requirement to establish the creep parameters of saline soils over a broader range of soil types, temperatures and ice contents. There is, in particular, a need to investigate the creep behaviour of ice poor saline soils.

Significant and as yet unexplained differences between creep rates observed in the field and those measured on natural samples of frozen soils in the laboratory have been noted. There are a number of possible reasons for these differences which should be investigated further. In particular, research into the effects which sample disturbance and sample size may have on creep behaviour observed in laboratory tests should be considered. It may be worthwhile to develop in situ methods for the measurement of creep parameters. Full scale field observations of creep behaviour in ice and frozen soils should be carried out whenever opportunities arise.

SECONDARY CREEP

LIST OF REFERENCES

Andersland, O.B. and Anderson, D.M., 1978. Geotechnical Engineering for cold regions. McGraw-Hill Book Company, New York, p.566.

Andersland, O.B., Sayles, F.H., and Ladanyi, B., 1978. Mechanical properties of frozen ground. Chapter 5 in Geotechnical engineering for cold regions. (Andersland and Anderson, 1978).

Hooke, R.L., Dahlin, B.B., and Kauper, M.T., 1972. Creep of ice containing dispensed fine sand, Journal of Glaciology. Vol. 11, No. 63, pp. 327-336.

Huang, S.L. and Speck, R.C., 1986. Laboratory creep tests of frozen gravels. Cold Regions Science and Technology, Vol. 13, pp. 101-104, Elsevier Science Publishers, Amsterdam.

Johnston, G.H., ed., Permafrost. Engineering Design and Construction. John Wiley and Sons, Canada, 1981.

Johnston, G.H., and Ladanyi, B., 1972, Field tests of grouted rod anchors in permafrost. Can. Geot. Journ., Vol. 9, pp. 176-194.

Ladanyi, B., 1972. An engineering theory of creep in frozen soils. Can. Geot. Journ. Vol. 9, pp. 63-80.

Ladanyi, B., 1975. Bearing capacity of strip footings in frozen soils. Can. Geot. Journ. Vol. 12, pp. 393-407.

Ladanyi, B., 1976. Use of the Static Penetration Test in Frozen Soils. Can. Geot. Journ., Vol. 13, No. 2, pp. 95-110.

Ladanyi, B., 1983. Shallow foundations on frozen soil: creep settlement. Journal of Geotechnical Engineering, Vol. 109, No. 11, pp. 1434-1448

Ladanyi, B., 1988a. Short and long term behaviour of axially loaded bored piles in permafrost. First Int'l Seminar on deep foundations on bored and augered piles, Ghent, June, 1988.

Ladanyi, B., 1988b. Information from course notes.

THURBER

LIST OF REFERENCES
(continued)

Ladanyi, B., and Johnston, G.H., 1973. Evaluation of insitu creep properties of frozen soils with the pressurementer. Second Int. Permafrost Conf., North American Contribution, National Academy of Sciences, Washington, D.C., pp. 310-318.

Ladanyi, B. and Johnston, G.H., 1974. Behaviour of circular footings and plate anchors embedded in permafrost. Can. Geot. Journ., Vol. 11, pp. 531-553.

Ladanyi, B., and Paquin, J., 1978. Creep Behavior of Frozen Sandunder a Deep Circular Load, Proceedings, 3rd Int. Conf. on Permafrost, Edmonton, Alberta, Vol. 1, pp. 679-686.

McRoberts, E.C., Law, T.C., and Murray, T.K., 1978. Creep tests on undisturbed ice-rich silt. Proceedings, 3rd International Permafrost Conference, Vol. 1., Edmonton, Alberta, pp. 539-545.

Morgenstern, N.R., Roggensack, W.D., and Weaver, J.S., 1980. The behaviour of friction piles in ice and ice-rich soils. Can. Geot. Journ., 17, pp. 405-415.

Nixon, J.F., 1978. Foundation Design Approaches in Permafrost Areas, Can. Geot. Journal, Vol. 15, pp. 96-112.

Nixon, J.F., 1988. Pile load tests in saline permafrost at Clyde River, N.W.T., Can. Geot. Journ., Vol. 25, pp. 24-32.

Nixon, J.F., and Lem, G., 1984. Creep and strength testing of frozen saline fine-grained soils. Can. Geot. Journ., Vol. 21, pp. 518-529.

Nixon, J.F., and McRoberts, E.C., 1976. A design approach for pile foundations in permafrost. Can. Geot. Journ., Vol. 13, pp. 40-58.

Roggensack, W.D., 1977. Geotechnical properties of fine-grained permafrost soils. Ph.D. thesis, University of Alberta, Edmonton, Alberta, 449 p.

THURBER

LIST OF REFERENCES
(continued)

Savigny, K.W., and Morgenstern, N.R., 1986a. Geotechnical condition of slopes at a proposed pipeline crossing, Great Bear River valley, N.W.T. Can. Geot. Journ., Vol. 23, pp. 490-503.

Savigny, K.W., and Morgenstern, N.R., 1986b. In situ creep properties in ice-rich permafrost soil. Can. Geot. Journ., Vol. 23, pp. 504-514.

Savigny, K.W., and Morgenstern, N.R., 1986c. Creep behaviour of undisturbed clay permafrost. Can. Geot. Journ., Vol. 23, pp. 515-527.

Sayles, F.H., 1968. Creep of frozen sand. U.S. Army Cold Regions Research and Engineering Laboratory, Technical Report 190, 54 p.

Sayles, F.H., 1973. Triaxial and creep tests on frozen Ottawa sand. Proceedings, 2nd International Conference on Permafrost, Yakutsk, USSR, North American Contribution, pp. 384-391.

Sayles, F.H., and Haines, D., 1974. Creep of frozen silt and clay, U.S. Army, Corps of Engineers, Cold Regions Research and Engineering Laboratory, Hanover, NH, Technical Report 252, 50 p.

Sego, D.C., and Morgenstern, N.R., 1983. Deformation of ice under low stresses. Can. Geot. Journ., Vol. 20, pp. 587-602.

Sego, D.C., Shultz, T., Banasch, R. Strength and deformation behaviour of frozen saline sand. Proc. of the Third Int'l Symposium on Ground Freezing, CRREL, Hanover, NH, pp. 11-17.

Vyalov, S.S. (Editor) 1959. Geological properties and bearing capacity of frozen soils. U.S. Army, Corps of Engineers, Cold Regions Research and Engineering Laboratory, Hanover, NH, Army Translation No. 74. 219 p. Translated from Russian in 1965).

Weaver, J.S., and Morgenstern, N.R. 1981. Pile design in permafrost. Can. Geot. Journ., Vol. 18, pp. 357-370.

THURBER

LIST OF FIGURES

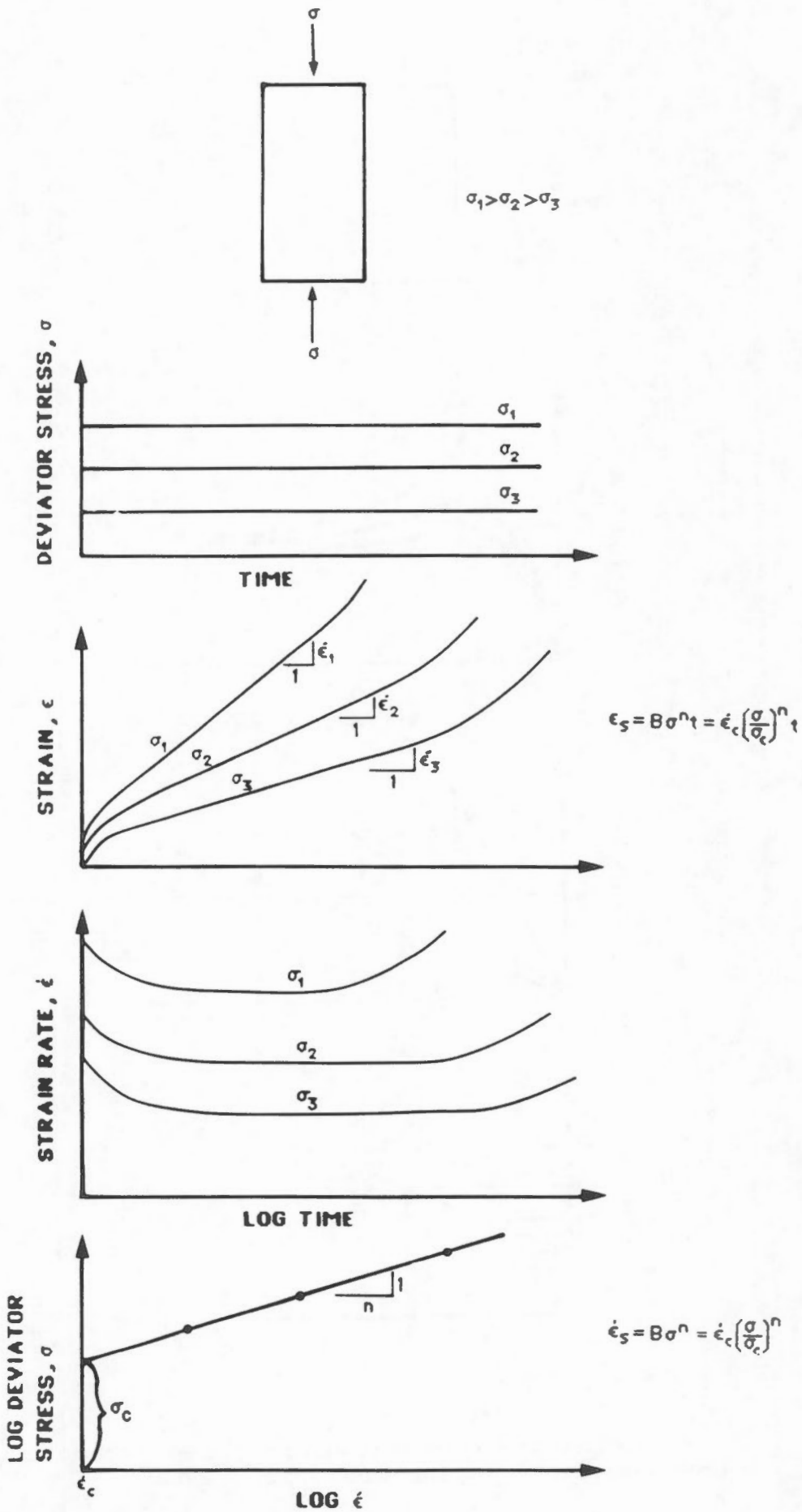

The determination of secondary creep parameters from constant stress tests.

FIGURE 6.1

THURBER

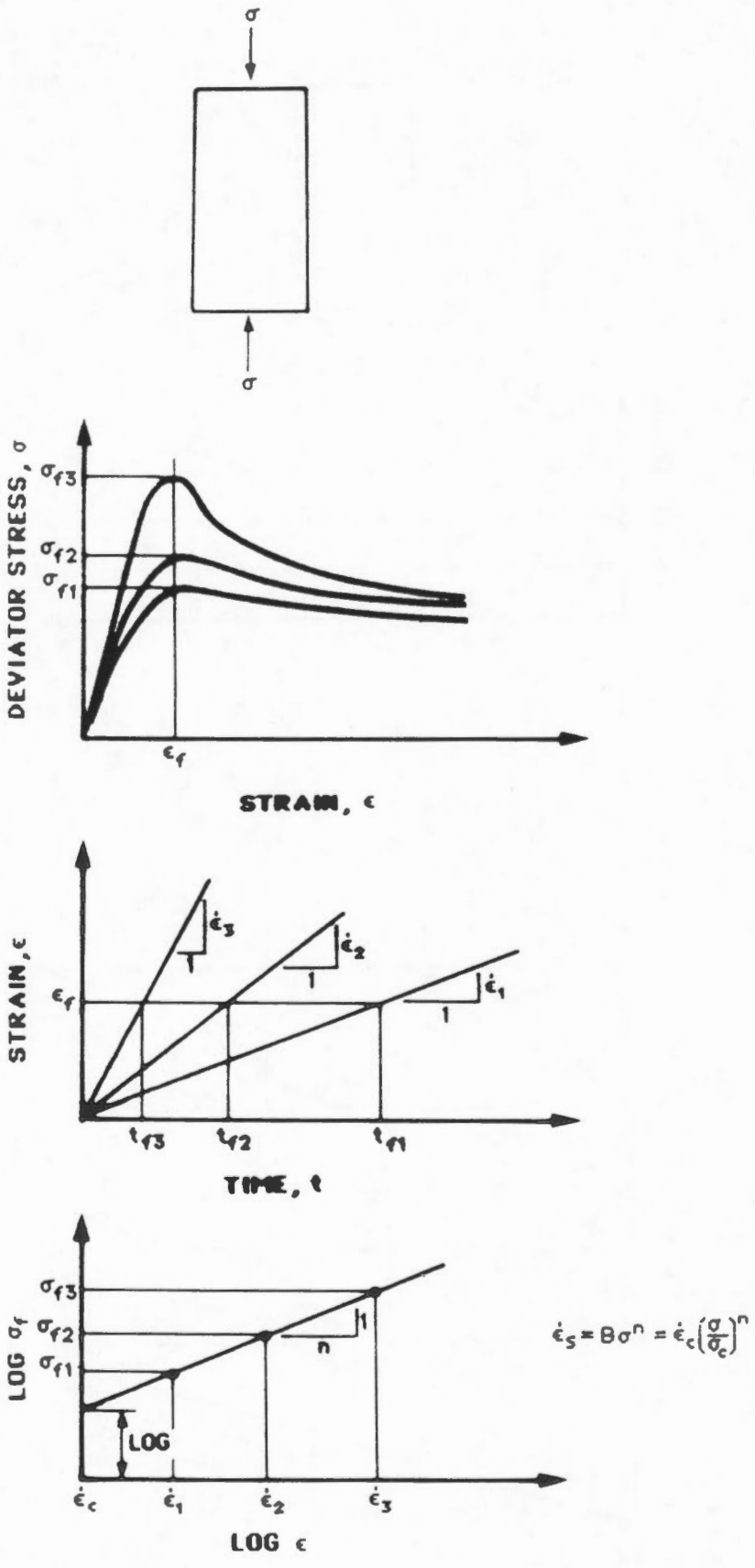

The determination of secondary creep parameters from constant displacement rate tests.

FIGURE 6.2

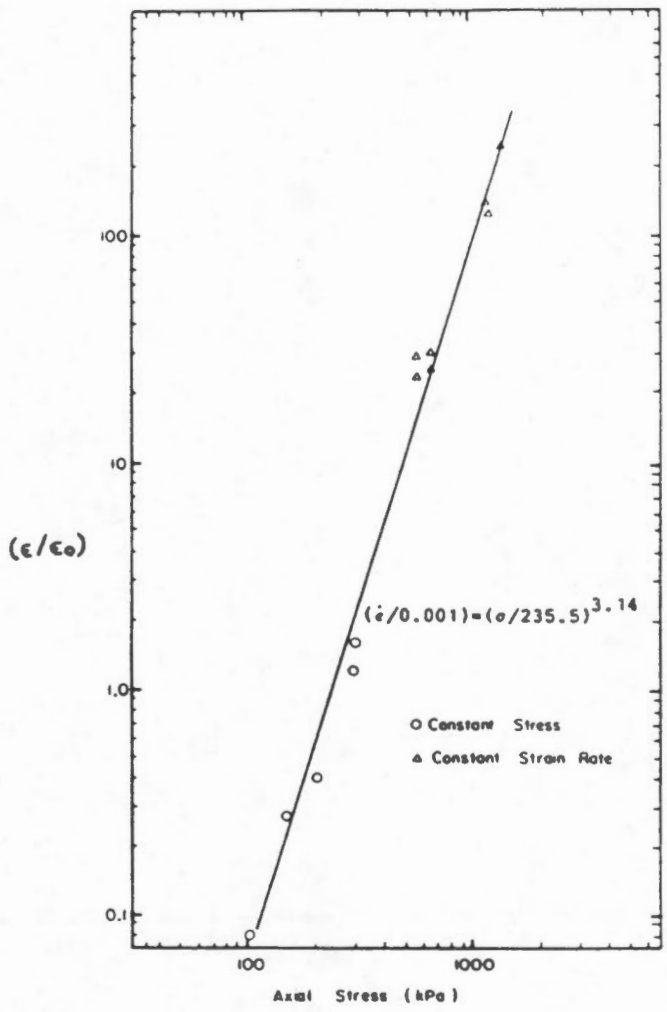

Normalized strain rate versus axial stress from combined constant stress and constant strain rate data for pure ice (Sego, 1983).

FIGURE 6.3

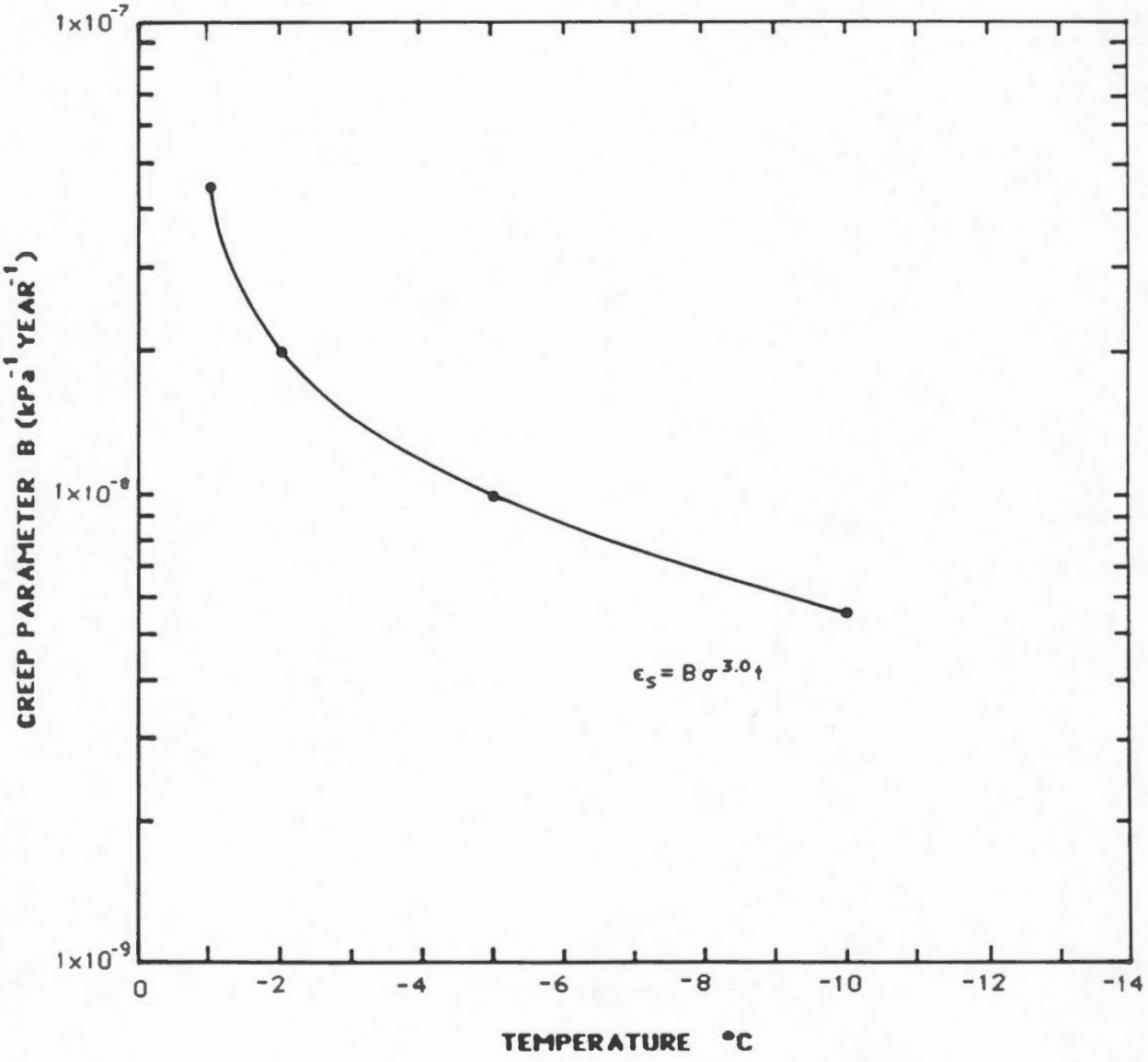

Relationship between the secondary creep parameter B and temperature for ice (after Morgenstern et al, 1980).

FIGURE 6.4

THURBER

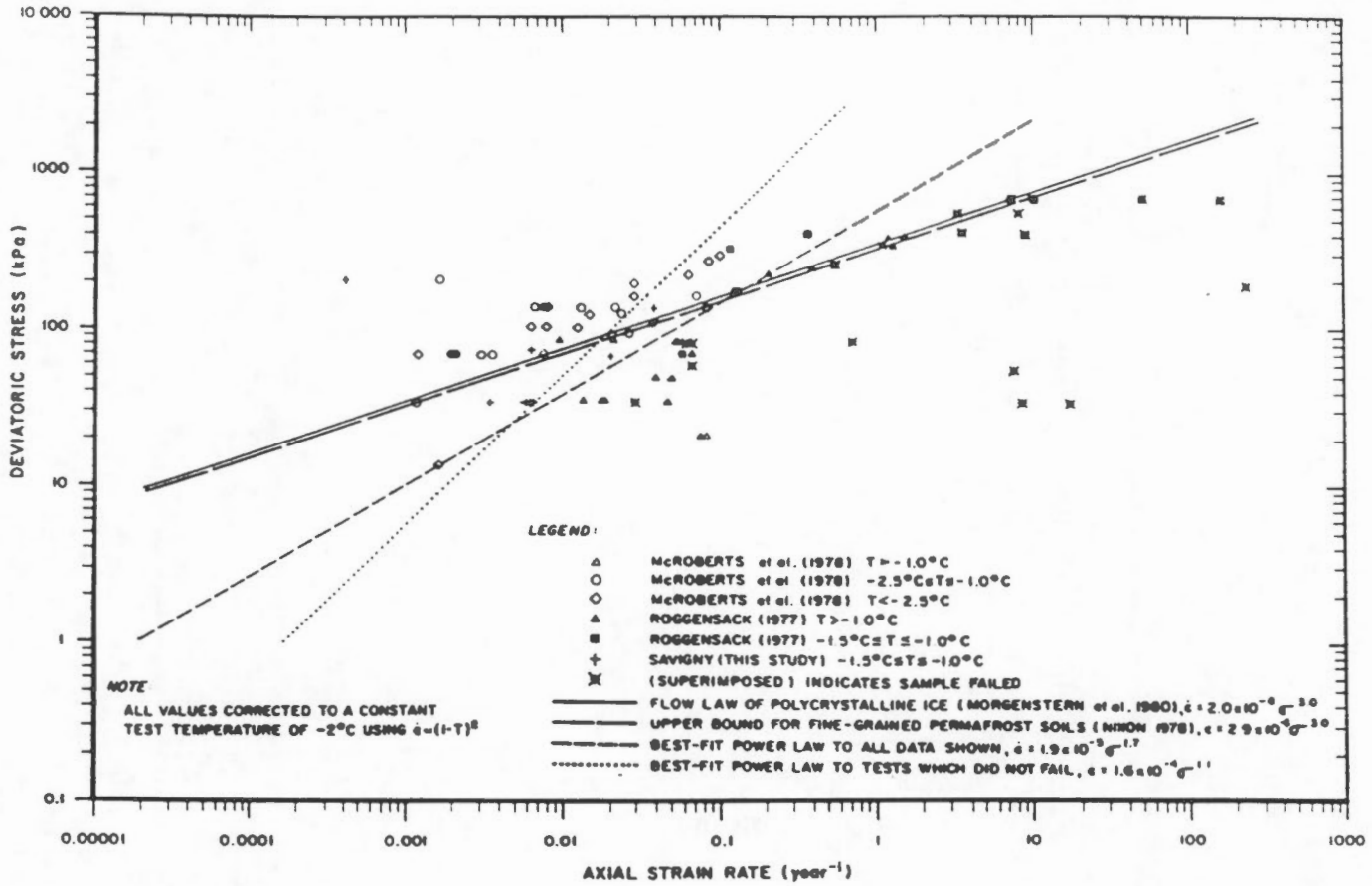

Steady state creep rate data for ice-rich glaciolacustrine clay from various locations in the Mackenzie Valley, N.W.T. (Savigny and Morgenstern, 1986).

THURBER

FIGURE 6.5

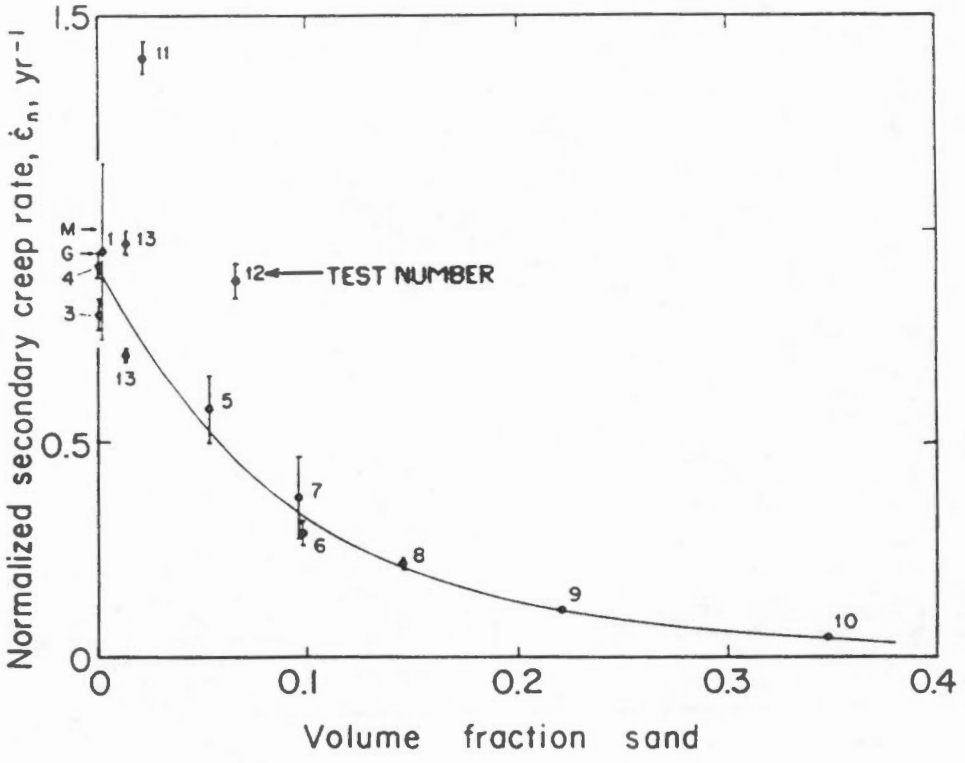

Normalized secondary creep rate versus volume fraction of sand (Hooke et al, 1972).

FIGURE 6.6

THURBER

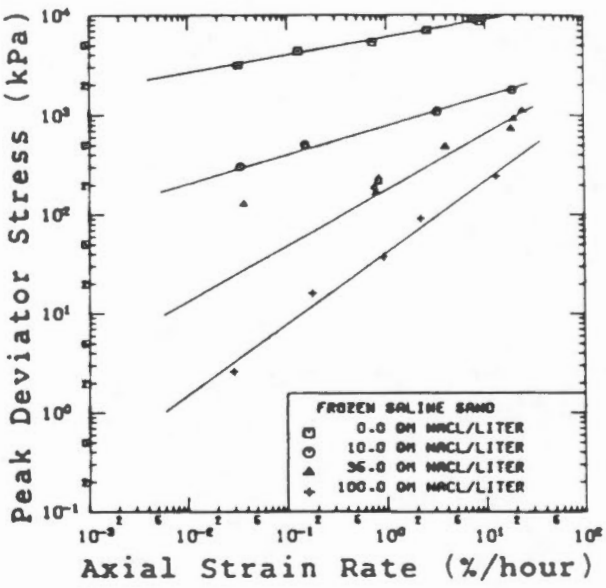

SOIL PROPERTIES

100% SAND	#10 TO #60 MESH
WATER CONTENT	16 - 19%
BULK DENSITY	18.9 TO 21.6 kN/m^3
TEMPERATURE	-7°C

CREEP PARAMETERS

SALINITY (ppt)	PROOF* STRESS (kPa)	n
0	1709.20	5.52
10	119.80	3.58
30	22.10	2.75
100	0.27	1.36

*proof stress determined at a strain rate of 0.001%/hour

Effect of pore fluid salinity on the secondary creep parameters of mortar sand at -7°C (Sego, 1982).

THURBER

FIGURE 6.7

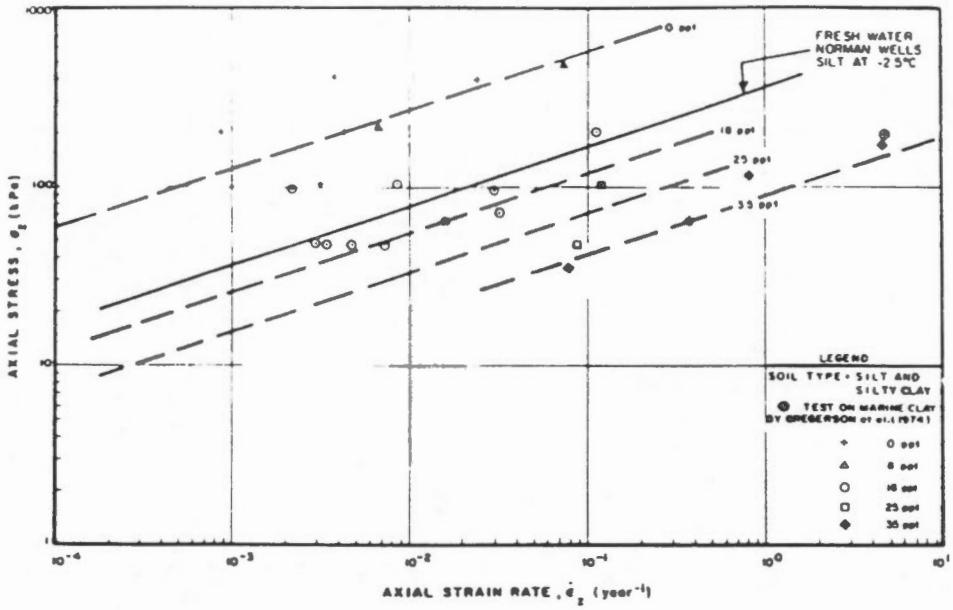

Effect of salinity on creep of frozen soils at -5°C (Nixon and Lem, 1984).

FIGURE 6.8

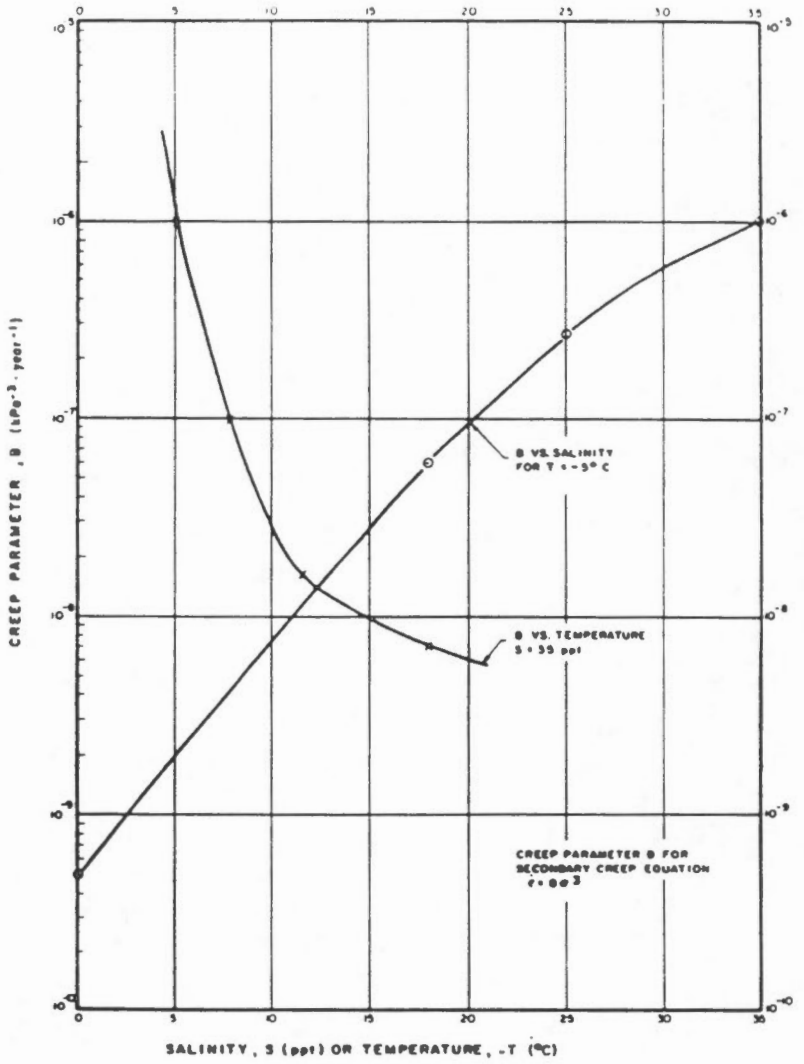

Relationship between the secondary creep parameter B, salinity and temperature (Nixon and Lem, 1984).

THURBER

FIGURE 6.9

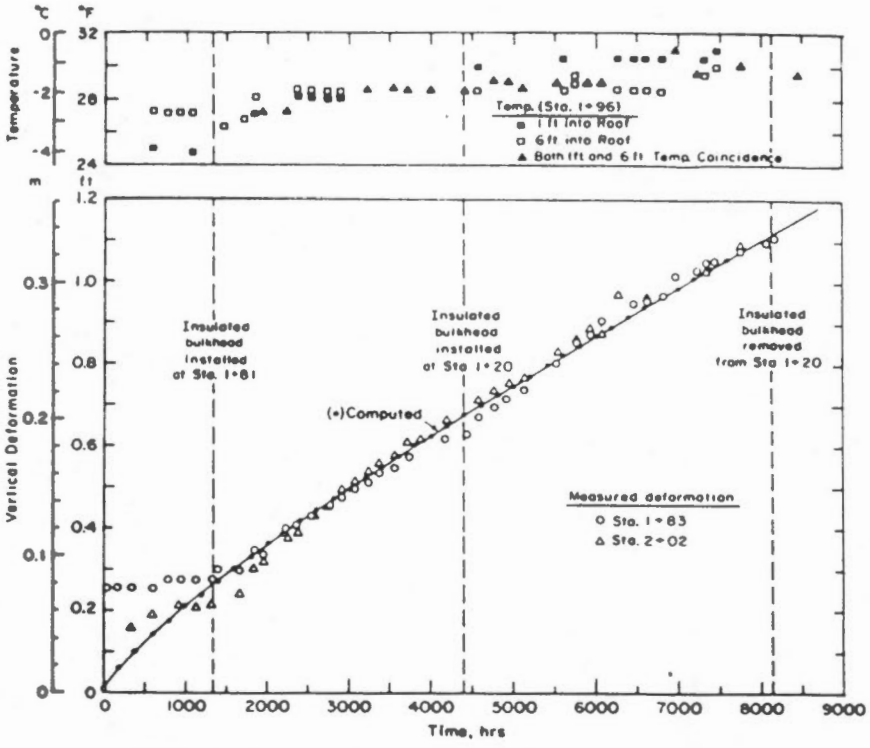

VERTICAL DEFORMATION AND TEMPERATURE VERSUS TIME

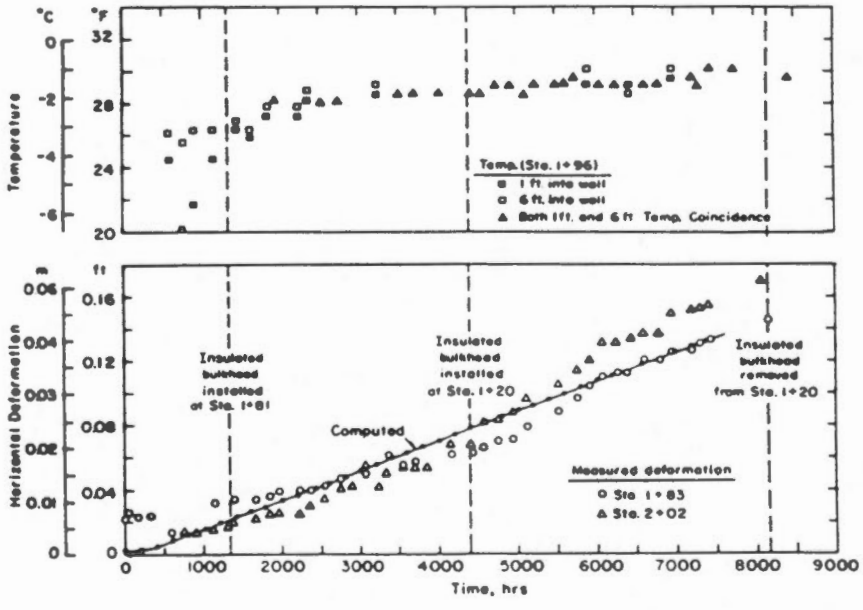

HORIZONTAL DEFORMATION AND TEMPERATURE VERSUS TIME

Observed vertical and horizontal deformations of a room in permafrost (Thompson and Sayles, 1972).

THURBER

FIGURE 6 .10

SECTION 7

STRENGTH PROPERTIES

SECTION 7

STRENGTH PROPERTIES

7.1 General

For many engineering design problems, it is necessary to consider possible failure of the frozen soil. The strength of ice and frozen soil is, however, time dependent, therefore the rate of load application and the duration of loading become important to the assessment of the strength of these materials.

The traditional method of establishing the time dependent strength of ice and frozen soil is to apply a constant stress to a cylindrical sample and determine time to failure (the onset of tertiary creep) as shown on Figure 7.1.

7.2 Vialov's Long Term Strength

Based on a series of constant stress creep tests, Vialov (1959) has suggested that the long term strength of ice or frozen soil could be established from short term constant stress tests, using an equation of the following form:

$$\sigma_f = \frac{\beta}{\log (t/B)} \qquad (7.1)$$

where

β and B are parameters which depend on soil type and temperature, and

t denotes the time to reach tertiary creep.

The parameters β and B are determined by plotting the reciprocal of the applied stress against the log of the time to failure. The parameters β and B can then be calculated from this plot as shown on Figure 7.1.

Sayles (1968) and Sayles and Haines (1974) carried out a series of tests to determine the creep strength of four different soils: Ottawa sand, Manchester fine sand, Hanover silt and Suffield clay. The duration of loading ranged up to 5000 hours (208 days).

THURBER

Their test results, together with the strength predicted using Equation 7.1 are shown in Figures 7.2, 7.3 and 7.4. The prediction of long term strength is seen to be reasonably good for Hanover silt and Suffield clay, but relatively poor for Ottawa sand and Manchester fine sand, particularly at the colder temperatures.

The instantaneous strength of each type of frozen soil was measured in unconfined compression tests at a constant displacement rate of 15% per minute. A summary of the measured instantaneous strength and the strength predicted at 100 years using Equation 7.1 for each soil type is presented in Figure 7.5.

The long term (100 year) strength is seen to range from 6 to 32 percent of the instantaneous strength, depending on soil type and temperature.

7.3 Failure Strain Concept

Recent research has indicated that ice and frozen soil will fail once the total strain reaches a specified value. On this basis, the long term strength can be established by rearranging Equation 6.1 to the following form:

$$\sigma_f = \sigma_{cuo}\left(\frac{\epsilon_f}{\dot{\epsilon}_o t_f}\right)^{1/n} \qquad (7.2)$$

where

$\dot{\epsilon}_o$ denotes strain rate under a proof stress σ_{cuo}

ϵ_f denotes the total strain at failure,

t_f denotes the time to failure under stress σ_f, and

n denotes the secondary creep exponent.

The time to failure, t_f in Equation 7.2 is normally taken as the design life of the structure times an appropriate factor of safety.

THURBER

The method of deriving the secondary creep parameters $\dot{\epsilon}_s$, σ_{ave} and n from the results of constant stress tests is illustrated in Figure 7.6, and is identical to the procedure described in Section 6 for establishing these parameters. As outlined previously in Section 6, the secondary creep also be established from constant displacement rate tests, as illustrated on Figure 7.7.

The accuracy to which the long term strength can be established from Equation 7.2 depends on the accuracy to which the secondary creep parameters can be determined. Hence the assessment of secondary creep behaviour (as discussed in Section 6) becomes extremely important to the assessment of the long term strength of ice and frozen soil.

The total strain at which failure will occur in the long term (ϵ_f) must be determined in order to use Equation 7.2. As shown on Figure 7.8, Sego and Morgenstern (1983) were able to demonstrate that the total strain at the onset of tertiary creep in the constant stress tests ranged from 0.4 to 1.8% for all levels of applied stress for both constant stress and constant displacement rate tests.

Parameswaran and Roy (1982) carried out a series of tests on frozen Ottawa sand at a temperature of -30°C. Their test results are presented in Figure 7.9. The results show that failure occurred at a total strain of between 1 to 1.5%. It is interesting that this result was obtained even for the very rapid rates of displacement (lower chart on Figure 7.9) where brittle failure occurred, rather than plastic failure.

The results of the foregoing studies indicate that the failure strain ϵ_f will be in the order of 1 to 1.5 percent. In some ice poor soils, however, the peak strength is not well defined and may occur at strains much greater than 2 percent. Further laboratory testing should be considered in order to confirm the strain at which failure takes place in ice poor soils.

It should be noted that in the very long term, both Equations 7.1 and 7.2 predict that the strength of ice and frozen soil will be zero. Most researchers believe that in the very long term, the strength of ice will be zero, while the strength of frozen soils will be equal to the thawed strength of the soil at the same void ratio as the frozen soil. This hypothesis, though reasonable, has never been proven.

It should be noted that validity of Equations 7.1 and 7.2 has only been established in laboratory tests which were undertaken for periods of up to 2 years. It is possible that under lower applied stresses, the behaviour of ice and frozen soils may be different from that observed in short term tests. For example, where stresses and creep rates are very low, recrystallization or healing processes may affect the deformation behaviour. It is possible that under such conditions creep rates may continue to decrease, such that tertiary creep is never reached. These aspects of the time dependent behaviour of ice and frozen soils appear worthy of further study.

It must be clearly understood that the use of Equation 7.2 implies that the ice or frozen soil behaves as a ductile continuum. Unfortunately, in the past, researchers have not always clearly differentiated between brittle failure (which takes place at relatively rapid strain rates) and ductile failure (which only takes place at relatively slow strain rates). No studies have been found in this review to indicate that there is a consistent relationship between brittle strength and ductile strength. This is an area in which a more detailed analysis of published data, compiled with laboratory tests, would appear to be of value.

In addition to time dependence, as discussed above, the strength of ice and frozen soil will also depend on the following variables:

- Confining stress,
- Temperature,
- Soil type,
- Ice content, and
- Unfrozen water content.

The effect which each of the foregoing variables has on the strength of ice and frozen soils is discussed in the following sections.

7.4 Confining Stress

As illustrated on Figure 7.10, a series of compression tests can be carried out (at a constant rate of displacement) to establish the failure stress under different confining stresses for a soil where all other variables (temperature, strain rate, soil type, etc) are held constant. The confining stress and the peak deviator stress can then

THURBER

be presented on a Mohr-Coulomb failure envelope under the specified test conditions. The failure envelope, derived from such tests, can be approximated by the following equation:

$$\tau_f = c + \sigma_m \tan \phi \qquad (7.4)$$

where

τ_f denotes the shear strength at failure.

c denotes the intercept of the failure envelope at zero confining stress.

σ_m denotes the mean confining stress acting on the sample.

ϕ denotes the angle of the failure envelope.

In unfrozen soils, the stresses on the sample may be expressed as effective stresses (total stresses minus the pore pressure in the sample) or as total stresses. In frozen soils, the stresses are commonly expressed as total stresses, unless the soil contains a significant unfrozen water content, in which case the stresses can be expressed either as total stresses or effective stresses.

The effect which confining stress will have on the strength of frozen soil will depend on the unfrozen water content.

7.4.1 No Unfrozen Water

In frozen soil where no unfrozen water is present, the short term, unconfined shear strength will generally range from 1000 to 5000 kPa, depending on temperature and strain rate. The confining stress σ_m in most civil engineering problems will range from 0 to 150 kPa, and hence the frictional term (σ_m Tan ϕ) in Equation 7.4 is small and can be neglected. In that case, Equation 7.4 reduces to:

$$\tau_f = \frac{\sigma_u}{2} = c_u \qquad (7.5)$$

THURBER

where

σ_u denotes the unconfined compressive strength, and

c_u denotes the unconfined shear strength.

As noted earlier, the long term strength of frozen soil is relatively low and hence the frictional component of strength may become significant. In addition, the frictional component becomes significant when confining stresses are very high.

Sayles (1973) investigated the effect of confining stress on the behaviour of ice and ice saturated soils in a series of direct shear tests, at high confining stresses. His test results are presented in Figure 7.11. The results demonstrate that significant increases in the shear strength of ice and frozen soils can be expected at high confining stresses. It is of interest that the strength envelopes for both ice and sand are curvilinear, behaviour which is common in unfrozen dense sands and heavily over consolidated clays.

As shown Figure 7.11, the confining stress applied to the samples in these tests ranged up to 28,000 kPa (4000 psi). This is very much higher than the range in confining stress normally encountered in geotechnical engineering practice.

7.4.2 High Unfrozen Water Content

For unsaturated frozen soils or frozen soils in which unfrozen water contents are high, the contribution to strength of the ice phase may be low, and hence the contribution to strength due to the frictional component ($\sigma_m \tan \phi$) may become significant. If the unfrozen water content is high enough, continuity throughout the pore fluid will occur and therefore drainage will result as the external confining stress is increased. As a result of this process, the strength of frozen soils which have high unfrozen water contents (for example saline soils or frozen clays at temperatures between 0 and -2°C) will increase as confining stress increases.

Ladanyi (1972) has proposed the following equation to account for the effects of confining stress in frozen soils which have a significant unfrozen water content and which can therefore consolidate when confining stress in applied:

THURBER

$$(\sigma_1-\sigma_3)_f = [\sigma_{cuo}+\sigma_3\ (f-1)] \left(\frac{\epsilon_f}{\dot{\epsilon}_o t_f} \right)^{1/n} \qquad (7.6)$$

where

$(\sigma_1-\sigma_3)_f$ denotes the deviator stress at failure,

σ_{cuo} denotes the unconfined compressive strength at a strain rate of $\dot{\epsilon}_o$,

σ_3 denotes the confining stress,

ϵ_f, t_f and n are as defined for Equation 7.2, and

$$f = \frac{1 + \sin \phi}{1 - \sin \phi} \qquad (7.7)$$

where

ϕ denotes the angle of friction of the soil which is approximately equal to the thawed angle of friction of the soil.

Roggensack (1977) carried out a series of tests which appear to confirm the relationship given in Equation 7.6 and shown schematically Section 5, Figure 5.5. Direct shear tests were carried out on samples of natural silty clay, at a temperature of -1.5°C, at various normal pressures and strain rates. The clay content of these samples ranged from 50 to 80% and hence the samples would contain significant unfrozen water at the test temperature.

A cohesion intercept and angle of friction was derived from the data at each strain rate, as indicated Figure 7.12. The angle of internal friction ranged from 16° to 23° depending on the strain rate, and generally increased as strain rate decreased. The cohesion intercept decreased as strain rate decreased. The values for the cohesion intercept are plotted as a function of time on Figure 7.13 and show a linear relationship between the cohesion intercept and the log of the time to failure (peak shear stress). Based on these results, a cohesion value of 0 would be obtained at about 100,000 hours (11 years) which for this material and test conditions appears reasonable.

THURBER

Roggensack has also plotted a similar set of data from tests carried out on Ottawa Sand by Sayles (1973) as shown on Figure 7.13. Based on Sayles' data, the cohesion for frozen sand would be zero at about 2,500 hours (4 months). This does not seem reasonable in view of the fact that most adfreeze piles are backfilled with frozen sand and have sustained adfreeze shear stresses greatly in excess of the frictional component alone, for periods of 5 to 10 years.

The unconfined shear strength of pure ice (from Sego and Morgenstern, 1983) has been plotted on Figure 7.13. While there is considerable scatter, the data shows a decrease in unconfined shear strength as strain rate is reduced. The relationship between unconfined shear strength and the logarithm of time for ice appears to be curvalinear, as indicated on Figure 7.13. Similarly, the relationship for soils may also be curvalinear. Further analysis of the available data, together with additional laboratory testing would be required before definite conclusions can be drawn with respect to the long term strength of frozen soils. This is an area in which further research appears to be worthwhile.

It would appear that further research into the effect of confining stress on the strength of frozen soils with and without unfrozen water content might be worthwhile.

7.5 Temperature

As might be expected, the short term strength of ice and frozen soils is temperature dependent with strength generally increasing as temperature is reduced.

Sayles (1966) summarized test results obtained from a variety of sources to demonstrate the variation in unconfined compressive strength of ice and a variety of frozen soils in the temperature range from 0 to -150°C. These results are presented in Figure 7.14. Soil properties for the soils shown were not obtained, however, the relative strength of the sand, silt, clay and ice can be observed. It should be noted that as the temperature approaches the thawing point, the strength of silt and clay drop below that of ice. This is due to the presence of unfrozen water at these higher temperatures.

THURBER

Bourbonnais and Ladanyi (1985) carried out a series of unconfined compression tests on sand (ASTM C-778 Standard Sand) down to temperatures of -160°C. These results, together with a summary of results reported by others are presented on Figure 7.15.

Kaplar (1971) reported the results of unconfined compressive strength tests for a variety of soils over a temperature range from 0 to -25°C. The results are presented on Figure 7.16. Kaplar also carried out a series of tests to measure the tensile strength of various types of frozen soils as a function of temperature, and these results are also presented on Figure 7.16. This figure shows that the tensile strength of a frozen soil is much less than the compressive strength, at a given temperature.

Haynes and Karalius (1977) reported the results of uniaxial compression and tension tests on Fairbanks Silt for temperatures down to -60°C. The test results are presented in Figure 7.17. The test results indicate that the tensile strength of frozen soil is more sensitive to temperature than the compressive strength at temperatures above about -5°C. At temperatures below about -10°C, however, the tensile strength becomes relatively insensitive to temperature, but the compressive strength continues to increase with decreasing temperature.

Ladanyi (1988) has provided a summary of the relationship between compressive strength and temperature for many of the soils tested by CRREL. The results are shown on Figure 7.18, together with the gradations of the various soils. A summary of the soil properties for these soils is tabulated on Figure 7.19.

Based largely on the results of the foregoing tests, the following empirical relationship between compressive strength and temperature has been accepted by many researchers:

$$\sigma_{c\theta} = \sigma_{co} (1 + \theta/\theta_c)^{k} \qquad (7.8)$$

where

$\sigma_{c\theta}$ denotes the short term compressive strength at temperature θ. The temperature is the absolute value of temperature in °C below freezing,

THURBER

σ_{co} denotes a reference stress obtained by extrapolating the results of unconfined compression tests at different temperatures back to 0°C,

θ_o denotes an arbitrary absolute value of temperature commonly taken as 1°C,

k denotes the temperature exponent.

The temperature reference stress (σ_{co}) and the temperature exponent (k) are readily derived from experimental data by plotting the log of unconfined compressive strength versus the log of $(1 + \theta/\theta_o)$. The technique is illustrated in Figure 7.20. The calculated value for σ_{co} is substituted for σ_{cuo} in Equations 7.2 or 7.6.

Figure 7.21 (Sayles and Haines, 1974) demonstrates that there is some basis for a normalized power law relationship of the form of Equation 7.8, because actual data does plot linearly. Typical values for k and σ_{co} for ice and various soils have been derived by Ladanyi (1988) and are as follows:

Soil	σ_{co} (kPa)	k
Suffield Clay	170	1.20
Bat-Baioss Clay	180	0.97
Hanover Silt	2250	0.87
Callovian Silt	310	0.89
Ottawa Sand	1050	1.00
Manchester Fine Sand	160	1.00
Polycrystalline Ice (or ice-rich soil)	103	0.37

7.6 Soil Type

As indicated on Figures 7.14 to 7.18, the short term compressive strength of soil depends not only on temperature but on soil type as well.

In general, the available data indicates that as the clay content of the soil increases, the unconfined strength decreases. This may be due to two effects. First of all, the unfrozen water content of fine grained soils (such as

THURBER

clays) is generally higher at a given temperature as compared to coarse grained soils (such as sands and gravels). Secondly, the angle of internal friction is generally lower for normally consolidated fine grained soils (25 to 30°) as compared to coarse grained soils (30 to 35°).

7.7 Ice Content

The effect which ice content has on the short term strength of frozen soil has been studied by a number of researchers. The test results reported by Kaplar (1971) which are presented in Figure 7.22 can be considered typical.

Where the ratio of the volume of ice to volume of soil is less than about 10 percent, (which corresponds to a water content of about 4 percent) the soil is essentially dry and the contribution to strength of interstitial ice is negligible.

As the water content exceeds 10%, the compressive strength is seen to increase dramatically. The maximum compressive strength is obtained at a water content of about 25%. At this water content, this soil, if thawed, would be in a loose saturated state. That is, it contains no excess ice. As the water content increases above 25% (and the excess ice content increases) the unconfined strength decreases dramatically as indicated on Figure 7.22.

Baker (1979) carried out a series of tests to establish the relationship between moisture (ice) content and compressive strength of Ottawa fine sand. The results of these tests are presented in Figure 7.23. The shape of the curve is similar to that reported by Kaplar, as shown on Figure 7.22.

The effect which the degree of ice saturation has on the short term strength of Ottawa sand was investigated by Alkire (1972), who obtained the interesting results presented on Figure 7.24. The tests were carried out at two different confining pressures (0 and 4830 kPa), and at two different degrees of ice saturation (59% and 98%). As indicated on Figure 7.24, the degree of ice saturation had a significant effect on the unconfined strength, but not on the confined strength.

7.8 Unfrozen Water Content

As unfrozen water content increases, the compressive strength of frozen soil will decrease. The unfrozen water

THURBER

content of frozen soil at a given temperature will be controlled by two factors:

- Grain size distribution, and
- Pore water salinity.

Haynes and Karalius (1977) carried out a series of unconfined compressive strength tests on Fairbanks Silt in order to establish the relationship between unconfined compressive strength and temperature. The unfrozen water content was calculated at each temperature using data from previous studies. The results are presented on Figure 7.25. In the case of Fairbanks Silt, the unfrozen water content is controlled by the grain size distribution of this material.

Baker and Kurfurst (1985) carried out a series of unconfined compression tests on frozen Ottawa fine sand, in which the pore fluid salinity was varied. The test results are presented on Figure 7.26 and illustrate a dramatic reduction in unconfined strength as salinity increases from 0 to 2 parts per thousand (ppt). These results may have been affected by the procedure used to freeze the saline samples, which may have resulted in a non-uniform distribution of pore fluid salinity within the sample. This has not been confirmed.

Stuckert and Mahar (1984) reported the results of a series of unconfined compression tests on frozen samples of Monterey uniform sand (D_{50} = 0.6 mm). The samples were prepared with a range of pore fluid salinities. The results of these tests are presented in the upper half of Figure 7.27. For each salinity concentration, these authors established the freezing point of the brine. They then tested each soil sample at a constant temperature below the freezing point of the brine. This makes it very difficult to apply their results in practice. In any event, the results demonstrate a significant reduction in unconfined compressive strength as pore fluid salinity increases.

Sego and Chernenko (1984) carried out a series of triaxial tests on samples of frozen mortar sand with pore fluid salinities ranging from 0 to 50 ppt. Test temperatures were maintained relatively constant, but ranged from -6.8 to -7.3°C. Tests were carried out at various confining stresses, so that the angle of friction and cohesion intercept could be determined for each value of pore fluid salinity. The results are presented on the lower half of Figure 7.27. As shown, these authors found a significant decrease in the cohesion intercept as pore fluid salinity

THURBER

increased from 0 to 10 ppt. The angle of internal friction rose to about 38° at a pore fluid salinity of 10 ppt and remained constant thereafter.

The foregoing results indicate the significant effect which salinity (and by inference unfrozen water content) has on the strength of frozen soil. Unfortunately, it is not possible to compile the existing information into a consistent format, because the various researches have used different testing procedures, strain rates and soil types. Consideration should be given to undertaking a comprehensive laboratory testing program to establish the strength properties of frozen soil over a range of temperatures, pore water salinities and clay contents, so that a consistent set of data could be made available for use by designers.

7.9 Summary

One of the major difficulties is interpreting between brittle failure (which occurs at relatively rapid strain rates) and ductile failure (which occurs only at relatively slow strain rates). The strain rate under which brittle failure will occur will depend on soil type and temperature. The strength measured in brittle failure is often not overly sensitive to strain rate. The relationship between brittle strength and ductile strength has not been investigated in a systematic way. This may be an area in which further research would be useful.

The theoretical relationships currently available appear to provide an excellent framework within which the strength behaviour of ice and frozen soil can be interpreted. The theory readily incorporates the major variables which affect strength, including time dependent behaviour, temperature, confining stress, soil type, ice content and unfrozen water content.

Unfortunately, no systematic laboratory studies have been undertaken to establish the validity of the theory over a broad range of temperatures and soil types. Consideration should be given to undertaking such a study.

At the present time, the long term strength of ice and frozen soils is established by extrapolating short term strength data. Such a procedure may not be valid if processes such as ice recrystallization or other healing mechanisms occur over a long period of time at low stress levels and strain rates in a manner which differ from that observed in the laboratory. This is an area in which further research would appear to be worthwhile.

THURBER

The current definition of long term failure strain should be reviewed. The current definition (the onset of tertiary creep) may be overly conservative at low stresses. This is an area in which further research should be considered.

A number of important laboratory investigations into the strength of frozen saline soils have been completed, and have provided considerable insight into the behaviour of these materials. These tests have generally been carried out on samples with relatively high void ratios. Preliminary information indicates that saline soils often exist at relatively low void ratios. Research into the creep and strength behaviour of saline soils at relatively low void ratios (high densities) should be considered.

STRENGTH PROPERTIES

LIST OF REFERENCES

Andersland, O.B. and Anderson, D.M., 1978. Geotechnical Engineering for cold regions. McGraw-Hill Book Company, New York, 566 p.

Andersland, O.B., Sayles, F.H., and Ladanyi, B., 1978. Mechanical properties of frozen ground. Chapter 5 in Geotechnical engineering for cold regions. (Andersland and Anderson, 1978).

Baker, T.H., 1978. Strain rate effect on the compressive strength of frozen sand. Engineering Geology, Vol. 13, pp. 223-231, Elsevier, Amsterdam.

Baker, T.H., and Kurfurst, P.J., 1985. Acoustic and Mechanical properties of frozen sand. Proc. of the Fourth Int. Symposium on ground freezing. pp. 227-234, Sapporo, Japan.

Bourbonnais and Ladanyi, 1985. The mechanical behaviour of frozen sand down to cryogenic temperatures. Proc. of the Fourth Int. Symposium on ground freezing. pp. 235-244, Sapporo, Japan.

Haynes, F.D., and Karalius, J.A., 1977. Effect of temperature on the strength of frozen silt. U.S. Army Corps of Engineers, CRREL Report 77-3, Hanover, NH.

Kaplar, C.W., 1971. Some strength properties of frozen soil and effect of loading rate, U.S. Army Corps of Engineers, CRREL, Hanover, NH.

Klein, J., Dr. Ing., 1985. Handbuch Des Gefrierschachtbaus Im Bergbau, Verlag Gluckauf GmbH., Essen.

Ladanyi, B., 1972. An engineering theory of creep in frozen soils. Can. Geot. Journ. Vol. 9, p. 63.

Parameswaran, V.R. and Roy, M., 1982. Strength and deformation of frozen saturated sand at -30°C. Can. Geot. Journ., Vol. 19, pp. 104-107.

Roggensack, W.D., 1977. Geotechnical properties of fine-grained permafrost soils. Ph.D. thesis, University of Alberta, Edmonton, Alberta, 449 p.

THURBER

LIST OF REFERENCES
(continued)

Sayles, F.H., 1966. Low temperature soil mechanics. Tech. Note, U.S. Army, CRREL, Hanover, NH.

Sayles, F.H., 1968. Creep of frozen sand. U.S. Army Cold Regions Research and Engineering Laboratory, Technical Report 190, 54 p.

Sayles, F.H., 1973. Triaxial and creep tests on frozen Ottawa sand. Proceedings, 2nd International Conference on Permafrost, Yakutsk, USSR, North American Contribution, pp. 384-391.

Sayles, F.H., and Haines, D., 1974. Creep of frozen silt and clay, U.S. Army, Corps of Engineers, Cold Regions Research and Engineering Laboratory, Hanover, NH, Technical Report 252, 50 p.

Sego, D.C. and Chernenko, D., 1984. Confining pressure influence on the strength of frozen saline sand. Proceedings of the Third Int'l. Specialty Conf. on Cold Regions Engineering, Edmonton, Alberta, pp. 565-578.

Sego, D.C., and Morgenstern, N.R., 1983. Deformation of ice under low stresses. Can. Geot. Journ., Vol. 20, pp. 587-602.

Sego, D.C., Shultz, T., Banasch, R. Strength and deformation behaviour of frozen saline sand. Proc. of the Third Int'l Symposium on Ground Freezing, CRREL, Hanover, NH, pp. 11-17.

Stuckert, J.A., and Mahar, L.J., 1984. The role of ice content in the strength of frozen saline coarse grained soils. Proceedings of the Third Int'l Specialty Conf. on Cold Regions Engineering, Edmonton, Alberta, pp. 579-588.

Vyalov, S.S. (Editor) 1959. Geological properties and bearing capacity of frozen soils. U.S. Corps of Engineers, Cold Regions Research and Engineering Laboratory, Hanover, NH, Army Translation No. 74. 219 p. (Translated from Russian in 1965).

THURBER

LIST OF FIGURES

THURBER

LIST OF FIGURES
(continued)

THURBER

LIST OF FIGURES
(continued)

THURBER

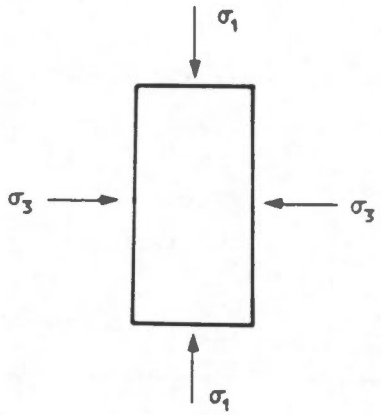

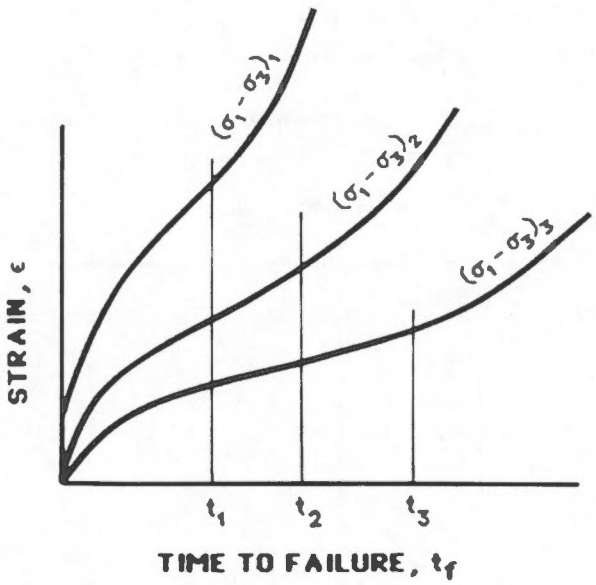

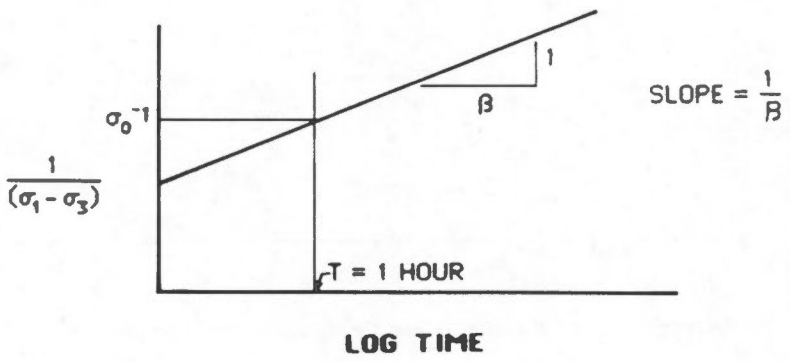

$$\sigma_f = \frac{\beta}{\log(t_f/B)} \qquad \log\frac{1}{B} = \frac{\beta}{\sigma_0}$$

The determination of Vialov's long term strength from constant stress tests.

FIGURE 7 1

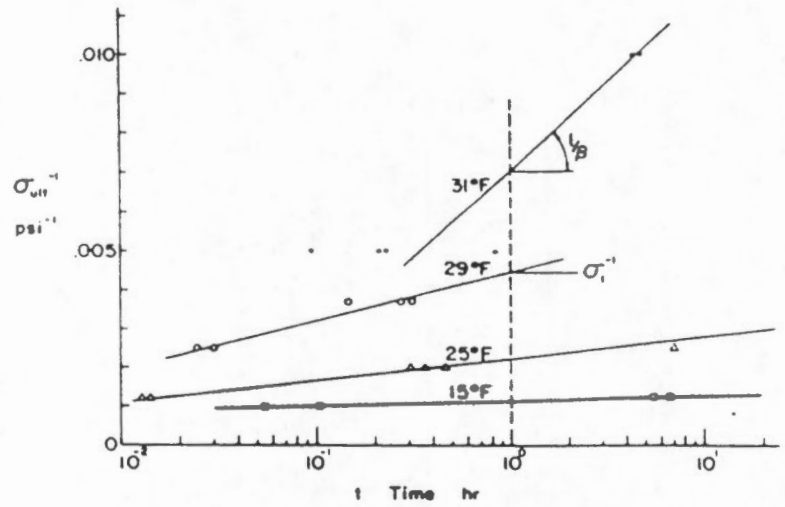

Determination of β and B values for Vialov's strength equation:

$$\sigma_u = \frac{\beta}{\log (t/B)} \qquad \frac{1}{\beta} = \text{slope} \qquad \log \frac{1}{B} = \frac{\beta}{\sigma_1}$$

a. *Hanover silt.*

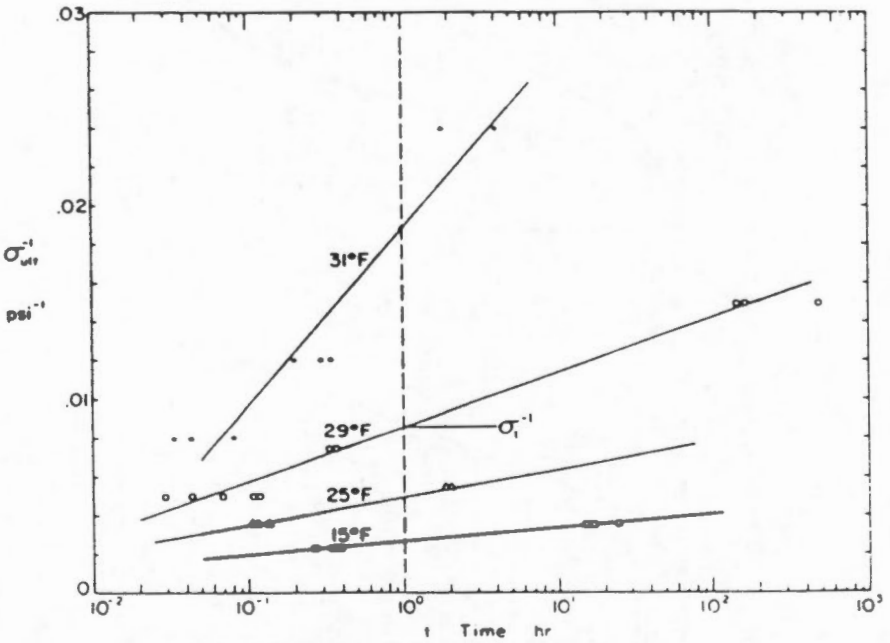

Determination of β and B values for Vialov's strength equation:

$$\sigma_u = \frac{\beta}{\log (t/B)} \qquad \frac{1}{\beta} = \text{slope} \qquad \log \frac{1}{B} = \frac{\beta}{\sigma_1}$$

b. *Suffield clay.*

Calculation of long term strength using Vialov's equation for strength (Sayles and Haines, 1974).

THURBER

FIGURE 7.2

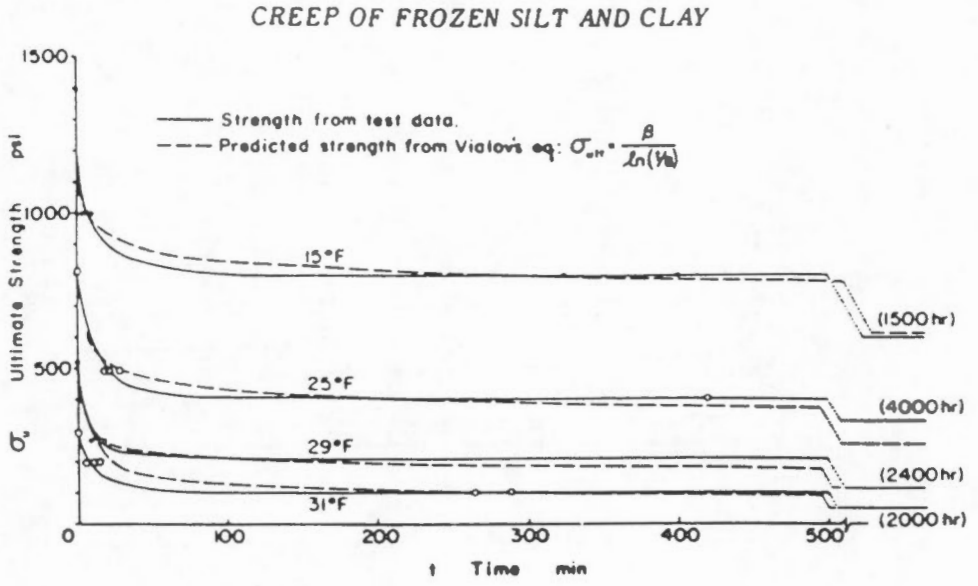

Hanover silt.

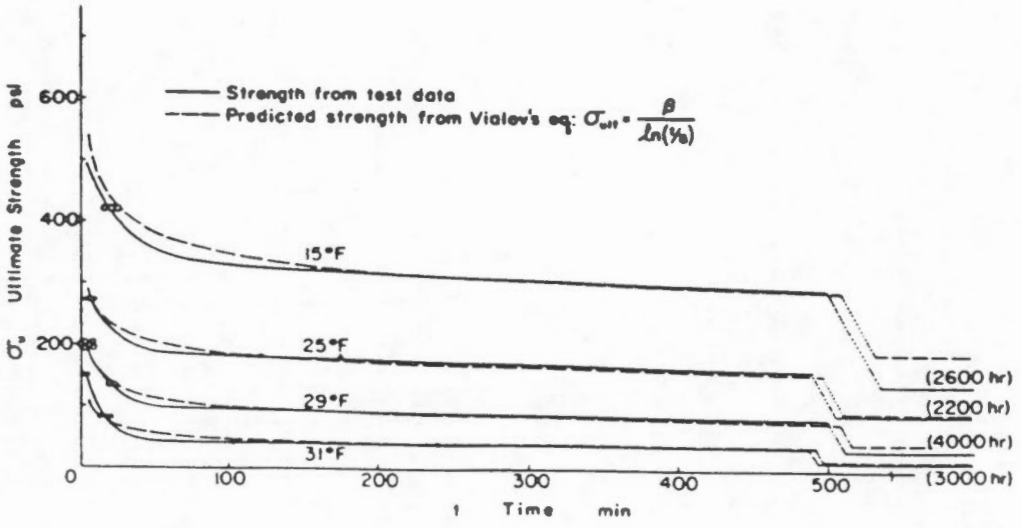

Suffield clay.

Measured and predicted long term strengths for Hanover silt and Suffield clay (Sayles and Haines, 1974).

FIGURE 7.3

THURBER

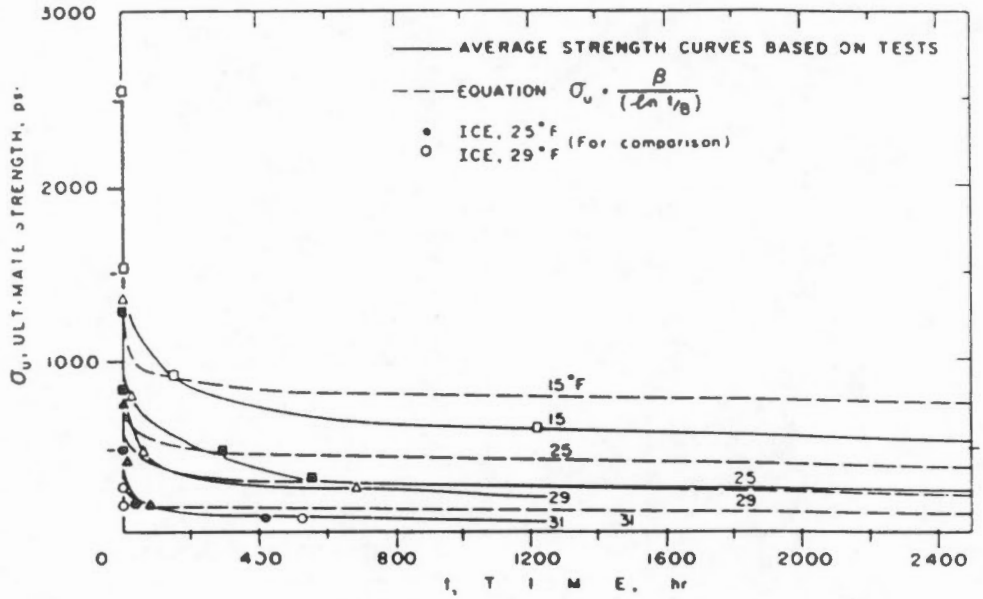

Ultimate strength and time to failure, Ottawa sand (20-30).

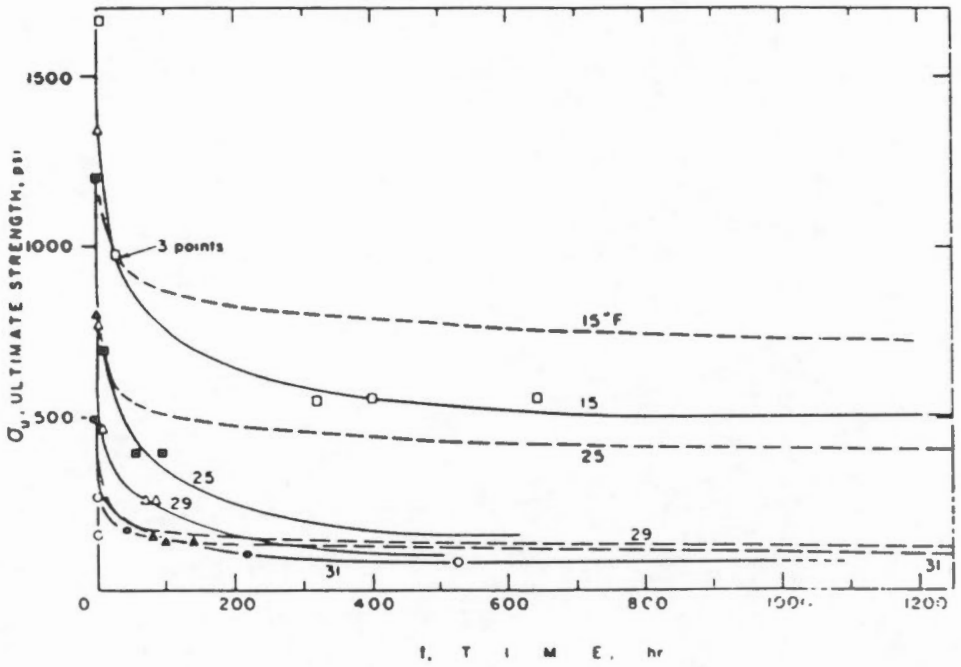

Ultimate strength and time to failure, Manchester fine sand.

Measured and predicted long term strengths for Ottawa sand and Manchester fine sand (Sayles, 1968).

THURBER

FIGURE 7.4

Soil	Temperature (°C)	Instantaneous Strength (kPa)	Predicted Strength (100 years) (kPa)	100 Years Strength/ Instantaneous (%)
Ottawa Sand	-9.5	17400	2900	17.
Ottawa Sand	-3.9	10000	1750	17.
Ottawa Sand	-1.7	9100	920	10.
Ottawa Sand	-0.6	5100	480	11.
Manchester Sand	-9.5	19200	2300	12.
Manchester Sand	-3.9	13800	1200	9.
Manchester Sand	-1.7	9200	790	9.
Manchester Sand	-0.6	5500	430	8.
Hanover Silt	-9.5	9900	3140	32.
Hanover Silt	-3.9	5600	1140	20.
Hanover Silt	-1.7	3600	510	14.
Hanover Silt	-0.6	2000	190	10.
Suffield Clay	-9.5	4900	840	17.
Suffield Clay	-3.9	3090	440	14.
Suffield Clay	-1.7	2300	230	10.
Suffield Clay	-0.6	1420	83	6.

Note: Instantaneous strength was measured in unconfined compression tests at a strain rate of 15% per minute.

Predicted 100 year strength as a percentage of the instantaneous strength (after Sayles, 1968 and Sayles and Haines, 1974).

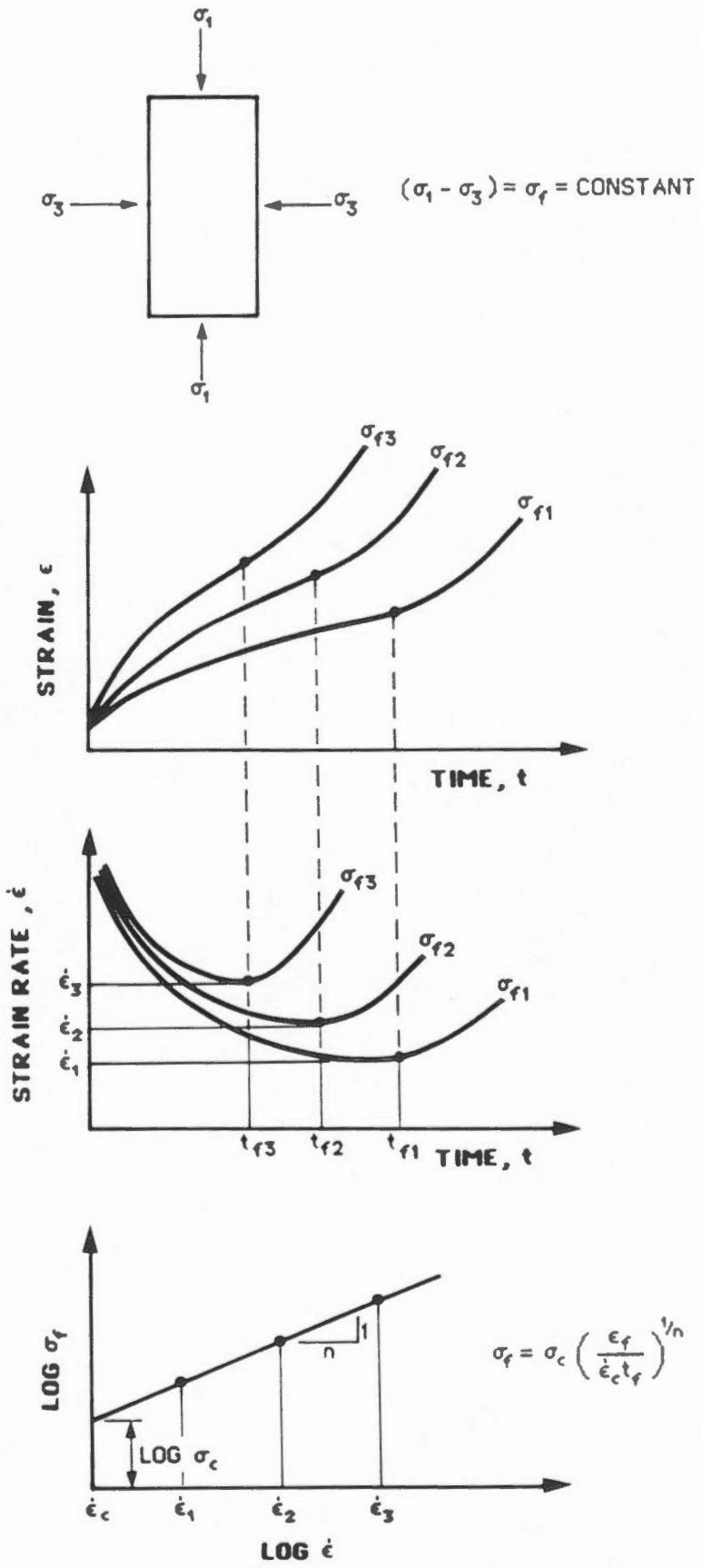

The determination of long term strength from constant stress tests, using the failure strain concept.

FIGURE 7.6

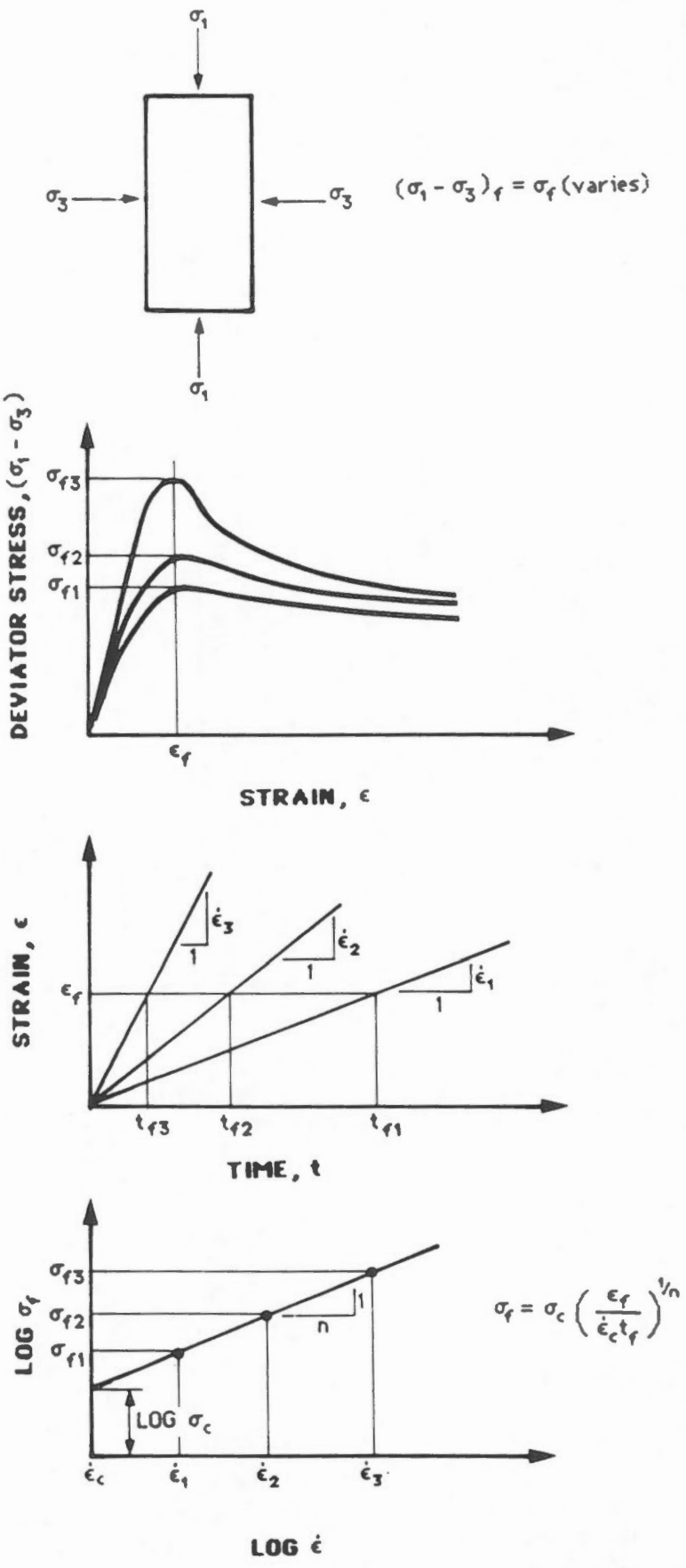

The determination of secondary creep parameters from constant displacement rate tests.

FIGURE 7.7

THURBER

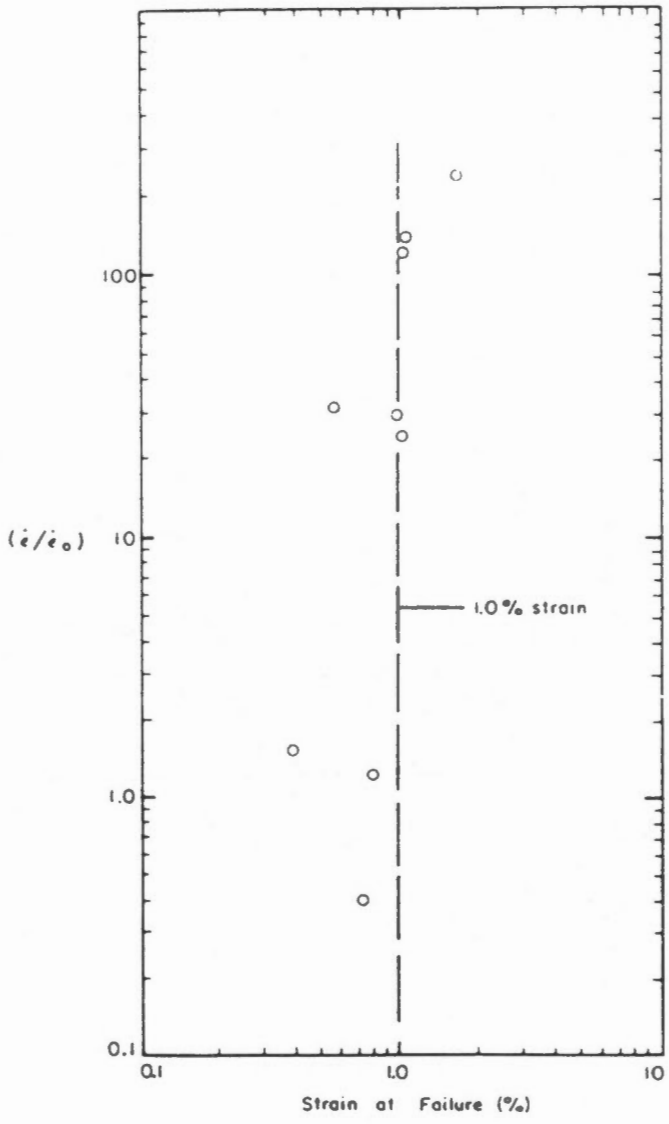

Normalized strain rate versus axial strain at the onset of tertiary creep of laboratory data.

Failure strains from constant stress and constant displacement rate tests on pure ice (Sego and Morgenstern, 1983).

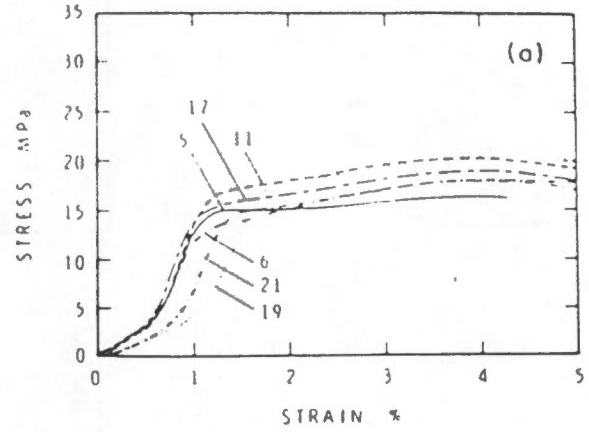

$\dot{\epsilon}$ = 0.2 to 1%/hour

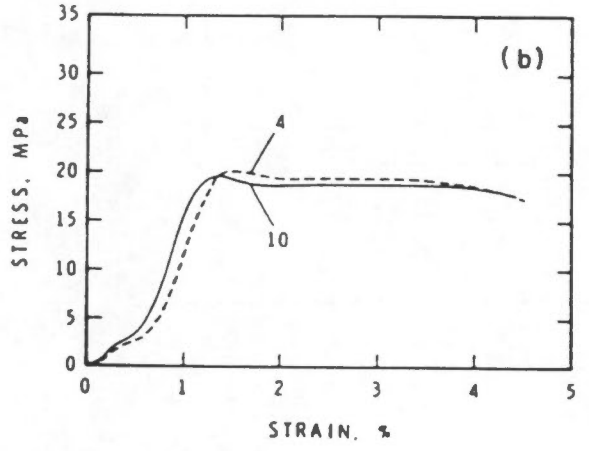

$\dot{\epsilon}$ = 2.1 to 2.4 %/hour

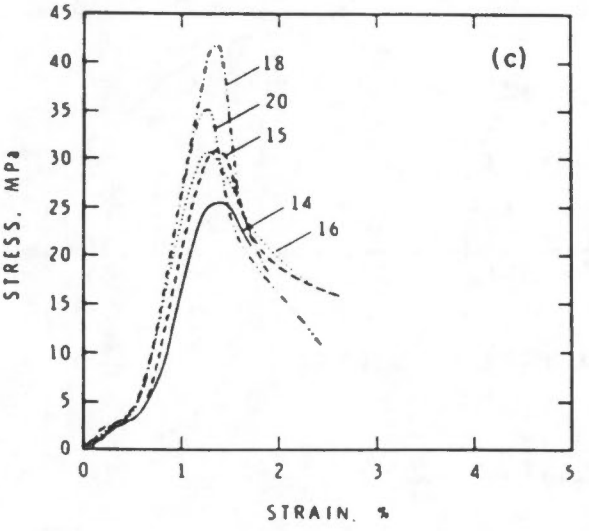

$\dot{\epsilon}$ = 18 to 2160 %/hour

SOIL DATA

Ottawa Sand
0.2 - 0.6 mm grain size
T = -30°C
w = 20%
S = 1

Stress-strain curves for frozen Ottawa sand at various strain rates (Parmeswaran and Roy, 1982).

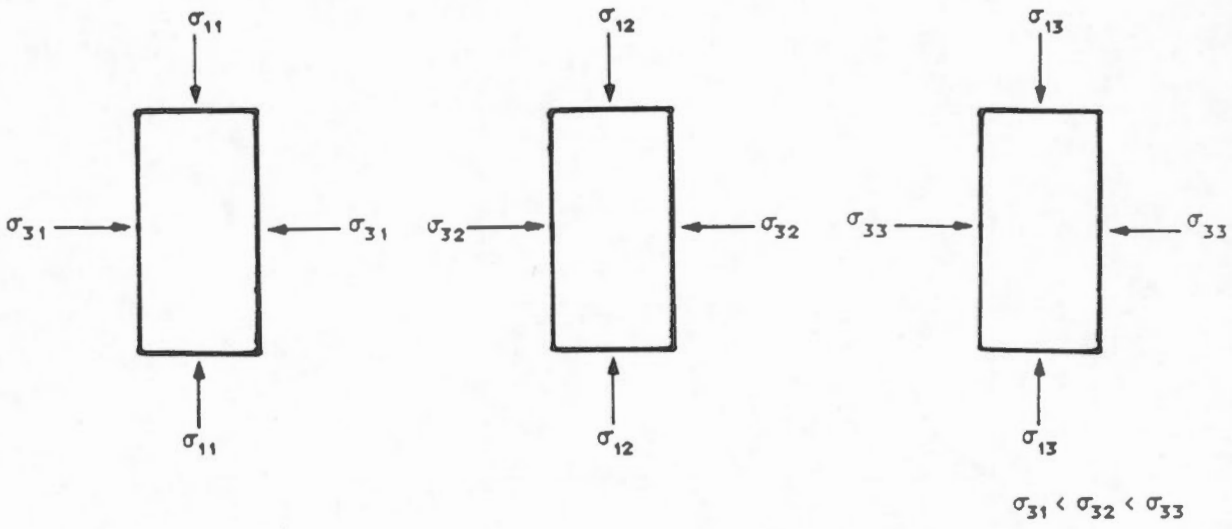

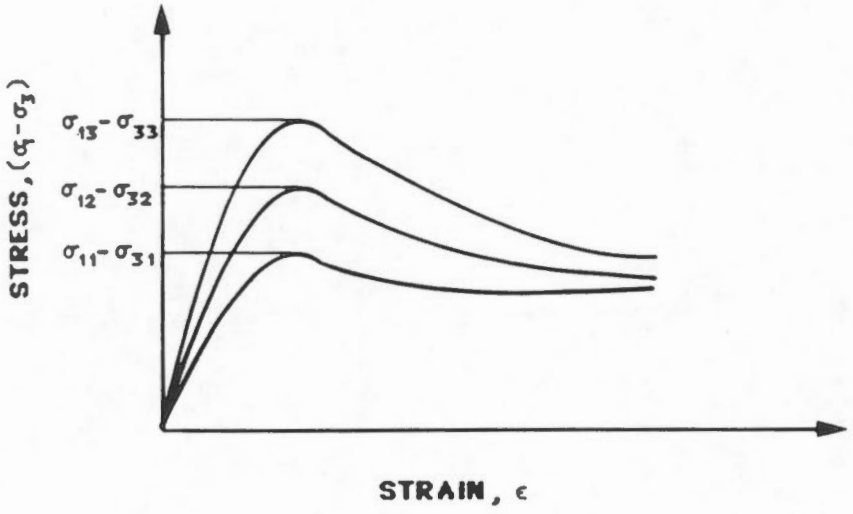

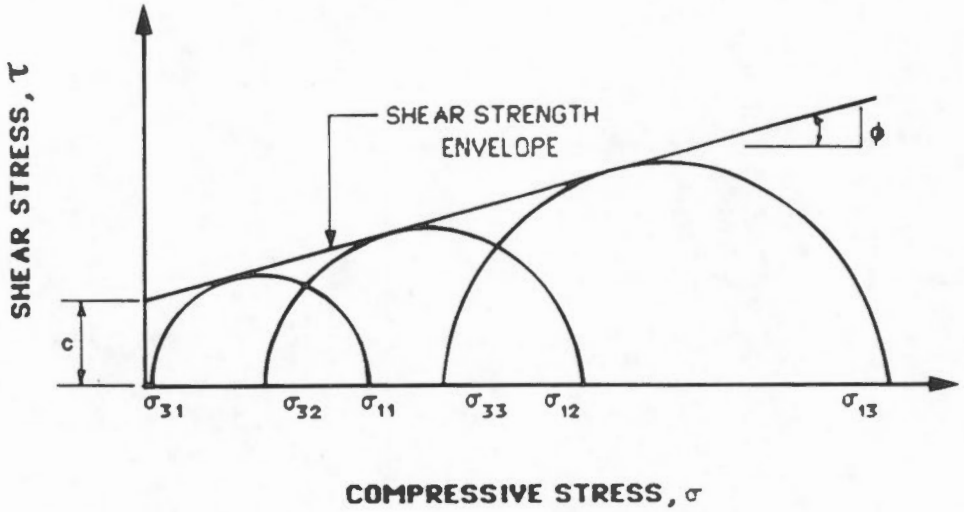

$$\tau_f = c + \sigma_m \tan\phi; \quad \sigma_m = \frac{\sigma_1 + \sigma_3}{2}$$

The effect of confining stress on the strength of frozen soil.

FIGURE 7.10

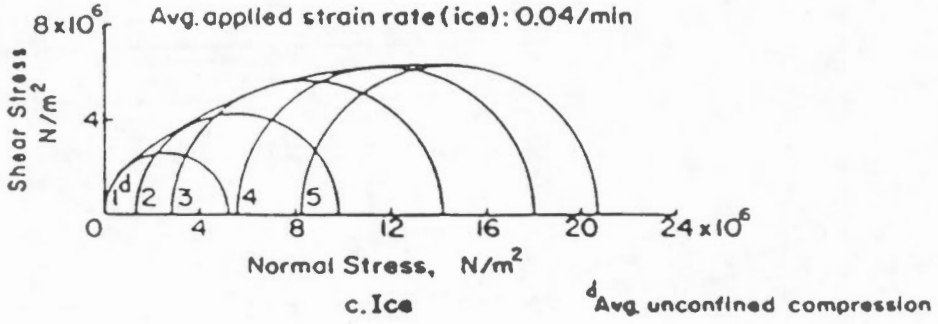

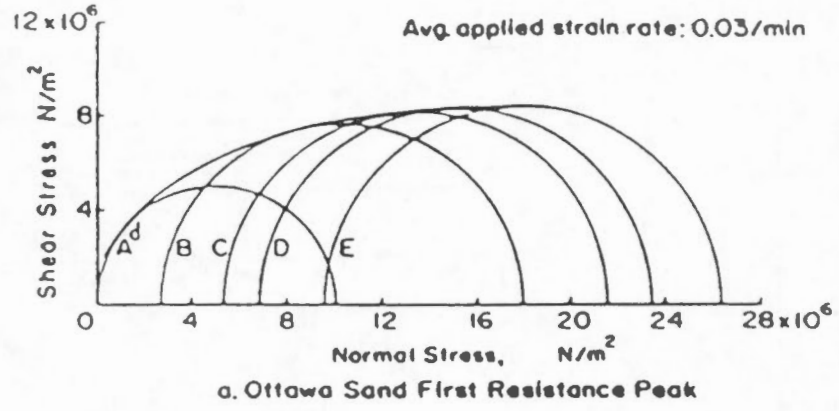

Ottawa Sand: 20 to 30 mesh
Dry Density: 16.4 kN/m^3
Degree of Saturation: 100%
Water Content: 22%
Temperature: -3.85°C

Failure envelopes for frozen Ottawa sand and ice (Sayles, 1973).

THURBER

FIGURE 7 11

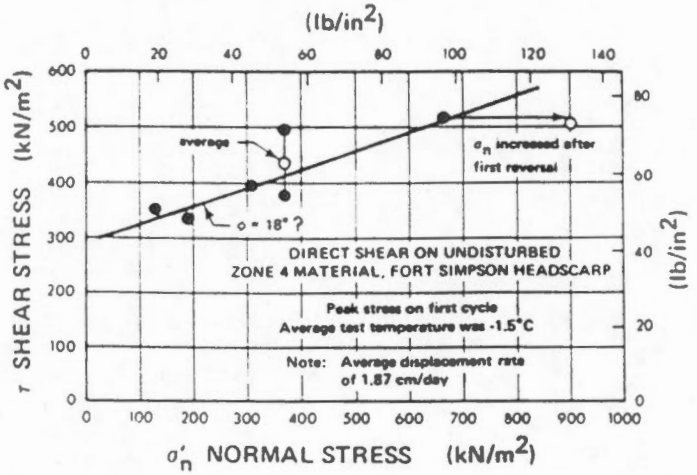

RATE 1

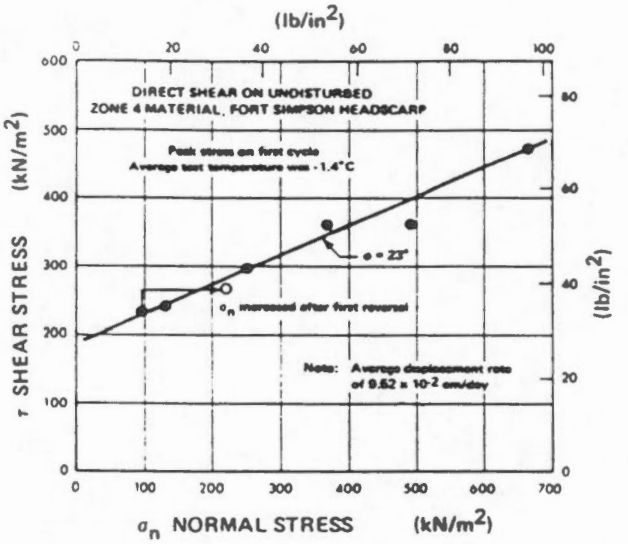

RATE 2

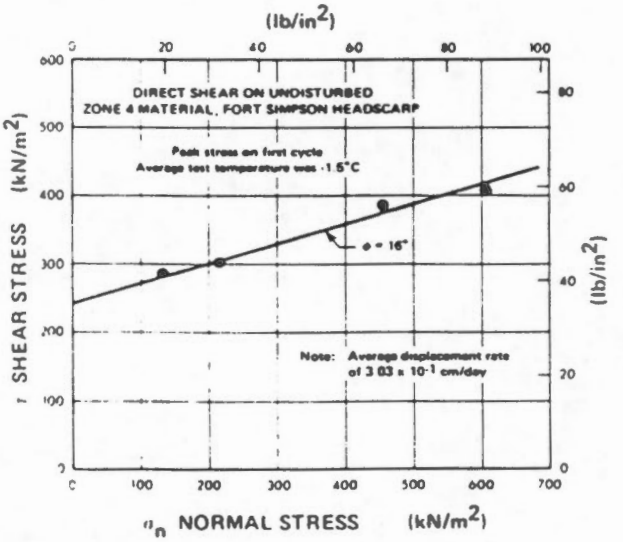

RATE 3

Results of direct shear tests on Fort Simpson clay at three different rates of displacement (Roggensack, 1977).

FIGURE 7.12

THURBER

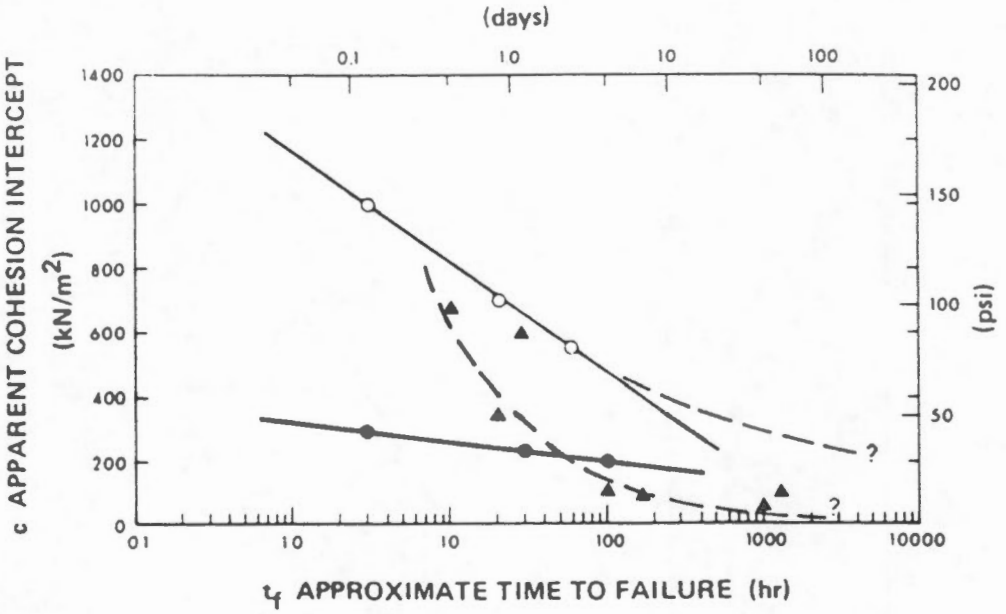

LEGEND :

20 - 30 MESH OTTAWA SAND, T = -3.85°C, TRIAXIAL COMPRESSION
(after Sayles, 1973)

FORT SIMPSON ZONE 4, SILTY CLAY, T = -1.5°C, DIRECT SHEAR

ICE, T =
(after Sego and Morgenstern, 1983)

Apparent cohesion intercept as a function of time to failure (after Roggensack, 1977).

THURBER

FIGURE 7.13

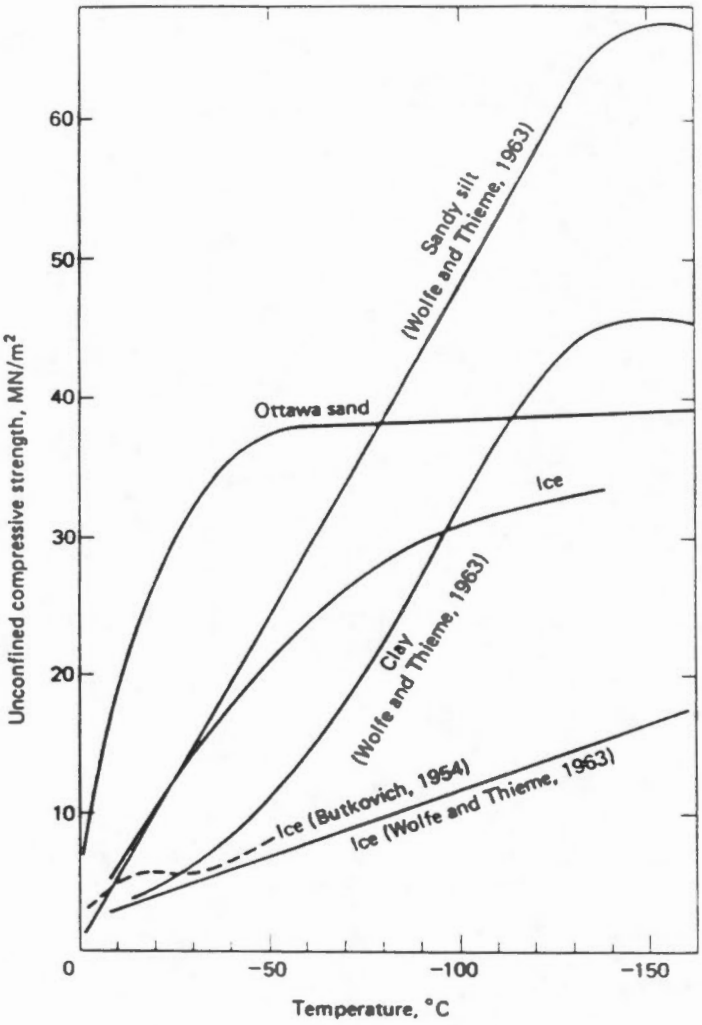

The effect of temperature on the unconfined compressive strength of various soils (Andersland et al, 1978; after Sayles, 1966).

THURBER

FIGURE 7 14

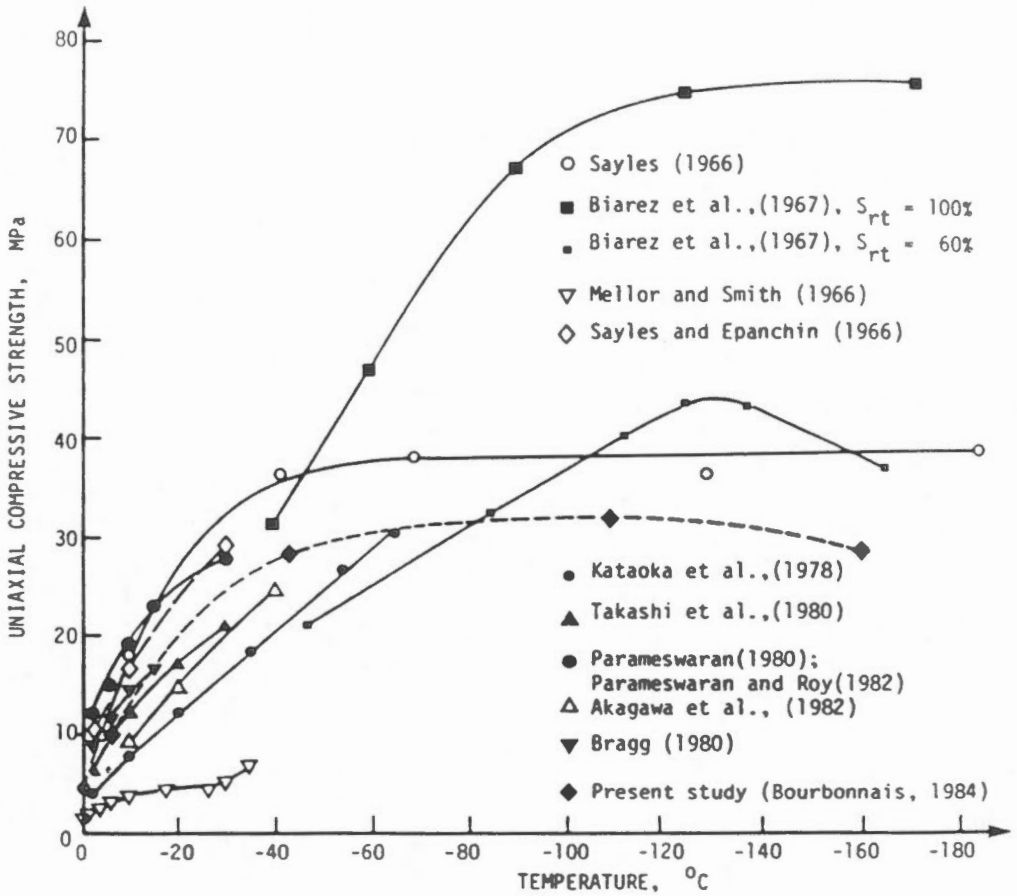

The effect of temperature on the strength of frozen sand (Bourbonnais and Ladanyi, 1985).

FIGURE 7.15

THURBER

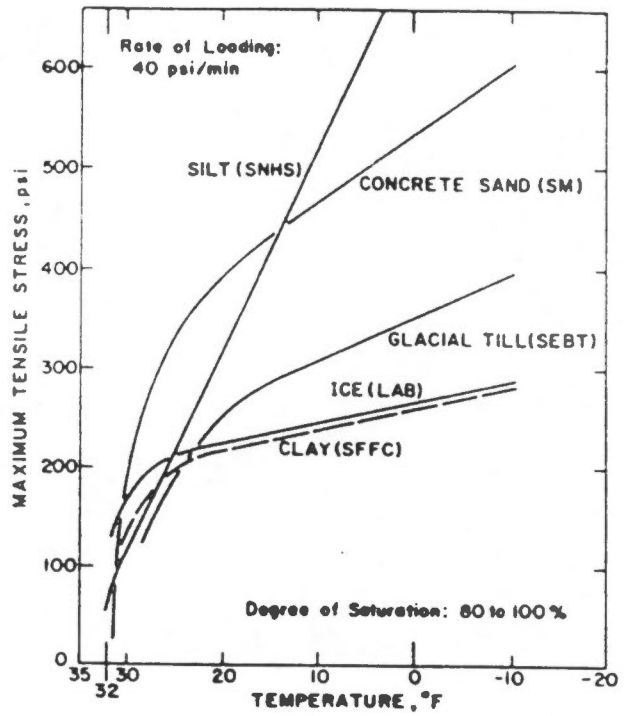

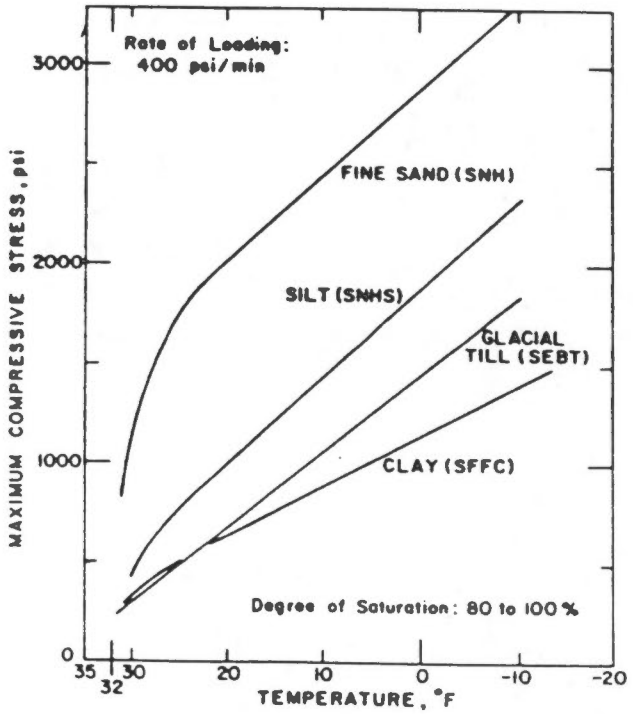

NOTE . SEE FIGURE 7.19 FOR SOIL DATA

The effect of temperature on the compressive and tensile strength of various soils (Kaplar, 1971).

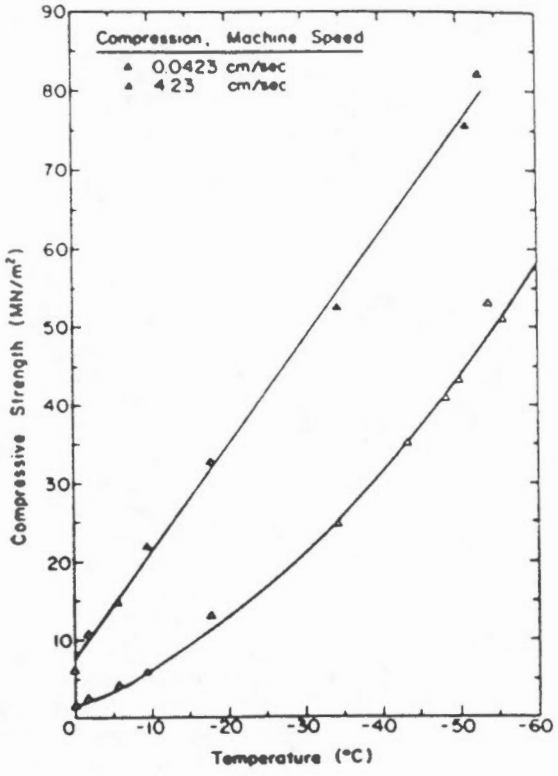

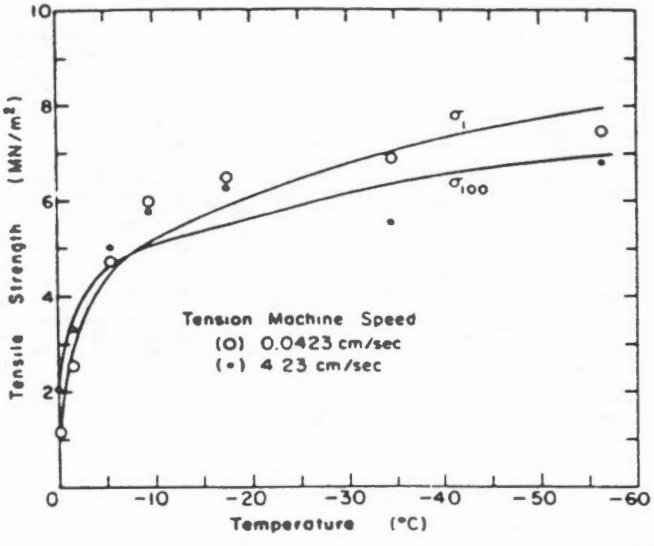

NOTE : FAIRBANKS SILT (SFS), SEE FIGURE 7.19

The effect of temperature on the compressive and tensile strength of Fairbanks silt (after Haynes and Karalius, 1977).

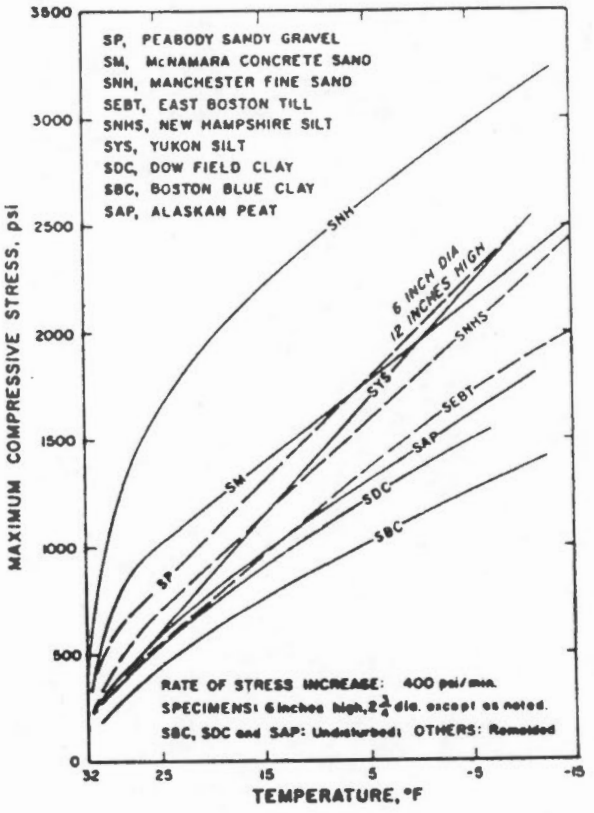

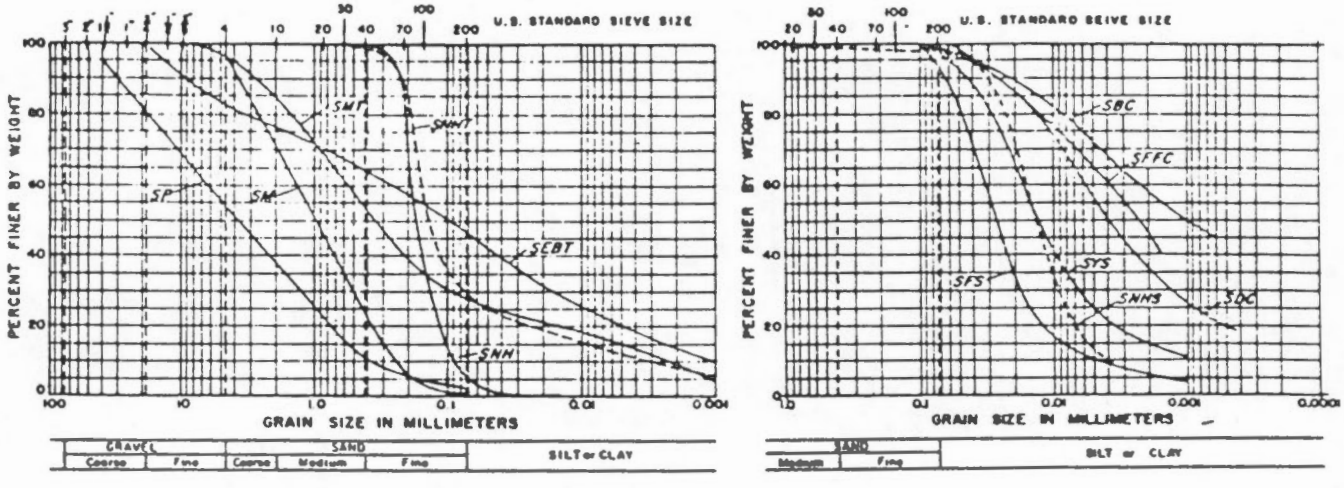

SEE FIGURE 7.19 FOR ADDITIONAL SOIL DATA

The effect of temperature on compressive strength for various soils tested by CRREL (Ladanyi, 1988).

THURBER

FIGURE 7.18

SOIL LEGEND	NAME	SOURCE	MAX. UNCONFINED COMPRESSIVE STRENGTH	DIRECT SHEAR TEST ANGLE OF INTERNAL FRICTION -
			psi	degrees
SP	Peabody Gravelly Sand	Peabody, Mass.	-	-
SM	McNamara Concrete Sand	Needham, Mass.	-	39
SMH	Manchester Fine Sand	Manchester, N.	-	35
SMT	Blend, McNamara Concrete Sand and East Boston Till	SM blended wit minus 40 mesh	-	38
SNHT	Blend, Manchester Fine Sand and East Boston Till	SNH blended wi minus 40 mesh	-	32
SEBT	East Boston till (-3/4")	East Boston Ma	-	28
SNHS	New Hampshire Silt (B)	Manchester, N	-	30
SFS	Fairbanks, Silt	Fairbanks, Ala	-	32
SYS	Yukon Silt	Whitehorse, Yu Territory, Can	-	38
SDC	Dow Field Clay	Dow Air Force Bangor, Me.	38.1	-
SBC	Boston Blue Clay	No. Cambridge,	21.9	-
SFPC	Fargo Clay	Fargo, North D	9.2	-
SAP	Alaskan Peat	Fairbanks, Ala	-	-

NOTES: (1) Providence V

(2) Modified AASI

(3) Standard Pro

(4) All specimens freezing. In with water su non-frost-sus soils.

FIGURE 7.19

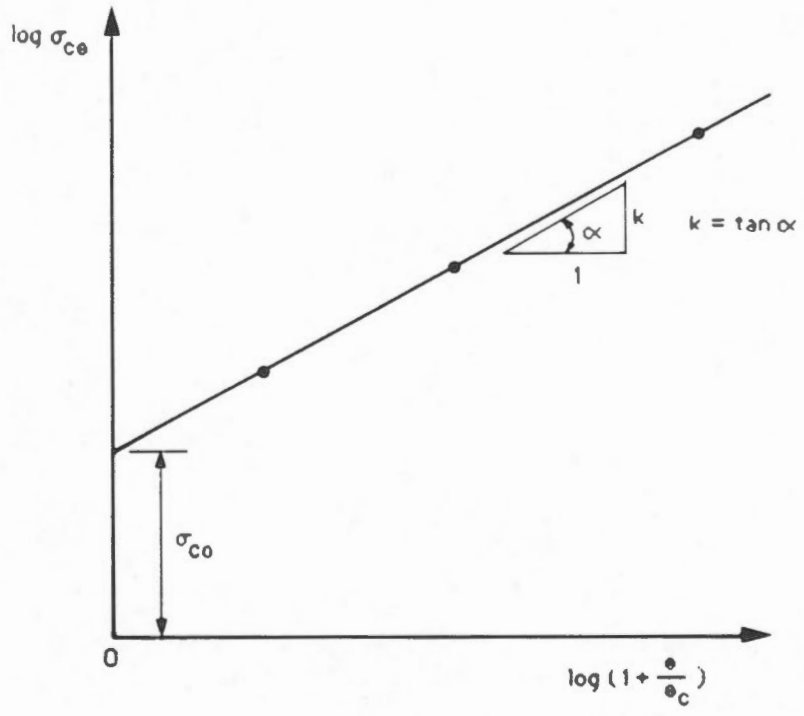

$$\sigma_{c\theta} = \sigma_{co}(1+\frac{\theta}{\theta_c})^{k}$$

$$\theta_c = 1^{\circ}C$$

The determination of the temperature reference stress and the temperature exponent (after Ladanyi, 1972).

FIGURE 7.20

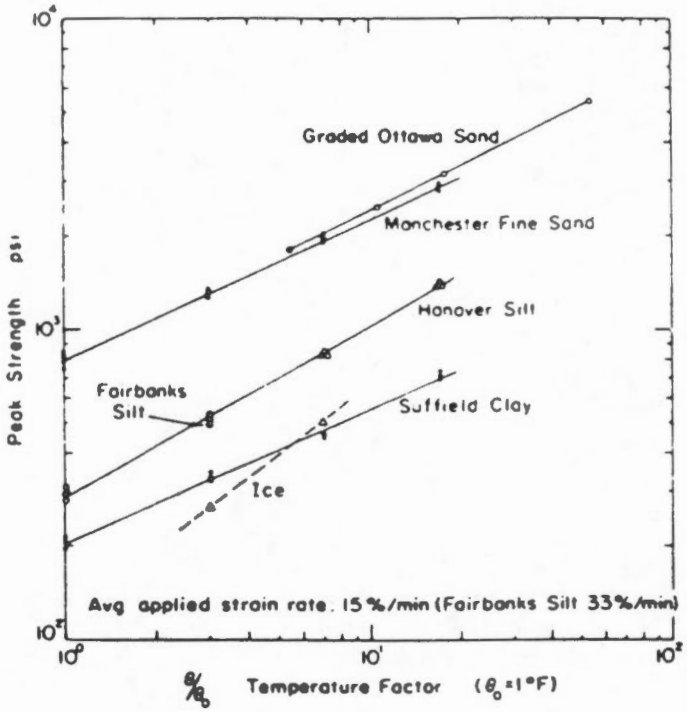

NOTE : SEE FIGURE 7.19 FOR SOIL DATA

Compressive strength versus the logarithm of normalized temperature (after Sayles and Haines, 1974).

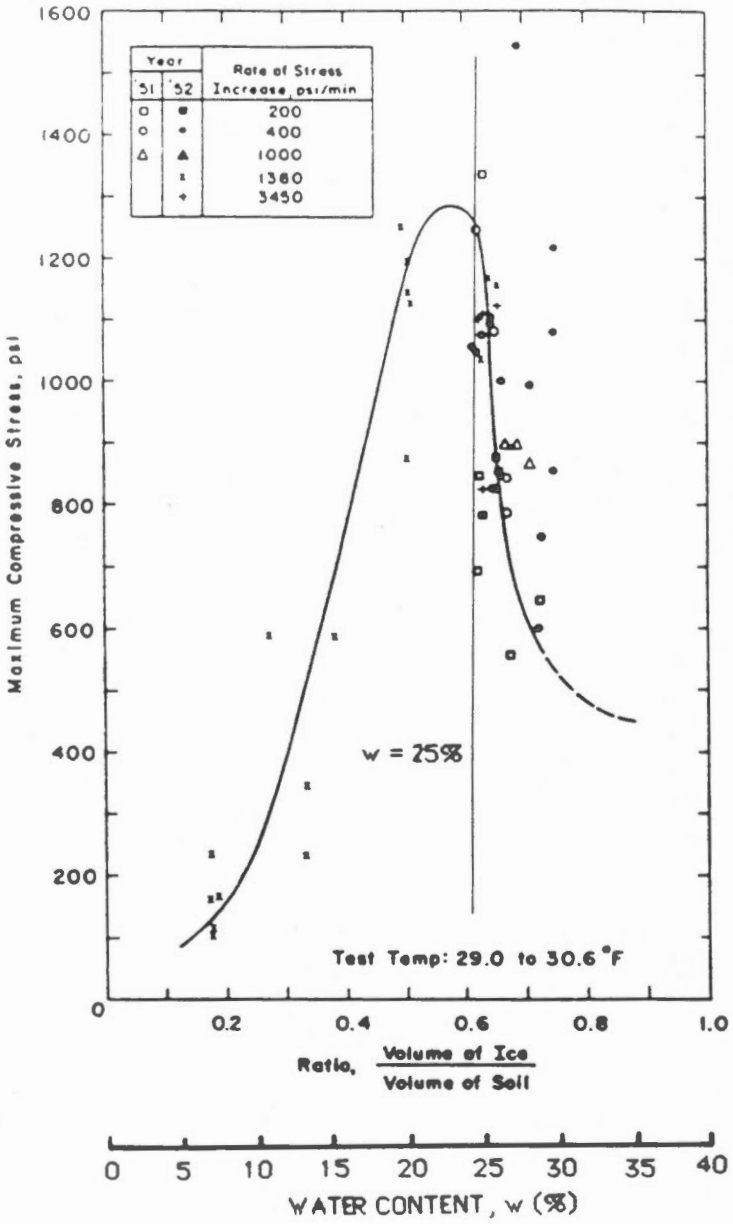

NOTE SEE FIGURE 7.19 FOR SOIL DATA

The effect of ice content on the unconfined compressive strength of Manchester fine sand (after Kaplar, 1971).

THURBER

FIGURE 7.22

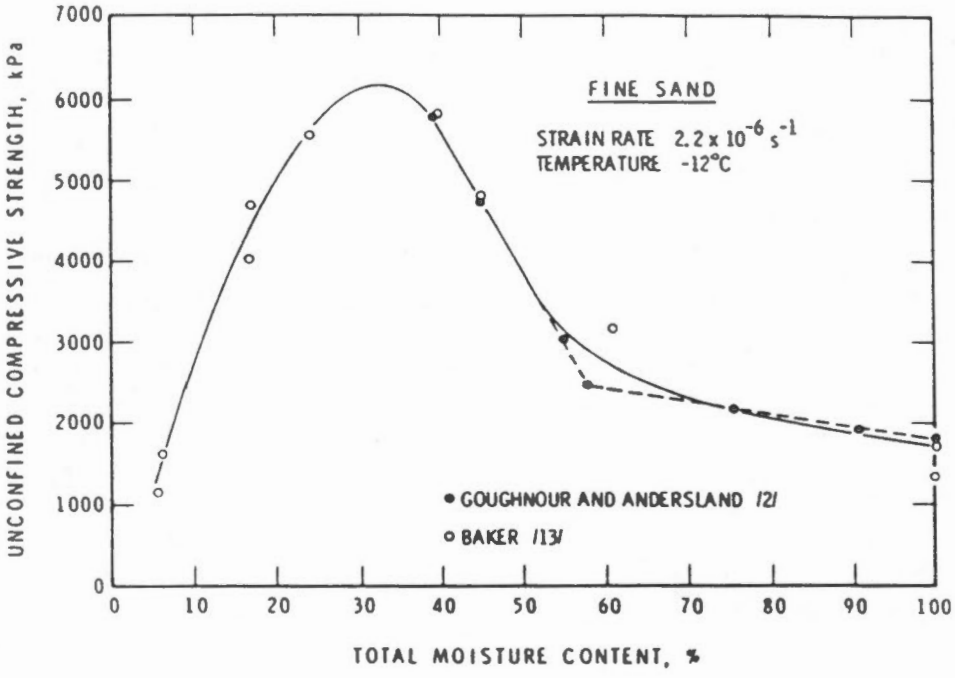

The effect of ice content on the unconfined strength of Ottawa fine sand (Baker, 1979).

THURBER

FIGURE 7.23

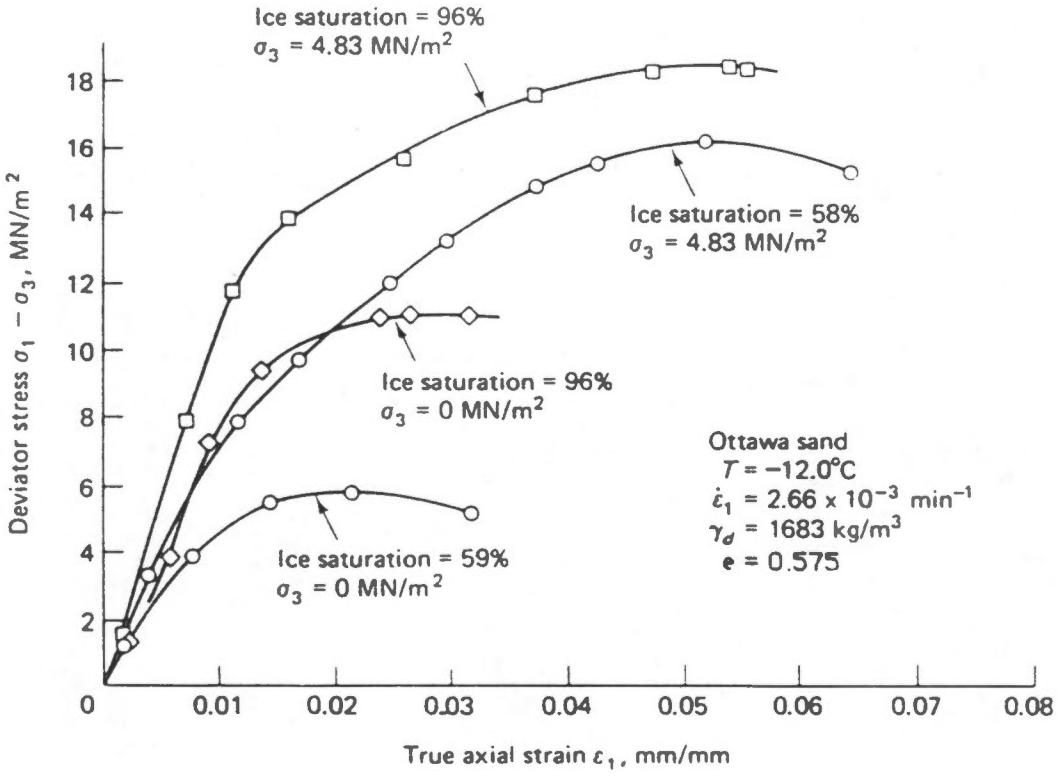

The effect of degree of ice saturation on the strength of frozen Ottawa sand (Andersland et al, 1978; after Alkeri, 1972).

FIGURE 7.24

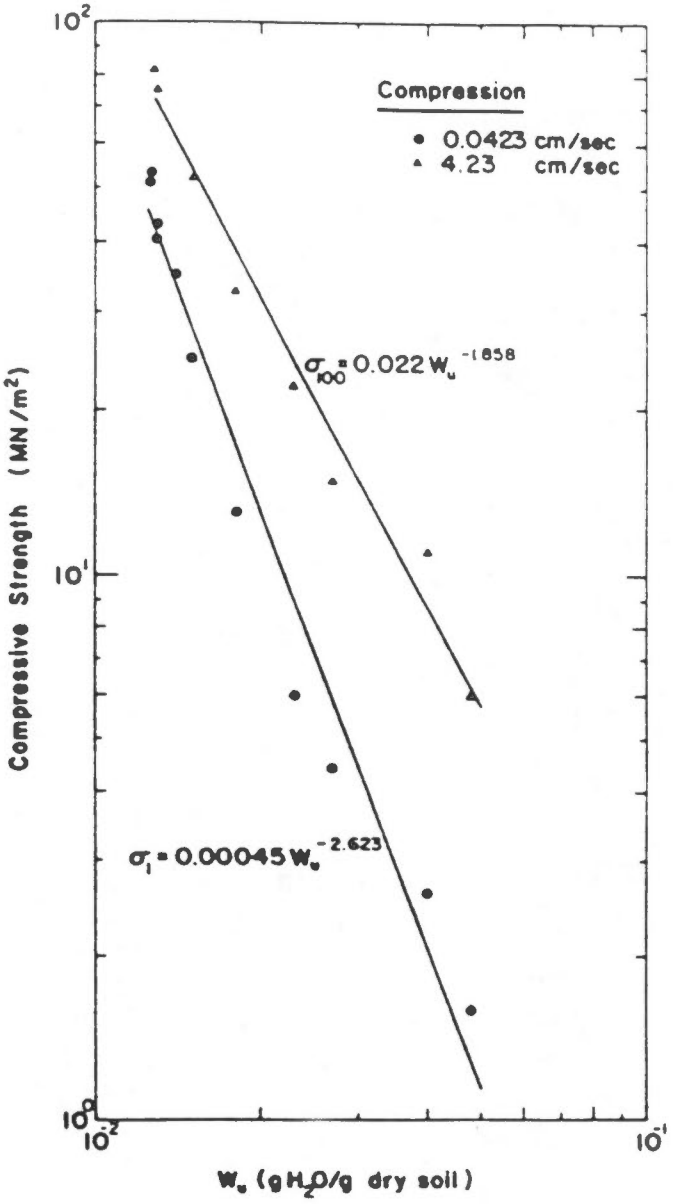

The effect of unfrozen water content on the unconfined strength of Fairbanks silt (Haynes and Karalius, 1977).

THURBER

FIGURE 7.25

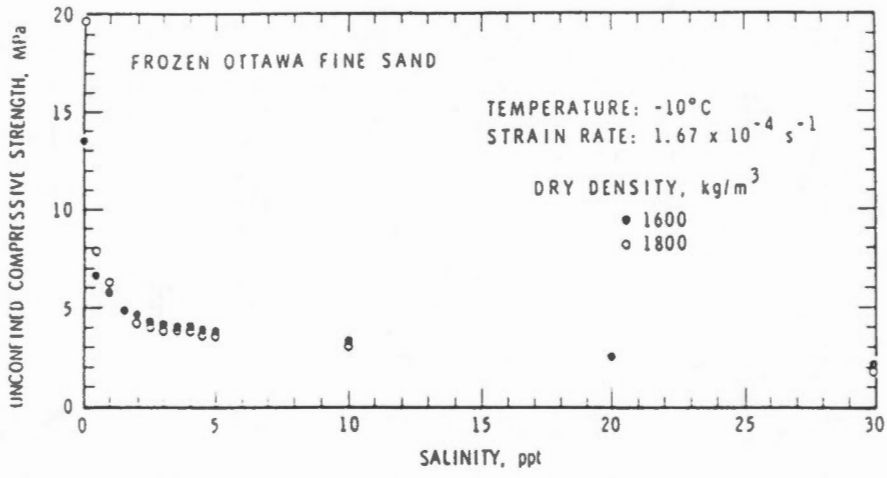

The effect of pore water salinity on the strength of Ottawa fine sand (Baker and Kurfurst, 1985).

THURBER

FIGURE 7.26

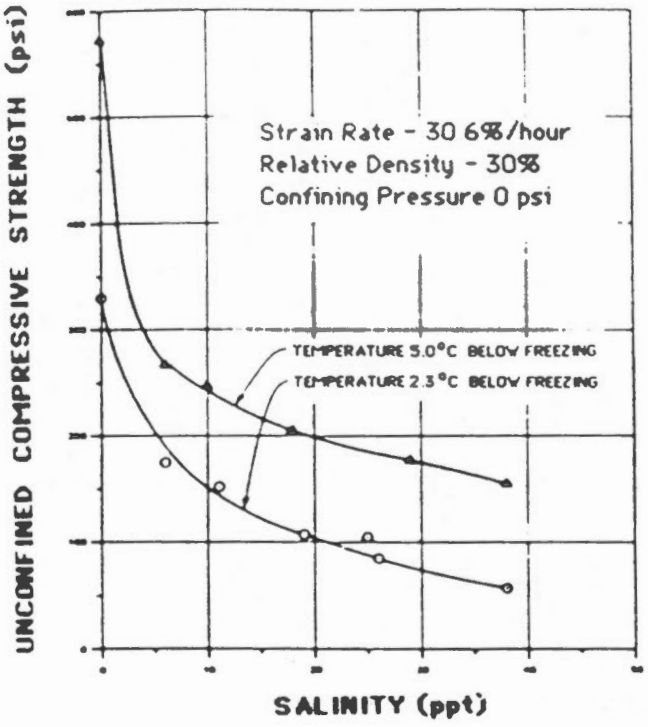

Note :
Temperatures shown are in °C below the depressed freezing point at each salinity concentration

Unconfined Compressive Strength versus Salinity. (Stuckert and Mahar, 1980)

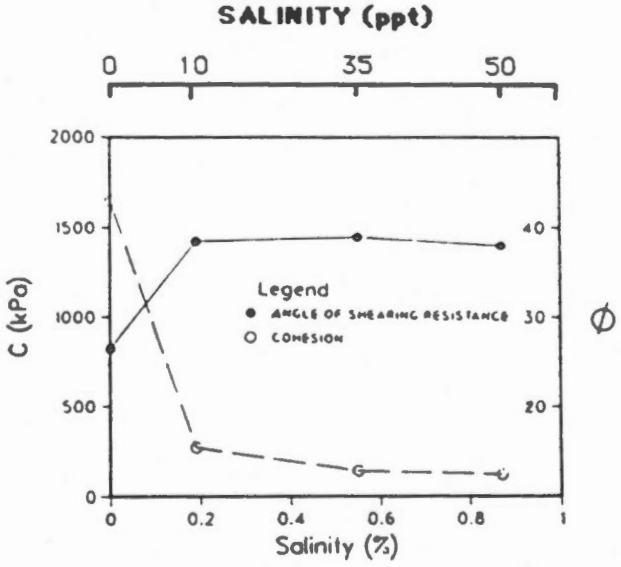

Strain Rate : 0.8%/hour
Temperature : -7°C

Effect of pore fluid salinity on the cohesion and angle of friction of mortar sand. (Sego and Chemenko, 1984)

The effect of pore water salinity on the strength of frozen soils.

SECTION 8

ADFREEZE STRENGTH

SECTION 8

ADFREEZE STRENGTH

8.1 General

When thawed soil is placed against a structural material such as concrete, timber or steel, and subsequently frozen, a bond develops between the frozen soil and the structural material. The shear strength due to ice bonding is commonly referred to as the adfreeze strength. The adfreeze strength between the frozen soil and the structure is of concern primarily with respect to the design of adfreeze piles in permafrost regions, however it is also important in calculating frost uplift forces against foundation walls in both permafrost and non-permafrost regions. This section of the report is primarily concerned with the adfreeze strength of piles installed in ice and frozen soil.

Weaver and Morgenstern (1981) provide an excellent summary of the factors controlling the design of adfreeze piles in permafrost. The design of piles in permafrost requires a consideration of two aspects:

1) Creep deformations, and
2) Adfreeze strength.

The analysis provided by Weaver and Morgenstern (1981) indicates that for relatively smooth shafted timber, concrete or steel piles, creep deformations may govern pile capacities in ice and ice rich soils, in some cases, depending on temperature and the factor of safety applied to the adfreeze strength. In ice poor silts and sands, the adfreeze strength, rather than creep deformations, will govern in most cases. It should be noted that the 'allowable' adfreeze strength presented on Figures 8 to 11 of Weaver and Morgenstern's paper are ultimate short term adfreeze strengths which should be reduced by an appropriate factor of safety in design.

Creep deformations of piles are controlled by the creep parameters of the soil surrounding the pile, as discussed in the previous sections, and therefore, this aspect of pile behaviour will not be considered further here.

Adfreeze strengths are usually measured by carrying out full scale pile load tests in the field or model pile tests

THURBER

in the laboratory. Where uplift forces due to frost heave are the primary concern, other test configurations may be more appropriate (Penner 1967, 1971 and 1974).

Field load tests on piles may be in either compression (downwards loading) or in tension (upwards loading). Field load test are most commonly carried out using hydraulic jacks and therefore the tests are load controlled, with the loads being applied in increments. A typical set up and test results are presented in Figure 8.1. Pile deformations are monitored until they either stabilize or a constant rate of deformation is achieved and the next higher load increment is then applied.

The interpretation of field load test data is usually based on the assumption that the pile is infinitely rigid with respect to the surrounding soil. The validity of this assumption has been investigated by Nixon and McRoberts (1976) and by Ladanyi (1988). These analyses indicate that for steel piles which are about 6 m in length, pile shaft stresses do not become relatively uniform with depth until after about 10 days at a temperature of -2°C and about 100 days at a soil temperature of -5°C. These results indicate that while it is reasonable to assume an infinitely rigid pile over the long term life of the pile, it is not always reasonable to make this assumption when interpreting the results of short term pile load tests. Unfortunately, the measurement of pile stress distribution with depth is not normally carried out when testing adfreeze piles in permafrost.

In most cases, the assumption is made that the pile is infinitely rigid and therefore the adfreeze strength is equal to the ultimate load applied to the pile divided by the area of the embedded shaft. That is:

$$\tau_f = P/\pi DL \qquad (8.1)$$

where

τ_f denotes the average stress at the pile/soil interface at failure,

P denotes the applied load,

D denotes the outside diameter of the pile, and

L denotes the embedded length of the pile.

THURBER

In theory, time deformation data from the pile loads prior to failure can be back-calculated to establish the creep parameters of the soil surrounding the pile. It is difficult, in practice, however, to derive the creep parameters from field tests for a number of reasons. First of all, it is necessary to measure deformations very accurately in order to obtain meaningful data with respect to creep deformations. This is difficult because changes in air temperature cause thermal expansion or contraction of the test pile and the measurement support piles. It is also difficult to maintain a constant load on the pile with conventional hydraulic jacking systems. Finally, daily expenses related to field testing are high, particularly in the north, and therefore load tests can only be run for periods of several hours or days. There is not usually sufficient time to achieve a uniform distribution of adfreeze stress along the length of the pile, nor sufficient time to obtain a reliable definition of pile creep rates.

Model pile tests in the laboratory can be carried out either at a constant rate of displacement, as shown in Figure 8.2, or in constant load tests, as shown in Figure 8.3. The interpretation of laboratory pile test data assumes that the pile is infinitely rigid with respect to the surrounding ice or frozen soil. This assumption is normally valid because of the relatively high pile diameter to length ratio of most laboratory tests, and provided displacement rates are reasonably slow, so that stresses remain relatively uniform along the outside surface of the pile.

As indicated on Figure 8.2, where constant rate of displacement tests are carried out, the load response is measured as a function of pile displacement. The ultimate average adfreeze strength, τ_f is calculated using Equation 8.1. The rate of strain, $\dot{\epsilon}$ is normally taken as being equal to the rate of displacement, $\dot{u}$ used in the test. Some researchers (Parameswaran, 1978) have measured pile displacements at the top and bottom of the pile and use the average rate of displacement in analysing their test data.

As indicated on Figure 8.2, the peak load response will be a function of the rate of displacement. As the rate of displacement is increased, the peak strength will increase. This behaviour is similar to that observed on constant displacement rate tests carried out on cylinders of ice or frozen soil as discussed in Section 7. It is not exactly the same, however, because a discontinuity is formed at or near the pile surface, a situation which does not occur when tests are carried out on cylinders.

THURBER

Assuming an infinitely rigid pile, the data from a series of constant displacement rate tests (at different rates of displacement but with all other conditions held constant) can be analysed using the same techniques which were used for tests on cylinders.

That is, the results of a series of constant displacement rate tests can be plotted as the log of the failure stress, τ_f versus the log of the average pile displacement rate, $\dot{u}$, as shown on Figure 8.2. The relationship will be approximately linear as shown. The relationship between adfreeze strength and displacement rate can be expressed using an equation which is the same as for similar tests on cylinders as discussed earlier. That is,

$$\tau_f = \tau_o \left(\frac{u_f}{\dot{u}_o \, t_f} \right)^{1/n} \qquad (8.2)$$

where

τ_o denotes the shaft stress which corresponds to a nominal pile deformation rate $\dot{u}_o$ as shown on Figure 8.2

u_f denotes the pile displacement at failure

t_f denotes the time to failure under shaft stress τ_f

n denotes the creep exponent which is established from the test data as shown on Figure 8.2.

Adfreeze strengths can also be established by carrying out constant load tests as shown in Figure 8.3. The magnitude of the applied stress must be such that the sample will reach tertiary creep within a reasonable length of time. The onset of tertiary creep (increasing rate of displacement) is considered to be the time to failure. A series of such tests are carried out (all at the same temperature) in order to establish the relationship between applied stress and time to failure for the specified conditions. As indicated on Figure 8.3 the time to failure will increase as the applied stress decreases.

The log of the applied stress τ_a is then plotted against the log of the minimum displacement rate $\dot{u}$, as shown on Figure 8.3.

THURBER

The proof stress τ_{oo} at a nominal strain rate $\dot{u}_o$ can be established from this plot, together with the creep exponent n, in the same way as was the case for the constant displacement rate test data. The values are then used in Equation 8.2.

As outlined in Section 7, Sego and Morgenstern (1983) have demonstrated that for tests on cylinders, the same results will be obtained from constant displacement rate tests as from constant stress tests. While it is reasonable to assume the same situation will occur with adfreeze strength, the necessary testing required to confirm this speculation has never been carried out. This is an area in which further research should be considered.

Many researches believe that Vyalov's (1959) relationship with respect to the time dependent strength of ice and frozen soils may also be adapted to adfreeze strength. That is,

$$\tau_f = \frac{\tau_o}{\ln\left(\frac{t_f}{t_o}\right)} \qquad (8.3)$$

where

t_o denotes the time to failure under some applied shaft stress τ_o , and

τ_f denotes the applied shaft stress which will result in failure at time t_f.

The parameters τ_o and t_o in Equation 8.3 can be established either from constant displacement rate tests or from constant load tests. In the case of constant displacement rate tests, τ_o is the measured peak stress and t_o is the time that the peak stress was reached. In constant stress tests, τ_o is the applied stress and t_o is the time at which tertiary creep begins.

Equations 8.2 and 8.3 both imply that the adfreeze strength will tend to zero at infinite time. Many researchers have suggested that the long term strength of piles in ice or ice rich soil will tend to zero, while the long term adfreeze strength of piles in ice poor soil will tend towards the thawed friction between the soil and the outside surface of the pile. While these speculations appear reasonable and provide a lower bound for adfreeze strength, they have never been proven.

THURBER

In addition to time dependence, as discussed above, the adfreeze strength of ice or frozen soil and structural materials will also be a function of the following variables:

1) Confining stress,

2) Load direction,

3) Pile surface properties,

4) Temperature, and

5) Backfill properties.

8.2 Confining Stress

Morgenstern and Weaver (1981) have discussed the effect which confining stress has on creep deformations of piles. Ladanyi (1988) has discussed the effect of confining stress on adfreeze strength. No quantitative data has been found in the literature.

Current pile installation procedures involve drilling a hole in the permafrost and placing sand slurry in the annulus between the pile and the pile hole. Under these conditions, the radial stress between the backfill and the pile surface will be relatively low, at least prior to freezing. The radial stress which develops as freezing takes place will depend on the direction and rate of freezing. It is conceivable that under some circumstances, the radial pressure which develops due to freeze back could be very high. This pressure can be expected to dissipate over a period of time, depending on the creep properties of the surrounding soil. Once freezeback pressure dissipates, the radial stress acting against the pile surface will be less than or equal to the vertical pressure and will therefore range from 0 to 150 kPa depending on depth.

The effect which confining pressure has on adfreeze strength can be approximated by:

$$\tau_a = c + \sigma_r \tan \phi \qquad (8.4)$$

where

τ_a denotes the adfreeze strength,

c denotes the adfreeze strength, under zero radial stress,

THURBER

σ_r denotes the radial stress acting on the pile surface, and

ϕ denotes the angle of friction between the frozen material and the pile.

No information was found in the literature with respect to the angle of friction between frozen soil and various structural materials. It is generally assumed by most researchers that for ice, $\phi = 0$, and the frictional component of adfreeze strength is therefore negligible. This appears to be a reasonable assumption, particularly where the long term adfreeze strength is of concern. In ice poor backfill soils, the angle of friction may have some finite value (20 to 35°) however the average radial stress is low (about 75 kPa) in most cases and so the net contribution to adfreeze strength due to friction will probably be negligible in comparison to unconfined adfreeze shear strength, at least in the short term. In view of these factors, most designers neglect the effect of confining pressure when establishing adfreeze strength for use in design. The influence of confining pressure may, however, be significant with respect to the long term adfreeze strength in ice poor soils. This is a subject which is now beginning to receive the attention of researchers.

8.3 Load Direction

Adfreeze piles may be subjected to net compressive loads (as in the case of building foundations) or tensile loads (for example in the case of tower anchors).

Steel piles subjected to compressive loads can be expected to increase in diameter as they are loaded, whereas piles subjected to tension can be expected to decrease in diameter. These changes in pile diameter may result in higher adfreeze strengths being achieved for compression tests as compared to tension tests.

It is speculated by most researchers that the effects of load direction on adfreeze strength of piles will be small, however no information to support this was found in the literature. It is difficult to establish the relative effects of load direction in the laboratory because it is difficult to induce the same magnitude of axial stress into a short pile in the laboratory, as occurs in a longer pile in the field, where the total applied load is much higher.

THURBER

In the absence of quantitative data, most designers adopt conservatively low values for adfreeze strength for piles subjected to tensile forces. A better alternative is to carry out field load tests which simulate design conditions, including the direction of loading.

8.4 Pile Surface Properties

As might be expected, the surface properties of piles can have a significant effect on the adfreeze strength.

Parameswaran (1978, 1979 and 1981) has reported the results of constant displacement rate tests and constant load tests on a variety of pile types including timber, concrete, steel H piles and steel pipe piles. These results, some of which are presented on Figure 8.4, provide a good indication as to the effect which pile type has on adfreeze strength All tests were carried out using Ottawa sand and distilled water.

These test results show that the highest adfreeze strengths were obtained with plain untreated timber (Figure 8.4). The results show that the adfreeze bond strength between frozen Ottawa sand and concrete, painted steel pipe and creosoted timber were roughly comparable.

The results show that the adfreeze strength between Ottawa sand and steel pipe piles and steel H-piles are also comparable (Figure 8.4).

The steel pipe piles were sandblasted prior to testing in all cases. In some cases, however, 1 coat of spray enamel was applied to the sandblasted pile prior to testing. It is of interest to compare the adfreeze strength between painted and unpainted piles, because pipe manufacturers routinely apply a lacquer coat to the pipe piles used in Northern Canada in order to reduce corrosion during transportation.

Parameswaran's, (1978) data for painted and unpainted pipe piles has been replotted in Figure 8.5. The results indicate that there is no significant difference between the adfreeze strength as a result of applying paint to the pipe.

Thurber Consultants Ltd. (1988) reported the results of a series of laboratory pile load tests carried out by the University of Alberta under contract with the Department of National Defense. The results of 13 pile load tests completed for this work are presented in Figure 8.8.

A detailed description of the apparatus and test procedure is outlined by Thurber Consultants (1988a and 1988b). Briefly, however, the tests involved preparing frozen ice poor samples of silty sand (saline or non-saline), drilling a 51 mm diameter pile hole, placing a 33 mm outside diameter steel pipe in the hole and backfilling the annulus with a variety of selected materials. Once the backfill was completely frozen, the piles were loaded to failure at a constant rate of displacement.

As part of the U of A test program, comparative tests were carried out to determine the difference in adfreeze strength between an untreated pile (as received from the supplier with one coat of black lacquer) which had not been sandblasted, with the same pile which was sandblasted prior to testing. The test results were as follows:

Test No.	Native Soil	Backfill	Peak Adfreeze Strength (kPa)	Temperature °C	Surface Treatment
1	Silty Sand	Sand	357	-4.8	Not sand blasted lacquer coated
12	Silty Sand	Sand	733	-5.3	Sand blasted, not painted

These test results are also shown on Figure 8.5. The test results with the sand blasted pile is comparable to the results obtained by Parameswaran (1978), whereas the results for the lacquer coated pile are very much lower. These results indicate that sand blasting steel piles will result in a significant increase in adfreeze strength. As demonstrated by Parameswaran's results, painting the pile after sand blasting will not reduce adfreeze strength significantly. It is not known whether the increase in strength due to sand blasting is because all contaminants are removed from the pile or because of the increased surface roughness due to sand blasting.

It is clear that further research concerning the effect of pile surface treatment (and in particular the surface treatment of steel pipe piles which are currently in widespread use) would be valuable.

8.5 Temperature

Adfreeze strength is known to increase significantly as temperature decreases. A summary of data for ultimate adfreeze strength as a function of temperature was compiled by Weaver and Morgenstern (1981), and the results are presented on Figure 8.6.

Johnston (1981) has also compiled data regarding adfreeze shear strengths as presented in Figure 8.7. As shown on the figure, Johnston has suggested a tentative relationship between ultimate short term (up to 24 hours) adfreeze strength for use in design. The ultimate short term strength determined from Figure 8.7 should be reduced by an appropriate factor of safety.

As discussed earlier, there is virtually no data with respect to long term adfreeze strengths and in the absence of data, Johnston has suggested that long term adfreeze strengths be taken as 50 percent of the short term strength. An appropriate factor of safety should also be applied.

8.6 Backfill Properties

Most researchers have recognized the important influence which backfill properties can have on adfreeze strength. For convenience, most laboratory studies involved placing a large amount of thawed soil around a pile and allowing it to freeze back. This procedure was used because it was convenient, and because it resulted in homogeneous soil properties from the outside surface of the pile shaft, which simplified interpretation of the test results The recent tests at the University of Alberta (Thurber Consultants Ltd., 1988), and as summarized in Figure 8.8, have demonstrated that the type of backfill, its method of placement and other factors can have a significant effect on the adfreeze strength and the capacity of the piles.

The test program indicated that the following backfill properties could influence the adfreeze strength:

1) Ice content,
2) Grain size distribution,
3) Salinity, and
4) Annulus size.

8.6.1 Backfill Ice Content

The U of A test data indicates, as expected, that where the ice content of the backfill is high, the short term adfreeze strength will be reduced significantly:

TEST NO.	NATIVE SOIL TYPE	NATIVE SOIL SALINITY	BACKFILL	BACKFILL SALINITY	PEAK ADFREEZE STRENGTH	TEMPERATURE (°C)
1	Silty Sand	0	Sand	0	357	-4.8
5	Silty Sand	0	Ice	0	217	-5.3

8.6.2 Backfill Grain Size Distribution

Two types of sand backfill were tested. In one case, uniform silty sand was used which had about 30% passing the No. 200 sieve. In the second test, a uniform sand which had 0% passing the No. 200 sieve was used. The following test results were obtained.

TEST NO.	NATIVE SOIL	NATIVE SOIL SALINITY (ppt)	BACKFILL	BACKFILL SALINITY (ppt)	PEAK ADFREEZE STRENGTH (kPa)	TEMPERATURE (°C)
1	Silty Sand	0	Uniform Sand	0	357	-4.8
7	Silty Sand	0	Silty Sand	0	360 (300)	-6.4 (4.8)

As indicated the test with the silty sand was carried out at a somewhat colder temperature than the tests with the uniform sand, and the adfreeze strength has been adjusted accordingly. The adfreeze strength with the uniform sand is seen to be somewhat higher (357 vs 300 kPa). Additional corroborative testing would be required to confirm this result.

8.6.3 Backfill Salinity

The effect which backfill salinity has on the adfreeze strength is indicated in the following results:

TEST NO.	NATIVE SOIL	SOIL SALINITY (ppt)	BACKFILL	NATIVE BACKFILL SALINITY (ppt)	PEAK ADFREEZE STRENGTH (kPa)	TEMPERATURE (°C)
4	Silty Sand	10	Sand	0	351	-4.5
6	Silty Sand	10	Silty Sand	10	190	-4.8

These tests indicate that if the backfill is saline, the adfreeze strength will be reduced by about 50 percent. The results demonstrated that great care must be taken to ensure that the sand and water used for the sand slurry backfill must be non-saline. While this seems straightforward, local contractors prefer to use drill cuttings (which are often saline) or local sand deposits which are generally not tested and which may be saline. An alternative is to use imported sand for the backfill.

8.6.4 Annulus Size

It may be deduced from the foregoing results that the size of the annulus between the pile and the pile hole will influence pile capacity. For example if a pile is installed in an ice rich or saline soil, the annulus could be increased and filled with non-saline sand such that the pile capacity will be controlled by the creep parameters and adfreeze strength of the sand backfill, rather than the properties of the native soil.

This is an area in which additional field and laboratory testing should prove useful.

8.7 Native Soil Properties

The properties of the native soil which surround the backfill can influence the pile capacity depending on the circumstances. The following backfill properties were investigated in the U of A tests

1) Ice content, and

2) Salinity.

8.7.1 Native Soil Ice Content

Comparative tests demonstrated that the ice content of the native soil (beyond the backfill) did not influence adfreeze strength:

TEST NO.	NATIVE SOIL TYPE	NATIVE SOIL SALINITY (ppt)	BACKFILL	PEAK ADFREEZE STRENGTH (kPa)	TEMPERATURE (°C)
1	Silty Sand	0	Imported Sand	356	-4.8
9	Ice	0	Imported Sand	353	-5.3

THURBER

It should be noted, however, that the ice content of the native soil will affect the creep parameters and hence the pile may experience significant deformations.

8.7.2 Native Soil Salinity

The data indicates that the salinity of the native soil may influence the adfreeze strength, depending on the pile surface treatment:

TEST NO.	NATIVE SOIL TYPE	NATIVE SOIL SALINITY (ppt)	BACKFILL	PEAK ADFREEZE STRENGTH (kPa)	TEMPERATURE (°C)	SURFACE TREATMENT
1	Silty Sand	0	Sand	357	-4.8	Untreated
4	Silty Sand	10	Sand	351	-4.5	Untreated
12	Silty Sand	0	Sand	733	-5.3	Sand blasted, unpainted
13	Silty Sand	10	Sand	581	-5.1	Sand blasted, unpainted

Failure occurred at the pile/backfill interface in all of the foregoing tests except for Test 13. Failure occurred at the backfill/native soil interface in Test 13. (The adfreeze strength given for Test 13 is the stress at the pile/backfill interface at failure).

For untreated piles, it is clear that the salinity of the native soil does not influence the short term adfreeze strength (Tests 1 and 4). It may, however affect their long term deformations. For sand blasted piles, the salinity of the native soil influenced the short term pile capacity because, in this case, the adfreeze strength between the backfill and the native soil governed (Test 13).

8.8 Comparisons with Field Data

As outlined by Thurber Consultants Ltd. (1988), there are a number of significant differences between the configuration of the pile load test used in the laboratory and actual field conditions. It is therefore useful to compare the laboratory results with the results of full scale field load tests. The available data can be conveniently grouped into saline and non-saline soils.

8.8.1 Non-Saline Soils

Three pile load tests were undertaken in Iqaluit (Thurber Consultants Ltd., 1983) in soils which are considered to be non-saline. The test results are summarized in Figure 8.9 and are compared to equivalent laboratory tests as follows:

TEST NO.	NATIVE SOIL	NATIVE SOIL SALINITY (ppt)	BACKFILL TYPE	BACKFILL SALINITY	AVERAGE PEAK ADFREEZE STRENGTH (kPa)	RANGE (kPa)	TEMPERATURE (°C)
1	Silty Sand	0	Sand	0	357 (300)	-	-4.8 (-3.5)
1,2 and 3	Sand	1.4	Sand	0	290	230 to 340	-3.5

As indicated above, if the laboratory test results are corrected for temperature, the measured adfreeze strength is in good agreement with the value determined in the field test. There is a significant scatter between the values determined in the field tests (230 to 340 kPa). It is speculated that the scatter is due to variations in density which occurred in placing the sand slurry in the annulus.

8.8.2 Saline Soils

Four field load tests were carried out by Hoggan Engineering and Testing Ltd., (1985) in Arctic Bay, N.W.T. Nixon (1988) reported the results of 3 pile load tests carried out in Clyde River, N.W.T. The test results are summarized on Figure 8.9. All 7 pile load tests were carried out on lacquer finished pipe piles which were not treated in any special way. Nixon (1988) has interpreted the pile deformations as being due to creep of the adjacent frozen soil. The deformations are relatively large and the interpretation presented here assumes that the piles exceeded the adfreeze strength at the pile/soil interface. It is difficult to establish which interpretation is correct, however, adfreeze failure definitely occurred in the tests at Arctic Bay, where deformations ranged from 7 to 10 mm. The site conditions (soil type, ice contents, ground temperatures and pore water salinity) were virtually the same at both sites. These field tests results can be compared to the equivalent laboratory test results as follows:

LOCATION	TEST NO.	NATIVE SOIL	AVERAGE NATIVE SOIL SALINITY	BACKFILL	BACKFILL SALINITY	AVERAGE PEAK ADFREEZE STRENGTH (kPa)	RANGE	AVERAGE TEMPERATURE (°C)
U of A Lab	4	Silty Sand	10	Sand	0	351	-	-4.5
U of A Lab	6	Silty Sand	10	Silty Sand	10	190	-	-4.8
Clyde River	1,2A,3	Silty Sand	10	Sand	0	96	81 to 124	-6.
Arctic Bay	2,3,4,5	Silty Sand	10	Sand	0	103	86 to 124	-6.

THURBER

The short term adfreeze strengths measured in the field are significantly lower than might be expected for clean, non-saline backfill soils (as was used at both Clyde River and Arctic Bay) placed in saline native material. Even if the backfill soils were contaminated by the native pore fluids, adfreeze strengths would be expected to be in the order of 190 kPa, (or higher if temperature corrected) not 100 kPa.

A number of possible reasons for the difference between the laboratory and field adfreeze strength have been suggested by Thurber Consultants Ltd., (1988). Unfortunately, there is not sufficient data available to confirm the actual reason for the difference. It may be possible to establish the reason through a series of appropriately planned laboratory and field pile test programs.

8.9 Summary

This review indicates that further research into the adfreeze strength of ice and frozen soil to piles would be worthwhile. The following areas appear to be of most concern at this time.

Pile Surface Treatment

Further laboratory and field testing should be undertaken to establish practical techniques for increasing adfreeze strengths to steel piles through surface treatment. Sandblasting, the use of degreasing agents and the addition of flanges and studs appear to be methods worth investigating further.

Backfill Properties

Further research should be carried out to establish the most suitable type of backfill for use in ice, ice rich soil and saline soils. Tests should be carried out to establish the effectiveness of increasing the size of the annulus as a means of increasing pile capacities. Improved methods of installing backfill slurries should be developed in order to increase slurry densities and reduce variations in slurry density which occur in the field.

Further research should be undertaken to establish whether saline pore fluids will diffuse from the native soil to the sand backfill and reduce pile load capacity in the long term.

Further research should be considered into the process of freezeback around piles including such aspects as the rejection of saline fluids towards the pile and the generation and dissipation of freezeback pressures around the piles.

Research should be carried out into the use of cement grouts as pile backfill. Concerns include set up times in freezing conditions, factors affecting cement bond values to the steel pile, and optimum mix design.

Long Term Loads

There is no reliable data concerning long term adfreeze strengths. Current approaches involve the extrapolation of data from relatively short term tests, which for ice and ice rich soils indicates that long term adfreeze strengths will be extremely low. It is possible that at very low rates of strain, other healing or strain hardening processes occur which will result in much higher adfreeze strengths than expected, based on the extrapolation of short term strength data. The definition of long term adfreeze strength should be reviewed. The current definition (the onset of tertiary creep) may be overly conservative at low stresses. This is an area in which further research should be considered.

Undetermined Field Effects

Seven pile load tests at two separate sites (both in saline soils) in the Northwest Territories resulted in adfreeze bond strengths which were significantly lower than would have been expected based on comparable laboratory test data. Saline soils are widespread in the Northwest Territories and therefore these field test results are significant. Research should be carried out aimed at establishing the reasons for the difference between these two fairly reliable sets of data.

Frost Heave

Frost heave of piles due to freezeback in the active layer is a concern. Methods of reducing the adfreeze strength to the pile shaft in the active layer should be investigated. Current techniques include greasing the upper portion of the pile and the use of plastic heat shrink sleeves. The effectiveness of these various techniques should be investigated.

THURBER

Dynamic or Cyclic Loads

A literature review of the effects of dynamic or cyclic loads and possible effects on adfreeze strength was not carried out as part of this study. This is an area which is of concern with respect to the design of compressor foundations. A literature review should be carried out and an evaluation of existing theory and data should be completed.

Lateral Loads

A literature review of the behaviour of piles subjected to lateral loads was not carried out as part of this study. It is recommended that such a review be carried out and an evaluation of existing theories and supporting data be made.

Driven Piles

Driven piles in permafrost have been used extensively in warm permafrost regions of Alaska, and should be suitable for similar areas in Northern Canada. Research into the use of driven piles (including a trial installation and field load tests) should be considered.

ADFREEZE STRENGTH

LIST OF REFERENCES

Hoggan Engineering and Testing (1980) Ltd., 1983. Pile Foundation Design for Kuluak School, Clyde River, N.W.T., report submitted to the Department of Public works and Highways, Government of the Northwest Territories.

Hoggan Engineering and Testing (1980) Ltd., 1985. Pile Load Tests, Arctic Bay Multi-Purpose Hall and School Extension, report submitted to the Department of Public Works and Highways, Government of the Northwest Territories.

Johnston, G.H., and Ladanyi, B., 1972. Field Tests of Grouted Rod Anchors in Permafrost, Cdn. Geot. Journ. Vol 9, pp. 176-194.

Johnston, G.H., 1981. Permafrost Engineering Design and Construction, John Wiley & Sons, Toronto.

Johnston, G.H., and Ladanyi, B., Field tests of deep power-installed screw anchors in permafrost, Cdn. Geot. Journ. Vol 11,, pp. 348-358.

Karpov, V.M. and Velli, Y.Y., 1968. Displacement Resistance of Frozen Saline Soils, Soil Mechanics and Foundation Engineering, Volume 4, pp. 277-279.

Kast, G. and Shermer, N., 1986. Dew Line Anchors in Permafrost, Geotechnical News, December, 1968, pp. 30-34.

Ladanyi, B., 1983. Design and construction of deep foundations in permafrost: North American practice. Fourth Int. Conf. on Permafrost, Fairbanks, 1983.

Ladanyi, B., 1988. Short and long term behaviour of axially loaded bored piles in permafrost. First Int. Seminar on deep foundations on bored and augered piles, Ghent, Belguim, June, 1988.

Nixon, J.F., 1988. Pile Load Tests in Saline Permafrost at Clyde River, N.W.T., Can. Geot. Journ., Vol. 25, pp. 24-32.

THURBER

LIST OF REFERENCES
(continued)

Nixon, J.F., and Neukirchner, 1984. Design of vertical and laterally loaded piles in saline permafrost, Proc. Cold Region Engineering Specialty Conf., CSCE, Montreal, Quebec.

Nixon, J.F., and Lem, G., 1984. Creep and strength testing of frozen saline fine grained soils, Cdn. Geot. Journ., Vol. 21, pp. 518-529.

Nixon, J.F., and McRoberts, E.C. A design approach for pile foundations in permafrost, Cdn. Geot. Journ., Vol. 13, pp. 40-57.

Ogata, N., Yasuda, M. and Katacha, T., 1983. Effects of salt concentration on strength and creep behaviour of artificially frozen soils, Cold Regions Science and Technology, Vol. 8, pp. 139-153.

Parameswaran, V.R., 1978. Adfreeze strength of frozen sand to model piles, Cdn. Geot. Journ., Vol. 15, pp. 494-500.

Parameswaran, V.R., 1979. Creep of model piles in frozen soil, Cdn. Geot. Journal., Vol. 16, pp. 69-77.

Penner, E., 1967. Heaving pressure in soils during unidirectional freezing, Cdn. Geot. Journ. Vol. 4, p. 398 Correction, Vol. 5, 1968, p. 119.

Penner, E., 1974. Uplift forces on foundations in frost heaving soils. Cdn. Geot. Journ. Vol. 11, p. 323-338.

Penner, E., and Gold, L.W., 1971. Transfer of heaving forces by adfreezing to columbs and foundation walls in frost-susceptible soils. Cdn. Geot. Journ., Vol. 8, pp. 514-526.

Sego, D.C., Shulz, T., and Banasch, R. Strength and deformation of frozen saline sand. Proc. of the Third International Symposium on Ground Freezing. Hanover, 1, pp. 11-18.

THURBER

LIST OF REFERENCES
(continued)

Stuckert, B.J., and Mahar, L.J. The role of ice content in the strength of frozen saline coarse grained soils. Proc. April 4-6, 1984. Canadian Society for Civil Engineering Speciality Conference, Quebec, Vol. 2, pp. 579-587.

Theriault, A., and Ladanui, B., 1988. Behaviour of long piles in permafrost. Fifth Int. Conf. on Permafrost, Trondheim, August, 1988.

Thurber Consultants Ltd., 1983. Pile load tests, Baffin Island Correctional Centre, report submitted to the Government of the Northwest Territories, Department of Public Works, October, 1983.

Thurber Consultants Ltd., 1988. North Warning System, Short Range Radar Sites - Zone 2, Pile Load Test Program, Model Pile Load Tests - Phase 1, report submitted to Stanley Associates Engineering Ltd., February, 1988.

Weaver, J.S., and Morgenstern, N.R., 1981. Pile design in permafrost. Can. Geot. Journ., Vol. 18, pp. 357-370.

SECTION 8

LIST OF FIGURES

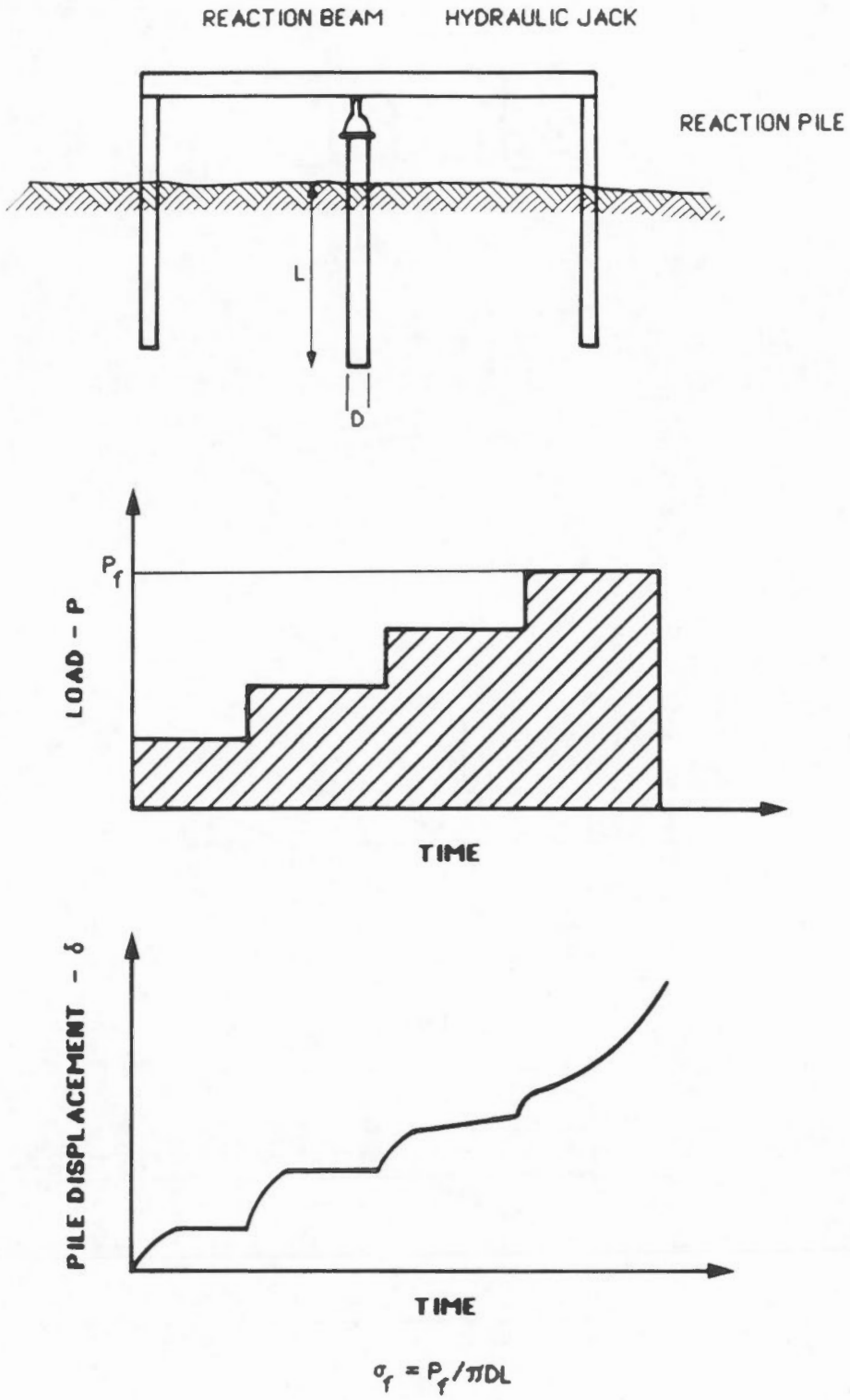

Typical field pile load test.

FIGURE 8.1

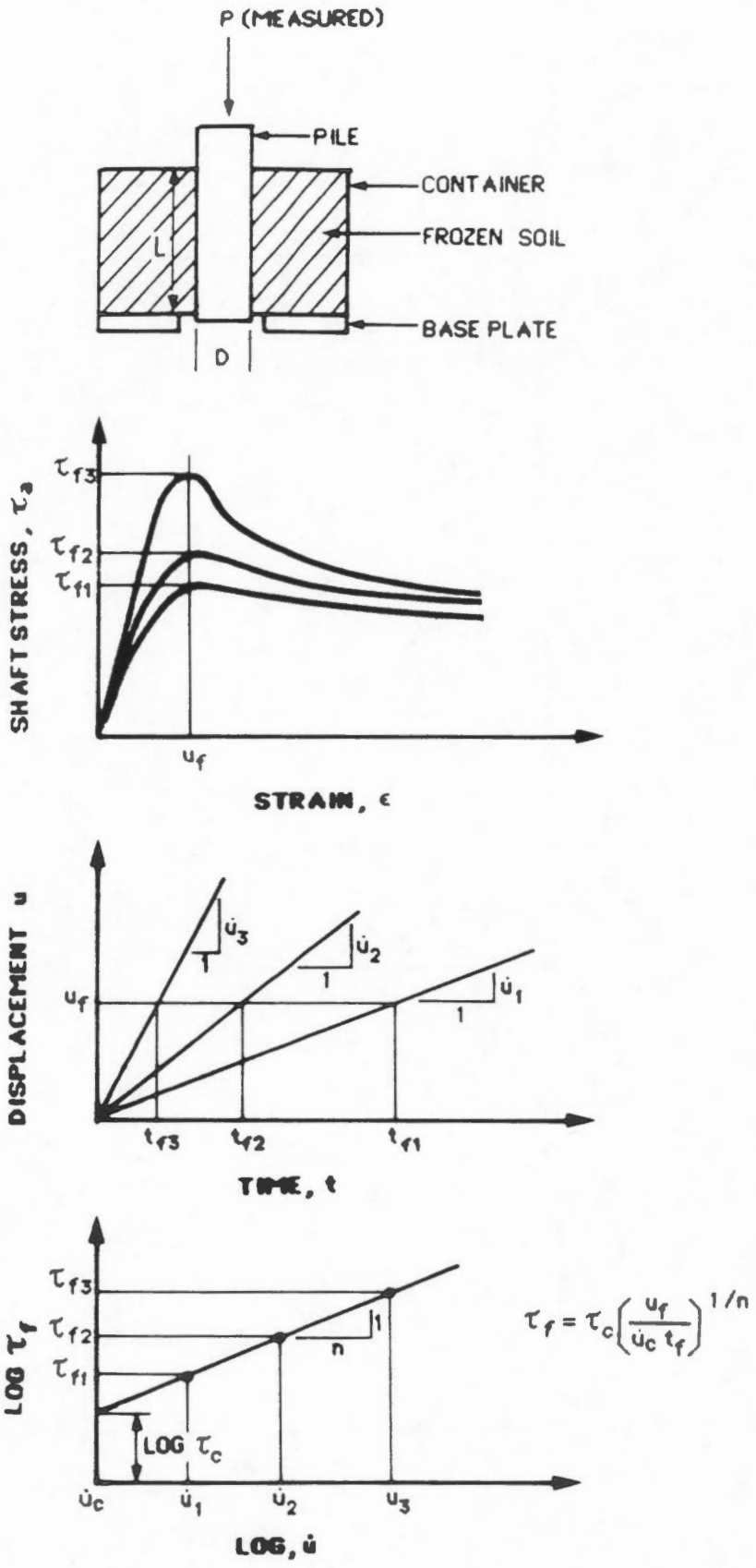

Typical laboratory pile load test (constant displacement rate test)

THURBER

FIGURE 8.2

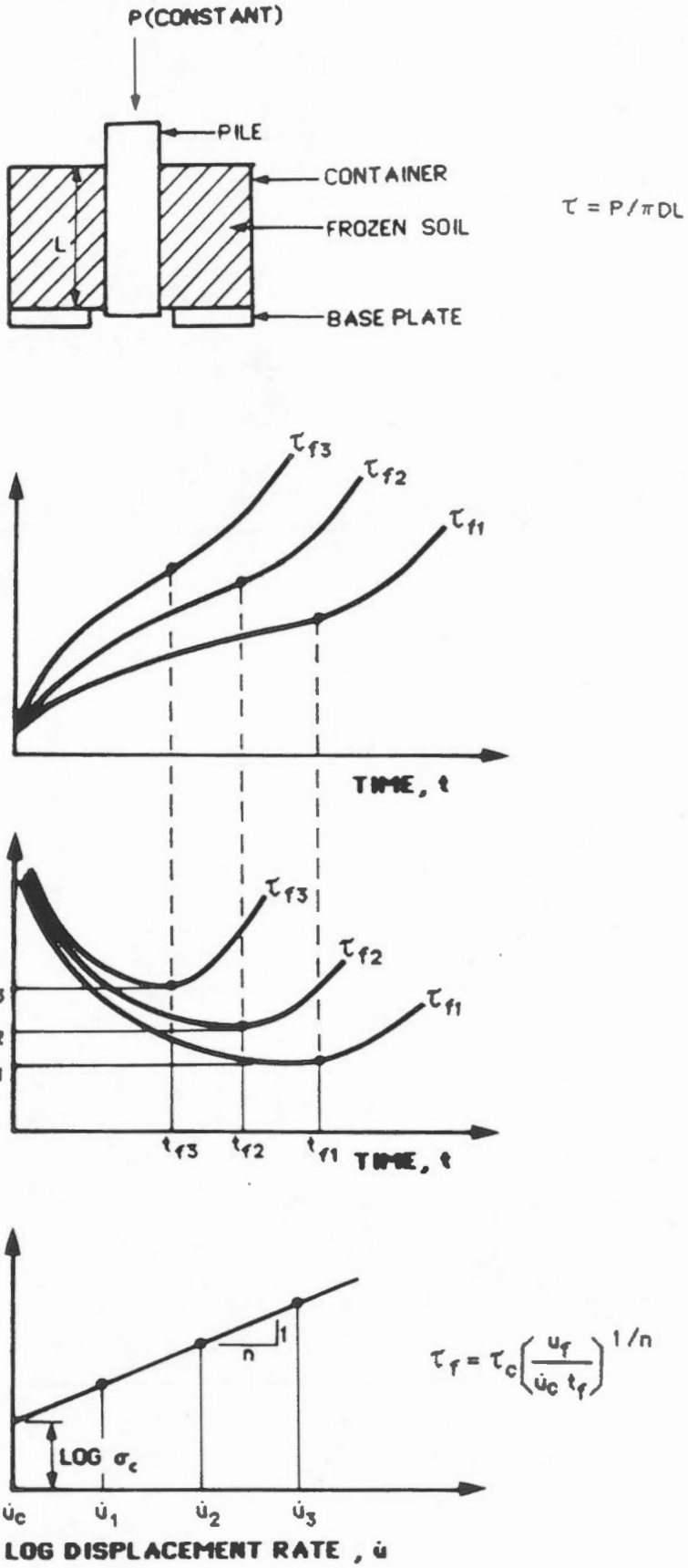

Typical laboratory pile load test
(constant load test)

FIGURE 8.3

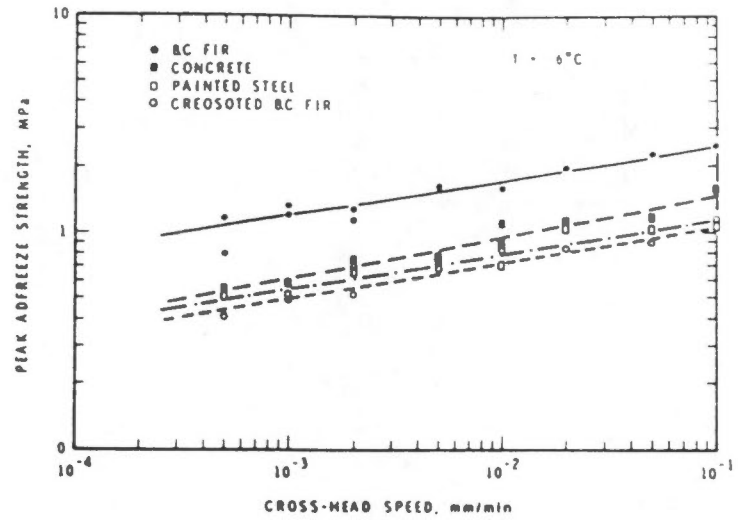

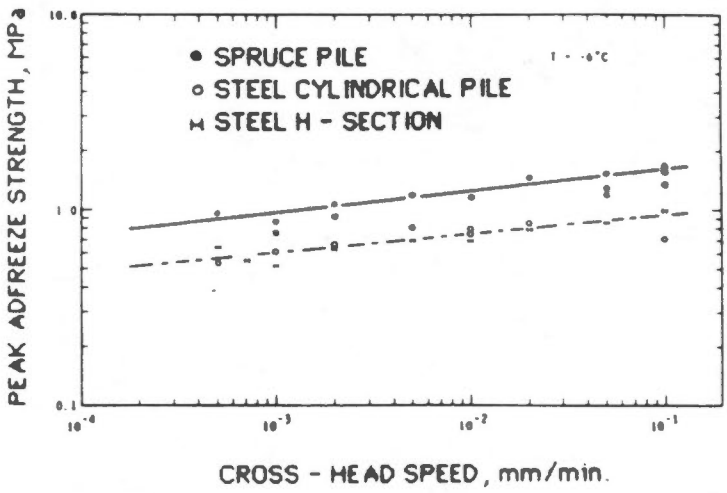

Effect of pile type on adfreeze strength (Parameswaran, 1978).

FIGURE 8 4

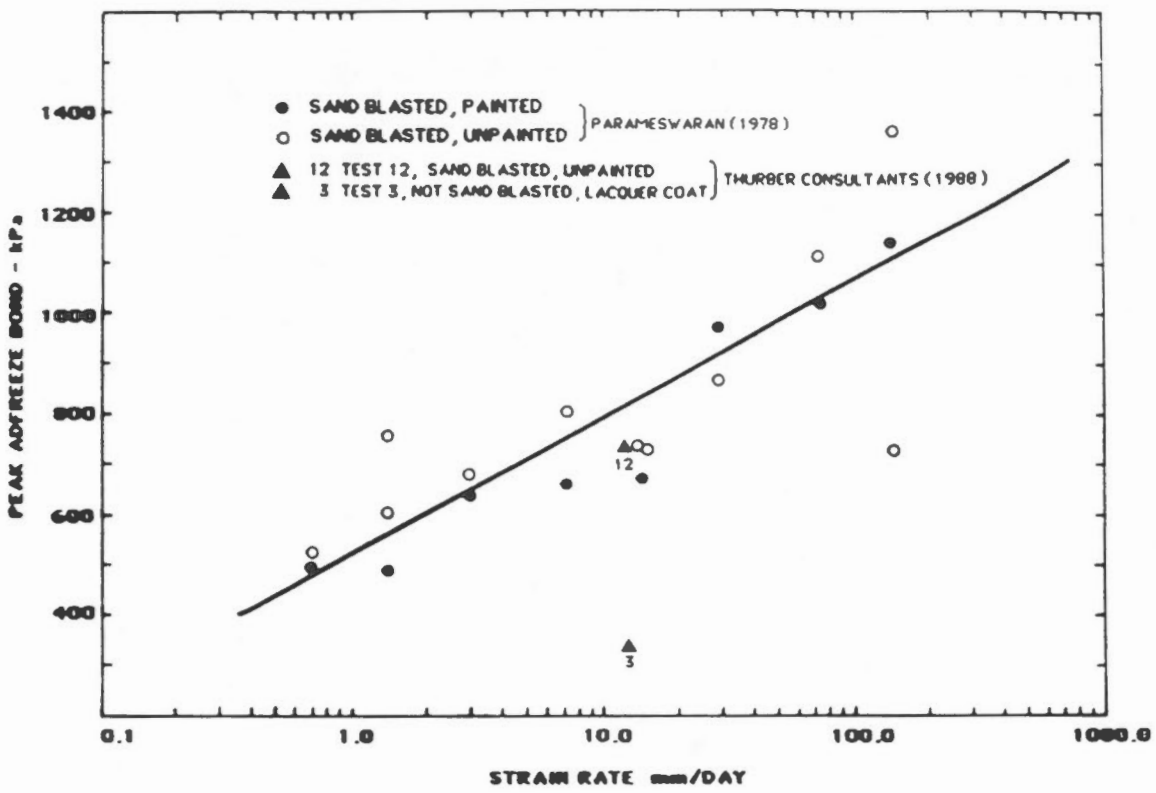

Effect of surface treatment on adfreeze strength (steel pipe piles).

THURBER

FIGURE 8.5

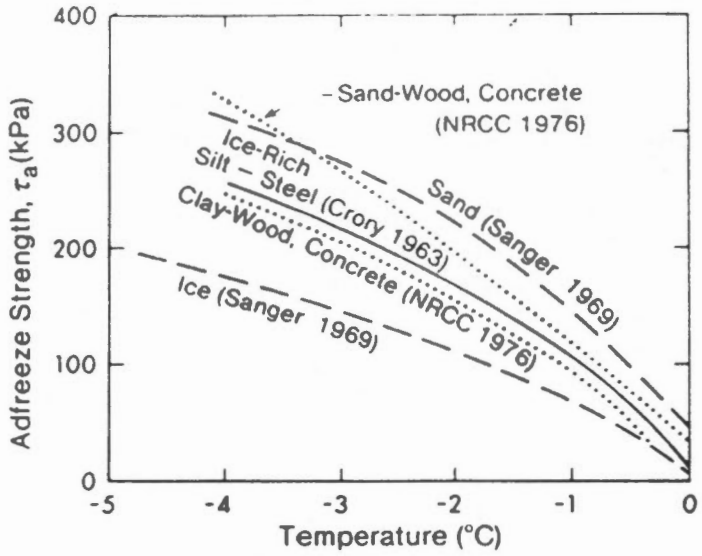

Effect of temperature on adfreeze strength (Weaver and Morgenstern, 1981).

FIGURE 8.6

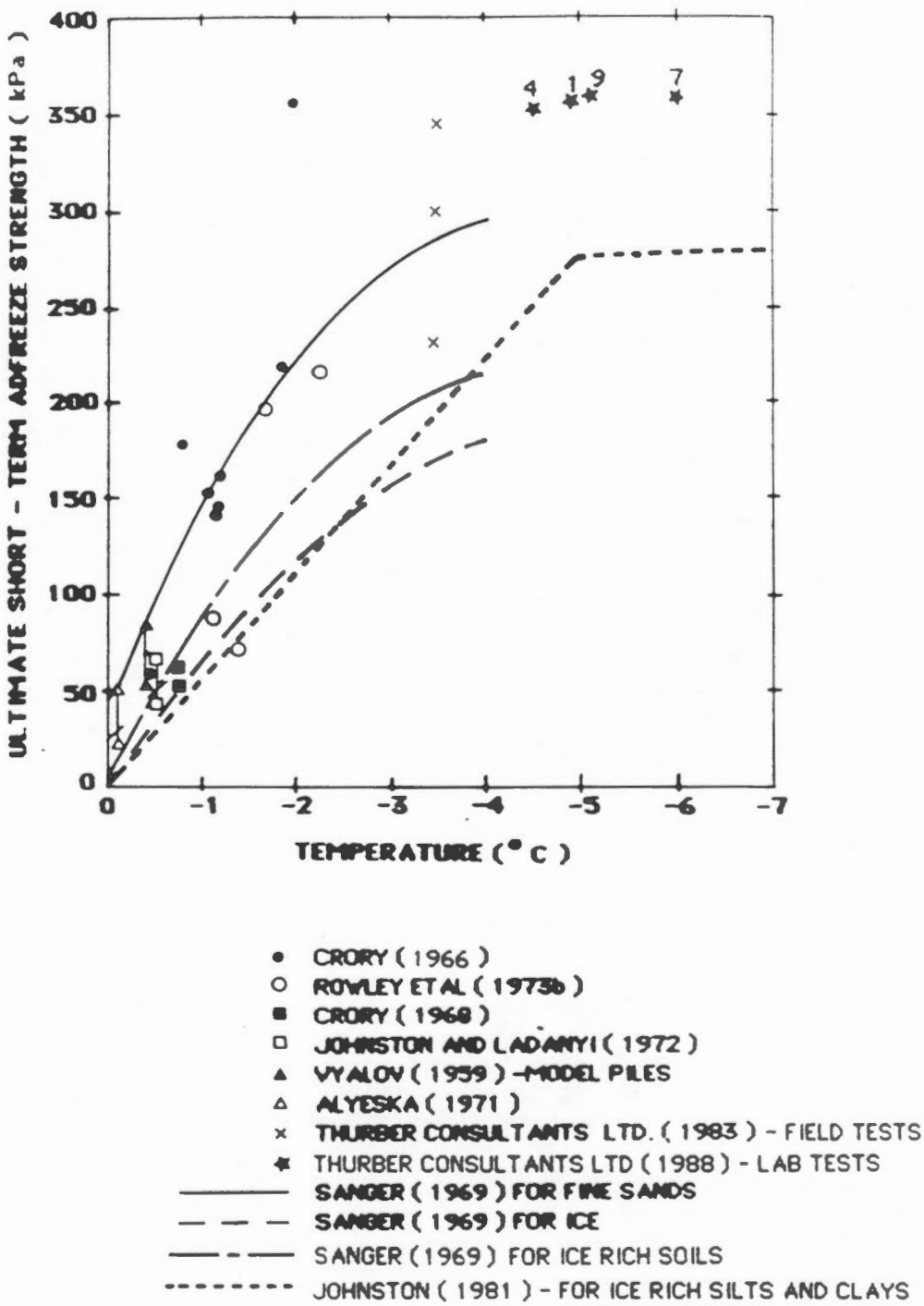

Effect of temperature on adfreeze strength (Johnston, 1981).

UNIVERSITY OF ALBERTA

LABORATORY PILE LOAD TEST RESULTS

Test No.	Native Soil Type	Native Soil Salinity (ppt)	Backfill Type	Backfill Salinity (ppt)	Peak Adfreeze Strength (kPa)	Displacement at Failure (mm)	time to Failure (hours)	Sample Temperature (°C)	Location of Failure Surface
1	SM	0	'Imported Sand'	0	357	0.77	2.7	-4.8	P/B
2	SM	10	H.P.C.	-	55	2.80	4.7	-4.8	B/N
3	SM	0	H.P.C.	-	72	0.78	2.0	-4.8	P/B
4	SM	10	'Imported Sand'	0	351	1.02	2.3	-4.5	P/B
5	SM	0	Ice	0	217	1.25	1.5	-5.3	P/B
6	SM	10	'Drill Cuttings'	10	190	0.98	2.7	-4.8	P/B
7	SM	0	'Drill Cuttings'	0	360	0.67	2.0	-6.4	P/B
8	SM	10	Ice	0	250	1.18	2.2	-5.9	P/B
9	Ice	0	'Imported Sand'	0	353	0.94	3.2	-5.3	P/B
10	Ice	0	Ice	0	216	0.67	3.0	-5.0	P/B
11	Ice	0	Ciment Fondu	-	736	1.93	5.3	-5.1	P/B
12	SM	0	'Imported Sand'	0	733	2.48	6.3	-5.3	P/B
13	SM	10	'Imported Sand'	0	581	5.33	9.9	-5.1	B/N

Note: 1) Failure occurred at pipe/backfill interface in all tests, except for Tests 2 and 13, in which failure occurred at the contact between the backfill and the 'native' soil. the peak shear stress at failure for these tests is the stress at the pipe/backfill interface.
2) H.P.C. denotes Halliburton Permafrost Cement.
3) Tests 12 and 13 were carried out on pipe piles which had been sand blasted prior to testing. All other tests were carried out on pipe piles which were as received from the supplier.
4) All tests were carried out under a displacement rate of 12 mm per day.
5) P/B denotes pile/backfill interface, B/N denotes 'native' soil interface.

Laboratory pile test results (Thurber Consultants Ltd., 1988).

THURBER

FIGURE 8.8

CLYDE RIVER SCHOOL
PILE LOAD TESTS
(NIXON, 1988)

Test No.	Native Soil Type	Average Native Soil Salinity	Backfill	Probable Backfill Salinity	Pile Diameter (mm)	Pile Hole Diameter (mm)	Peak Adfreeze Strength (kPa)	Approx. Time to Failure (hours)	Average Temperature (°C)
1	Silty Sand	10	Sand	1	140	150-175	124	24	-6.
2A	Silty Sand	10	Sand	1	140	150-175	83	144	-6.
3	Silty Sand	10	Sand	1	140	150-175	81	66	-6.

ARCTIC BAY SCHOOL
PILE LOAD TESTS
(HOGGAN, 1985)

Test No.	Native Soil Type	Average Native Soil Salinity	Backfill	Probable Backfill Salinity	Pile Diameter (mm)	Pile Hole Diameter (mm)	Peak Adfreeze Strength (kPa)	Approx. Time to Failure (hours)	Average Temperature (°C)
2	Silty Sand	10	Sand	1	114	180	109	75.	-6.
3	Silty Sand	10	Sand	1	114	180	93	22.	-6.
4	Silty Sand	10	Sand	1	114	180	86	25.	-6.
5	Silty Sand	10	Sand	1	140	180	124	73.	-6.

BAFFIN CORRECTIONAL CENTRE (IQALUIT)
PILE LOAD TESTS
(THURBER CONSULTANTS LTD., 1983)

Test No.	Native Soil Type	Average Native Soil Salinity	Backfill	Probable Backfill Salinity	Pile Diameter (mm)	Pile Hole Diameter (mm)	Peak Adfreeze Strength (kPa)	Approx. Time to Failure (hours)	Average Temperature (°C)
1	Sand	1.4	Sand	0	102	165	340	22	-3.5
2	Sand	1.4	Sand	0	127	165	300	23	-3.5
3	Sand	1.4	Sand	0	127	165	230	6	-3.5

Field pile load test data for steel pipe piles (Iqaluit, Clyde River and Arctic Bay).

THURBER

FIGURE 8.9

SECTION 9

THAW CONSOLIDATION

SECTION 9

THAW CONSOLIDATION

9.1 General

When frozen soils thaw, significant settlement may occur, depending on the volume of excess ice present within the frozen soil. There are two aspects of the thaw consolidation process which are of concern to geotechnical engineers:

1) Thaw settlements, and
2) excess pore pressures.

The magnitude and distribution of settlements are of concern for any structure (pipelines, roads, embankments and buildings) which could cause a change in the thermal regime such that thaw settlement will occur. The structure must be designed to either tolerate the expected settlements or measures must be taken to reduce or eliminate thaw.

As frozen soil thaws, excess pore water pressure may be generated at the thaw front. The magnitude of the pore water pressure controls the strength of the thawing soil and hence is of interest in assessing the stability of slopes and embankments constructed in permafrost regions.

These two aspects of the thaw consolidation process are discussed in the following sections.

9.2 Thaw Settlements

For many design applications, the rate of consolidation and the pore pressures generated during thaw consolidation are not a major concern. It is therefore acceptable to ignore time dependent effects and thereby simplify the analysis of the thaw consolidation process (Watson et al., 1973).

If a sample of ice rich frozen soil is thawed uniaxially under a nominal applied pressure σ_o , the total thaw strain can be measured, as shown in Figure 9.1. Once the sample has thawed completely, an additional pressure (σ_1) can be applied and additional vertical deformation will occur as the thawed sample consolidates further.

THURBER

For ice rich soils, the thaw strain which occurs under the nominal pressure σ_o is normally much greater than the strain which will occur under subsequent increased pressures. Therefore, it can be assumed that the strain which occurs after thawing is a linear function of applied pressure, and total strain due to thaw consolidation will be given by the following expression:

$$\epsilon_t = A_o + m_v \sigma \qquad (9.1)$$

where

ϵ_t denotes the total strain under applied stress σ,

A_o denotes the intercept of the thawed applied pressure - strain relationship at an applied pressure of zero, as shown on Figure 9.1, and

m_v denotes the compressibility of the soil after thawing.

For many practical design applications, the sample can be thawed under a single applied load, which is selected to be representative of the expected effective stress which will exist in the thawed soil after consolidation is completed. For most pipeline design applications an applied pressure of 50 to 100 kPa can be used, which will yield a reasonable, but conservative estimate of total thaw strain. Thus, Equation 9.1 can be simplified further to:

$$\epsilon_t = A_p \qquad (9.2)$$

Equation 9.2 is particularly useful for estimating thaw settlements below linear structures such as roads and warm oil pipelines because it permits the use of simplified test procedures, so that a large number of samples can be tested and analysed statistically to establish a range of expected thaw settlements. The procedure, as applied to the design of a warm oil pipeline is described in detail by Hanna et al (1983).

The water content of frozen soils is routinely measured in most subsurface investigations. It is of interest, therefore to relate the water (ice) content of the frozen soil to thaw strain. Hanna et al (1983), have summarized such data from a variety of sources. The data are presented on Figures 9.2 to 9.6, for different soil types.

THURBER

Water contents shown on these figures are expressed in terms of volumetric water content rather than the usual gravimetric water content, so that the full range of water contents will be confined between 0 and 100%. The volumetric water content is the ratio of the volume of water to the total volume of the frozen soil. It can be calculated from the gravimetric water content through the use of the following equation:

$$w_v = \frac{w_g}{\left(\frac{1}{G_s} + \frac{w_g}{S}\right)} \qquad (9.3)$$

where

w_v denotes the volumetric water content,

w_g denotes the gravimetric water content,

G_s denotes the specific gravity of the soil particles, and

S denotes the degree of saturation.

The specific gravity of most mineral soils falls within a range from 2.5 to 2.7. The specific gravity of peat can range from 1.1 to 2.5.

Crory (1973) and others have suggested the use of a correlation between thaw strain and frozen bulk density. Correlations between these variables are presented on Figures 9.7 to 9.9.

Total thaw strains in saturated ice rich soils can also be estimated from the void ratio before and after thawing, since:

$$\epsilon_t = \frac{e_f - e_t}{1 + e_f} \qquad (9.4)$$

where

e_f denotes the void ratio of the frozen soil, and

e_t denotes the void ratio of the thawed soil.

THURBER

The void ratio of the frozen and thawed soil can be readily calculated from the water content since:

$$e = \frac{w_g G_s}{S} \qquad (9.5)$$

Once the total thaw strain for a particular soil type has been established, an estimate of the total thaw settlement which will occur in the field can be established from the equation:

$$\Delta x = A_\sigma \; x + m_v \; \Delta\sigma x \qquad (9.6)$$

or

$$\Delta x = A_p x \qquad (9.7)$$

where

Δx denotes the total thaw settlement, and

x denotes the depth of thaw.

In practice, the thaw settlement parameters A_σ, m_v and A_p can be expected to vary with depth and therefore it is usually necessary to calculate the thaw settlement within discrete soil layers and add the calculated settlement for each layer to obtain an estimate of total settlement.

It will be noted on Figures 9.3 to 9.9 that there is considerable scatter to the data relating thaw strains to soil water content or frozen bulk density. This will, of course, reflect the accuracy to which thaw settlements can be calculated. In addition, significant variations in thaw settlements, due to the random orientation and distribution of excess ice within the frozen soil must be expected. Despite these limitations, the foregoing relationships have been found to be very useful as a means of predicting the average total settlement and the probable range in total settlement which can be expected in the field.

It is understood (Morgenstern, 1988) that the magnitude of thaw settlements observed in the field are generally less than those calculated using the relationships given in Figures 9.3 to 9.9. The lower observed settlement is believed to be due to arching and other 3 dimensional effects. This is an area in which further research should be considered.

THURBER

9.3 Excess Pore Pressures

As mentioned earlier, when frozen soil thaws, water is liberated at the thaw front. In many ice rich soils the water pressure at the thaw front may exceed the hydrostatic water pressure at that depth. The water pressure above hydrostatic is termed the excess pore pressure. The excess pore pressure at the thaw front will be controlled by the rate at which water is liberated by thaw and the rate at which the water can drain from the thaw front. A sketch which shows the physical process of thaw consolidation is presented on Figure 9.10.

For many field problems (particularly one dimensional problems) the rate of advance of the thaw front can be approximated by an equation of the form:

$$x = \alpha \sqrt{t} \qquad (9.8)$$

where

- x denotes the depth below the surface at which a step temperature has been applied,
- α denotes a thermal coefficient, and
- t denotes time.

The thermal coefficient, is a function of the thermal properties of the soil and the temperature boundary conditions. It can be readily established using a thermal analysis appropriate to the problem at hand. Values for which are commonly encountered in practice range from 0.1 to 1.0 mm per second $^{0.5}$ and can normally be calculated to an accuracy of $\pm$ 10 percent.

The dissipation of pore pressure within the thawed portion of the soil is controlled by the coefficient of consolidation, c_v, which is defined as follows:

$$c_v = \frac{k}{m_v \; w} \qquad (9.9)$$

where

- k denotes the hydraulic permeability of the thawed soil,

THURBER

γ_w denotes the unit weight of water, and

m_v denotes the coefficient of compressibility.

The coefficient of volume compressibility, m_v is defined as follows:

$$m_v = \frac{\Delta \epsilon}{\Delta \sigma'} \qquad (9.10)$$

where

$\Delta \epsilon$ denotes the thaw strain which occurs under an increase in effective stress $\Delta \sigma'$.

Typical values for the coefficient of compressibility range from 0.01 mm^2/sec for clays to 10 mm^2/sec for sandy silts.

Morgenstern and Nixon (1971) developed a one-dimensional theory for the thaw consolidation process depicted in Figure 9.10, by coupling the constitutive equation governing consolidation with the equation which defines the advance of the thaw front. Initially the theory assumed that void ratio was a linear function of effective stress, as shown in the upper half of Figure 9.10. The theory was later extended to incorporate a non-linear relationship between void ratio and effective stress which is more appropriate to ice rich, thawed soils (Morgenstern and Nixon, 1973a).

A key parameter which governs the process is the thaw consolidation ratio, R, which is defined as follows:

$$R = \frac{\alpha}{2\sqrt{c_v}} \qquad (9.11)$$

The thaw consolidation ratio, R, represents a coupling of the thermal and consolidation processes within the thawing soil. It is a measure of the relative rate at which excess water is generated (by thawing) at the thaw front, and the rate at which it can drain from the thaw front by consolidation. Where thaw rates (as embodied in) are rapid, the value of R will be high and high excess pore pressures will be generated at the thaw front. Where the coefficient of compressibility is high (indicating rapid dissipation of pore pressure), R will be low and the excess pore pressure at the thaw front will be low.

THURBER

The predicted excess pore pressure at the thaw front based on an assumed linear relationship between void ratio and effective stress is shown in the upper half of Figure 9.11. An exact solution for both the self weight case and a weightless soil with an external applied pressure was possible. The total excess pore pressure can be obtained by adding the excess pore pressure for each case.

The predicted excess pore pressure at the thaw front assuming a non-linear relationship between void ratio and effective stress is presented in the lower half of Figure 9.11. This solution assumes a linear relationship between void ratio and the logarithm of effective stress. The solution shown on Figure 9.11 assumes externally applied loads are large relative to the self weight of the soil. An exact solution for the non-linear self weight case was not possible and hence numerical methods must be used to solve the equation for that case.

As indicated by the results presented on Figure 9.11, the pore pressure at the thaw front will be primarily a function of the following variables:

1) The rate of thaw as embodied in the thermal coefficient α,

2) The rate of consolidation as defined by the coefficient of consolidation c_v, and

2) The residual effective stress σ'_o, which is the effective stress of the soil after it has thawed but before any drainage has occured.

As a first approximation, a value of R greater than about 0.5 would indicate a probability of significant excess pore pressures being generated at the thaw plane. The theory can therefore be used to provide an indication of those soils which might be thaw unstable, provided α, c_v and σ'_o are known or can be estimated.

A summary of pertinent properties of various soils from the Mackenzie Valley is presented in Figure 9.12. It is apparent that under the rates of thaw normally encountered in civil engineering practice, significant pore pressures will normally be generated during thawing of ice rich silts, silty clays and clays. Excess pore pressures will not normally be generated in sands and gravels. This predicted behaviour is consistent with field experience.

The thaw consolidation theory has been extended in a number of ways. For example, the rate of thaw may be expressed as an arbitrary power law (Nixon and Morgenstern, 1973a). The movement of the heat source may be taken as finite (Nixon 1973a) and a solution for layered systems has been obtained (Nixon, 1973b). This latter solution is of particular value because it can be used to predict the stability of soils which overlie thick ice layers. Nixon and Morgenstern (1973b) have also examined the effect which high values of the residual effective stress will have on the process of thaw consolidation.

The theory of thaw consolidation has been applied to a variety of practical problems. The stability of dam foundations on thawing ground has been discussed by Nixon (1973a), the settlement and stability of the thaw bulb around a buried pipeline by Nixon (1973a) and Morgenstern and Nixon (1975). The application of thaw consolidation theory to slope stability problems has been discussed by McRoberts (1973), McRoberts and Morgenstern (1974) and McRoberts and Nixon (1977).

9.4 Laboratory Confirmation Tests

Laboratory tests have been carried out by a number of researchers, to test the validity of the thaw consolidation theory proposed by Morgenstern and Nixon. Tests on reconstituted samples were reported by Morgenstern and Smith (1973) and on undisturbed samples by Nixon and Morgenstern (1974). The results of these tests are presented on Figures 9.13 and 9.14. The test results confirm, in general, the validity of the non-linear theory of consolidation.

Roggensack (1977) carried out an extensive and detailed program of laboratory tests on undisturbed samples of ice rich soils from three separate sites in the Mackenzie River Valley.

Roggensack measured the residual effective stress on a large number of samples and found a good correlation between the thawed, undrained void ratio (prior to consolidation) and the measured values of residual effective stress for the various soil types. He also found a good correlations between soil type, residual effective stress and liquidity index. These correlations are presented on Figures 9.15 and 9.16.

Roggensack found that both hydraulic permeability k and the coefficient of compressibility m_v were very sensitive to effective stress in the thawed soil. However, in most

THURBER

soils, as effective stress increased, both permeability and compressibility decreased, with the result that c_v was not overly sensitive to changes in effective stress for a given soil type. Typical tests results which illustrate the relationship between c_v and effective stress are presented in Figures 9.17 and 9.18. The test results show that c_v typically decreases in the stress range from 0 to 50 kPa and remains relatively constant thereafter. As discussed by Roggensack, the use of the lower constant value for c_v over the entire stress range will cause predicted pore pressures to be higher than actual field values in the stress range from 0 to 50 kPa, which is conservative.

A comparison between the pore pressure at the thaw front as measured experimentally by Roggensack on laboratory samples, and the pore pressure predicted by the Morgenstern and Nixon non-linear thaw consolidation theory is presented in Figure 9.19. The excellent agreement between the measured and predicted values confirms the validity of the theory.

9.5 Comparisons with Field Data

9.5.1 Inuvik Pipeline

In order to study the behaviour of a warm oil pipeline in ice rich permafrost, Mackenzie Valley Pipeline Research Limited installed a 27 m test section of 0.61 m diameter pipe near Inuvik, N.W.T. The surrounding soils consisted of ice rich silty clay. Oil, at a temperature of 71°C was circulated through the pipe. The test section was fully instrumented to measure settlements, temperatures and pore pressures. A complete description of the instrumentation is given by Slusarchuk (1973) and a summary of the observations is given by Watson et al (1973). A sketch showing the stratigraphy below the pipeline is shown in Figure 9.20.

Morgenstern and Nixon (1975) carried out an analysis of the data obtained from the test facility. The problem is not one-dimensional, however it is reasonable to assume one-dimensional conditions exist directly below pipe centreline.

The predicted and measured position of the thaw front below the centreline of the pipeline, as a function of time, is shown on Figure 9.21. The results indicate excellent agreement between the predicted and observed rates of thaw. A value for the thermal coefficient of 0.773 $mm/sec^{0.5}$ was calculated from this data.

THURBER

A value for the coefficient of consolidation of 1.03 mm^2/sec was established from laboratory tests on undisturbed core samples taken from the site. The value for the thaw consolidation ratio, R, was therefore calculated to be 0.383.

Using this value for the thaw consolidation ratio, the maximum excess pore pressure at the thaw front was calculated using the thaw consolidation theory. The predicted and measured pore pressures at the thaw front are compared in Figure 9.22. While there is some scatter, there is reasonable agreement between the observed and predicted pore pressures. The scatter is most likely due to natural variations in soil water content and grain size distribution.

The observed and predicted settlement behaviour below the pipeline is compared in Figure 9.23. The observed settlement, as measured at two locations, is seen to vary significantly, reflecting variations in ice content over the site. The settlement predicted from the thaw consolidation theory is seen to be in good agreement with the observed settlements.

9.5.2 Sans Sault and Martin River Slopes

McRoberts et al (1978) measured pore water pressures in thawing slopes at test sites located near Sans Sault Rapids and Martin River in the Mackenzie River Valley. In this case, the pore pressures were measured periodically as the active layer thawed during the summer months. No attempt was made to monitor the associated surface settlements. The soil properties and pore pressure observations are summarized on the upper half of Figure 9.24.

McRoberts used the Morgenstern and Nixon thaw consolidation theory to predict the coefficient of consolidation which would have been operative in order to achieve the observed pore pressures. The back calculated coefficient of consolidation was then compared to that established from laboratory test data, and field permeability test data.

The comparison between the laboratory measured values and the back calculated values for c_v are presented on the lower half of Figure 9.24. While the two sets of data are in reasonable agreement, it is not possible to draw definite conclusions from this study. As

THURBER

discussed by McRoberts, there are a number of complicated and inter-related factors which make it difficult to reconcile the predicted and measured pore pressures at these two sites.

9.6 Summary

A considerable volume of data is available which can be used to provide an indication of the range in total settlements which will occur in frozen soils, provided soil water contents or frozen bulk densities are known. The simplified method of calculating thaw settlements has proven to be adequate for many design applications.

The magnitude of thaw settlements observed in the field is often less than predicted values due to three dimensional effects. This is an area in which further research should be considered.

The Morgenstern and Nixon thaw consolidation theory provides an excellent framework within which the stability of thawing soils can be evaluated. Laboratory tests have shown that the theory models the thaw consolidation behaviour of both reconstituted and undisturbed soils reasonably well. Reasonable agreement has been obtained between predicted and observed thaw consolidation behaviour in the field.

No further research into the process of thaw consolidation appears to be warranted at this time, however field studies related to thaw consolidation would be of great value, if opportunities arise.

THURBER

THAW CONSOLIDATION
LIST OF REFERENCES

Andersland, O.B., and Anderson, D.M., 1978. Geotechnical engineering for cold regions. McGraw-Hill Book Company, New York.

Brown, W.G., and Johnston, G.H., 1970. Dykes on permafrost predicting thaw and settlement. Canadian Geotechnical Journal, Vol. 7, pp. 365-371.

Carlslaw, H.S., and Jaeger, J.C., 1947. Conduction of heat in solids. Clarendon Press, Oxford.

Crory, F.E., 1973. Settlement associated with the thawing of permafrost. Permafrost: The North American contribution to the Second International Conference on Permafrost, Yakutsk, National Academy Science, Washington, D.C., pp. 599-607.

Hanna, A.J., Saunders, R.J., Lem, G.M., and Carlson, L.E., 1983. Alaska highway gas pipeline project (Yukon) section thaw settlement design approach. Proceedings of the Fourth International Conference on Permafrost, Fairbanks, National Academy Science, Washington D.C. pp. 439-444.

Johnson, G.H., 1981. Permafrost, engineering design and construction, John Wiley and Sons, New York.

Johnson, G.H., Ladanyi, B., Morgenstern, N.R., and Penner, E., 1981. Chapter 3, engineering characteristics of frozen and thawing soils. In permafrost engineering design and construction (Johnson, 1981).

Lachenbruch, A.H., 1970. Some estimates of the thermal effects of a heated pipeline in permafrost. U.S. Geol. Survey Circ. 632.

Luscher, U. and Afifi, S.S., 1973. Thaw consolidation of Alaskan silts and granular soils. Permafrost: The North American contribution to the Second International Conference on Permafrost, Yakutsk, National Academy Science, Washington, D.C. pp. 325-333.

MacPherson, J.G., Watson, G.H. and Koropatnick, A., 1970. Dykes on permafrost foundations in northern Manitoba, Canadian Geotechnical Journal, Vol. 7, pp. 356-364.

THAW CONSOLIDATION
LIST OF REFERENCES
(continued)

McRoberts, E.C., 1973. Stability of slopes in permafrost. Ph.D. Thesis, University of Alberta, Civil Engineering, Edmonton, Alberta.

McRoberts, E.C., and Morgenstern, N.R., 1974. Stability of slopes in frozen soil, Mackenzie Valley, N.W.T. Canadian Geotechnical Journal, Vol. 11, No. 4, pp. 554-573.

McRoberts, E.C., Flectcher, E.B. and Nixon, J.F., 1978. Thaw consolidation effects in degrading permafrost. Proceedings of the Third International Conference on Permafrost, Edmonton, National Research Council of Canada, Ottawa, pp. 693-699.

McRoberts, E.C., and Nixon, J.F., 1977. Extensions to thawing slope stability theory. Proc. 2nd International Symposium on Cold Regions Eng. (1976), Fairbanks, University of Alaska, Department of Civil Engineering, pp. 262-276.

McRoberts, E.C., Law, T.C., and Moniz, E., 1978. Thaw settlement studies in the discontinuous permafrost zone. Proceedings of the Third International conference on Permafrost, Edmonton, National Research Council of Canada, Ottawa, pp. 700-706.

Morgenstern, N.R., 1988. Personnel Communication.

Morgenstern, N.R., and Nixon, J.F., 1971. One dimensional consolidation of thawing soils. Canadian Geotechnical Journal, Vol. 8, pp. 558-565.

Morgenstern, N.R., and Smith, L.B., 1973. Thaw-consolidation tests on remoulded clays. Canadian Geotechnical Journal, Vol. 10, pp. 25-40.

Morgenstern, N.R., and Nixon J.F., 1975. An analysis of the permformance of a warm-oil pipeline in permafrost, Inuvik N.W.T. Canadian Geotechnical Journal, Vol. 12, pp. 199-208.

THURBER

Nixon, J.F., 1973a. The consolidation of thawing soil. Unpublished Ph.D. Thesis, University of Alberta, Dept. of Civil Engineering, Edmonton, Alberta.

Nixon, J.F., 1973b. Thaw consolidation of some layered systems. Canadian Geotechnical Journal, Vol. 10, pp. 617-631.

Nixon, J.F., and Ladanyi, B., 1978. Chapter 4, Thaw consolidation. In geotechnical engineering for cold regions (Andersland and Anderson, 1978).

Nixon, J.F., and Morgenstern, N.R., 1973a. Practical extensions to a theory of consolidation for thawing soils. The North American contribution to the Second International Conference on Permafrost, Yakutsk, National Academy Science, Washington, D.C., pp. 369-376.

Nixon, J.F., and Morgenstern, N.R., 1973b. The residual stress in thawing soils. Canadian Geotechnical Journal, Vol. 10, pp. 571-580.

Nixon, J.F., and Morgenstern, N.R., 1974. Thaw-consolidation tests on undisturbed fine-grained permafrost. Canadian Geotechncial Journal, Vol. 11, pp. 202-214.

Palmer, A.C., 1972. Thawing and differential settlement close to oil wells through permafrost. Division of Engineering, Brown University, Report ARPA E-83.

Palmer, A.C., 1972. Settlement of a pipeline on thawing permafrost. Transmission from the Engineering Journal of the American Society of Civil Engineers, 98, pp. 477-491.

Roggensack W.D., 1977. Geotechnical properties of fine-grained permafrost soils. Unpublished Ph.D. thesis, University of Alberta, Dept. of Civil Engineering, Edmonton, Alberta.

Ryden, C.G., 1985. Pore pressure in thawing soil. Proc. of the Fourth Int. Symposium on ground freezing, Sapporo, Japan, A.A. Balkema, Boston, pp. 223-226.

THURBER

Slusarchuk, W.A., Watson, G.H., and Speer, T.L., 1973. Instrumentation around a warm-oil pipeline buried in permafrost. Canadian Geotechnical Journal, Vol. 10, pp. 227-245.

Smith, L.B., 1972. Thaw consolidation tests on remoulded clays. Unpublished M.Sc. Thesis, University of Alberta, Dept. of Civil Engineering, Edmonton Alberta.

Smith, W.S., Nair, A., and Smith, R.E., 1973. Sample disturbance and thaw consolidation of a deep sand permafrost. The Northern American contribution to the Second International Conference on Permafrost, Yakutsk, National Academy Science, Washington, D.C. pp. 392-399.

Speer, T.L., Watson, G.H., and Rowley, R.K., 1973. Effects of ground-ice variability and resulting thaw settlements on buried warm oil pipelines. The North American contribution to the Second International Conference on Permafrost, Yakutsk, National Academy Science, Washington, D.C., pp. 746-751.

Watson, G.H., Slusarchuk, W.A., and Rowley, P.K., 1973. Performance of a warm-oil pipeline buried in permafrost. The North American contribution to the Second International Conference on Permafrost, Yakutsk, National Academy Science, Washington, D.C., pp. 759-766.

Watson, G.H., Slusarchuk, W.A., and Rowley, R.K., 1973. Determination of some frozen and thawed properties of permafrost soils. Canadian Geotechnical Journal, Vol. 10, pp. 592-606.

Zaretskii, Y.K., 1968. Calculation of the settlement of thawing soil. American society of Civil Engineers, Soil mechanics and foundations division, pp. 151-155.

THURBER

THAW CONSOLIDATION
LIST OF FIGURES

THURBER

THURBER

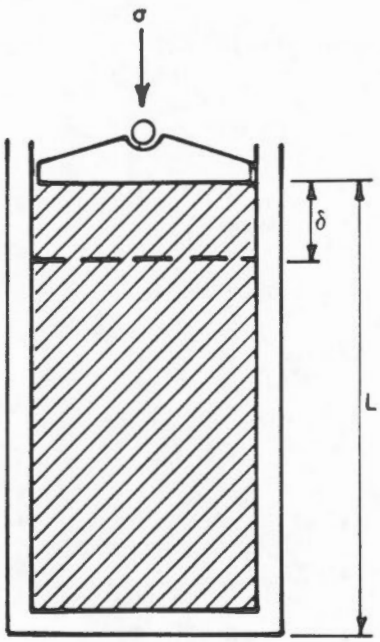

$$\varepsilon_t = \frac{\delta}{L} = \frac{\Delta e}{1 + e_0}$$

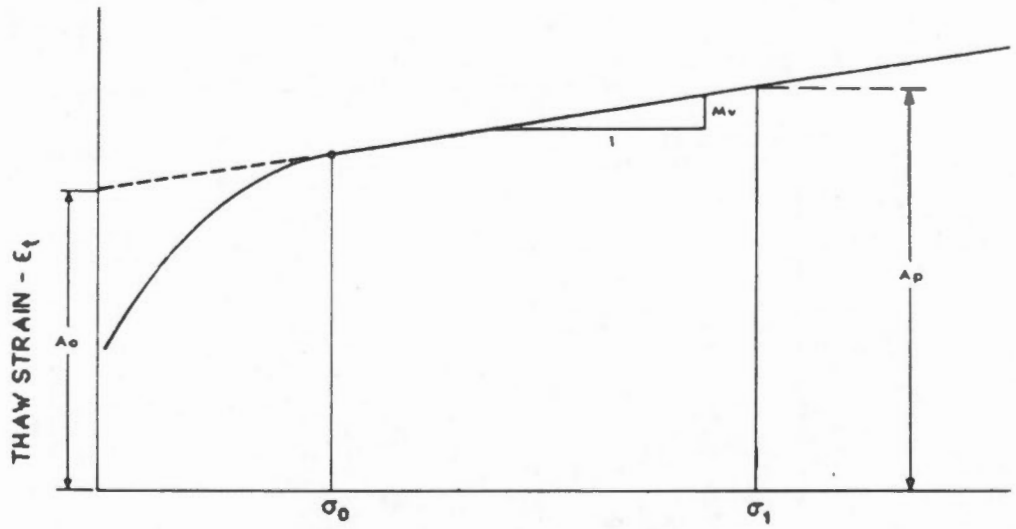

$$\varepsilon_t = A_0 + m_v \sigma$$

Simplified thaw settlement behaviour of ice rich frozen soil (after Watson et al., 1973).

FIGURE 9.1

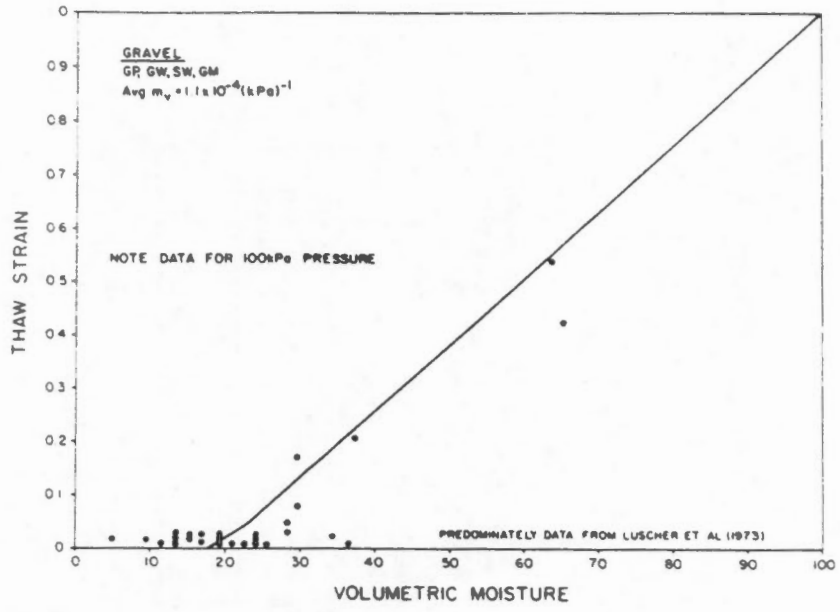

Thaw-strain water content correlation for gravel (Hanna et al., 1983).

FIGURE 9.2

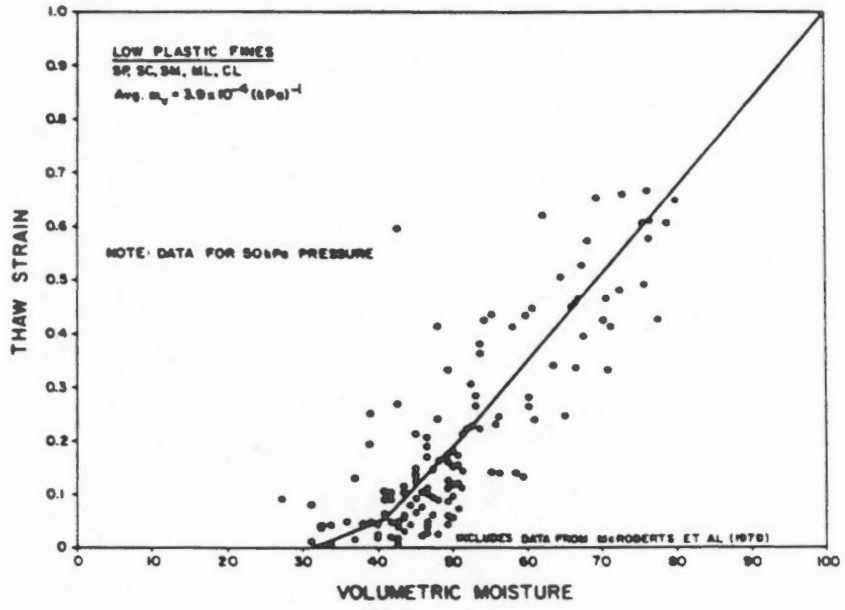

Thaw-strain water content correlation for low plastic fine grained soils (Hanna et al., 1983).

FIGURE 9.3

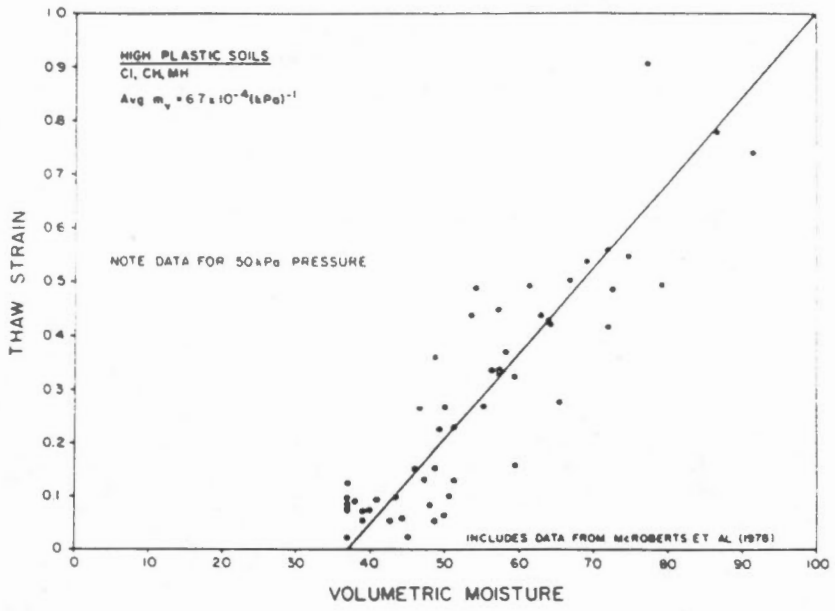

Thaw-strain water content correlation for high plastic soils (Hanna et al, 1983).

FIGURE 9.4

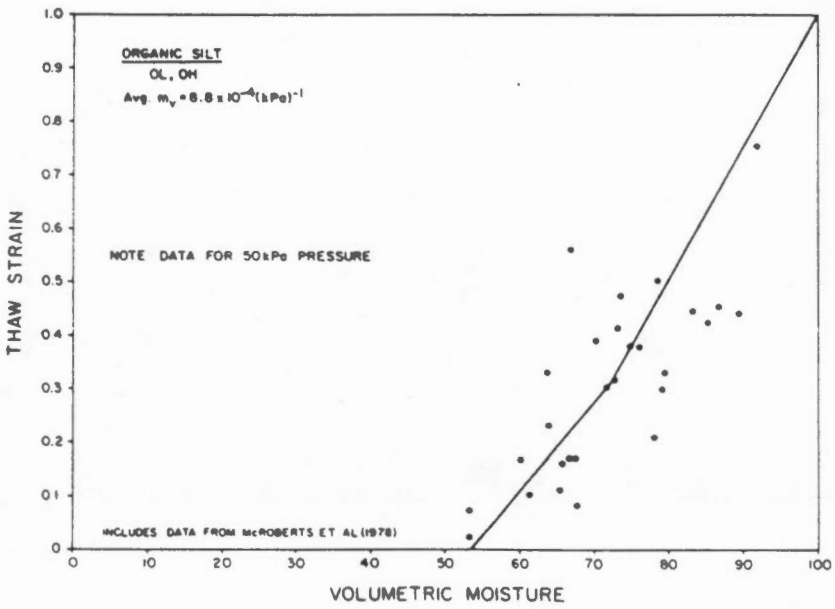

Thaw-strain water content correlation for organic silt (Hanna et al., 1983).

FIGURE 9.5

THURBER

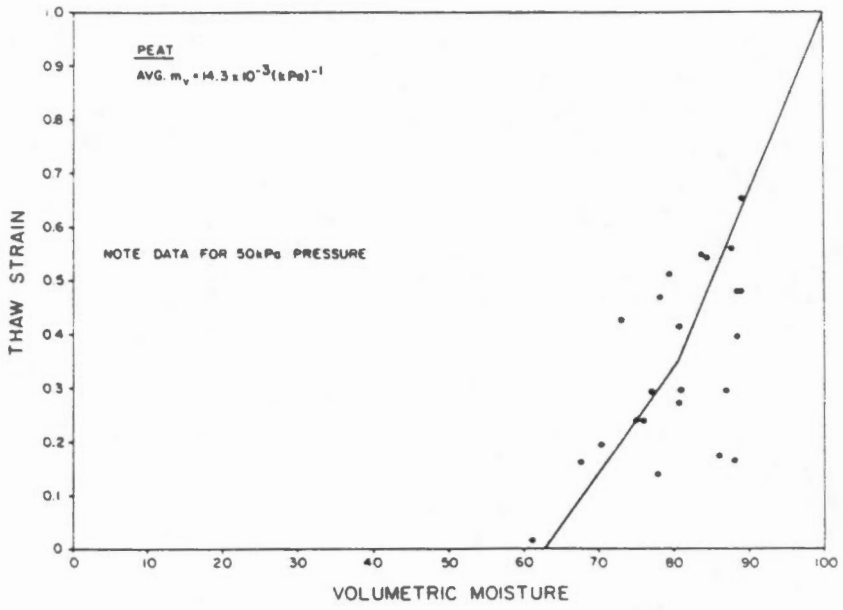

Thaw-strain water content correlation for peat (Hanna et al., 1983).

THURBER

FIGURE 9.6

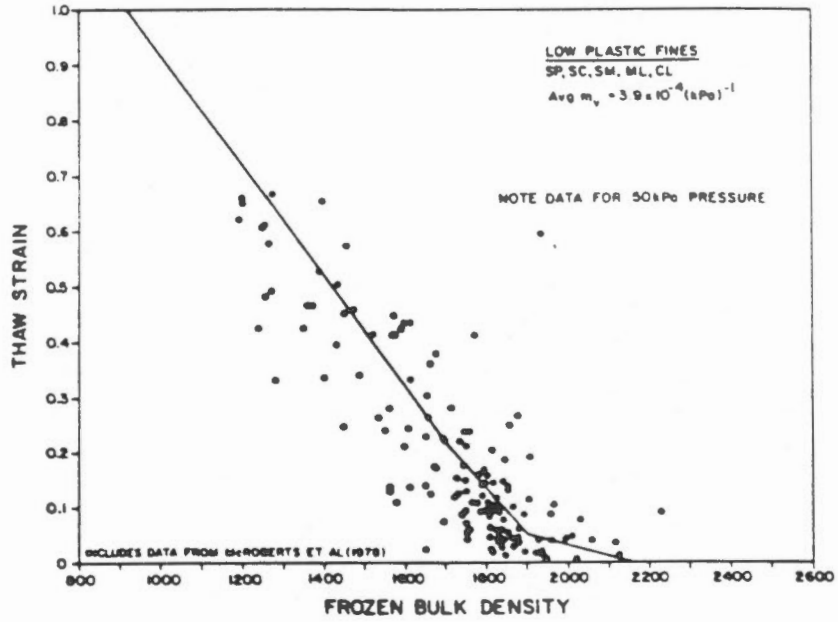

Thaw-strain frozen bulk density correlation for low plastic fine grained soils (Hanna et al., 1983).

FIGURE 9.7

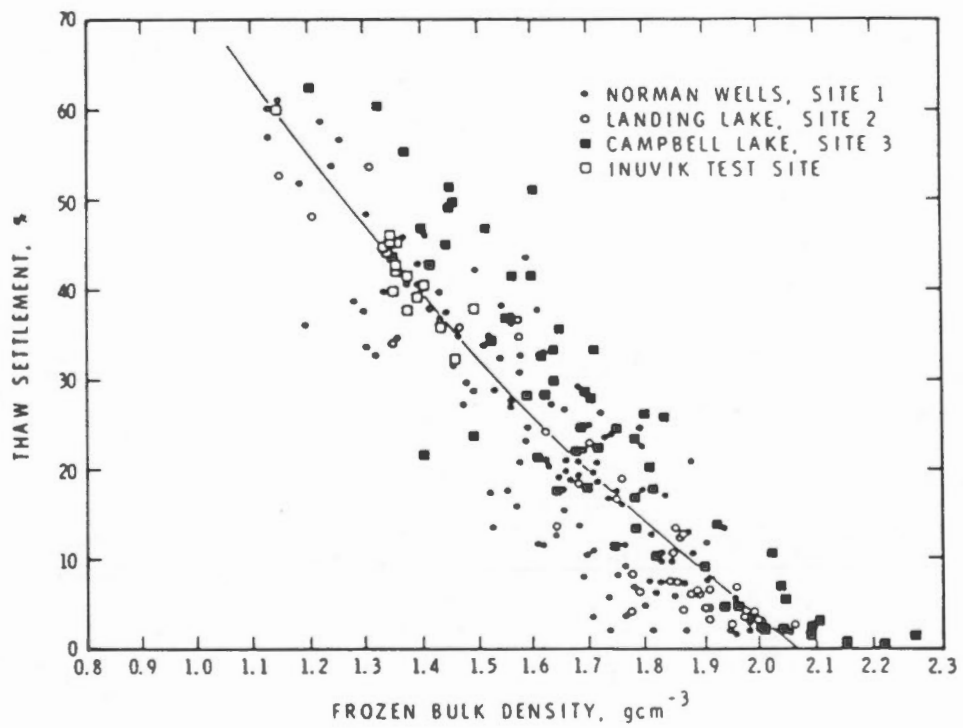

Thaw-strain frozen bulk density correlation (Speer et al., 1973, from Johnston, 1981).

FIGURE 9.8

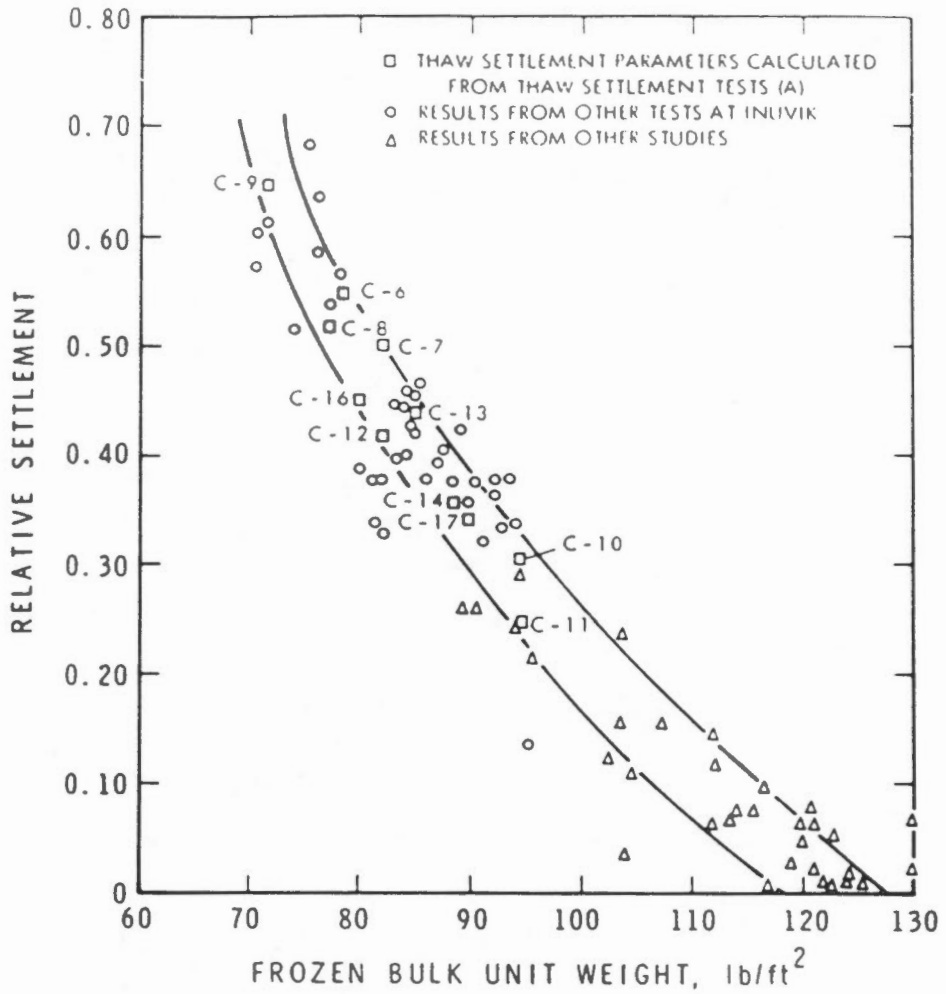

Thaw-strain frozen bulk density correlation (Watson et al., 1973, from Johnston, 1981).

FIGURE 9.9

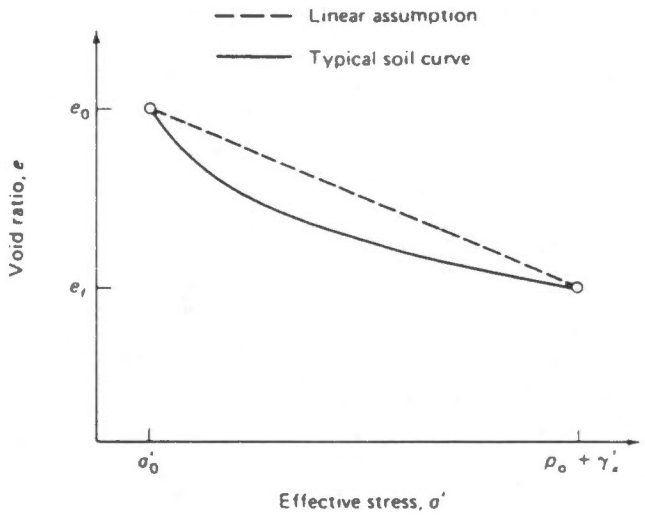

Void-ratio–effective-stress relationships.

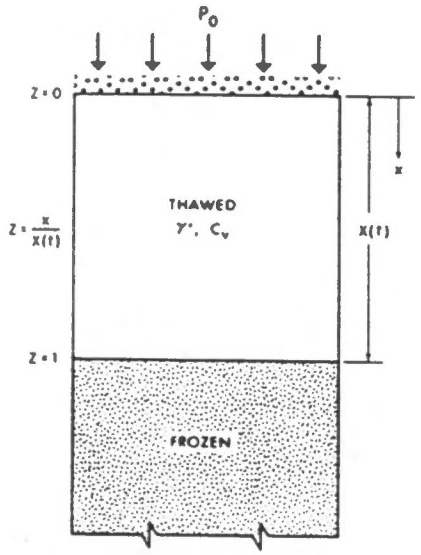

One-dimensional thaw-consolidation.

Idealized one dimensional thaw consolidation (Morgenstern and Nixon, 1971 and 1973).

FIGURE 9.10

THURBER

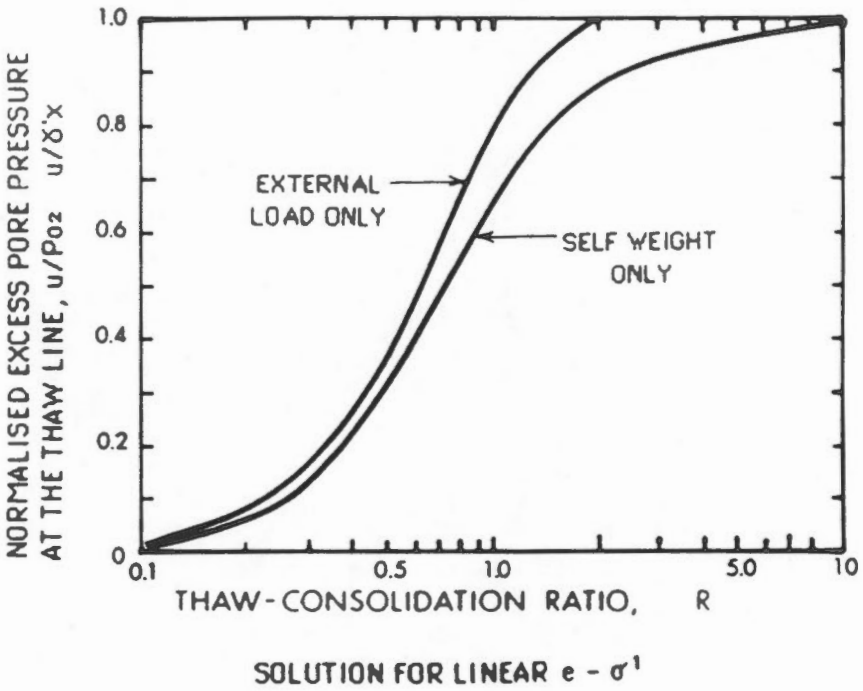

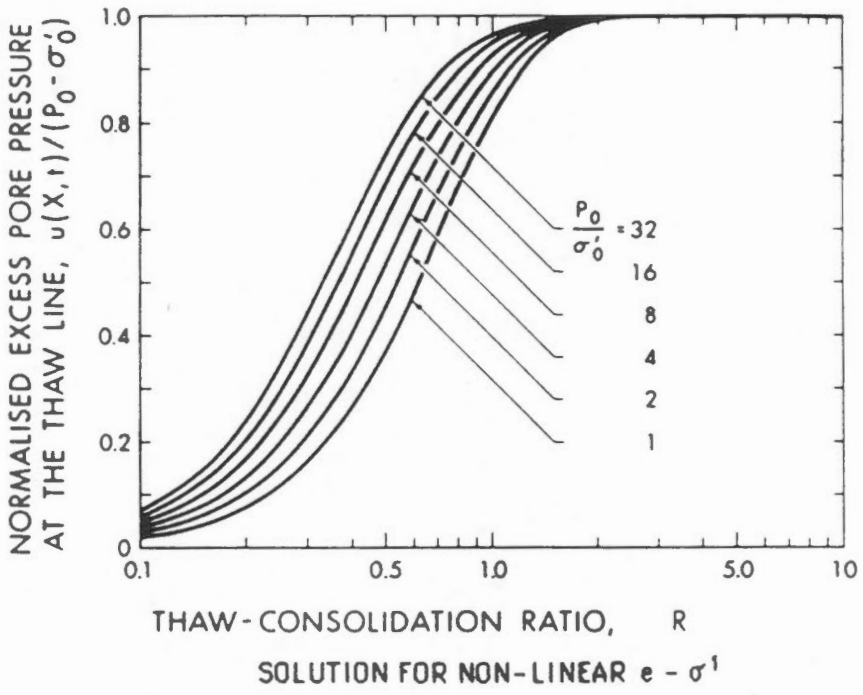

Relationship between the thaw consolidation ratio and excess pore pressure at the thaw front (Nixon and Morgenstern, 1971 and 1973a).

FIGURE 9.11

THURBER

SOIL	SAMPLE CONDITION[1]	PLASTIC LIMIT	LIQUID LIMIT	G_s	PERCENT SILT	PERCENT CLAY	PERMEABILITY $X10^{-8}$ cm^2/sec	COEFFICIENT OF CONSOLIDATION C_v mm^2/sec	SOURCE
Athabasca Clay	R	20	41	2.65	-	45	.004 to .26	.03 to .17	1
Lake Edmonton Clay	R	29	70	2.76	-	65	0.3 to 0.4	.18 to .27	1
Bentonite	R	87	591	2.75	-	94	.003 to .01	.0004 to .0003	1
Norman Wells Silt	U	19	29	2.65	67	23	1 to 10	2.5	2
Mountain River Clay	R	20	40	2.73	44	55	.05	0.1	2
Noell Lake Clay	U	23	41	2.65	50	40	0.1	0.2	2
Devon Silt	R	22	30	2.65	55	23	1.0	0.5	2
Sans Sault Clay	U	18 to 25	31 to 44	-	-	23 to 40	1 to 100	0.1 to 7.0	3
Martin River Clay	U	17 to 31	24 to 43	-	-	10 to 45	1 to 100	0.7 to 7.0	3
Inuvik Silt	U	29 to 32	50 to 63	2.66	53	40	1 to 100	1.0 to 74	4

NOTES: 1) Sample condition is designated U for undisturbed and R for reconstituted.
2) G_s denotes the specific gravity of the soil particles.

SOURCES:
1 Smith (1972)
2 Nixon (1974)
3 McRoberts et al (1978)
4 Watson et al (1973)

Consolidation properties of selected soils.

THURBER

FIGURE 9.12

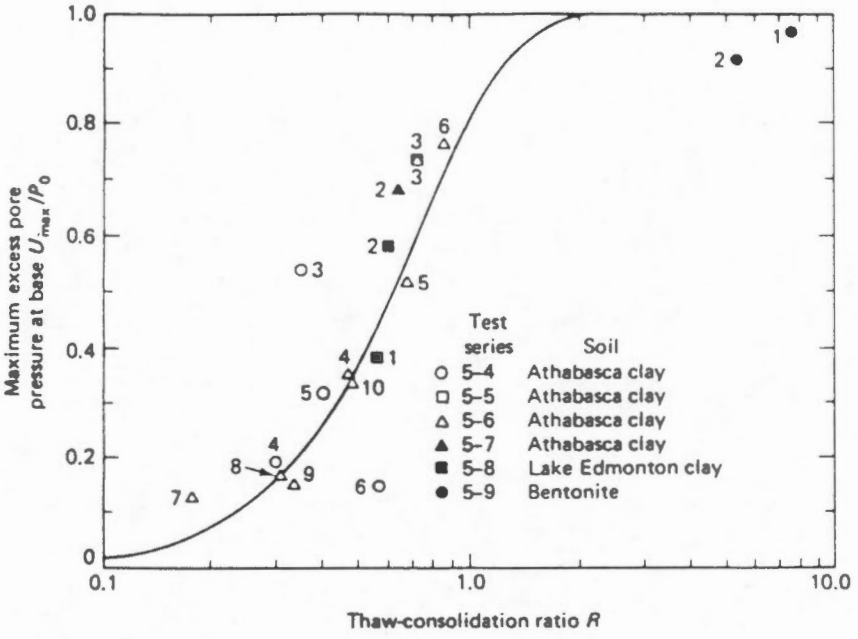

Observed and predicted pore pressures for reconstituted samples in laboratory tests (Morgenstern and Smith, 1973).

FIGURE 9.13

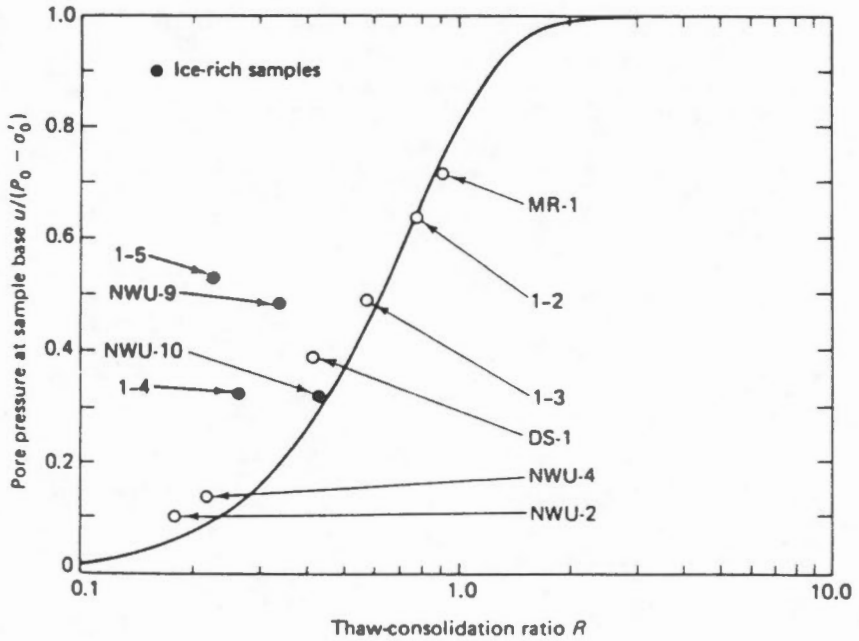

Observed and predicted pore pressures for undisturbed samples (Nixon and Morgenstern, 1974).

FIGURE 9.14

THURBER

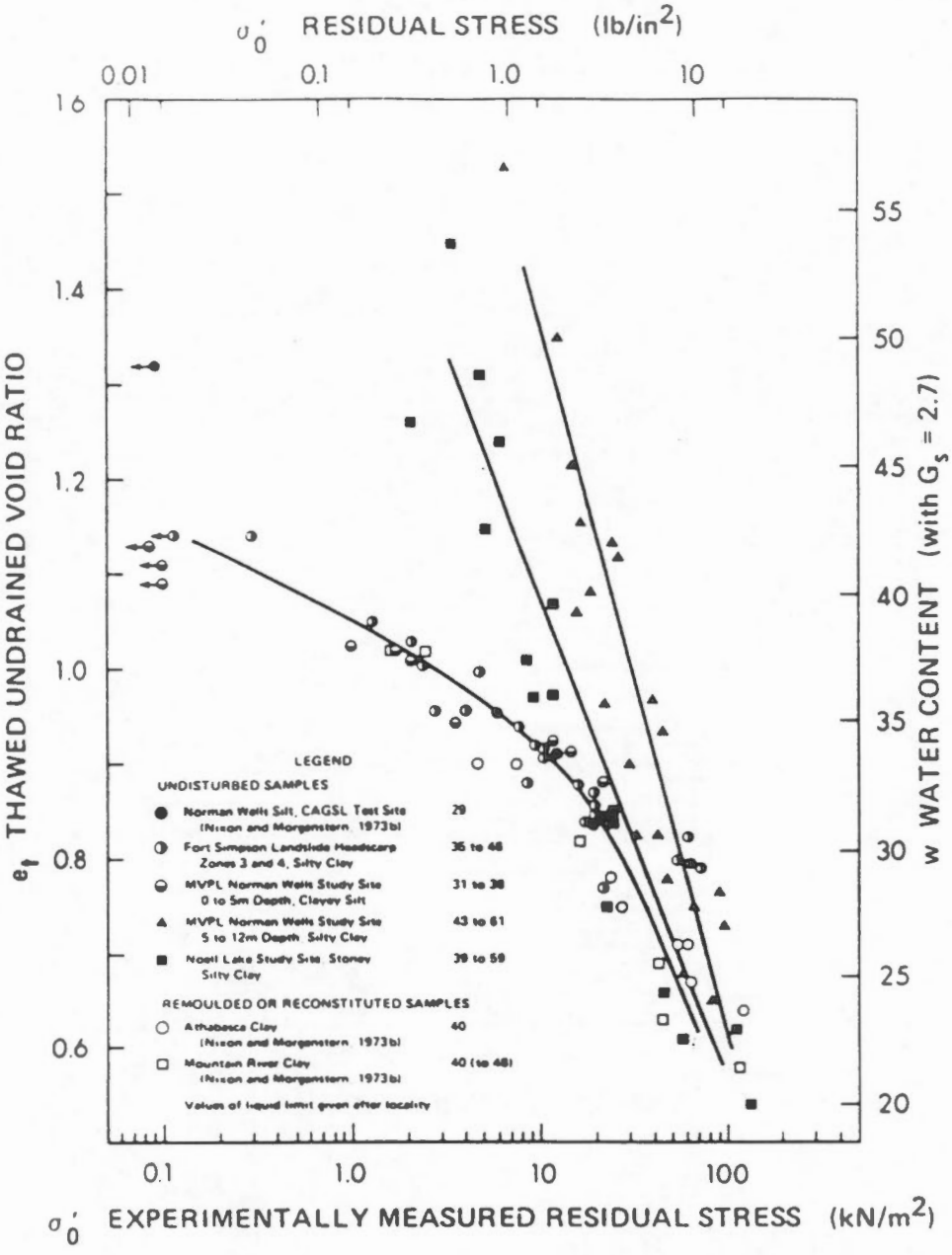

Correlation between thawed undrained void ratio and residual effective stress (Roggensack, 1977).

FIGURE 9.15

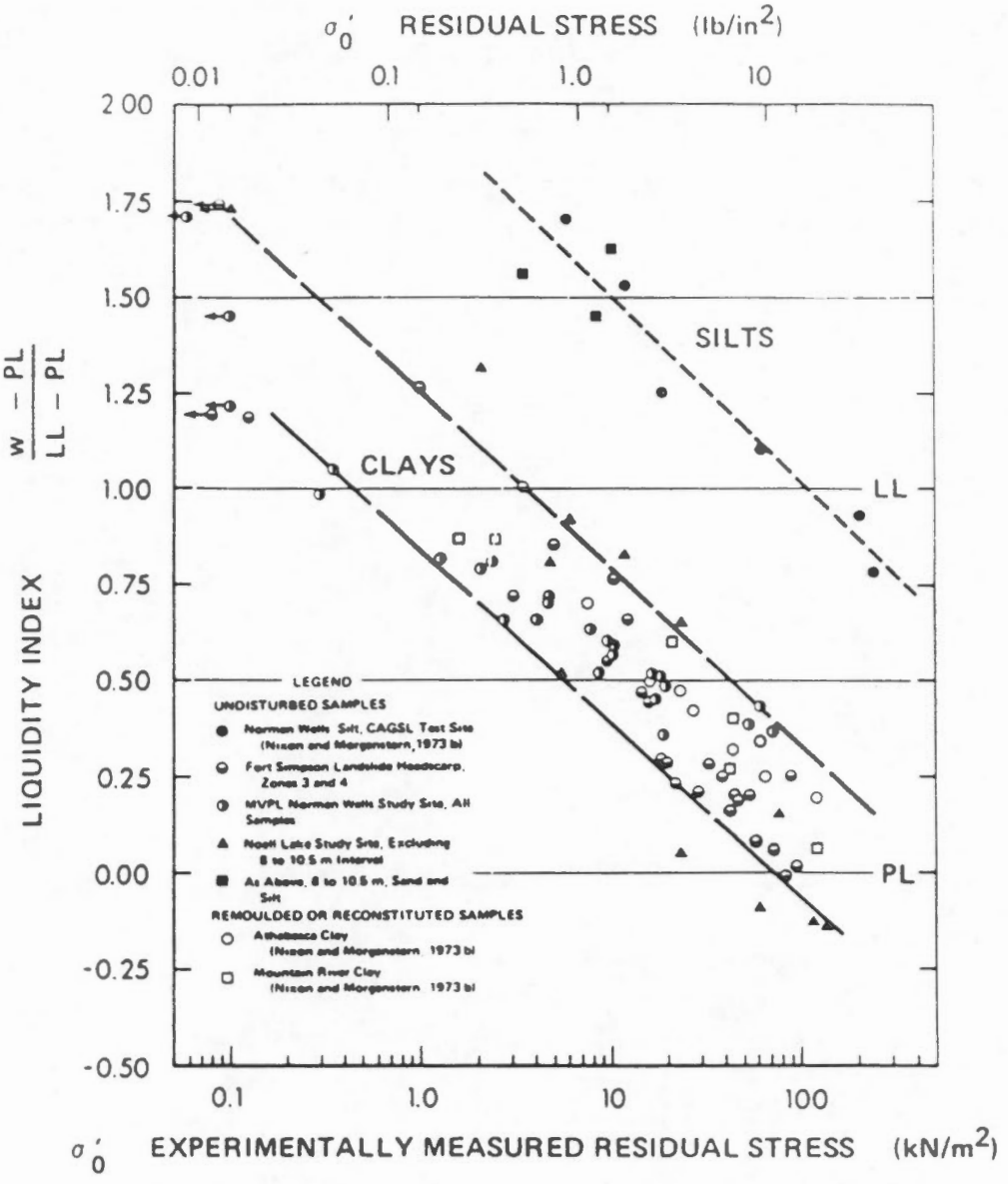

Correlation between liquidity index and residual effective stress (Roggensack, 1977).

FIGURE 9.16

THURBER

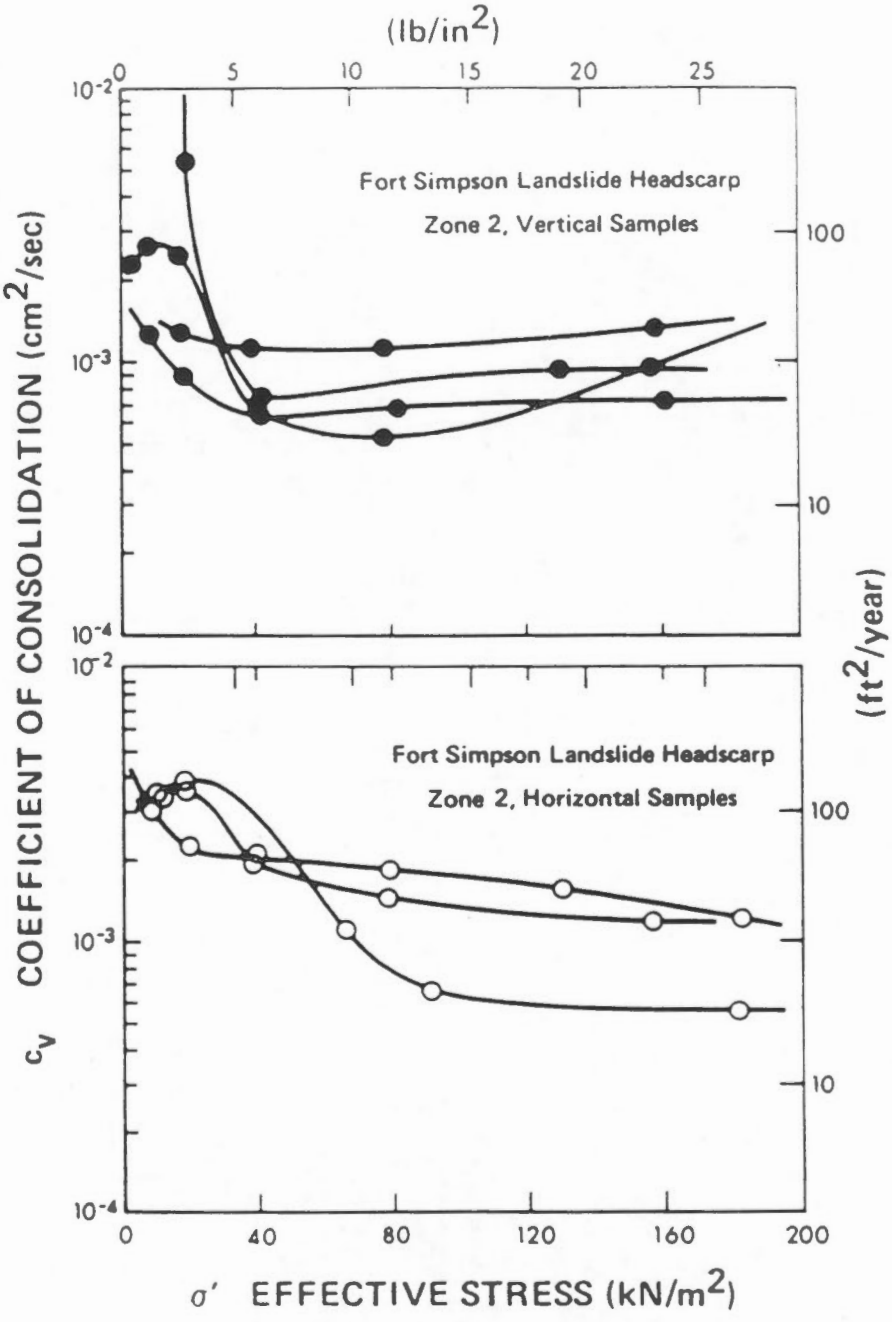

c_v versus σ', stratified structure, Zone 2, Fort Simpson landslide headscarp

Coefficient of consolidation versus effective stress - Fort Simpson clay (Roggensack, 1977).

FIGURE 9.17

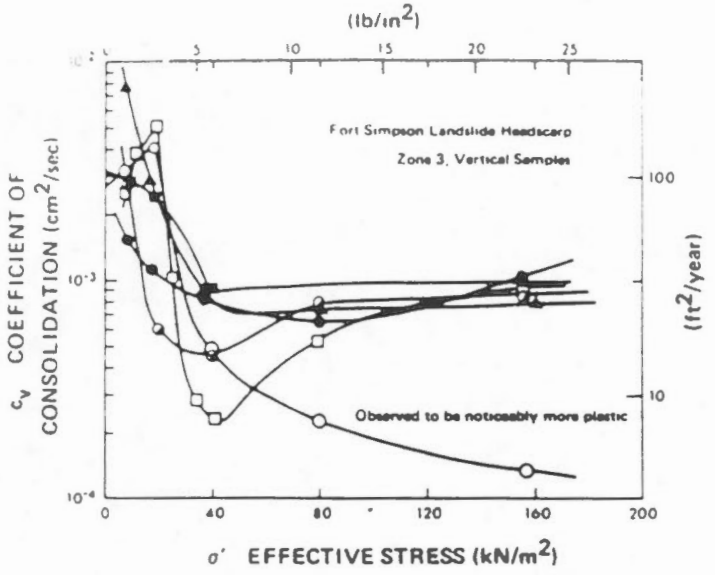

c_v versus σ', reticulate structure, Zone 3, Fort Simpson landslide headscarp

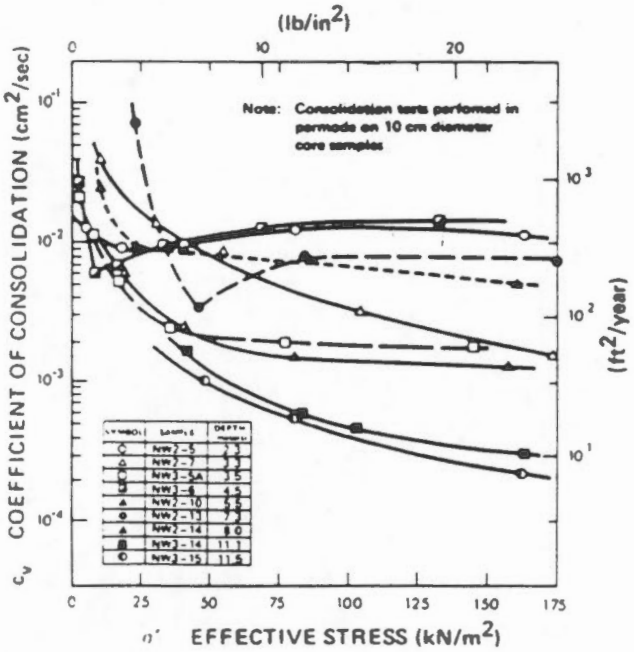

c_v versus σ', Norman Wells site

Coefficient of consolidation versus effective stress - Norman Wells silt (Roggensack, 1977).

FIGURE 9.18

THURBER

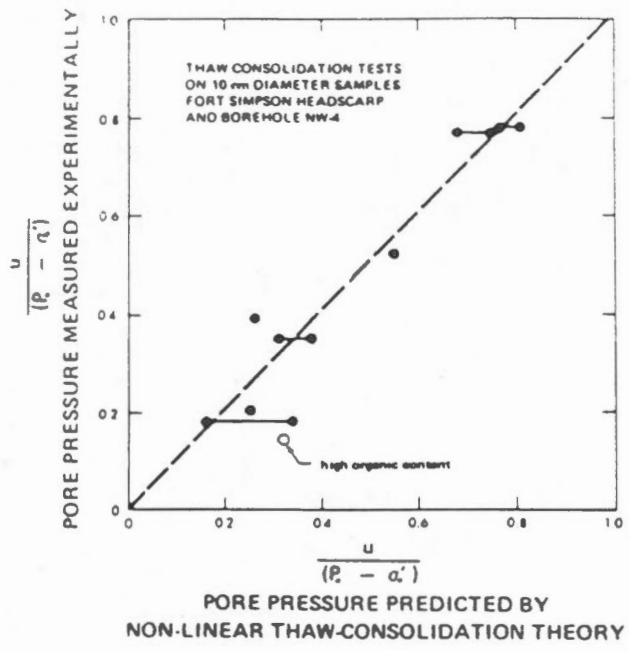

Observed and predicted pore pressures for undisturbed samples (Roggensack, 1977).

FIGURE 9.19

THURBER

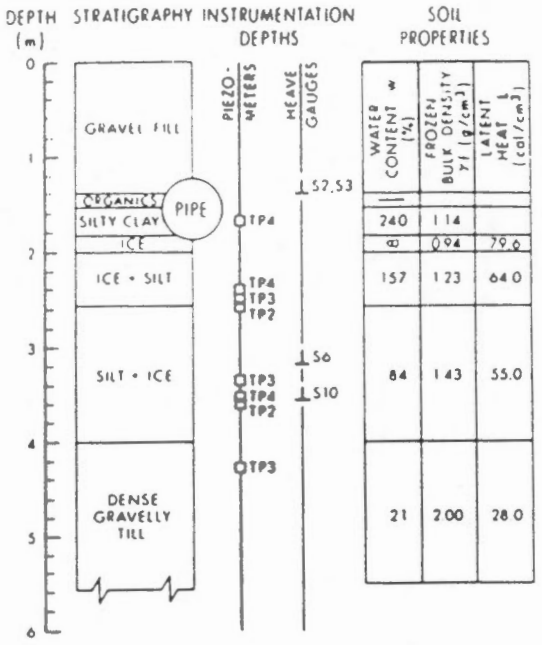

Stratigraphy at the Inuvik Test Facility (Morgenstern and Nixon, 1979).

FIGURE 9.20

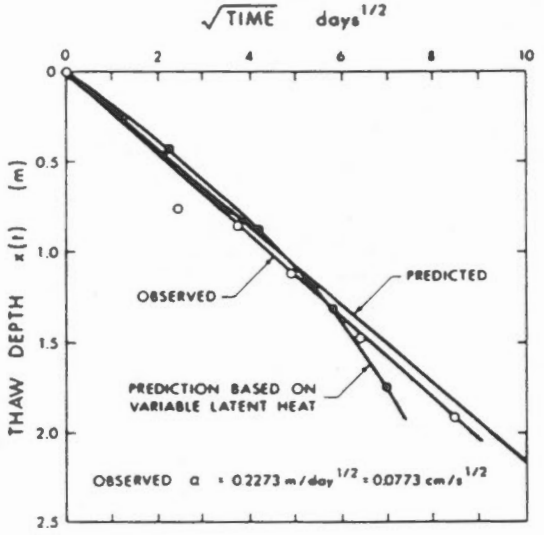

Predicted and observed thaw depths at the Inuvik Test Facility (Morgenstern and Nixon, 1975).

FIGURE 9.21

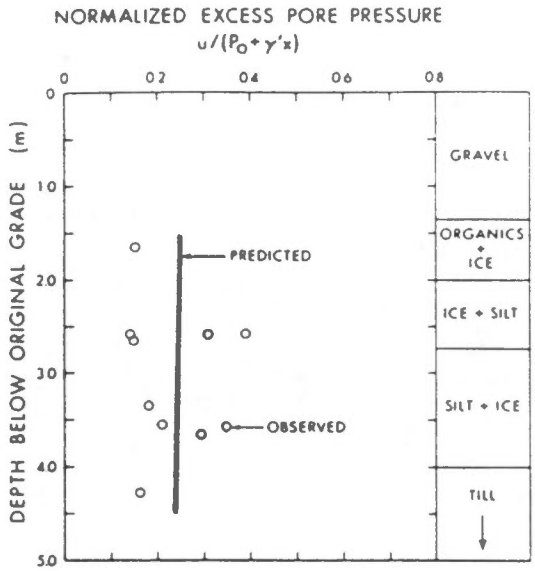

Predicted and observed maximum pore pressures at the thaw front at the Inuvik Test Facility (Morgenstern and Nixon, 1975).

FIGURE 9.22

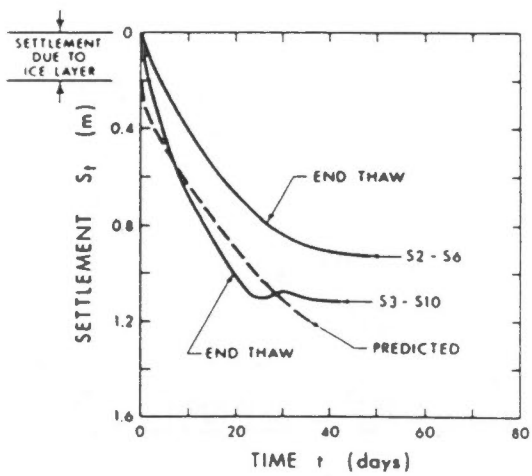

Predicted and observed settlements at the Inuvik Test Facility (Morgenstern and Nixon, 1975).

FIGURE 9.23

TABLE 1

SUMMARY OF SOIL PROPERTIES

SANS SAULT	MARTIN RIVER
Before thaw consolidation	Before thaw consolidation
$86 \leq \gamma_f \leq 117$ pcf	$70 \leq \gamma_f \leq 109$ pcf
$939 \leq e_1 \leq 2.637$	$1.148 \leq e_1 \leq 1.864$
$23 \leq w \leq 63\%$	$40 \leq w \leq 80\%$
After thaw consolidation	After thaw consolidation
$121 \leq \gamma_b \leq 128$ pcf	$110 \leq \gamma_b \leq 133$ pcf
$0.61 \leq e \leq 0.67$	$0.59 \leq e \leq 0.73$
$23 \leq w \leq 28\%$	$20 \leq w \leq 30\%$
$18 \leq PL \leq 25\%$	$17 \leq PL \leq 31\%$
$31 \leq LL \leq 44\%$	$24 \leq LL \leq 43\%$
$23 \leq$ % clay $\leq 40\%$	$10 \leq$ % clay $\leq 45\%$
$29 \leq \phi' \leq 32.5^0$	$23.5 \leq \phi' \leq 38^0$
$0 \leq c' \leq 0.5$ psi	$0 \leq c' \leq 2$ psi
$320 \leq c_u \leq 2000$ psf	$320 \leq c_u \leq 2870$ psf

TABLE 2

NORMALIZED EXCESS PORE-WATER PRESSURE

	AUG 8/75	AUG 24/75	SEPT 7/75	OCT 6/75	JULY 24/76
SSC1	- (1)	0.07	-	drawdown	drawdown
SSC3	-	0.35	-	0.34	drawdown
SSG2	-	-	-	0.40	drawdown
MRP2	0.25	-	drawdown(2)	-	0.06
MRP6	0.20	-	0.27	-	0.24
MRGP1	0.17	-	0.10	-	0.02
MRGP2	-	-	0.12	-	0.25
MRGP3	-	-	0.27	-	0.26

NOTES 1 DASH (-) INDICATES NO READING TAKEN

2 DRAWDOWN - LEVEL OF WATER IN THE PIEZOMETER WAS LOWER THAN THE GROUND-WATER LEVEL

Site	Calculated Value for c_v Based on Laboratory Data mm^2/sec Range	Average	Value of c_v Back Calculated from Pore Pressures Measured in the Field mm^2/sec
Sans Sault Rapids	0.1 to 7.0	1.0	0.09 to 0.15
Martin River	0.7 to 7.0	0.5	0.15 to 0.40

Pore pressure observations in a natural slope in ice rich permafrost during annual thaw (McRoberts et al., 1978).

THURBER

FIGURE 9.24

SECTION 10

FROST HEAVE

SECTION 10

FROST HEAVE

10.1 General

As the ground freezes each fall (in permafrost or non permafrost regions) ice lenses can develop at the frost front, with the result that the ground surface will heave. The heaving can cause uplift of building foundations, lateral movement of retaining walls and heaving of roads and airfields. In the case of roads and airfields, when the ground thaws the following spring, the ice lenses melt out, resulting in an oversaturated subgrade and potential failure of the pavement structure. Frost heave and its control have therefore been the focus of a considerable research effort over the last 50 years or so.

In recent years, a number of projects have been proposed which involve the installation of chilled (below 0°C) gas pipe lines in permafrost areas. The use of chilled gas greatly improves the efficiency of the system, while at the same time reducing thaw degradation of frozen ground. However, in sporadic permafrost areas, the chilled line must pass through areas of both frozen and unfrozen soil. Where unfrozen ground is present, a frost bulb will develop around the pipeline. Frost heaving of the pipeline is therefore of concern, since, if heave is excessive, the line could be damaged.

Some examples of frost heave below various structures are shown in Figure 10.1. The phenomenon of frost heave involves a complex coupling of thermal and hydraulic processes within the soil. In the past, researchers established that three conditions were necessary for the formation of segregated ice during freezing.

1) Ground temperatures must be sufficiently cold for a prolonged period.
2) The water table must be close to the freezing front.
3) The soil must be susceptible to the formation of segregated ice.

Frost heave can be reduced by removing at least one of the foregoing conditions. Where ground temperatures or the water table cannot be changed, then the approach would

THURBER

often be to replace the frost susceptible soil with non-frost susceptible soil. This is the approach which is commonly used in order to control frost heave below pavement structures.

Frost susceptible soils have been broadly classified based on grain size distribution as shown on Figure 10.2. As indicated on the figure, those soils which have a high percentage of silt are normally highly frost susceptible, whereas clean sands and gravels are normally not frost susceptible. Soils which contain a significant percentage of clay are not normally regarded as being frost susceptible. It is believed that the low permeability of clayey soils supresses the development of ice lenses, at least for a limited time.

One of the most widely used frost susceptibility criteria was developed by the U.S. Army Corps of Engineers (Johnson, 1981). The results of studies undertaken by the Corps indicated that frost susceptible soils include all inorganic soils which contain more than 3 percent by weight finer than 0.02 mm. Frost susceptible soils were grouped into several categories according to their degree of frost susceptibility as shown on Figure 10.3. The F1 soils shown on Figure 10.3 are considered to be the least frost susceptible and the F4 soils are considered the most frost susceptible.

Unfortunately, while frost susceptibility criteria such as those given above have proven to be extremely valuable to designers, the approach has a number of serious drawbacks. First of all, as indicated on Figure 10.2, it has been found that there is no sharp dividing line between frost susceptible and non frost susceptible materials. Secondly, the frost susceptibility criteria do not reflect other factors (such as the thermal regime) which can affect frost heaving. In critical situations, therefore, designers have been forced to take a conservative approach in evaluating the acceptability of materials where frost heaving is a concern. Finally, the foregoing frost susceptibility criteria provide no theoretical basis on which to evaluate the probable magnitude of frost heave which might occur or the measures which might be considered to reduce or eliminate frost heave.

A number of behavioural models for frost heave have been proposed by researchers over the years. The majority of these models are either overly complex or require a knowledge of parameters which cannot be reliably determined.

THURBER

A relatively simple and practical theory, which appears to incorporate the major factors which control the process of frost heave in soils has been developed by Konrad and Morgenstern. The theory is described in a series of five papers (Konrad and Morgenstern, 1980, 1981, 1982a, 1982b, 1984). The following sections review the Konrad and Morgenstern model and its application.

10.2 Description of the Model

All researchers accept that as a frost front advances into the soil mass, water will be drawn to the freeze front as a result of a suction which develops at that point. The physical situation is shown in Figure 10.4.

At some point above the ice lens, a cold side temperature T_c exists, while below the frost front the warm side temperature is denoted T_w. The temperature gradient between these two points is assumed to be constant. The temperature at which ice first begins to form in the soil will be near 0°C and is designated T_i. The temperature at the base of the ice lens T_m, is seen to be somewhat lower than 0°C. The surface defined by T_i is termed the freezing or frost front. The zone between the ice lens and the freezing front is termed the frozen fringe.

Within the frozen fringe, water exists in equilibrium with pore ice at temperatures below 0°C, The water is present as adsorbed films on the surface of the soil particles. The thickness of the adsorbed films is a function of temperature, soil particle sizes, void ratio and a number of other variables.

The suction pressure at the base of the ice lens is denoted P_w while the suction pressure at the frost front is denoted P_u.

If the frost front is not advancing (that is steady state temperature conditions exist) water will flow from the frost front to the base of the growing ice lens through the low permeability frozen fringe. The volumetric heat and latent heat, which are released as the water at the base of the lens turns to ice, equal the heat removed when the ice lens is stationary. If the heat removed exceeds the heat released when ice forms at the base of the ice lens, then the frost front will advance.

The rate at which the frost front advances controls the thickness of the ice lens which can develop. In the field, at shallow depths where temperature gradients are large,

THURBER

and the rate of advance of the freeze front is rapid, segregated ice lenses are thin or non-existent. At greater depths, the temperature gradient is small (with the result that the frozen fringe is thicker) and the rate of advance of the freeze front is slow, therefore thicker ice lenses can form.

In formulating their theory, Konrad and Morgenstern have made the following assumptions:

1) The soil voids are saturated and contain either water or ice.
2) The temperature gradient within the frozen fringe is constant.
3) Darcy's law is valid for the flow regime that exists in the vicinity of the frost front, and within the frozen fringe.
4) The permeabilities in the frozen fringe and the unfrozen soil are constant (but not necessarily the same).
5) The temperatures at the frost front and at the base of the ice lens are constant for given soil properties.
6) The suction pressure at the base of the ice lens is constant for given soil properties.
7) Under steady state conditions, water accumulates only at the base of the warmest ice lens. Water does not accumulate within the frozen fringe or above the base of the ice lens, although redistribution of ice and water may occur in both areas.

If the foregoing assumptions are made, Konrad and Morgenstern have established that the velocity of water flow, v to the growing ice lens will be proportional to the thermal gradient G_f in the frozen soil above the ice lens. That is:

$$v = SP\ G_f \qquad (10.1)$$

where

SP denotes a constant which is termed the Segregation Potential.

The segregation potential constitutes a coupling between the thermal and mass flow phenomenon which occurs in frost heave. It can be established from suitable laboratory tests for a particular soil type, and the temperature

THURBER

gradient at the frost front can be determined as a function of time for most field problems from a geothermal analysis. Therefore, the rate of heave, h can be calculated from the following equation:

$$h = 1.09\ SP\ G_s + 0.09\ n \frac{dx}{dt} \qquad (10.2)$$

where

n denotes the porosity (which should be reduced to account for that portion of the pore water which does not freeze), and

$\frac{dx}{dt}$ denotes the rate of advance of the frost front.

As mentioned, the segregation potential can be established in laboratory frost heave tests for a specific soil. A sample of the soil to be tested is consolidated from a slurry to a specified pressure in order to achieve a uniform void ratio throughout. The sample is then placed in a freeze cell, a designated external pressure is applied and the sample is allowed to consolidate. Freezing is commenced either from the top down or from the bottom up. The advantage of freezing from the bottom up is that heave of the unfrozen soil above the frozen soil occurs, so that side friction is reduced. A sketch of a typical set up (freezing from the bottom up) is presented in Figure 10.5. The samples are typically 100 mm in diameter and 100 mm high.

It is desirable that the frost front be as close to the warm plate and the water source as possible in order to minimize head losses due to water flow through the unfrozen soil. In order to achieve this, a warm plate temperature of about +1°C and a cold plate temperature of -5 to -8°C are recommended (Konrad and Morgenstern, 1984).

As freezing progresses, the temperature profile, water movement into the soil and total heave are monitored. Typical data are presented on Figure 10.6. During the initial stages of the test, when the frost front is advancing, non-steady state heat flow persists. When the frost front becomes stationary, steady state is reached. This marks the beginning of Phase 3 as shown on Figure 10.6, and coincides with the growth of the last ice lens, unless the temperature boundary conditions are changed. As indicated on Figure 10.6, the rate of heave decreases with time and will ultimately stop. As discussed by Konrad and Morgenstern,

THURBER

this behaviour is believed to be due to warming of the base of the last ice lens due to the fixed thermal boundary conditions and the increasing height of the sample due to heave. For no applied load, when the temperature of the bottom of the ice lens reaches 0°C, the suction will also be zero and water flow will stop.

The rate of heave at the time that the last ice lens forms is determined from the data. The temperature gradient at that time is also determined by assuming a linear gradient throughout the sample.

Frost heave tests can then be repeated for different temperature gradients. It is possible to plot water velocity (at the formation of the last ice lens) versus G_f. The slope of this line is the segregation potential. Typical results are presented on Figure 10.7.

Research has indicated that the segregation potential is a function of the following variables:

1) Suction at the frost front,
2 Rate of cooling of the frozen fringe,
3) Stress state, and
4) Soil properties, including grain size distribution, particle shape, particle mineralogy, void ratio, and soil structure.

10.3 Suction at the Frost Front

Konrad and Morgenstern (1981) have investigated and discussed the effect which the suction at the frost front will have on the values of segregation potential measured in the laboratory.

It is important to understand how the selection of the cold and warm side temperatures can affect the value of the suction at the frost front P_u, and hence the measured value of SP (which is a function of P_u).

Konrad and Morgenstern (1981) have demonstrated that, under steady state temperature conditions, varying the cold side temperature in a laboratory frost heave cell will not affect the magnitude of the suction at the frost front. This is illustrated on the upper half of Figure 10.8. As shown, no matter how the cold side temperature is varied, as long as the warm side temperature remains constant, the ratio of the length of the frozen fringe to the length of the unfrozen soil below the frost front remains constant.

THURBER

Therefore, because the total head loss between the warm plate and the bottom of the ice lens is constant, then the suction at the frost front must also remain constant. (The total head loss between the warm plate and the bottom of the ice lens actually increases slightly as the elevation of the frost front rises but the change is negligible in comparison to the magnitude of the total suction head).

Since the suction at the frost front remains constant the segregation potential will also remain constant as the cold side temperature is varied. Therefore, the relationship between water intake velocity and temperature gradient (segregation potential) can be readily established by holding the warm side temperature constant and progressively decreasing the cold side temperature. A rigorous proof that the suction at the frost front and segregation potential will remain constant as the cold side temperature is varied is presented by Konrad and Morgenstern (1981).

On the other hand, if the cold side temperature is held constant and the warm side temperature is varied, then the suction at the frost front will vary as will the measured value for the segregation potential. This effect is illustrated on Figure 10.9. In this case, as the warm side temperature is increased, the ratio of the length of the frozen fringe to the length of the unfrozen zone decreases dramatically, as shown. Therefore the proportion of the total head loss within the unfrozen zone is increased, with the result that the suction at the frost front is increased. Therefore, the measured value for segregation potential will be reduced as the warm plate temperature (and consequently P_u) is increased.

Konrad and Morgenstern carried out a range of tests on Devon silt in which the suction at the frost front was varied by varying the warm side temperature. The suction at the frost front was calculated at steady state from the following equation:

$$P_u - P_b = \frac{v_u \, l_u}{K_u} \qquad (10.3)$$

where

P_u denotes the suction at the frost front,

P_b denotes the pore pressure at the bottom of the unfrozen soil,

THURBER

v_u denotes the water velocity in the unfrozen soil,

l_u denotes the length of the unfrozen soil below the steady state ice lens, and

K_u denotes the hydraulic permeability of the unfrozen soil, which is measured prior to starting the freeze test.

These researchers were therefore able to establish the relationship between the segregation potential and suction at the frost front for Devon silt. The test results are presented on Figure 10.10. They also established that, for a given suction the segregation potential is unique for a particular soil under specified conditions.

These experimental results are significant for a number of reasons. First of all, the results demonstrate that the warm side temperature must be carefully controlled in frost heave tests, in order to obtain consistent measurements of SP. Secondly, the warm side temperature must be kept as low as possible (+1°C) in order to minimize the suction at the frost front and measure a maximum value for SP.

Konrad and Morgenstern have established values of SP for Devon silt at suction values as low as about 5 kPa as shown on Figure 10.10. The results have been extrapolated back to determine a value for SP of about 175 x 10^{-5} mm^2s^{-1} $°C^{-1}$, at a suction of zero. It is possible that under very low suction values, SP may increase more rapidly than indicated by the available test data. This is an area in which further research should be considered.

The selection of a suitable value for the suction at the frost front is, of course, necessary in order to analyse field problems. At the present time, there is no reliable method of predicting the suction which will occur in field situations. However, Konrad and Morgenstern have suggested that since the average permeability within the frozen fringe is lower than the average permeability of the unfrozen soil below the fringe, it is reasonable to expect that suction pressures at the frost front will be very low in the field. In any event, such an assumption is conservative, because it results in a maximum value for SP and consequently a maximum value of predicted heave. The assumption may not be valid for soils which have a significant clay content, however. The suction at the frost front for

THURBER

clays in the field may be high, which may explain the observed fact that frost heaving in clays is very low under most field conditions. This is an area in which further research may be worthwhile.

10.4 Rate of Cooling

Konrad and Morgenstern (1982) have addressed the effect which the rate of cooling of the frozen fringe has on the segregation potential. The effect for a particular soil can be established from the results of a frost heave test using the following procedure.

At any particular time during a freezing test, as the frost front is advancing, it is possible to establish the average temperature and temperature gradient across the frozen fringe (or near it) from measured temperatures at various depths within the sample. The change in the average temperature across the fringe can therefore be determined as a function of time and represents the rate of cooling of the fringe. Typical results are presented on Figure 10.11. As these researchers note, a freezing test with fixed boundary conditions provides a complete range of heat extraction rates.

The time corresponding to specific rates of cooling can then be determined. The corresponding measured water intake rate, combined with the measured length of unfrozen soil allows the suction at the frost front to be calculated for each time step, using Equation 10.3. The segregation potential at each time interval is calculated from Equation 10.1. It is therefore possible to plot, at selected times, the segregation potential as a function of suction at the frost front and rate of cooling. The results of a series of tests carried out on Devon silt by Konrad and Morgenstern are presented on Figure 10.12. The results can be presented in the form of a three dimensional plot as shown on Figure 10.13. The surface defined in the three dimensional plot has been termed the characteristic frost heave surface for that material.

Konrad and Morgenstern demonstrate that having defined the characteristic frost heave surface, as shown, they are able to mathematically simulate the observed frost heave which occurs during transient freezing in the laboratory.

The test results for Devon silt indicate that for this material, at the test void ratio, the suction at the frost front does not exceed a limiting value of about 80 kPa. This is speculated to be the critical suction beyond which

THURBER

cavitation will occur in this silt. The results also indicate that there is a limiting rate of cooling (about 2.5°C/hour) above which water flow to the freezing front does not occur.

The relatively complex behaviour of segregation potential with respect to rate of cooling and suction at the frost front could make the practical application of the theory to field situations difficult. However, it must be recognized that rates of cooling which occur in the field are typically very much lower than the rates of cooling used in laboratory frost heave tests. For most field situations, the rate of cooling at the frost front is in the order of 0.01°C per hour or less. Konrad and Morgenstern suggest that since this is the case, soil frost heave characteristics in the field can be approximated by the characteristics corresponding to the formation of the final ice lens, as measured in the laboratory with constant temperature boundary conditions. That is, when the rate of cooling of the frost front in the laboratory is near zero.

The assumption that the rate of cooling in the field is very low, combined with the conservative assumption that the suction at the frost front is near zero, greatly simplify the calculations and make the application of the theory to design problems practical.

Many researchers have observed that during the initial stages of a laboratory freezing test, when the rate of cooling of the frozen fringe is very rapid, water will be expelled from the frost front. This phenomenon was investigated by Nixon (1987) and is worthy of further discussion here.

As outlined by Nixon, Gilpin (1980) suggested that the mass balance of water at an advancing frost front would be given by:

$$v_{ff} = v_u + 0.09\ n \frac{dx}{dt} \qquad (10.4)$$

where

v_{ff} denotes the velocity of water within the frozen fringe

v_u denotes the velocity of water within the unfrozen soil below the frost front

THURBER

n denotes the porosity (which should be reduced to account for that portion of the pore water which does not freeze), and

$\frac{dx}{dt}$ denotes the rate of advance of the frost front.

From an examination of Equation 10.4, it can be seen that for rapid rates of frost advance, the externally measured pore water velocity v_u may be negative, even through frost heave and water migration to the active ice lens is continually taking place. That is, the equation correctly predicts the expulsion of water from the frost front during the initial stages of frost heave tests, when rates of freezing are very rapid.

Based on the foregoing considerations, Nixon suggested that the segregation potential should be more precisely defined as:

$$SP^{*} = v_{zz}/G_{zz} \qquad (10.5)$$

where

v_{zz} denotes the water velocity within the frozen fringe, and

G_{zz} denotes the temperature gradient within the frozen fringe.

Nixon then derived the following expression from which segregation potential could be calculated from measurements made in conventional frost heave tests.

$$SP^{*} = (h/1.09)/(G_z - Lh/1.09\ K_z) \qquad (10.6)$$

where

h denotes the rate of heave,

G_z denotes the temperature gradient in the frozen soil near the frost front,

K_z denotes the thermal conductivity of the frozen soil and fringe (which are assumed to be equal), and

L denotes the latent heat of water.

THURBER

The value for SP^* can be readily calculated at any time during the frost heave test from the measured heave rate and thermal gradient at the frost front. Equation 10.6 will provide a somewhat larger value for SP than that obtained with the Konrad-Morgenstern definition.

Equation 10.6 can be rearranged to provide the following equation for predicting frost heave in the field:

$$h = 1.09\ SP^* G_f / (1 + L\ SP^* / K_f) \qquad (10.7)$$

It should be noted that at the present time, most of the laboratory data for segregation potential has been calculated using the definition proposed by Konrad and Morgenstern (Equation 10.1). The definition proposed by Nixon more accurately reflects observed behaviour and merits further consideration.

10.5 Stress State

A number of researchers have demonstrated that if an external pressure is applied to a freezing soil, total frost heave can be reduced. The effect which external applied pressure has on the segregation potential was investigated by Konrad and Morgenstern (1982b) through a series of tests on Devon silt, together with a re-evaluation of test data reported by others on other soil types.

Konrad and Morgenstern found that the correlation between the log of SP and applied external pressure was linear, as illustrated on Figure 10.14. As the applied load is increased, SP is seen to decrease for Devon silt. The data shown on Figure 10.14 are for SP as measured during the formation of the final ice lens in frost heave tests. That is, the rate of cooling and the suction at the frost front are both relatively low.

The relationship between applied pressure and segregation potential for Calgary silt is presented in Figure 10.15. There is considerable scatter to the test results obtained for Calgary silt. The scatter is attributable to variations in grain size and density of the samples tested, as well as variations in the method of testing. These factors can have a significant effect on the measured values for segregation potential.

As indicated by the test data, the influence of applied pressure at the frost front on segregation potential is significant and cannot be neglected. Konrad and Morgenstern have suggested the following relationship between SP and applied pressure:

THURBER

$$SP_o = ae^{-bP} \qquad (10.8)$$

where

SP_o denotes the segregation potential when the final ice lens is being formed under steady state temperature conditions.

a and b denote soil parameters which are determined from laboratory tests.

e denotes the base of the exponential function (2.718).

and P denotes the total pressure acting on the frost front, including the weight of soil and any load applied at ground surface.

Nixon (1988) has pointed out that the value of segregation potential will vary significantly in the pressure range from 0 to 15 kPa, as a consequence of the relationship given by Equation 10.8. In addition, the proportion of the applied pressure at the frost front due to side friction in laboratory frost heave cells will be significant, if the external applied load is small. As a result, it will be difficult to obtain consistent test results in the laboratory at low values of applied pressure, unless measures are taken to reduce side friction.

Nixon (1987) has suggested that heave rates measured in confined frost heave cells in the laboratory may be greater than those which occur in the field, because of the lateral constraint imposed by the frost heave cell. In the field, where lateral constraint is reduced, frost heave may occur in a horizontal direction as well as a vertical direction, with the result that vertical heave may be reduced. It is understood that Nixon is currently investigating this effect through a series of triaxial frost heave tests.

10.6 Soil Properties

The properties of the soil, will of course, have a significant effect on the segregation potential. Past research has indicated that the segregation potential will be affected primarily by the following soil properties:

1) Void ratio,
2) grain size distribution,
3) soil particle mineralogy, and
4) soil particle shape.

THURBER

Other soil properties, such as hydraulic permeability, thermal properties, density, degree of saturation, and water content will all affect the segregation potential, however these properties are embodied in the parameters listed above, and hence these latter variables will not be considered separately.

It is clear that in determining the segregation potential in laboratory tests, the foregoing soil properties must be carefully controlled in order to obtain a consistent set of test results. In addition the effects which factors such as the method of soil placement in the field, freeze thaw cycles (which will affect the void ratio) must be carefully evaluated in order to ensure that the laboratory test results will be representative of field conditions.

No systematic studies of the effect which void ratio (or density, or initial water content) has on segregation potential have been found in this review. Konrad and Morgenstern have indicated from the results of a limited number of tests, that varying the void ratio will have a significant effect on the segregation potential for Devon silt. The externally applied pressure will of course, also affect the void ratio. The relationship between void ratio, external applied pressure and segregation potential deserves further investigation.

Rieke et al (1983) and Vinson et al (1986) investigated the segregation potential of various mixtures of sands and gravels which contained up to 20 percent material passing the No. 200 sieve. An attempt was made to establish correlation between various soil index properties (such as percent passing .02 mm and specific surface area of soil particles) and segregation potential. Their findings can be summarized as follows:

1) SP increased as fines content increased,
2) SP increased with decreasing activity of the fines fraction, and
3) SP increased as the liquid limit of the fines fraction increased, for a specific fines fraction mineralogy.

These researchers found that there was no consistent correlation between the more common soil index properties and segregation potential. They therefore introduced a new index, referred to as the fines factor, R_f, which incorporates the significant variables which appear to have a strong influence on the segregation potential.

THURBER

$$R_f = \frac{F_t \, F_c}{L_f} \qquad (10.9)$$

where

R_f denotes the fines factor,

F_t denotes the percentage, by weight passing the No. 200 sieve,

F_c denotes the percentage by weight of clay sizes to the total passing the No. 200 sieve, and

L_f denotes the liquid limit of the material passing the No. 200 sieve.

As shown on Figures 10.16 and 10.17, the correlation between the fines factor and segregation potential was found to be reasonably good for the soils tested, particularly for the coarser grained materials.

It is understood that other attempts to correlate basic soil indices (including the fines factor) have not been successful for finer grained materials (Sego, 1988). Further research into the fundamental processes which control segregation potential is required in order to establish useful correlationship between soil indices and segregation potentially particularly for silts and clays.

Nixon (1987) has compiled data on the segregation potential of a wide variety of soils as a function of applied pressure. This data is presented on Figure 10.18. This data indicates that the segregation potential of silts and clayey silts is much more sensitive to applied pressure as compared to clays.

10.7 Saline Soils

Chamberlain (1982) investigated the process of frost heave in soils which contain saline pore water. The salinity of the pore water tends to depress the freezing point of the water. However, the freezing process is made more complex because of the exclusion of salt from the ice, with the result that the concentration of salt in the unfrozen water increases, depressing the freezing point of the unfrozen water still further.

THURBER

An idealized sketch which shows the sequential development of ice lenses in saline soils is presented in Figure 10.19. The net result of the presence of saline pore water is that the thickness of the frozen fringe is greatly increased over that which normally occurs in non-saline soils. In addition, however, ice lenses tend to develop within the frozen fringe, a condition which is assumed not to occur in the Konrad and Morgenstern theory.

There may also be zones or pockets of highly concentrated saline pore fluids which will be present behind the frost front and which have virtually no hydraulic connection with the frozen fringe.

Further research into the process of frost heaving in saline soils appears to be worthwhile. It may be possible to modify or extend the concept of segregation potential such that the same theoretical framework can be used to predict frost heave in saline soils.

10.8 Other Factors

A number of other factors have been shown or can be expected to influence segregation potential. These factors include stress history (overconsolidation), freeze-thaw history (which imparts a secondary structure and permeability to the soil) and natural variations in soil properties due to its geological origin. No systematic research into the effects which these factors may have on segregation potential was found in this review.

10.9 Comparisons with Field Data

The frost heave theory proposed by Konrad and Morgenstern has been used to match frost heaving observations for a number of case histories.

Nixon (1982) used the theory to match observed heave of cold plates installed at the Calgary frost heave test facility (Nixon et al, 1981). A sketch of the test set up and test results is presented on Figure 10.20. The overburden pressure during the initial stage of the test (about 200 days), prior to retreat of the frost bulb was measured to be 60 to 120 kPa.

Nixon selected a value for SP of 90 x 10^{-5} mm^2/s ^oC) which is the midpoint of the available data (Figure 10.15) at an applied pressure of 100 kPa, and calculated frost heave as a function of time using this value of

THURBER

SP. The calculated and observed values are compared on Figure 10.20. There is reasonably good agreement between the calculated and measured values, both in terms of the shape of the heave curve with time, as well as the absolute magnitude of heave at specific times.

Konrad and Morgenstern (1984) compared measured frost heave rates of various chilled pipeline test sections at the Calgary test facility, with predicted values obtained using the segregation potential concept. Konrad and Morgenstern accounted for the scatter in the SP test results for Calgary silt (Figure 10.15) by calculating heave rates using reasonable upper and lower bounds as well as the average values for segregation potential from the available data as shown on Figure 10.21. A comparison between predicted and measured heave for the various test sections is presented in Figures 10.22 to 10.23.

Relative to the level of predictive accuracy commonly encountered in many other areas of geotechnical engineering, the agreement between predicted and measured heave is considered to be excellent.

Smith and Dallimore (1985) used the concept of segregation potential to compare predicted frost heave of a chilled pipeline at the Caen test facility with observed heave. The results of frost heave tests on the Caen silt are shown on the upper half of Figure 10.24. Frost heave tests were carried out on compacted samples of silt as well as on samples which were consolidated from a slurry. In the case of the consolidated samples, tests were run on the samples, which were then thawed and subjected to a second frost heave test. The significant effects which sample preparation procedure and freeze-thaw history have on segregation potential is apparent from these test results.

Predicted frost heave is compared to measured heave of the pipeline in the lower half of Figure 10.24. When the value for segregation potential as measured on consolidated samples is used, the predicted and measured heave are in excellent agreement. The heave predicted using values for segregation potential as measured on compacted samples is significantly lower, however, than the observed heave rate. This is surprising, because the silt at the Caen test facility was placed and compacted in layers and subsequently saturated from below. The reason for this discrepancy has not been established, however, it may be due to variations in void ratio which occur throughout the laboratory compacted samples. The method of compaction used in the field

THURBER

is not strictly comparable to the method used in the laboratory and somewhat different soil structures may occur, even though the resulting densities are the same. The reasons for the discrepancy between the segregation potentials measured on compacted laboratory samples and the values which are apparently operative at the Caen test facility should be investigated further.

Smith and Dallimore found a significant variation in the segregation potential values measured on the consolidated silt samples. The reasons for this variability are not discussed in the paper, and may be due to variations between sample properties (grain size, void ratio) variations between test procedures or side friction in the frost heave cell. The authors suggest that it would be preferable to undertake a number of frost heave tests so that the consistency of laboratory measured values can be assessed and the range in segregation potential values which may be encountered in the field can be evaluated.

The monitoring arrangement at the Caen test facility was such that it was possible to monitor heave behind the frost front. Heave within the frozen soil behind the frost front has been termed secondary heave. The secondary heave measurements made at the Caen test facility are presented in Figure 10.25. During the period of monitoring, secondary heave apparently accounted for 14% of the total heave. This heave could not be accounted for by the progressive freezing of unfrozen pore water behind the frost front. These observations deserve further study.

Konrad and Morgenstern (1984) have used the concept of segregation potential to assess the effect which selected variables will have on a chilled pipeline in permafrost. While these predictions cannot be confirmed, they are presented here in order to indicate the value of the theory to designers.

The effect which initial ground temperature has on total heave is indicated on Figure 10.26. These results indicate that total heave is not significantly affected by initial ground temperature, although the depth of frost penetration is.

The effect which pipeline operating temperature can be expected to have on total heave is presented on Figure 10.27. Total heave after 30 years is in the order of 0.5 m for a pipeline operating at -1°C and 1.1 m for a pipeline operating at -10°C.

THURBER

The effect which insulating the pipelines has on total heave and frost penetration is indicated on Figure 10.28.

10.10 Summary

The thermodynamic and hydraulic processes which control frost heave are complex. It has taken a considerable research effort to isolate the various factors which control frost heave and establish those that are most significant.

Konrad and Morgenstern have presented a frost heave theory which appears to incorporate those factors which, on the basis of available laboratory and field data, appear to have the most significant control over frost heave. Nixon (1987) has suggested a useful modification to this theoretical model. Further research and laboratory studies aimed at extending the theory and defining the limitations of the theory more precisely should be considered.

Consideration should be given to establishing values for segregation potential at very low values of suction at the frost front. Such situations commonly arise in the field where silt overlies a water-bearing sand, and heave rates may be significantly faster under such circumstances.

Correlations between segregation potential and applied pressure for a variety of soils have been established and a useful index (the fines factor) has been proposed which may be used to provide a preliminary assessment of the frost susceptibility of various coarse grained soils. Recent research (Sego, 1988) has indicated, however, that the correlation between fines factor and segregation potential is not consistent over a broad range of soils types. Further research into the fundamental factors affecting segregation potential is required so that meaningful correlations between segregation potential and soil index properties can be established.

On the one hand, clean sands and gravels have a very low segregation potential and are therefore not frost susceptible. On the other hand, soils with a high clay content have an apparent high segregation potential and yet do not heave significantly in the field due to their low unfrozen permeability. The usefulness of the Konrad-Morgenstern theory could be greatly enhanced if the effects of low permeability in the unfrozen zone could be incorporated into the theory.

In non-permafrost areas, frost heave below roads and airstrips can be reduced if the water table is lowered or if the finished grade is raised. Presumably this effect occurs because of the increased suction at the frost front as freezing occurs. Research should be considered to investigate this effect in order to establish whether the theory can be extended and used to predict frost heave as a function of depth to the water table below roads and airstrips.

Comparisons between observed frost heave and frost heave measured in the field have been extremely encouraging. The agreement between predicted and observed behaviour is well within the level of accuracy commonly accepted in other areas of geotechnical engineering practice. In the case of the Caen test facility observations, there is an unexplained discrepancy which should be investigated further.

Natural frost heave phenomenon such as pingos, hydrolaccoliths and ice wedge polygons are very common throughout Northern Canada. Consideration should be given to using the Konrad-Morgenstern frost heave theory to explain these natural phenomenon. Such work may greatly increase the level of confidence with respect to the validity of the theory, particularly with respect to the prediction of long term behaviour.

There appears to be a requirement to investigate the effect which void ratio has on segregation potential. The factors which affect void ratio include initial water content, method of sample preparation, freeze thaw cycles, overconsolidation, applied pressure and other factors.

Observations from the Caen test facility indicate that secondary frost heave occurred in frozen soil behind the frost front. Secondary frost heave was not observed at the Calgary test facility. The observed secondary frost heave at Caen deserves further investigation.

Extensive deposits of unfrozen, saline, frost susceptible soils are unlikely to be found onshore in Northern Canada, however chilled pipelines may be placed offshore and if this is the case, they will be laid in saline unfrozen soil. Further research into the factors which control frost heave in saline soils should be considered, with the objective of extending the Konrad-Morgenstern theory or developing a new behavioural theory which can be used by design engineers.

Heave rates in the field may be less than those observed in the laboratory due to reduced horizontal constraint. It is understood that the effect of horizontal restraint on frost heave is currently being investigated (Nixon, 1987).

A number of chemical additives have been used in the past to reduce the frost susceptibility of soils below pavement structures. It would be useful to study a number of these additives in order to interpret the behaviour in terms of the segregation potential concept.

A number of researchers have expressed concern that segregation potential is so sensitive to soil density, grain size distribution, and structure, as well as to test procedure, that it is difficult to obtain consistent results, which will be representative of field conditions. These concerns have some validity, particularly in view of the inhomogeneity of natural deposits. It is difficult, and possibly impossible, to completely resolve these concerns. Additional field observations of frost heave may be of value in this regard. This could include observation of heave under natural freezing conditions, as well as the use of small scale insitu frost heave tests, using apparatus similar to the cold plate tests reported by Nixon (1982).

THURBER

FROST HEAVE
LIST OF REFERENCES

Chamberlain, E.J., 1983. Frost heave of saline soils. Proc. of the Fourth Int'l. Permafrost Conf., National Academy Press, Washington, D.C., pp. 121-126

Chamberlain, E.J., 1981. Frost susceptability of soil, review of index tests. U.S. Army Corps of Engineers, CRREL, Hanover, NH, CRREL Monograph 81-2.

Gilpin, R., 1979. A model of the "liquid-like" layer between ice and a substrate with applications to wire regulation and particle migration. J. Colloid Interface Science, Vol. 8, pp. 235-251.

Gilpin, R., 1980. A model for the prediction of ice lensing and frost heave in soils. Water Resources Research, Vol. 16, pp. 918-930.

Gilpin, R., 1982. A frost heave interface condition for use in numerical modelling. Proc. 4th Can. Permafrost Conf. (R.J. Brown Memorial Volume) NRCC 20124. pp. 459-465.

Dallimore, S.R., 1984. Laboratory characterization of frost heaving of Caen silt. In pipelines and frost heave, Proc. of a seminar at Caen, France, Carleton University Press, Ottawa, pp. 23-26.

Johnson, G.H., Ladanyi, B., Morgenstern, N.R., and Permer, E., 1981. Engineering characteristics of frozen and thawing soils. In permafrost engineering design and construction (Johnson, 1981).

Konrad, J.M., and Morgenstern, N.R., 1980. A mechanistic theory of ice lens formation in fine grained soils. Can. Geot. Journ. Vol. 17, pp. 473-486.

Konrad, J.M., and Morgenstern, N.R., 1981. The segregation potential of a freezing soil. Can. Geot. Journ. Vol. 18, pp. 482-491.

Konrad, J.M., and Morgenstern, N.R., 1982a. Prediction of frost heave in the laboratory during transient freezing. Can. Geot. Journ. Vol. 19, pp. 250-259.

THURBER

Konrad, J.M., and Morgenstern, N.R., 1982b. Effects of applied pressure on freezing soils. Can. Geot. Journ. Vol. 19, pp. 494-505.

Konrad, J.M., and Morgenstern, N.R., 1983. Frost susceptability of soils in terms of their segregation potential. Proc. of the Fourth Int'l. Permafrost Conf., Fairbanks.

Konrad, J.M., and Morgenstern, N.R., 1984. Frost heave prediction of chilled pipelines buried in frozen soils. Can. Geot. Journ. Vol. 21, pp. 100-115

Nixon, J.F., 1982. Field frost heave predictions using the segregation potential concept. Can. Geot. Journ. Vol. 19, pp. 526-529.

Nixon, J.F., 1983. Frost heave pipeline interaction using continuum mechanics. Can. Geot. Journ. Vol. 20, pp. 251-261.

Nixon, J.F., 1984. A method for predicting frost heave of buried chilled pipelines. Pipeline and frost heave proceedings, Caen, France, Carlton University Press, Ottawa pp. 55-59.

Nixon, J.F., 1987. Ground freezing and frost heave - a review. American Soc. of Mechanical Engineers, Proc. of the Int'l. Symp. on Cold Regions Heat Transfer, University of Alberta, Edmonton, June 4 to 6, 1987, pp. 1-10.

Nixon, J.F., 1988. Personnel communication.

Nixon, J.F., Ellwood, J.R., Slusarchuk, W.A., 1982. In situ frost heave testing using cold plates. Proc. 4th Can. Permafrost Conf. National Academy Press, Washington D.C. pp. 466-474.

Northern Engineering Services, 1975. Internal report on results from frost effects study. Unpublished report, Calgary, Alberta.

THURBER

Rieke, R.D., Vinson, T.S., and Mageau, D.W., 1983. The role of specific surface area and related index properties in the frost heave susceptability of soils. Proc. Fourth Int'l. Conf. on Permafrost, National Research Council, Washinton, D.C.

Road Research Laboratories, 1961. Soil mechanics for road engineers. Dept of Scientific and Industrial Research, H.M. Stationery Office, London, U.K.

Sego, D.C., 1988. Personnel communication.

Smith, M.W., and Dallimore, S.R., 1985. Observations and prediction of frost heave of an experimental pipeline. Fourth International Symposium on Ground Freezing, Sapporo, pp. 297-304.

Vinson, T.S., Ahmad, F., Rieke, R.D., 1986. Factors important to the development of frost heave susceptability criteria for coarse grained soils. Transportation Research Record 1089. Transportation Research Board, National Research Council, Washington D.C.

THURBER

FROST HEAVE
LIST OF FIGURES

THURBER

LIST OF FIGURES
(continued)

THURBER

THURBER

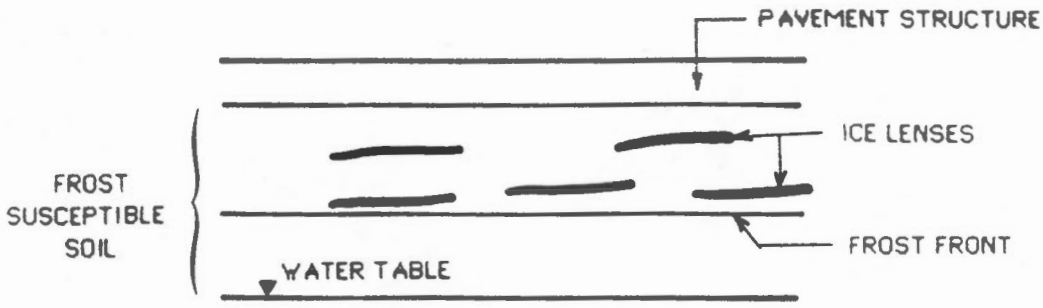

FROST HEAVE BELOW ROADS

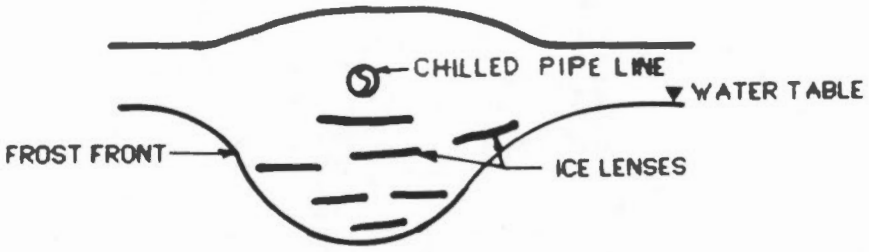

FROST HEAVE BELOW CHILLED PIPE LINES

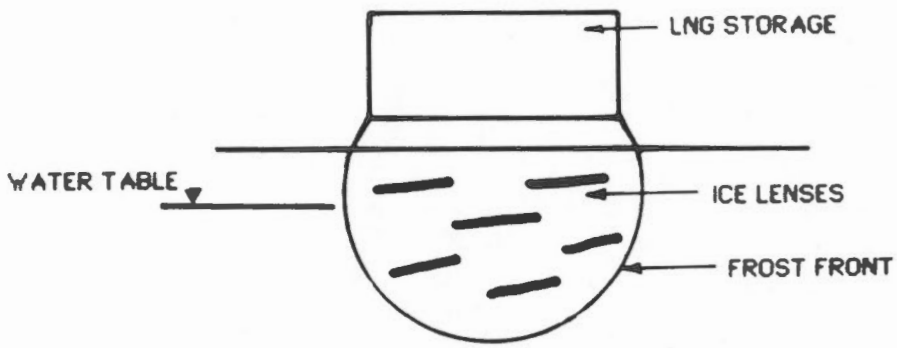

FROST HEAVE BELOW LNG STORAGE TANKS

Some examples of potential frost heave below various types of structures.

FIGURE 10.1

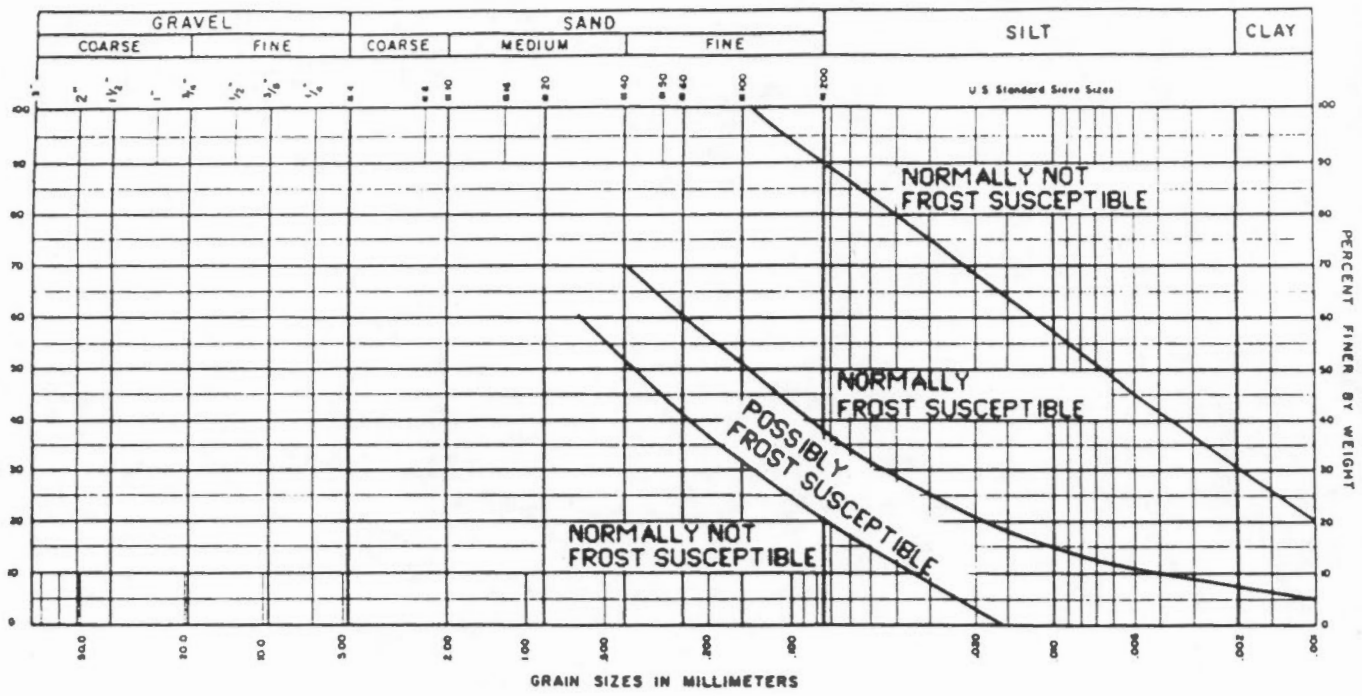

Frost susceptibility criteria based on grain size distribution (adapted from Road Research Laboratories, 1961).

FIGURE 10.2

Frost group	Soil type	Percentage finer than 0.02 mm, by weight	Typical soil types under Unified Soil Classification System
F1	Gravelly soils	3 to 10	GW, GP, GW-GM, GP-GM
F2	(a) Gravelly soils	10 to 20	GM, GW-GM, GP-GM
	(b) Sands	3 to 15	SW, SP, SM, SW-SM, SP-SM
F3	(a) Gravelly soils	>20	GM, GC
	(b) Sands, except very fine silty sands	>15	SM, SC
	(c) Clays, PI >12	—	CL, CH
F4	(a) All silts	—	ML, MH
	(b) Very fine silty sands	>15	SM
	(c) Clays, PI < 12	—	CL, CL-ML
	(d) Varved clays and other fine-grained, banded sediments	—	CL and ML; CL, ML, and SM; CL, CH, and ML; CL, CH, ML, and SM

NOTES: 1. With a sufficient water supply, ice segregation should be expected in non-uniform soils containing more than 3% of grains smaller than 0.02 mm and in very uniform containing more than 10% smaller than 0.02 mm.

2. The soils classified as F1 are the least frost susceptible, while the soils classified as F4 are the most frost susceptible.

U.S. Army Corps of Engineers, Frost susceptibility classification of soils (from Johnson, et al, 1981).

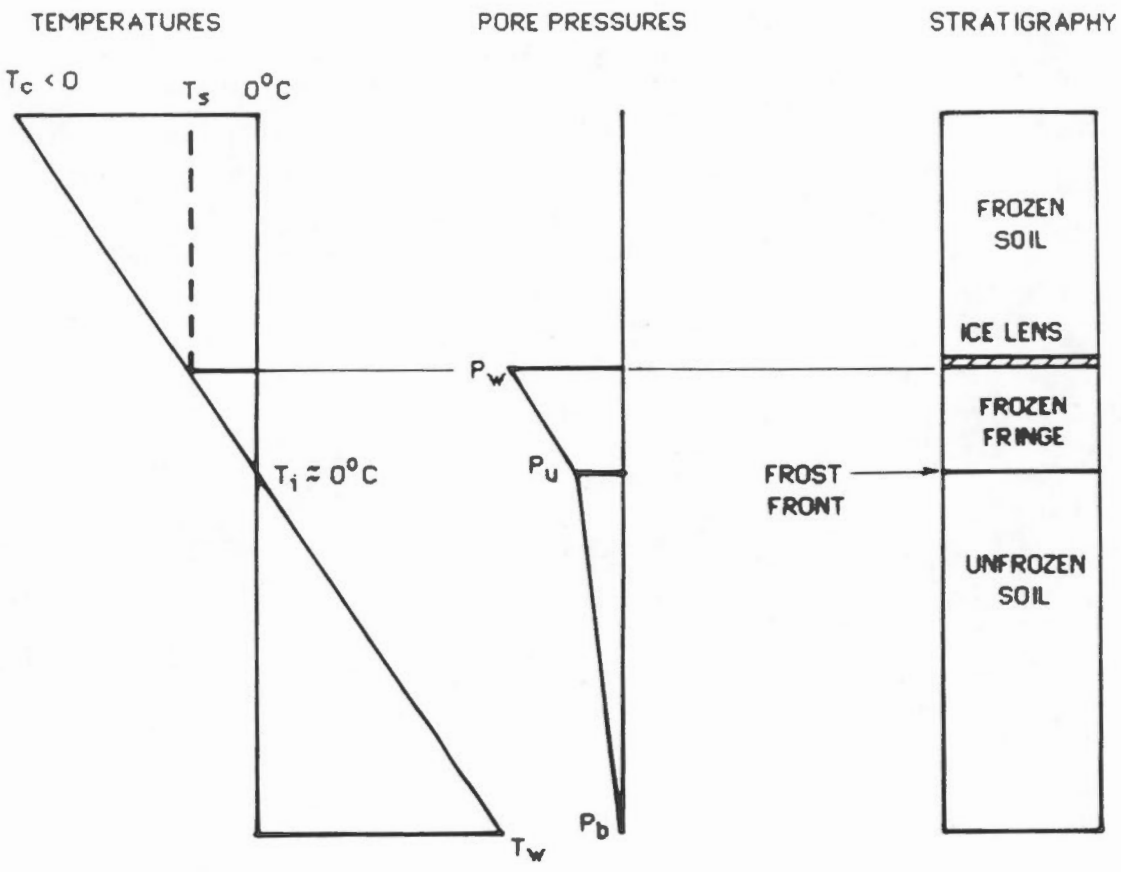

Idealized steady state frost heave (after Konrad and Morgenstern, 1980).

FIGURE 10.4

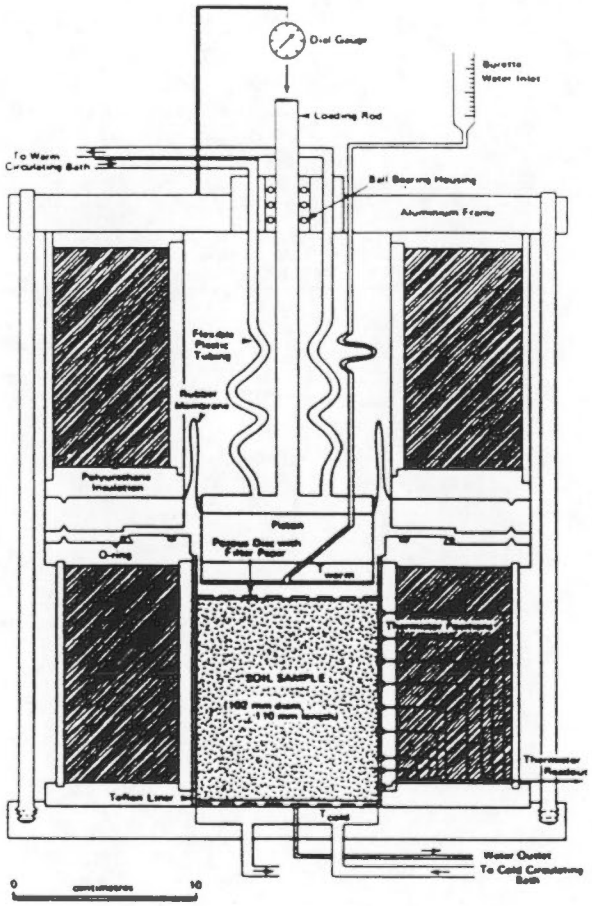

Cross-section of a frost heave cell (Dallimore, 1984).

FIGURE 10.5

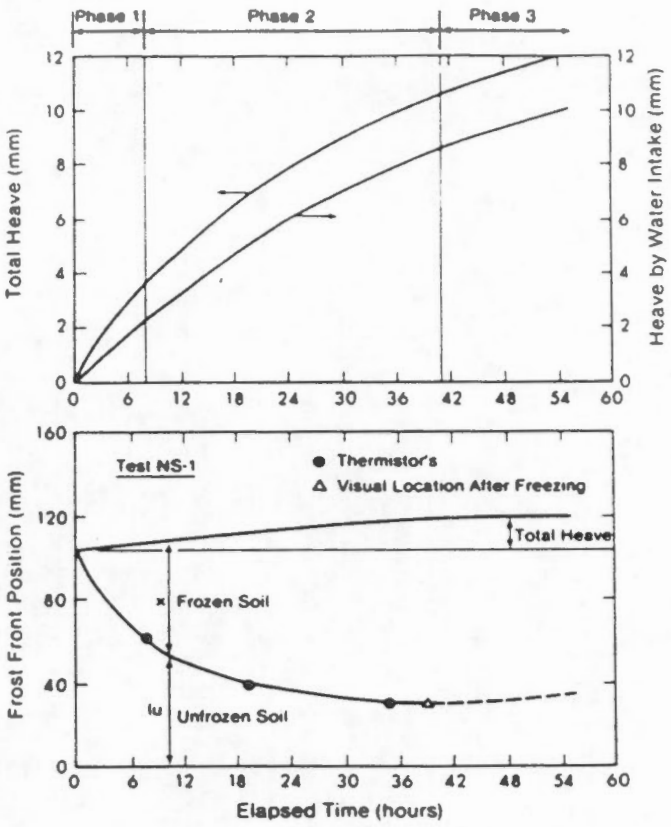

Example of data obtained from a frost heave test (Konrad and Morgenstern, 1980).

FIGURE 10.6

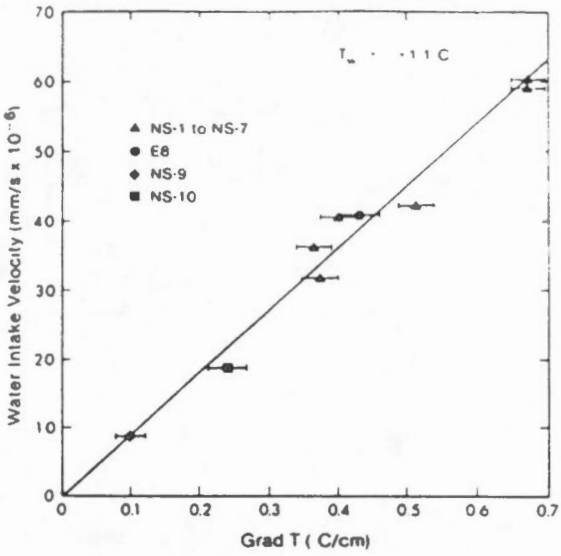

Water intake velocity versus temperature gradient at steady state temperature (Konrad and Morgenstern, 1980).

FIGURE 10.7

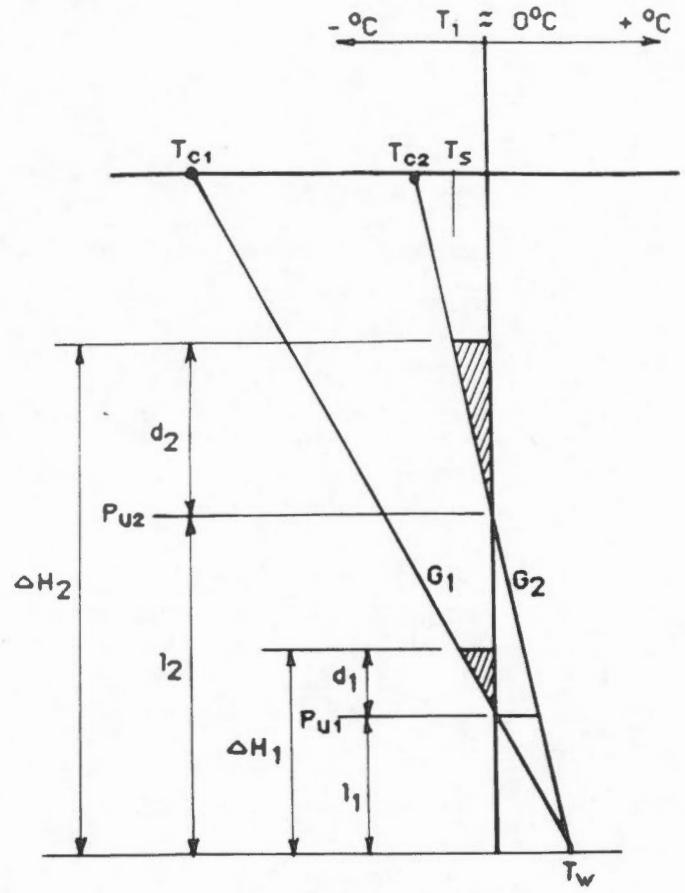

$$\Delta H_1 = \Delta H_2$$

$$\frac{d_1}{l_1} = \frac{d_2}{l_2}$$

$$\therefore P_{u1} = P_{u2} = \text{Constant}$$

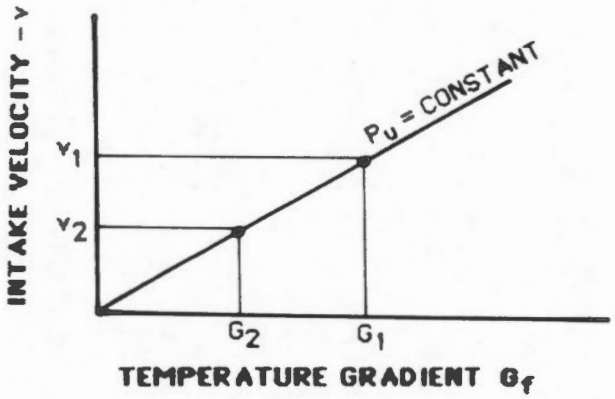

The effect of varying the cold side temperature on P_u and SP (after Konrad and Morgenstern, 1981).

FIGURE 10.8

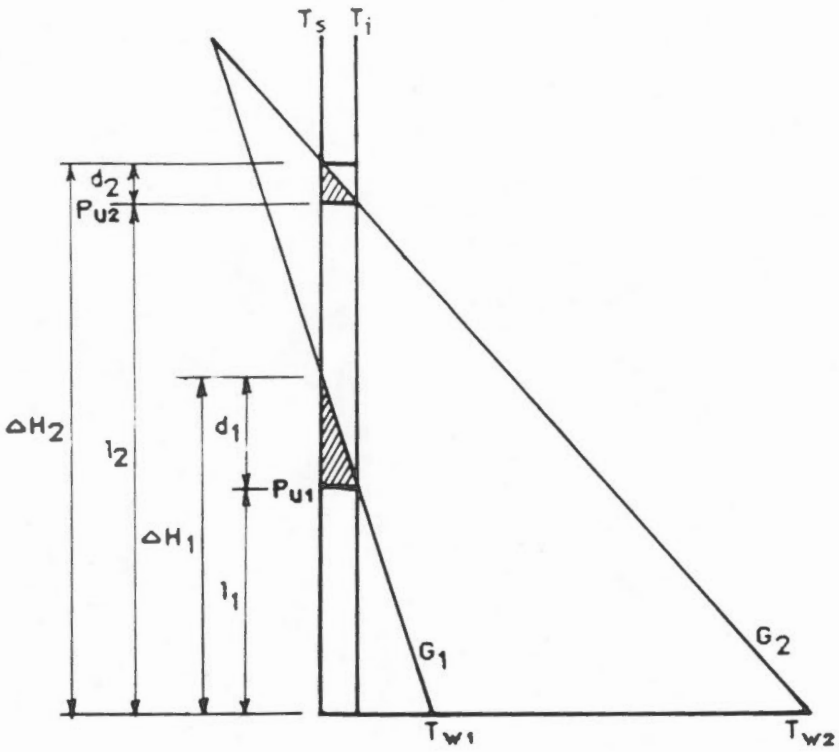

$$\Delta H_1 = \Delta H_2$$

$$\frac{d_1}{l_1} \neq \frac{d_2}{l_2}$$

$$\therefore P_{u1} \neq P_{u2}$$

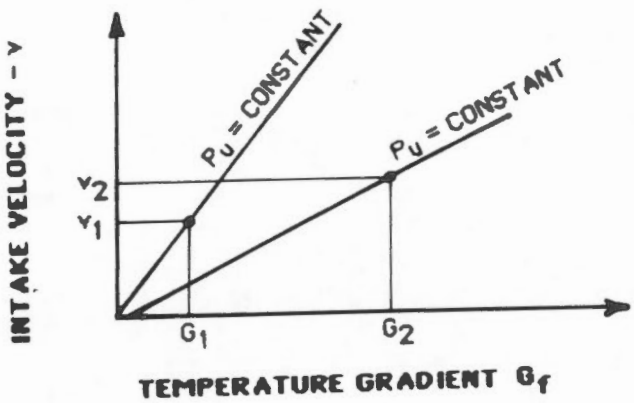

The effect of varying the warm side temperature on P_u and SP (Konrad and Morgenstern, 1981).

FIGURE 10.9

THURBER

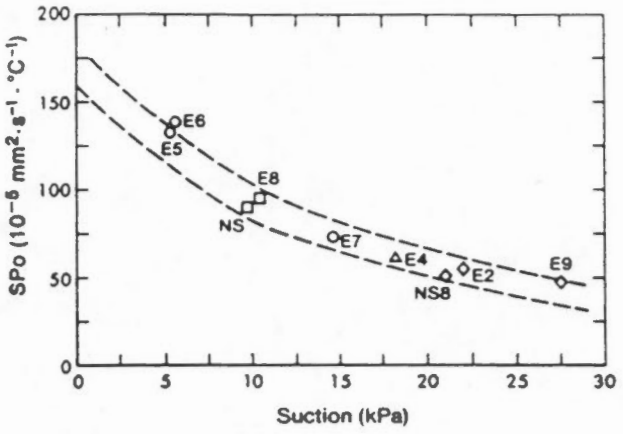

Segregation potential versus suction at the frost front for Devon silt (Konrad and Morgenstern, 1981).

FIGURE 10.10

THURBER

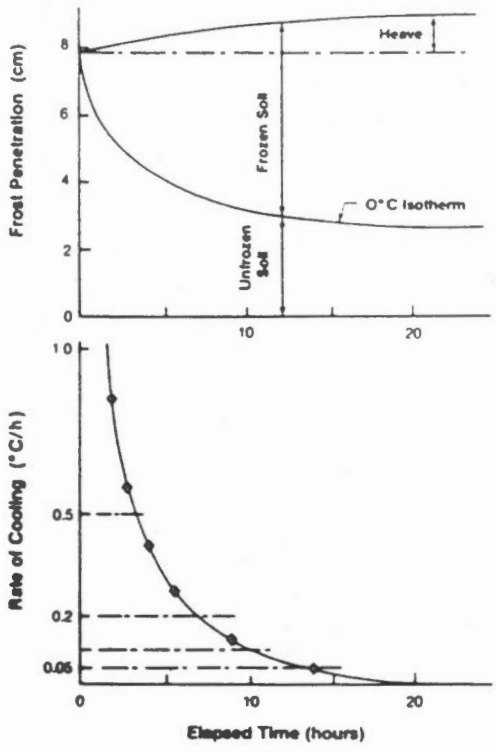

Rate of cooling of the frost front as a function of time (Konrad and Morgenstern, 1982a).

FIGURE 10.11

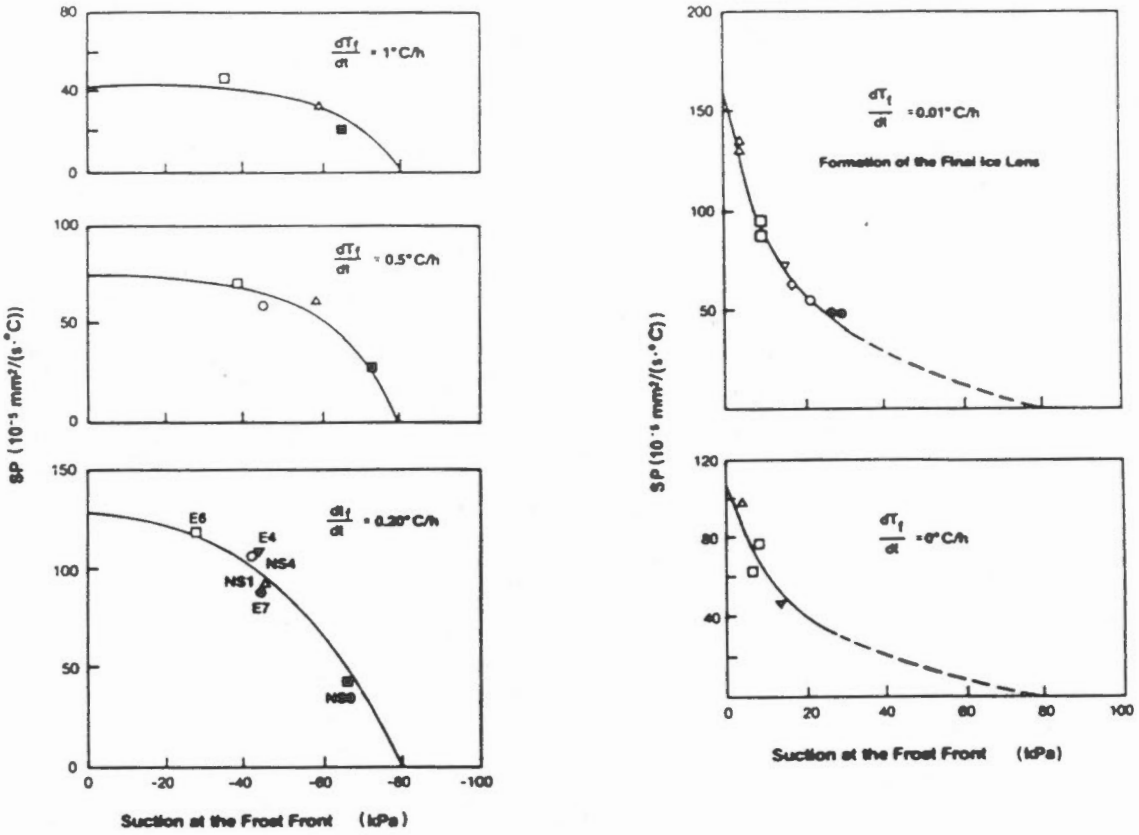

The effect of rate of cooling and suction at the frost front on the segregation potential of Devon silt (Konrad and Morgenstern, 1982a).

FIGURE 10.12

THURBER

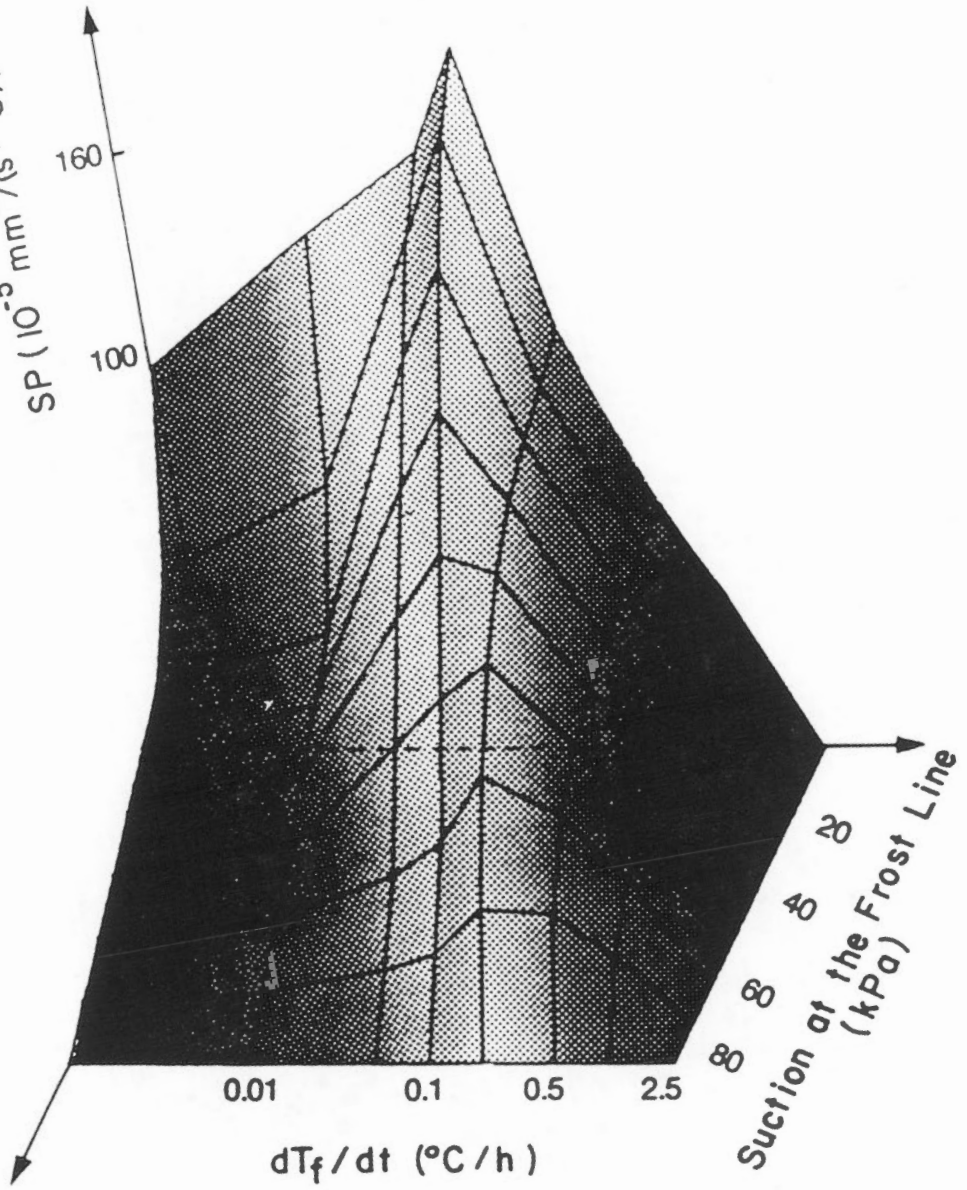

The characteristic frost heave surface for Devon silt (Konrad and Morgenstern, 1982a).

FIGURE

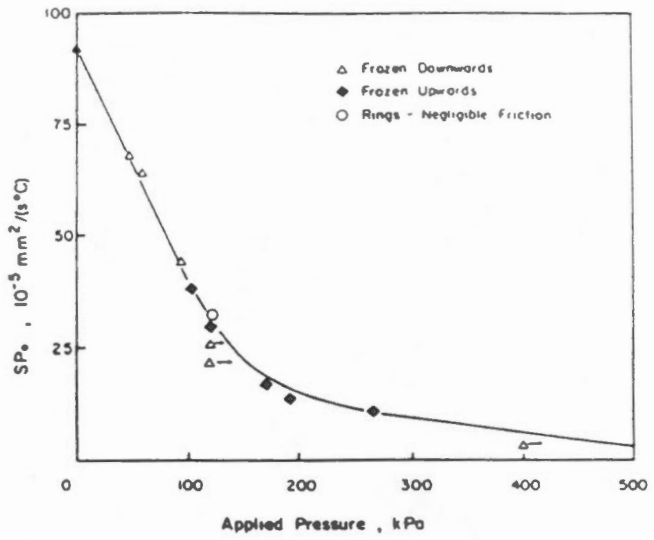

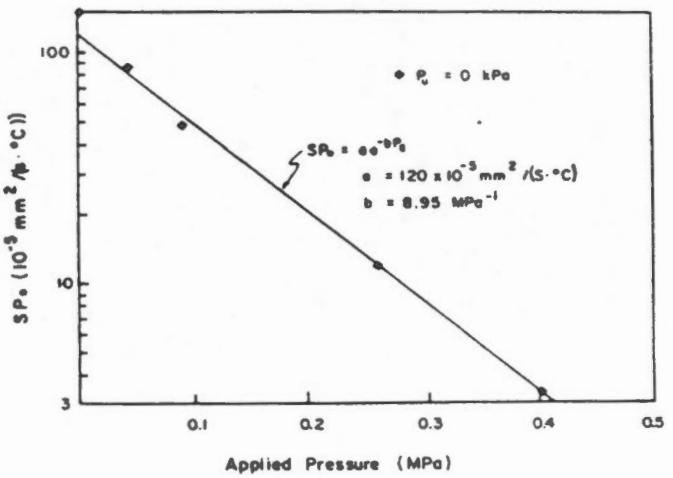

Segregation potential as a function of applied pressure for Devon silt (Konrad and Morgenstern, 1982b).

FIGURE 10.14

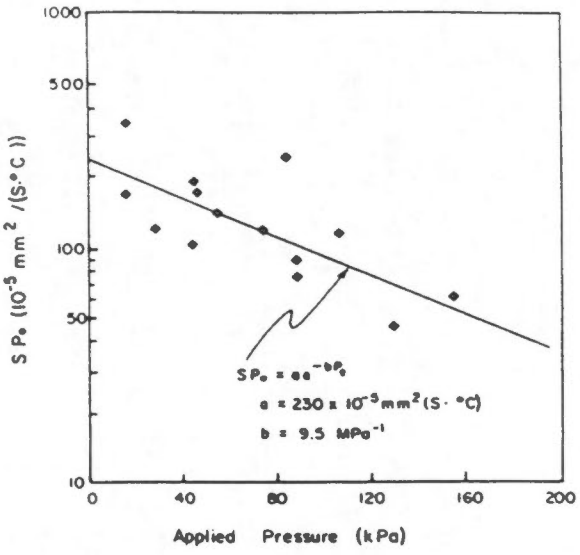

Segregation potential as a function of applied pressure for Calgary silt. Test results from Northern Engineering Services (1975) (Konrad and Morgenstern, 1982b).

FIGURE 10.15

THURBER

TABLE 1 Frost Heave and Index Property Test Results for Soil Mixtures.

Test	Percent Astoria Sand	Percent Hanover Silt	Percent Clay	Specific Surface Area m^2/g	Liquid Limit of Fine Fraction (LL_{ff}) %	Fines Factor[2] (R_f) %	Segregation Potential (SP_o) $10^{-6}\ \frac{mm^2}{°C\text{-}sec}$
1	80	0	20 (M)[1]	19.5	135	14.8	2561
2	95	5	0	0.25	-	-	-
3	95	0	5 (M)	4.87	135	3.70	227
4	90	0	10 (M)	9.74	135	7.41	1565
5	90	10	0	0.50	-	-	293
6	80	20	0	1.0	-	-	1063
7	80	14	6 (M)	6.54	56	10.7	1846
9	90	7	3 (M)	3.27	56	5.36	841
10	90	6	4 (M)	4.20	66	6.06	1112
11	90	3	7 (M)	6.97	99	7.07	1338
13	95	1.5	3.5 (M)	3.48	99	3.54	302
14	95	3	2 (M)	2.10	66	3.03	212
15	95	3.5	1.5 (M)	1.64	56	2.68	295
16	95	1	4 (PK)[1]	0.99	58	6.90	1601
17	80	4	16 (PK)	3.96	58	27.6	4229
18	80	10	10 (PK)	2.85	40	25.0	3165
19	80	15	5 (PK)	1.93	29	17.1	2395
20	90	2	8 (PK)	1.98	58	13.8	2223
21	90	7.5	2.5 (PK)	0.96	29	8.53	1361
22	95	3.75	1.25 (PK)	0.48	29	4.27	541
23	95	3.75	1.25 (MK)[1]	0.31	26	2.88	478
24	80	15	5 (MK)	1.25	26	11.5	1916
25	80	4	16 (MK)	1.80	37	25.9	3870
26	95	1	4 (MK)	0.45	37	6.5	1176
27	80	12	8 (M)	8.39	66	12.1	2156
28	80	6	14 (M)	13.9	99	14.1	2159
29	90	5	5 (PK)	1.43	40	12.5	2189
30	95	2.5	2.5 (PK)	0.71	40	6.25	1036
31	95	0	5 (PK)	1.18	75	6.67	2319
33	90	0	10 (PK)	2.35	75	13.3	3353
34	80	0	20 (PK)	4.70	75	26.7	4737

[1] M = montmorillonite; MK = well-crystallized kaolinite; PK = poorly crystallized kaolinite.

[2] $R_f = \frac{(\%\text{fines})\ (\%\text{ clay sizes in fine fraction})}{LL_{ff}}$

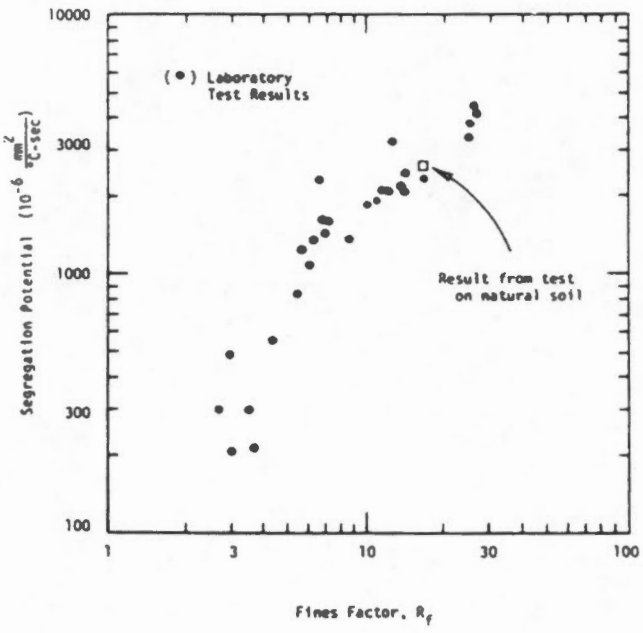

The correlation between the fines factor and segregation potential (Rieke et al, 1983).

FIGURE 10.16

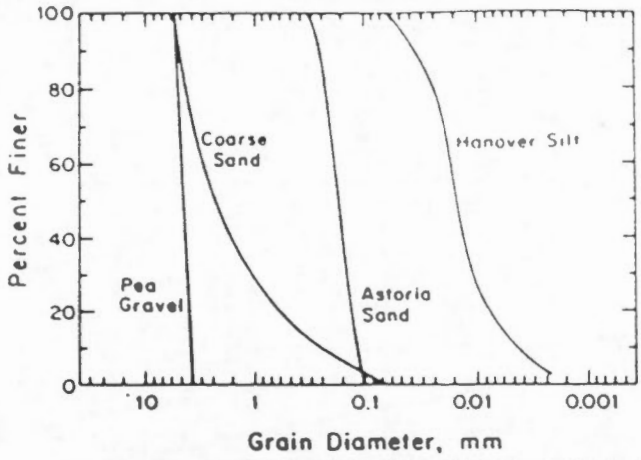

Grain size distributions for soil employed in test program.

PERCENTAGE OF SOIL MIXTURE COMPONENTS, COEFFICIENT OF UNIFORMITY, AND COEFFICIENT OF CURVATURE OF TEST SAMPLES

Test No.	Coarse Material		Silt	Clay		Percent Finer Than	Percent Finer Than			Segregation Potential	Heave Rate
	Percent	Type	(%)	Percent	Type	0.074 mm	0.02 mm	C_u	C_c	(mm^2/°C-day)	(mm/day)
1	100	Well-graded sand	–	–	–	–	–	11	1.1	0.0	0.0
2	98	Well-graded sand	1.5	0.5	PCK	2	1.3	15	1.7	0.0	0.0
3	96	Well-graded sand	3.0	1.0	PCK	4	2.5	16	1.8	0.0	0.9
4	92	Well-graded sand	6.0	2.0	PCK	8	5.0	19	1.9	73	2.3
5	80	Well-graded sand	15.0	5.0	PCK	20	12.5	150	5	147	5.0
6	80	Well-graded sand	10.0	10.0	PCK	20	15.0	1350	46	232	7.8
7	95	Well-graded sand	1.0	4.0	WCK	5	4.5	17	1.8	86	3.2
8	92	Pea gravel	6.0	2.0	PCK	8	5.0	1.2	0.9	76	2.5
9	80	Pea gravel	15.0	5.0	PCK	20	12.5	370	323	203	6.7
10	80	Pea gravel	10.0	10.0	PCK	20	15.0	2900	2421	300	12.7
11	95	Pea gravel	1.0	4.0	WCK	5	4.5	1.1	0.9	67	2.5
12	91	Pea gravel	1.8	7.2	PCK	9	8.1	1.1	0.9	90	4.6
13	96	Pea gravel	3.0	1.0	PCK	4	2.5	1.1	0.9	0.0	0.8

Note: PCK = poorly crystallized kaolinite; WCK = well-crystallized kaolinite; $C_u = D_{60}/D_{10}$; $C_c = D_{30}^2/(D_{60} \times D_{10})$.

NOTE: $1 mm^2 / {}^{\circ}C - day$ equals $1.15 \times 10^{-5}\ mm^2 / {}^{\circ}C - SEL$

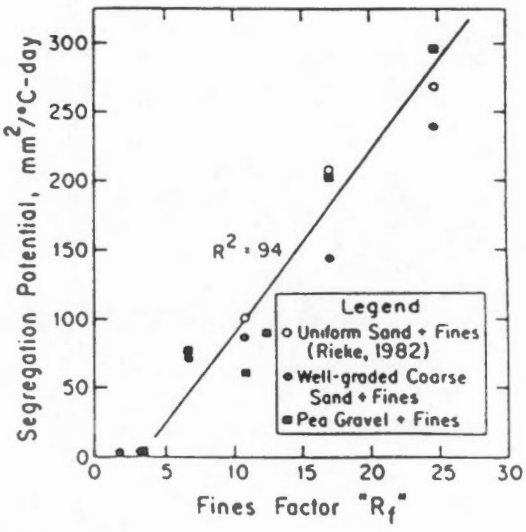

The correlation between the fines factor and segregation potential (Vinson et al, 1986).

FIGURE 10.17

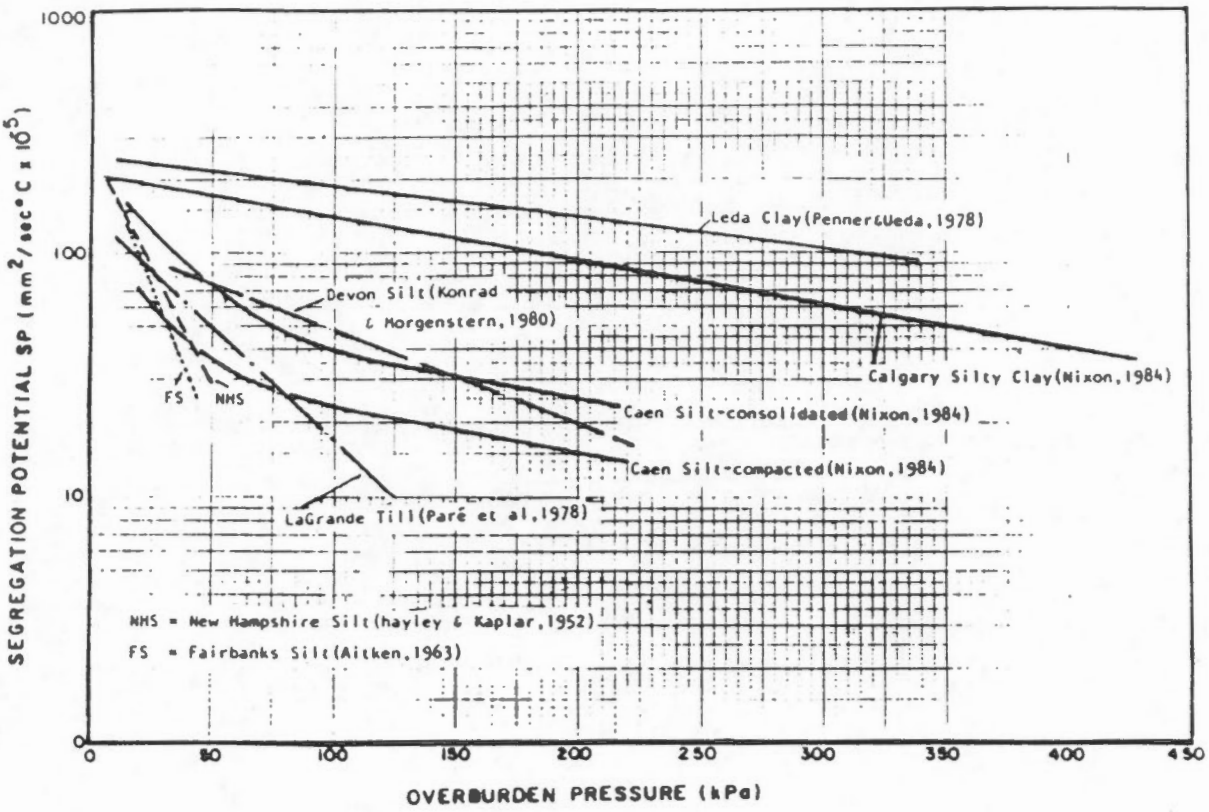

Segregation potential as a function of soil type and applied pressure (Nixon, 1987).

FIGURE 10.18

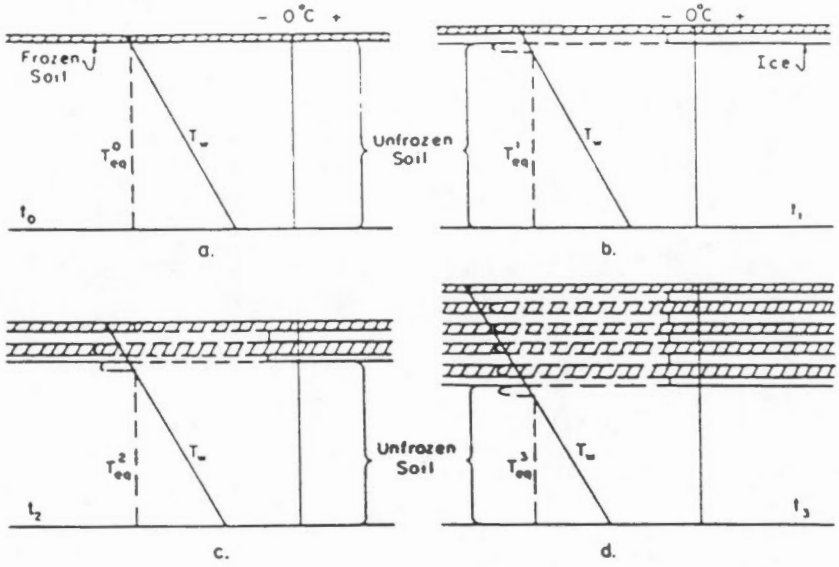

FIGURE 5 Schematic diagram of ice segregation process in saline soils. (a) At time zero (t_0), the pore water temperature profile is T_w and a thin soil layer has frozen; (b) at time t_1, an ice lens is growing and a freezing point depression bulb has formed beneath it due to the exclusion of salts. The segregation freezing temperature at the first ice lens growth site decreases because of the brine concentration, and a second ice nucleation site forms; (c) at time t_2, a third ice nucleation site has formed below the freezing point depression bulb formed by the second ice lens; (d) the process continues at time t_3, with many ice lens growth sites. Ice lens growth at the original nucleation site is shut off by reduced hydraulic conductivity.

Schematic diagram of ice segregation in saline soils (Chamberlain, 1983).

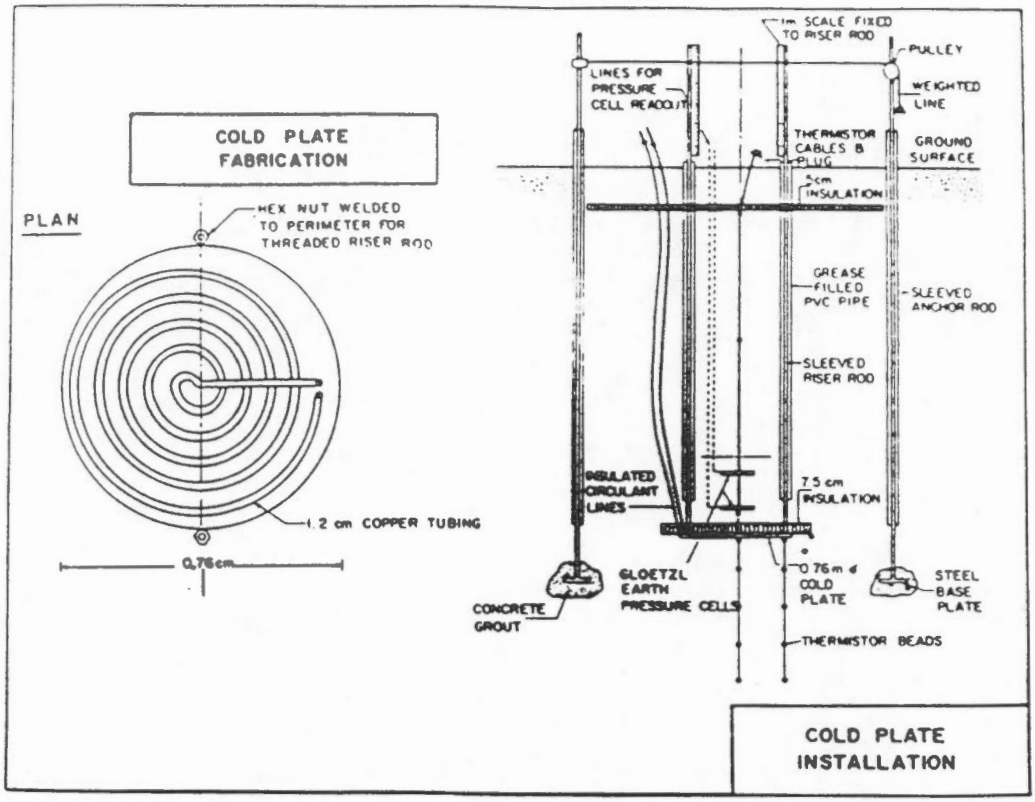

Frost heave test plates at Calgary test facility (from Nixon *et al.* 1981).

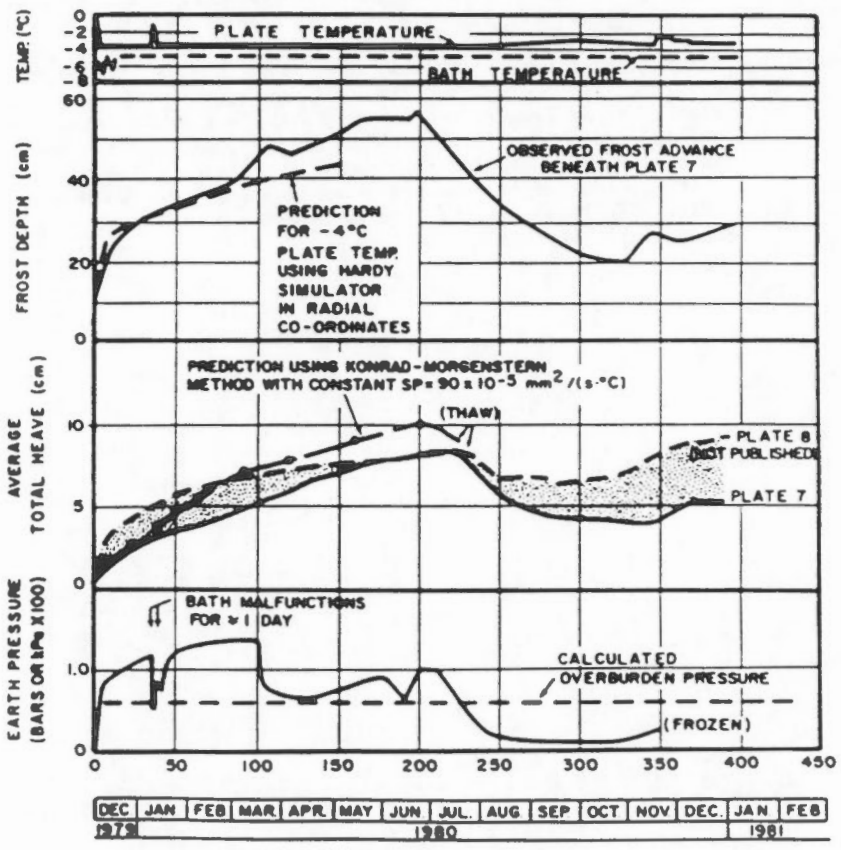

Frost heave plate tests—observations and predictions (1 bar = 100 kPa).

Comparison between predicted and measured frost heave for test plates at the Calgary Test Facility (Nixon, 1982).

FIGURE 10.20

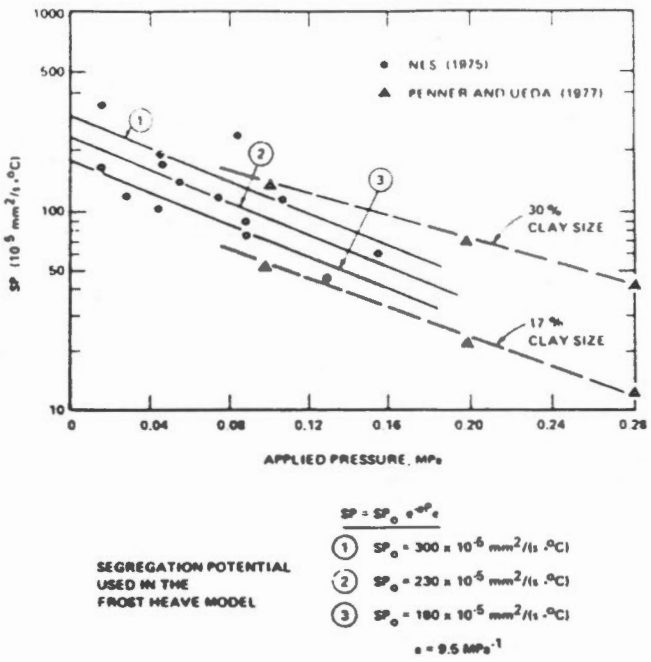

The segregation potential of Calgary silt as a function of applied pressure. The range in values used in the comparison between predicted and measured frost heave of the pipe sections is indicated on the figure (Konrad and Morgenstern, 1984).

THURBER

FIGURE 10.21

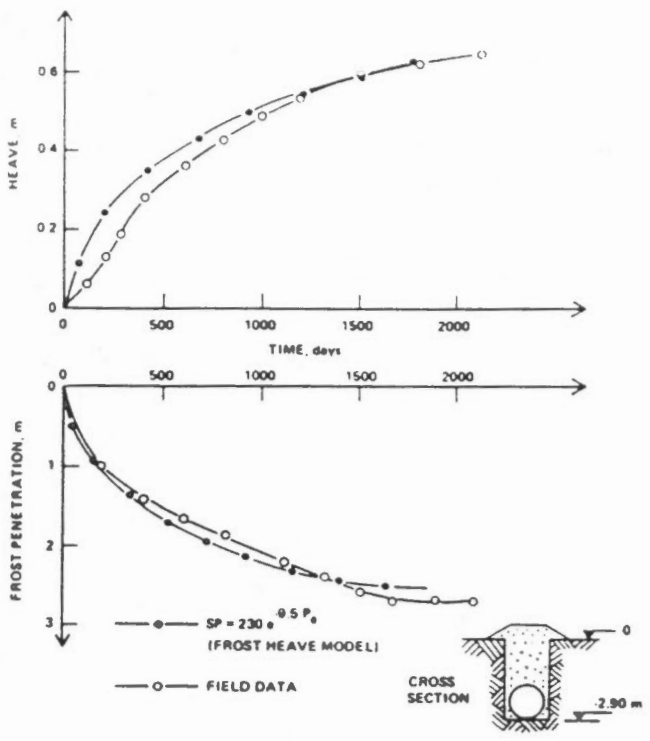

Predictions and observations for the deep burial section.

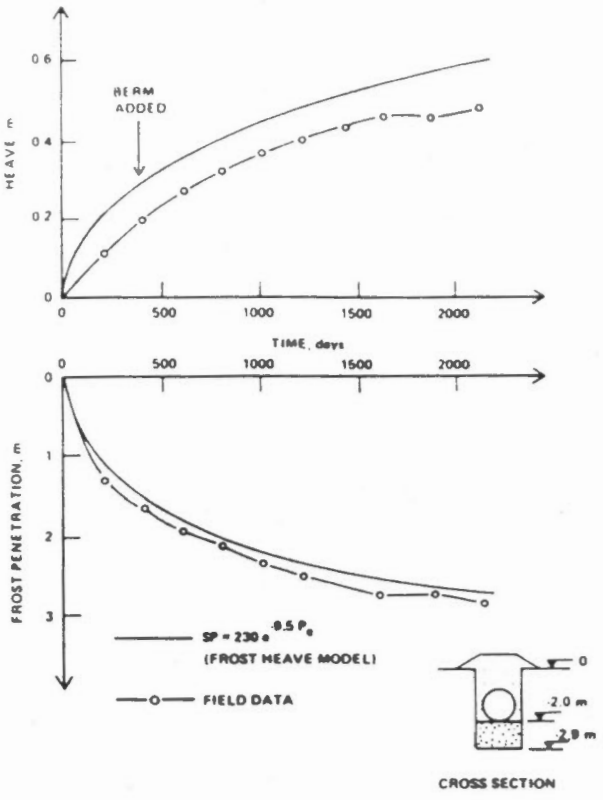

Predictions and observations for the gravel section.

Predictions and observations for the deep buried and gravel pipeline sections at the Calgary Test Facility (Konrad and Morgenstern, 1984).

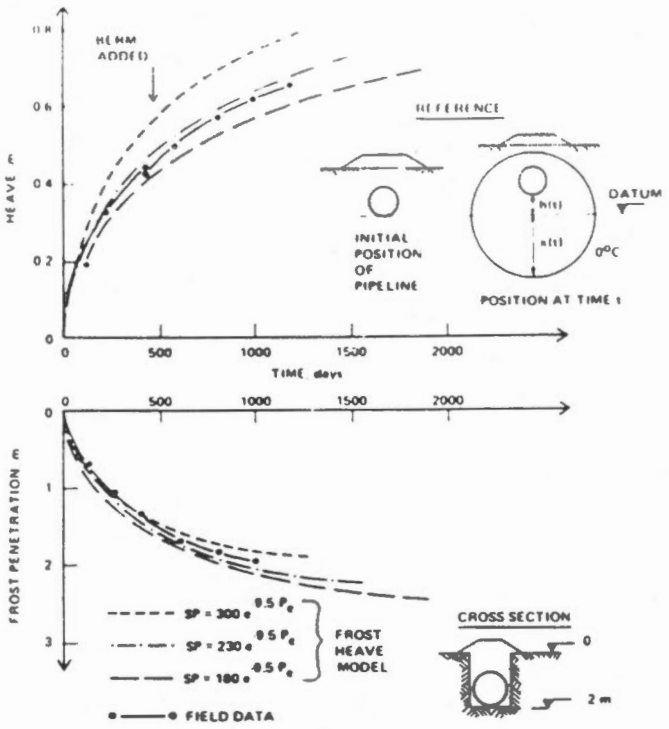

Predictions and observations for the control section.

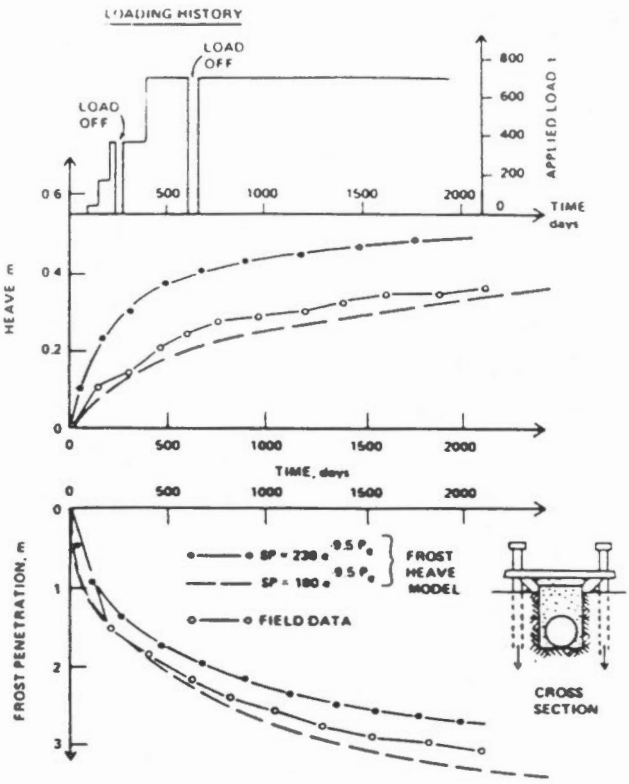

Predictions and observations for the restrained section.

Predictions and observations for the control and restrained pipeline sections at the Calgary Test Facility (Konrad and Morgenstern, 1984).

FIGURE 10.23

THURBER

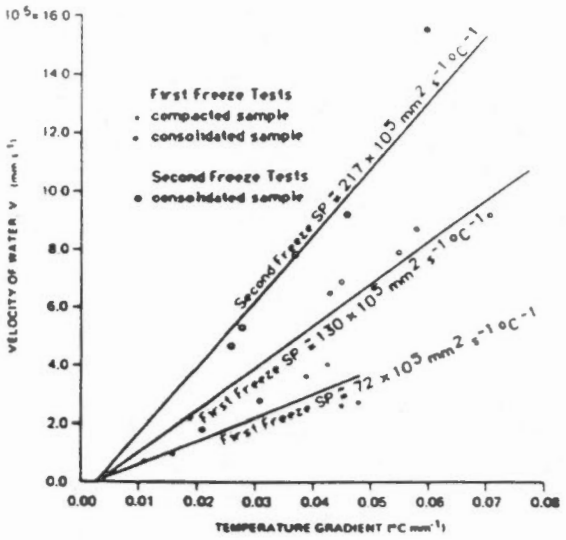

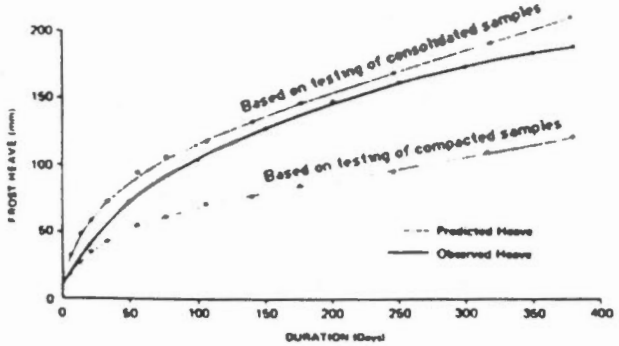

Observed and predicted frost heave of the chilled pipeline at the Caen Test Facility (Smith and Dallimore, 1985).

THURBER

FIGURE 10.24

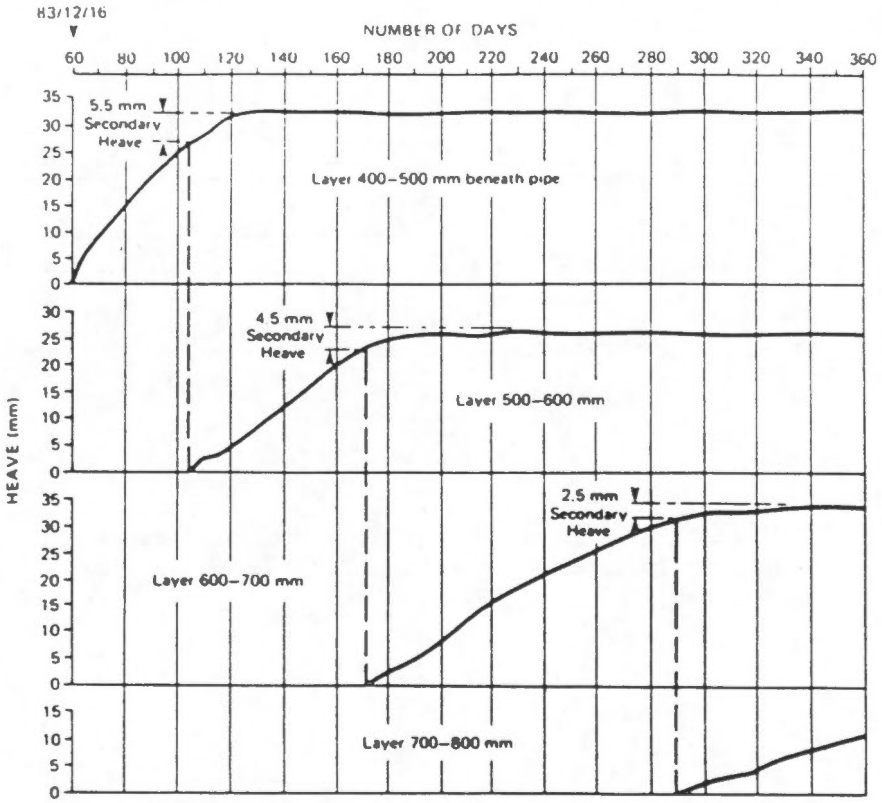

Differential frost heave with depth at the Caen Test Facility. The data shows secondary frost heave occurring (Smith and Dallimore, 1985).

FIGURE 10.25

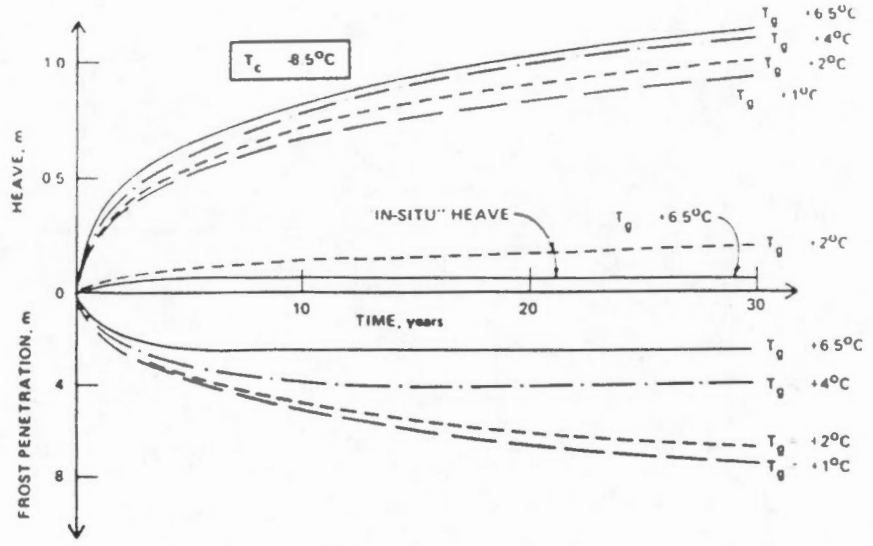

Effect of initial ground temperature on frost heave below a pipeline (Konrad and Morgenstern, 1984).

FIGURE 10.26

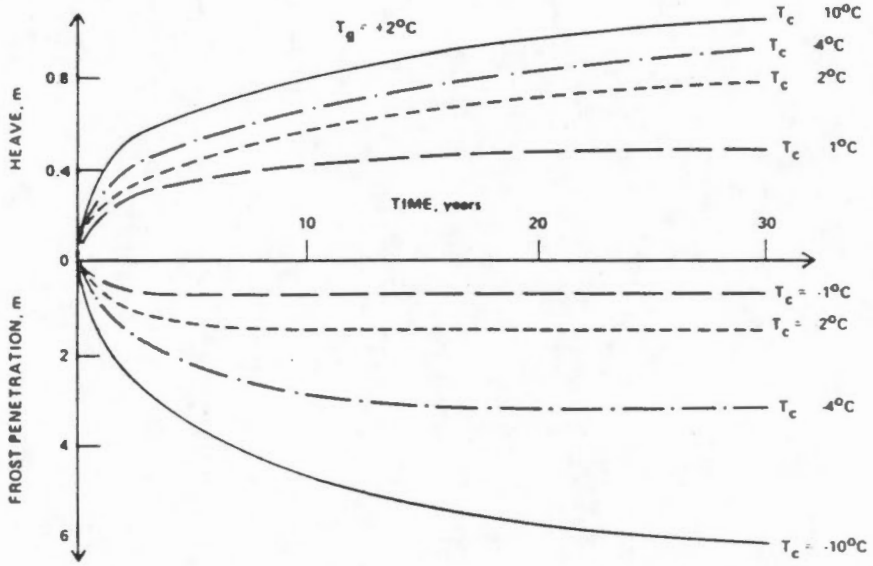

Effect of pipe temperature on frost heave below a pipeline (Konrad and Morgenstern, 1984).

FIGURE 10.27

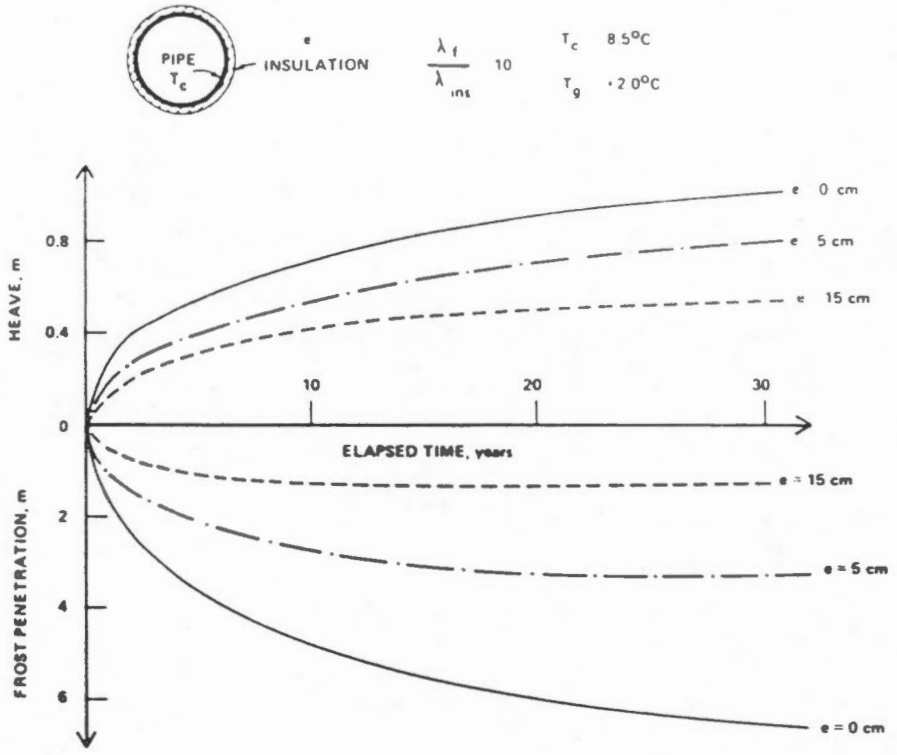

Effect of pipeline insulation on frost heave below a pipeline (Konrad and Morgenstern, 1984).

THURBER

FIGURE 10.28

SECTION 11

DYNAMIC PROPERTIES

SECTION 11

DYNAMIC PROPERTIES

11.1 General

Vinson (1978) presents an excellent review of the dynamic properties of ice and frozen soils and the factors which affect the dynamic properties. This section summarizes Vinson's review and provides additional relevant data that has become available since 1978.

A knowledge of the dynamic properties of frozen soil is required in the analysis of the following situations:

1) vibrating equipment (compressors, pumps, turbines, radar towers),
2) excavation by blasting,
3) earthquake loadings, and
4) geophysical exploration (permafrost delineation, mineral exploration).

As indicated in Figure 11.1 (Vinson, 1978), dynamic loadings can be characterized by the following variables:

1) frequency,
2) amplitude (stress or strain magnitude), and
3) duration (attenuation, if transient loading).

The dynamic response of frozen ground to dynamic loading is defined by two types of properties:

1) dynamic stress-strain properties, and
2) energy-absorbing properties.

The dynamic stress-strain properties normally include dynamic Young's Modulus, E_d, or dynamic shear modulus, G_d and Poisson's Ratio. These properties can be determined from either field or laboratory tests where the velocity of wave propagation through a frozen soil is measured. The velocity of wave propagation is directly related to the dynamic stress-strain properties. There are four types of strain waves which are commonly referred to:

1) Compressional wave (P-wave): This wave travels throughout a soil mass, reflects from interfaces, and is the fastest of all body waves.

THURBER

2) Shear wave (S-wave): This wave causes particle motions transverse to the direction of travel; it can be transmitted throughout solids, but not liquids.

3) Longitudinal wave (L-wave also known as bar-wave): This wave is similar to the compression wave but can only be propagated in thin bars or columns of material (ie, laboratory test specimens).

4) Rayleigh wave (R-wave): This is a surface wave which induces motions in the shape of a vertical ellipse.

Of the four waves, the R-wave is not particularly useful for determining dynamic stress-strain properties, but it is mentioned because it can cause interference in devices intended to monitor the arrival of other waves. The velocities of propagation of the four waves are uniquely related, for a given Poisson's ratio, as shown in Figure 11.2 (McNeill, 1969). It is apparent that the velocity of R-waves are practically the same as S-waves and virtually independent of Poisson's ratio. The P-wave and L-wave have similar velocities for Poisson's ratios up to about 0.2.

The energy-absorbing properties are normally determined by measuring the decreasing amplitudes of consecutive cycles or by relating the work performed to the energy dissipated in a given cycle. McNeill (1969) indicates that damping in thawed soil is around 5 percent and is often insignificant when compared to the damping in other foundation elements.

11.2 Methods of Measurement

Vinson (1978) describes five test methods from which the dynamic properties can be determined; they are:

1) Field Tests
   - Seismic Method
   - Cylindrical In Situ Test

2) Laboratory Tests
   - Ultrasonic Methods
   - Resonant-Frequency Method
   - Cyclic Triaxial Method

11.2.1 Seismic Method

The seismic method evolved out of geophysical exploration work. A compressional wave or shear wave is generated near the ground surface and the time required

for the wave to travel through the ground is monitored on seismographs placed at varying distances from the source, such that the wave velocities can be determined. This method is schematically shown in Figure 11.3 (Vinson, 1978). The waves are transmitted as either direct, reflected or refracted waves. Of these, the refracted waves are the most useful for determining velocities.

Once the compressional and shear wave velocities are measured, the dynamic stress-strain properties can be calculated from the following relationships:

$$G_d = \rho V_s^2 \qquad (11.1)$$

where

G_d denotes the dynamic shear modulus,

ρ denotes the mass density of the soil, and

V_s denotes the shear wave velocity.

$$\mu = 0.5\ (V_p^2-2V_s^2)/(V_p^2-V_s^2) \qquad (11.2)$$

where

μ denotes Poisson's Ratio, and

V_p denotes the shear wave velocity.

The dynamic Young's Modulus, E_d can then be calculated from the following equation:

$$E_d = 2(1+ \mu)G \qquad (11.3)$$

The seismic method does not provide sufficient data to permit the damping properties to be readily determined.

11.2.2 Cylindrical In Situ Test

The cylindrical in situ test is conducted by detonating a charge along the full length of a borehole, which sends a compression wave radially out from the borehole. The times for waves to reach geophones located in boreholes at various distances from the charged borehole are monitored, so that velocities can be determined. The test set-up is illustrated in Figure 11.4 (Vinson, 1978).

THURBER

Only the compressional wave velocity, V_p can be measured with this technique. Therefore, Poisson's Ratio must be known or estimated to calculate dynamic Young's Modulus from the following equation:

$$E_d = V_p^2 \rho \frac{(1+2\mu)(1+\mu)}{(1-\mu)} \qquad (11.4)$$

Damping can be determined from the cylindricial in situ test by relating the lower amplitudes measured at increasing distances from the borehole. The method is described by McNeill (1969). The response in a single seismograph would appear as shown in the upper half of Figure 11.5. The damping ratio can then be determined from the lower half of Figure 11.5 as follows:

$$D = \Delta/(4\pi^2 + \Delta^2)^{0.5} \qquad (11.5)$$

where

D denotes the damping ratio

Δ denotes the change in wave amplitude over one log decrement (log cycle).

This technique has not been used extensively in frozen ground, because it is expensive. The in situ cylinder test does, however, have promise as a field technique which allows the stress-strain properties, and energy absorbing properties to be evaluated.

11.2.3 Ultrasonic Methods

There are two ultrasonic methods for determining the dynamic properties of frozen ground in the laboratory. They are the pulse-transmission and critical angle methods. Both methods are schematically shown in Figure 11.6 (Vinson, 1978).

The pulse transmission technique is simple and commonly used. A compression or shear wave is driven into a sample at one end and the response is monitored at the other end in order to establish the P and S-wave velocities. The dynamic moduli and Poisson's ratio can be calculated using the equations given previously.

THURBER

In the critical angle method, a pulse is transmitted to a sample through a liquid bath. The sample can be rotated relative to the incident wave so that longitudinal waves and shear waves are transmitted through the sample. At two critical angles, only shear waves or only longitudinal waves are transmitted, these angles are characterized by minimum (zero) amplitudes of the alternate waves.

The dynamic shear modulus, G_d is then calculated from Equation 11.1. The dynamic Young's Modulus, E_d, is calculated from the following relationship.

$$E_d = \rho V_1^2 \qquad (11.6)$$

where

E_d denotes dynamic Young's Modulus,
ρ denotes mass density of the frozen soil, and
V_1 denotes longitudinal wave velocity.

11.2.4 Resonant-Frequency Method

In the resonant frequency method, also referred to as the sonic method, a sample is excited in a longitudinal or torsional mode and V_1 or V_s, respectively is determined from the frequency of resonance. A schematic of the test set up is shown in Figure 11.7 (Vinson, 1978). The computations associated with this technique are rather complex and are discussed in Vinson (1978) and Stevens (1975). The following parameters are determined:

V_1 - velocity of the L-wave,

V_s - velocity of the S-wave,

δ_1 - lag angle in the longitudinal mode,

δ_2 - lag angle in the torsional (shear) mode.

The lag angles, δ_1 and δ_2, are a measure of the energy-absorbing behaviour of the test specimen and are related to the damping ratio as follows:

$$D = \sin \frac{\delta}{2} \qquad (11.7)$$

THURBER

where

D denotes damping ratio

δ denotes phase lag

The complex dynamic stress-strain properties can be calculated from the following:

$$E^* = \frac{V_1^2 \rho}{1 + \tan^2(\delta_1/2)} \qquad (11.8)$$

$$G^* = \frac{V_s^2 \rho}{1 + \tan^2(\delta_s/2)} \qquad (11.9)$$

where

E^* denotes complex Young's Modulus,

G^* denotes complex shear modulus,

ρ denotes mass density of the soil specimen.

Vinson (1978) notes that E^* is approximately the same as E_d and G^* is approximately the same as G_d if the damping is low (which is generally the case for frozen soil).

11.2.5 Cyclic Triaxial Method

In cyclic triaxial tests, a cylindrical sample is placed in a triaxial cell and a specified confining pressure is applied. The deviator stress is then cycled so that the principal stress direction is rotated through 90° and the shear stresses are reversed over every half cycle of loading. A schematic of the test set-up is shown in Figure 11.8 (Vinson, 1978). The stress-strain behaviour is shown in Figure 11.9.

The dynamic Young's Modulus is readily determined from this method as follows:

$$E_d = \frac{\sigma_m}{\epsilon_m} \qquad (11.10)$$

THURBER

where

E_d denotes dynamic Young's Modulus,

σ_m denotes the maximum deviator stress ($\sigma_1 - \sigma_3$), and

ϵ_m denotes the maximum axial strain.

Young's Modulus is the only dynamic stress-strain property that can be easily measured in the cyclic triaxial test. Poisson's Ratio must be estimated in order to determine other dynamic stress-strain properties from cyclic triaxial data.

The damping ratio can be calculated from the test results from the following equation:

$$D = \frac{A_L}{4\ \pi A_T} \qquad (11.11)$$

where

D denotes the damping ratio,

A_L denotes the dissipated energy per cycle (hatched area on Figure 11.9), and

A_T denotes the work done per cycle (hatched area on Figure 11.9).

11.2.6 Summary of Relationships

A summary of the relationships between the various wave velocities and the dynamic stress-strain properties is presented on Figure 11.10.

11.2.7 Effect of Strain Amplitude

As might be expected the stress-strain properties measured using the various test procedures will be affected by the strain amplitude imposed by the method of measurement. It is therefore important that the strain amplitude used in the test correspond to the strain amplitude expected under field loading. Figure 11.11 shows the range strain amplitudes commonly used in the various test methods, in comparison to the range in strain amplitudes which occur due to dynamic loads in the field.

THURBER

The frequency of the dynamic test should also correspond to the frequency of the dynamic loading expected to occur in the field. In general, lower strain amplitudes are associated with higher frequencies.

11.3 Dynamic Properties of Ice

The dynamic properties of ice are considered separately from frozen soil because there exists both field and laboratory test data, which can be compared. The field data was obtained from seismic work on glaciers.

The dynamic stress-strain properties of ice are known to be a function of the following variables:

- tempertaure,
- strain amplitude,
- frequency, and
- confining pressure.

11.3.1 Temperature

The effect of temperature on the dynamic stress-strain and energy absorbing properties of ice for various test methods is shown in Figure 11.12 (Vinson, 1978). The effect of temperature is small. Wave velocities increase slightly at colder temperatures, while damping decreases slightly at colder temperature.

11.3.2 Strain or Stress Amplitude

No systematic studies into the effect of stress or strain amplitude on the dynamic properties of ice have been found in this review. Some limited testing has been conducted within the scope of their studies (Vinson and Chaichanavong, 1976 and Stevens, 1975). Most researchers agree that the amplitude and frequency of the test procedure should be selected so that it is comparable to the dynamic field loading.

11.3.3 Frequency

The effect of frequency on the dynamic stress-strain and energy-absorbing properties of ice is shown in Figure 11.13 (Vinson, 1978). There is a gap in the laboratory test data, however a trend of increasing wave velocity with increasing frequency is apparent. The effect appears to be more pronounced at lower frequencies (0.1 to 10 Hz) than at higher frequencies

THURBER

(1000 to 10,000 Hz). There is some indication, from cyclic triaxial testing, that damping decreases between about 0.1 and 1.0 Hz and increases slightly between 1.0 Hz and 10 Hz. No indication of the scatter in the data is provided, however, so it is not known how distinct this trend is.

11.3.4 Confining Pressure

The effect of confining pressure on the longitudinal wave velocity in ice is shown in Figure 11.14 (Vinson, 1978). These are results from cyclic triaxial tests. An increase in the longitudinal velocity with increasing confining pressure is indicated. The increase is most pronounced between 200 and 1000 kPa and at warm ice temperatures.

No clear relationship between confining pressure and the energy absorbing properties has been determined.

11.4 Dynamic Properties of Frozen Soil

Only limited field testing has been carried out to determine the dynamic properties of frozen soil. The field data that is available was obtained primarily from geophysical exploration surveys. A summary of compressional wave velocities obtained in the field is presented in Figure 11.16.

The influence of various parameters on the dynamic properties of frozen soil can only be examined on the basis of laboratory tests. Vinson (1978) compiled such a review, based largely on work carried out by CRREL. A summary of the soil characteristics for the soils discussed in the following sections is presented in Figures 11.17 and 11.18.

The dynamic stress-strain properties of frozen soils are known to be a function of the following variables:

- Temperature
- Strain Amplitude
- Frequency
- Confining Pressure
- Void Ratio
- Unfrozen Water Content
- Soil Type
- Unconfined Compressive Strength

THURBER

11.4.1 Temperature

The effect of temperature on the dynamic stress-strain and energy absorbing properties of frozen soil is shown in Figure 11.19. The longitudinal wave velocity for all soils is shown to increase significantly with decreasing temperature. The influence is most pronounced in the range from 0 to -5°C.

The influence of temperature on the energy-absorbing properties of frozen soils is shown in the lower half of Figure 11.19. Some soils exhibit a decrease in damping with decreasing temperature in the range of 0°C to -10°C, as might be expected. Other soils exhibit negligible sensitivity. The differing behaviour cannot be attributed to soil type because both coarse and fine-grained soils exhibit each type of behaviour. The test method would seen to be of most significance. The samples exhibiting a temperature dependence were tested using the cyclic triaxial method the other samples were tested using the resonant frequency method. Further investigation into these results should be considered.

Stevens (1975) tabulated values of complex dynamic Poisson's Ratio for different soils under various loading conditions, as shown in Figure 11.20. No temperature dependence is evident. Stevens cautions that the values may not be reliable because they have been indirectly calculated from the complex moduli, E* and G*, which themselves may have small inaccuracies. The Poisson's Ratios are presented here, however, because they provide an indication of typical values for Poisson's Ratio for frozen soils. This information can be used together with the longitudinal wave velocities to estimate other dynamic stress-strain moduli for frozen soil.

11.4.2 Strain Amplitude

The effect of strain amplitude on the dynamic properties of frozen soil is shown in Figure 11.21. Both the dynamic stress-strain properties and energy-absorbing properties exhibit no strain amplitude dependence below amplitudes of about 10^{-3} percent. Between amplitudes of 10^{-3} percent and 10^{-1} percent, wave velocities decrease and damping increases with increasing strain amplitude. The test method appears to affect these results. The soils tested with the resonant frequency method exhibited no dependence on strain

amplitude. On the other hand, the dynamic properties for those soils tested with the cyclic triaxial method are seen to vary with strain amplitude. Further study into this behaviour should be considered.

11.4.3 Frequency

The effect of frequency on the dynamic properties of frozen soil is shown in Figure 11.22. Although there is a gap in the available data between 10 Hz and 1000 Hz, some trends are evident. The wave velocities appear to increase gradually with increasing frequency. The energy absorbing properties appear to decrease with increasing frequency. The effect is most pronounced in the range of frequencies between 0.1 and 10.0 Hz, the range of frequencies corresponding to the cyclic triaxial method.

11.4.4 Confining Pressure

The effect of confining pressure on the dynamic properties of frozen soils is shown on Figure 11.23. The dynamic Young's modulus of coarse-grained soils is shown to increase with increasing confining pressure while the dynamic Young's Modulus of fine-grained soils appears to be independent of confining pressure. The energy-absorbing properties of all soils appear to have no dependence on confining pressure.

It should be noted that only limited data is available concerning the effect which confining pressure has on the dynamic stress-strain properties. The only laboratory test method that routinely uses confined samples is the cyclic triaxial method.

11.4.5 Void Ratio

The effect of void ratio on the dynamic properties of frozen soil is shown in Figure 11.24. The complex shear modulus, G*, decreases with increasing void ratio, approaching that of ice. The effect is most pronounced in the range of void ratios between 0.5 and 1.0, where soils lose intergranular contact.

As indicated on the lower half of Figure 11.24, no clear trends between void ratio and damping are indicated. It does appear that as the void ratio is increased to the point where the soil is oversaturated

with ice, the damping becomes quite insensitive to void ratio. The damping of frozen soil tends to be greater than that of ice.

11.4.6 Unfrozen Water Content

The degree of ice saturation and unfrozen water content are directly related by the following relationship:

$$S_{ice} = \frac{(w - w_u)\, G_s\, \gamma_w}{e\, \gamma_{ice}} \qquad (11.13)$$

where

S_{ice} denotes degree of ice saturation,

w denotes total moisture content,

w_u denotes unfrozen water content,

γ_w denotes the unit weight of water,

γ_{ice} denotes the unit weight of ice,

G_s denotes the specific gravity of the soil particles, and

e denotes the void ratio.

The effect of degree of ice saturation on the dynamic stress-strain properties is shown in Figure 11.25. The shear wave velocity of all soils increases with increasing ice saturation. The shear wave velocity of sand becomes relatively insensitive at degrees of ice saturation above about 40%, whereas the shear wave velocity of clay continues to increase at all levels of ice saturation. Conversely, it can be said that the wave velocities decrease with increasing unfrozen water content. It is expected that the dependency on degree of ice saturation (or unfrozen water content) will be more pronounced with the shear wave velocity than with the compressional or longitudinal wave velocities, because water does not transmit the shear waves.

King (1984) has determined that the compressional wave velocity can be directly related to the water filled porosity. He tested a variety of saturated soil

THURBER

samples from locations in the Canadian Arctic islands, the Beaufort Sea, and the Mackenzie River valley. The data is shown in Figure 11.26.

It is known that increasing salinity increases the unfrozen water content in a frozen soil. A corresponding decrease in wave velocity would be expected. This was investigated and confirmed by Baker and Kurfurst (1985). The results are shown in Figure 11.27.

Although quantitative relationships have not been found, Vinson (1978) suggests that damping decreases with increasing ice content, up to saturation.

11.4.7 Soil Type

The effect of soil type on the dynamic properties of frozen soils can be inferred from the figures presented in the previous discussions in this section. Coarse-grained soils have higher dynamic stress-strain properties than fine-grained soils. This is evident in Figure 11.28 (Vinson, 1978), where a linear relationship between the modulus or velocity and the logarithm of D_{50} is shown.

No clear relationship between soil type or grain size distribution and energy-absorbing properties has been established.

11.4.8 Unconfined Compressive Strength

Stevens (1975), presents an interesting correlation between maximum compressive strength and complex Young's Modulus. The relationship appears to be linear for a range of soil types, as shown in Figure 11.29. This data suggests that the maximum compressive strength may be used to provide a preliminary estimate of dynamic modulus values.

11.5 Summary

The variables which influence the dynamic properties of frozen soil have been identified. A qualitative summary of the significance of the effect which different variables have on the dynamic stress-strain and energy absorbing properties of ice and frozen soils is presented on Figure 11.30.

THURBER

SECTION 11

DYNAMIC PROPERTIES
LIST OF REFERENCES

Baker, T.H.W., and Kurfurst, P.J., 1985. Acoustic and mechanical properties of frozen sand. Proceedings of the Fourth International Symposium on Ground Freezing. Sapporo, Japan, August 5-7, pp. 227-234.

Barnes, D.F., 1963. Geophysical methods for delineating Permafrost, Proc. 1st Int. Conf. Permafrost, Lafayette, Ind., NAS-NRC Publ. 1287, pp. 349-355.

Bell, R.A.I., 1966. A seismic Reconnaissance of the McMurdo Sound region, Antarctica, J. Glaciol., Vol. 6, pp. 209-221.

Bennett, H.F., 1972. Measurements of ultrasonic wave velocities in ice cores from Greenland and Antarctica, U.S. Army Cold Region Res. Eng. Lab. Res. Rep. 237, Hanover, NH, June.

Chaichanavong, T. 1976. Dynamic properties of ice and frozen clay under cyclic triaxial loading conditions, unpublished Ph.D. thesis, Michigan State University, East Lansing.

Czajkowski, R.L., 1977. The dynamic properties of frozen soils under cyclic triaxial loading conditions, unpublished M.S. thesis, Michigan State University, East Lansing.

Hobson, G.D., 1962. Seismic exploration in the Canadian Arctic Islands, Geophysics, Vol. 27, pp. 253-273.

Hunter, J.A., 1974. Seismic velocity measurements in permafrost, Fox Tunnel, Fairbanks, Alaska, Geol. Surv. Can. Pap. 74-1, pt. B, pp. 89-90.

Kaplar, C.W., 1969. Laboratory determination of dynamic moduli of frozen soils and of ice, U.S. Army Cold Reg. Res. Eng. Lab. Res. Rep. 163, Hanover, NH.

King, M.S., 1984. The influence of clay-sized particles on seismic velocity for Canadian Arctic permafrost. Canadian Journal of Earth Sciences, Vol. 21, pp. 19-24.

THURBER

King, M.S., Bamford, T.S., and Kurfurst, P.J., 1974. Ultrasonic velocity measurements on frozen rocks and soils, proc. Symp. Permafrost Geophys., Calgary, pp. 35-42.

Kohnen, H., and Bentley, C.R., 1973. Seismic refraction and reflection measurements at Byrd Station, Antarctica. J. Glaciol., Vol. 12, pp. 101-111.

Kolsky, H., 1963. Stress waves in solids. Dover Publications Inc., New York, U.S.A.

Kurfurst, P.J., and Pullan, S., 1985. Field and laboratory measurements of seismic and mechanical properties of frozen ground. in Proceedings of the Fourth International Symposium on Ground Freezing. Sapporo, Japan, August 5-7, pp. 255-262.

McGinnis, L.D., Nakao, K., and Clark, C.C., 1973. Geophysical identification of frozen and unfrozen ground, North Am. Contrib. 2d Int. Conf. Permafrost, Yakutsk, U.S.S.R., National Academy of Science, Washington, pp. 136-146.

McNeill, R.L., 1969. Machine foundations: the state-of-the-art. in Proceedings of Specialty Session 2, Seventh International conference on Soil Mechanics and Foundation Engineering. Mexico, pp. 67-100.

Nakano, Y., Martin, R.J., and Smith, M., 1972. Ultrasonic velocities of the dilational and shear waves in frozen soils, J. Water Resour. Res. Vol. 8, pp. 1024-1030.

Robin, G. de Q., 1958. Seismic shooting and related investigations, Glaciology III, Norw.-Br. Swed, Antarct. Exped. 1949-52, Sci. Res., Vol. 5, pp. 48-80.

Roethlisberger, H., 1961. Applicability of seismic refraction soundings in permafrost near Thule, Greenland, U.S. Army cold Region. Res., Eng. Lab. Tech. Rep. 81, Hanover, NH.

THURBER

Roethlisberger, H., 1972. Seismic exploration in cold regions, U.S. Army Cold Reg. Res. Eng. Lab. Techn. Monogr. II-A2a, Hanover, NH.

Sartoelli, A.N., Pesowski, M.S., Henderson, J.D., Fenton, M.M. and Green, D.H., 1986. Compression and shear wave methods applied to the recognition of glaciotectonic deformation. in Geotechnical Stability in Surface Mining. edited by R.K. Singhal, A.A. Balkema, Boston, Mass., U.S.A., pp. 235-244.

Smith, N. 1969. Determining the dynamic properties of snow and ice by forced vibration, U.S. Army Cold Reg. Res. Eng. lab. Tech. Rep. 216, Hanover, NH.

Stevens, H.W., 1975. The response of frozen soils to vibratory loads, U.S. Army Cold Reg. Res. Eng. Lab. Techn. Rep. 265, Hanover, NH.

Vinson, T.S., 1978. Response of frozen ground to dynamic loading. Chapter 8 in Andersland, O.B., and Anderson, D.M. (Editors), Geotechnical Engineering for Cold Regions. McGraw-Hill, pp. 405-458.

Vinson, T.S., and Chaichanavong, T.. 1976. Dynamic properties of ice and frozen clay under cyclic triaxial loading conditions. Mich. State. Univ. Div. Eng. Res. Rep. MSU-CE-76-4.

Vinson, T.S., Czajkowski, R., and Ki, J., 1977. Dynamic properties of frozen cohesionless soils under cyclic triaxial loading conditions, Mich. State Univ. Div. Eng. Res. Rep. MSU-CE-77-1.

Woolson, J.R., 1963. Seismic and Gravity Surveys of Naval Petroleum Reserve No. 4 and Adjoining Areas, Alaska, U.S. Geol. Surv. Prof. Pap. 304-A.

THURBER

SECTION 11

DYNAMIC PROPERTIES
LIST OF FIGURES

THURBER

DYNAMIC PROPERTIES
LIST OF FIGURES
(continued)

THURBER

THURBER

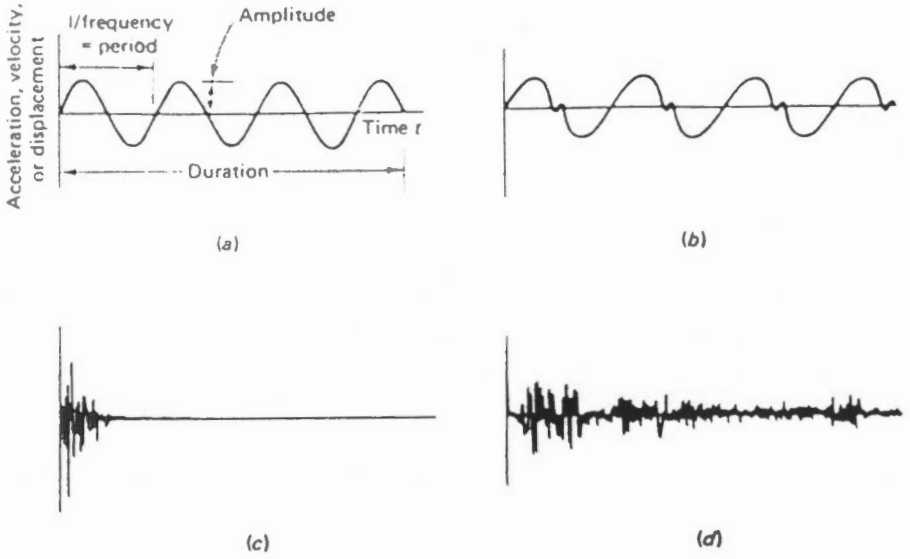

Dynamic-loading motion characteristics: (a) harmonic, periodic, vibrating machinery; (b) nonharmonic, periodic, vibrating machinery; (c) transient blasting, geophysical exploration; (d) irregular, earthquake (Vinson, 1978).

FIGURE 11.1

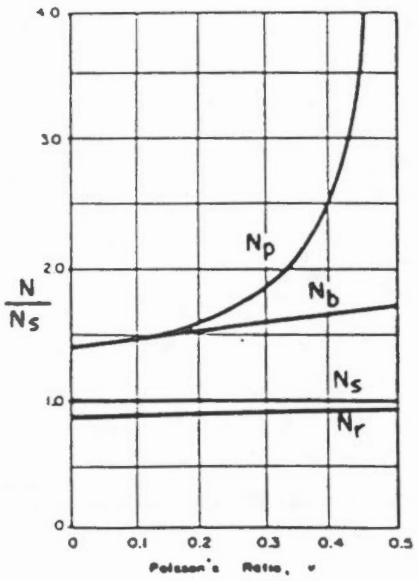

Relationship between wave velocities (after McNeill, 1969).

FIGURE 11.2

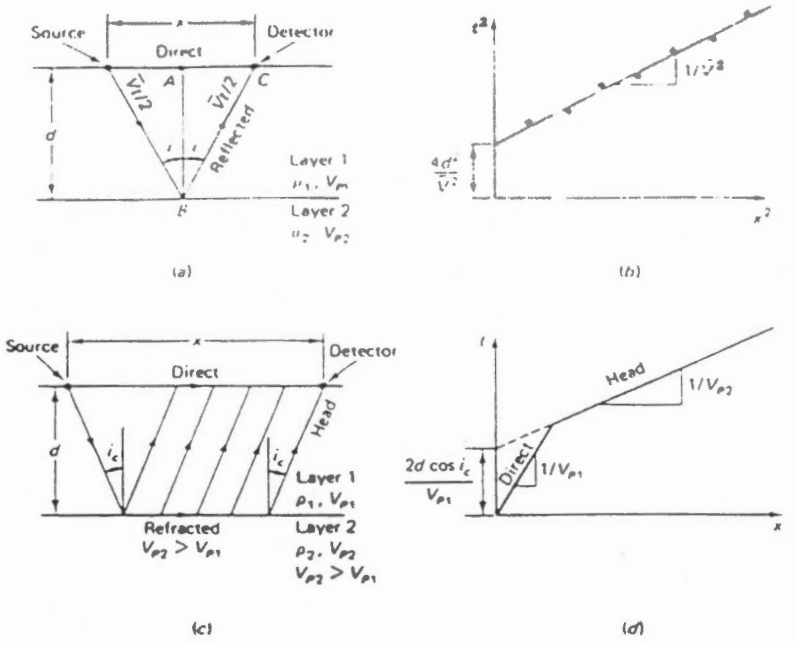

Seismic methods of determining wave velocities: (a) reflection survey; (b) t^2 vs. x^2; (c) refraction survey; (d) travel time vs. distance (Vinson, 1978).

FIGURE 11.3

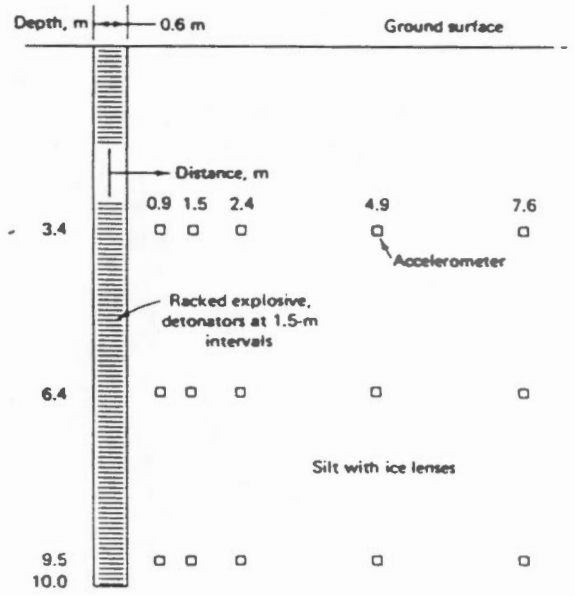

Configuration for cylindrical in situ test (Vinson, 1978).

FIGURE 11.4

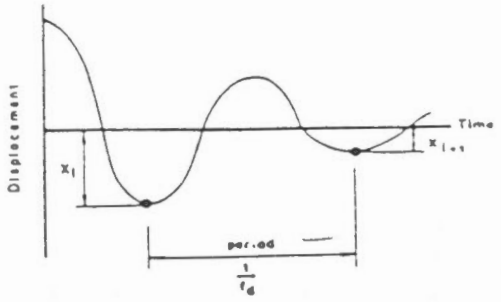

x_i = Amplitude of one cycle

$x_i + 1$ = Amplitude of next cycle

f_d = Damped natural frequency

Oscillation to Rest

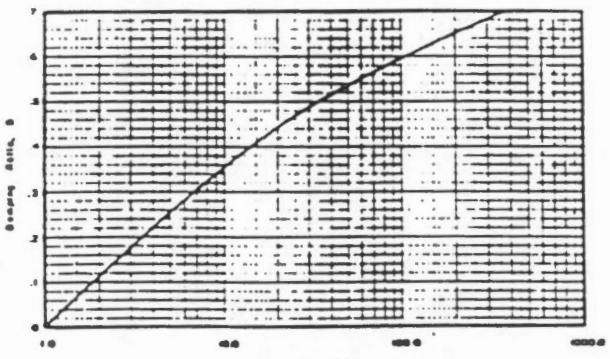

$$\text{RATIO} = \frac{x_i}{x_i + 1}$$

Estimate of Damping from Succeeding Oscillations

Determination of damping ratio (McNeill, 1969).

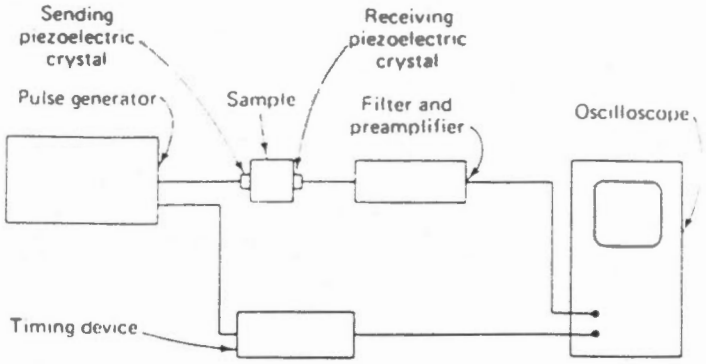

(a)

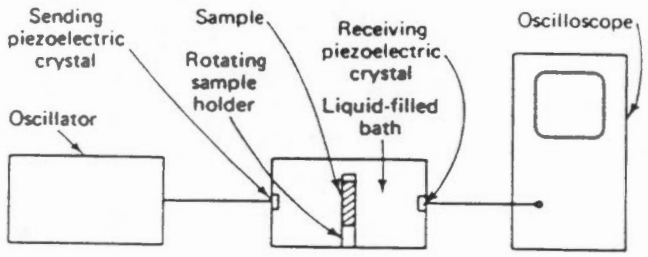

(b)

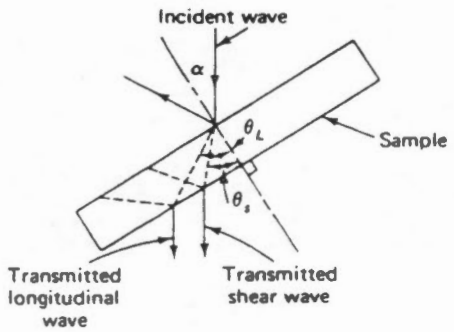

(c)

Schematic diagram of ultrasonic test equipment: (a) pulse-transmission method; (b) critical angle method; (c) wave transmission through parallel plate (Vinson, 1978).

FIGURE 11.6

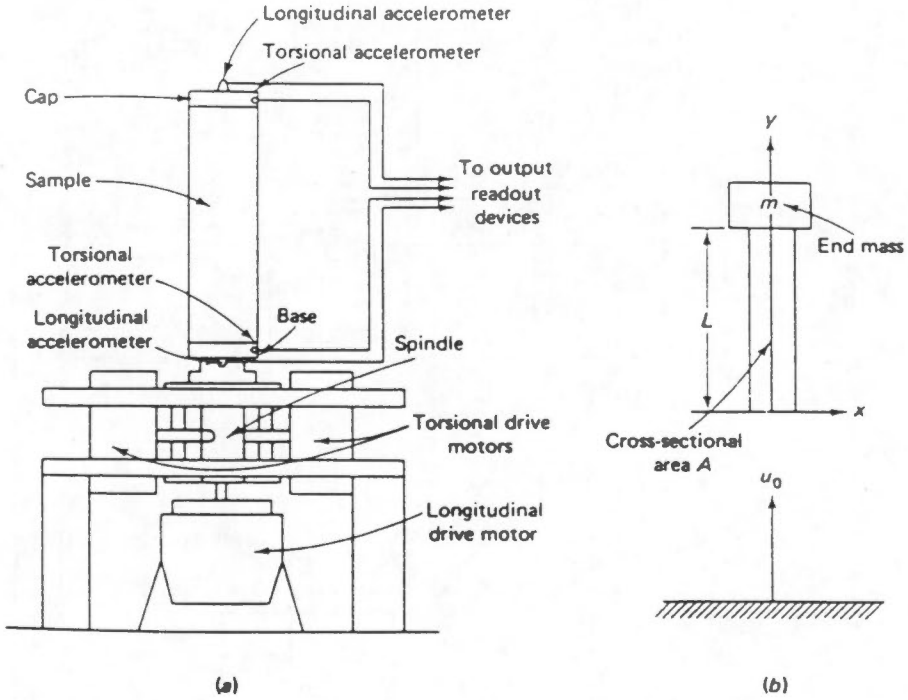

Resonant-frequency test equipment: (a) schematic of resonant-column-test equipment; (b) mathematical representation of resonant-column test (Vinson, 1978).

FIGURE 11.7

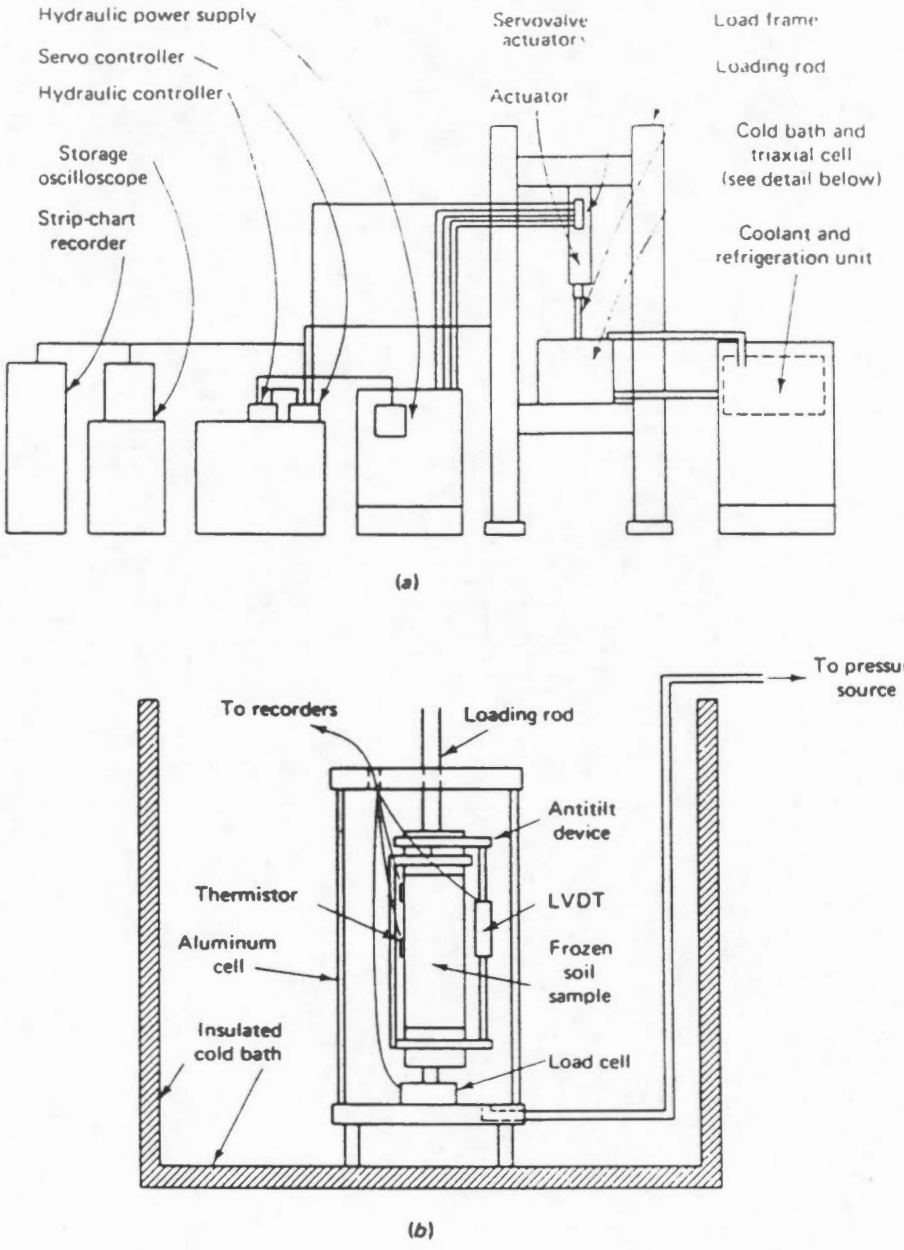

Cyclic triaxial test equipment: (a) schematic of cyclic triaxial test system; (b) triaxial cell inside cold bath (Vinson, 1978).

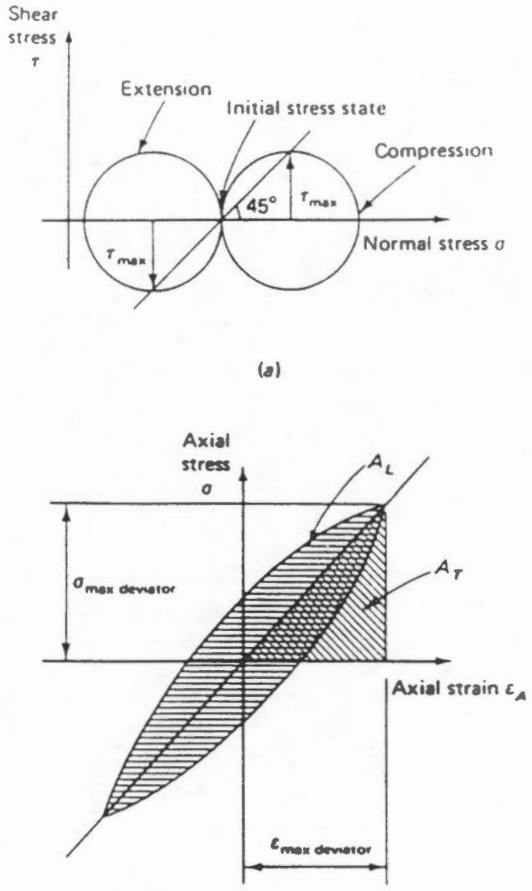

Stress state and stress vs. strain for cyclic triaxial test: (a) Mohr's-circle representation of cyclic stress states; (b) stress vs. strain for one load cycle (Vinson, 1978).

THURBER

FIGURE 11.9

Dynamic stress-strain properties

Given	To calculate: Dynamic or complex Young's modulus E or E^*†	Dynamic or complex shear modulus G or G^*†	Poisson's ratio μ or μ^*†	Compression-wave velocity V_p	Shear-wave velocity V_s	Longitudinal-wave velocity V_L
E, ρ, μ	E	$\frac{E}{2(1+\mu)}$	μ	$\left[\frac{E}{\rho}\frac{1-\mu}{(1+\mu)(1-2\mu)}\right]^{1/2}$	...	$\left(\frac{E}{\rho}\right)^{1/2}$
G, μ, ρ	$2(1+\mu)G$	G	μ	$\left[\frac{(1-\mu)2G}{(1-2\mu)\rho}\right]^{1/2}$	$\left(\frac{G}{\rho}\right)^{1/2}$	
E, G	E	G	$\frac{E}{2G}-1$	...	$\left(\frac{G}{\rho}\right)^{1/2}$	$\left(\frac{E}{\rho}\right)^{1/2}$
ρ, μ, V_p	$\frac{V_p^2\rho(1-2\mu)(1+\mu)}{1-\mu}$	$\frac{(1-2\mu)\rho V_p^2}{2(1-\mu)}$	μ	V_p	$V_p\left[\frac{1-2\mu}{2(1-\mu)}\right]^{1/2}$	$V_p\left[\frac{(1+\mu)(1-2\mu)}{1-\mu}\right]^{1/2}$
ρ, μ, V_s	$2\rho(1+\mu)V_s^2$	ρV_s^2	μ	$V_s\left[\frac{2(1-\mu)}{1-2\mu}\right]^{1/2}$	V_s	$V_s[2(1+\mu)]^{1/2}$
ρ, V_p, V_s	$\frac{V_s^2(3V_p^2-4V_s^2)\rho}{V_p^2-V_s^2}$	ρV_s^2	$\frac{1}{2}\frac{V_p^2-2V_s^2}{V_p^2-V_s^2}$	V_p	V_s	

Energy-absorbing properties‡

Given	To calculate: Damping ratio D	Loss factor $\tan\delta$	Quality factor Q
Phase lag δ	$\sin\frac{\delta}{2}$	$\tan\delta$	$\frac{1}{\tan\delta}$
Attenuation coefficient a and wavelength λ			
	$\sin\frac{\tan^{-1}(a\lambda/2\pi)}{2}$	$a\frac{\lambda}{2\pi}$	$\frac{2\pi}{a\lambda}$
Damping coefficient β and angular frequency ω			
	$\sin\frac{\tan^{-1}(2\beta/\omega)}{2}$	$\frac{2\beta}{\omega}$	$\frac{\omega}{2\beta}$
Log decrement Δ	$\left(\frac{\Delta^2}{4\pi^2+\Delta^2}\right)^{1/2}$	$\tan 2\left[\sin^{-1}\left(\frac{\Delta^2}{4\pi^2+\Delta^2}\right)^{1/2}\right]$	$\frac{\pi}{\Delta}$

† Complex moduli are not significantly different from elastic moduli for materials with low damping.
‡ Conversion equations for materials with low damping.

Summary of theoretical relationships between dynamic properties (Vinson, 1978).

THURBER

FIGURE 11.10

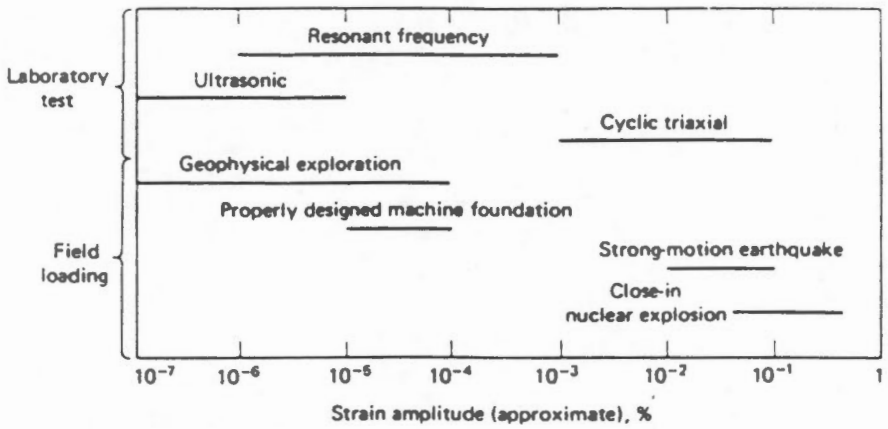

Relationship between laboratory and field strain amplitudes of loading (Vinson, 1978).

THURBER

FIGURE 11.11

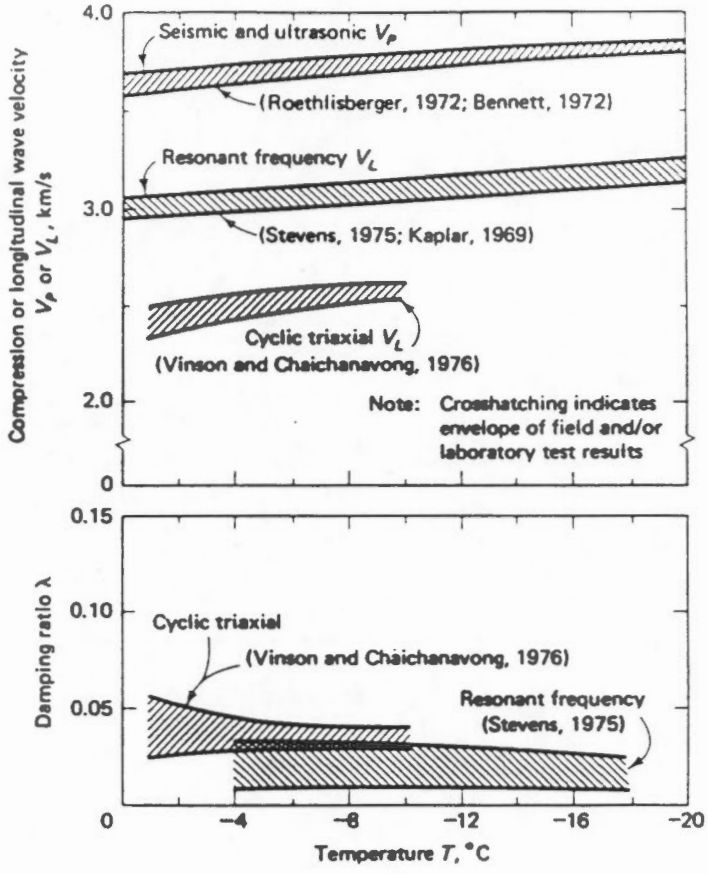

The effect of temperature on the dynamic properties of ice (Vinson, 1978).

THURBER

FIGURE 11.12

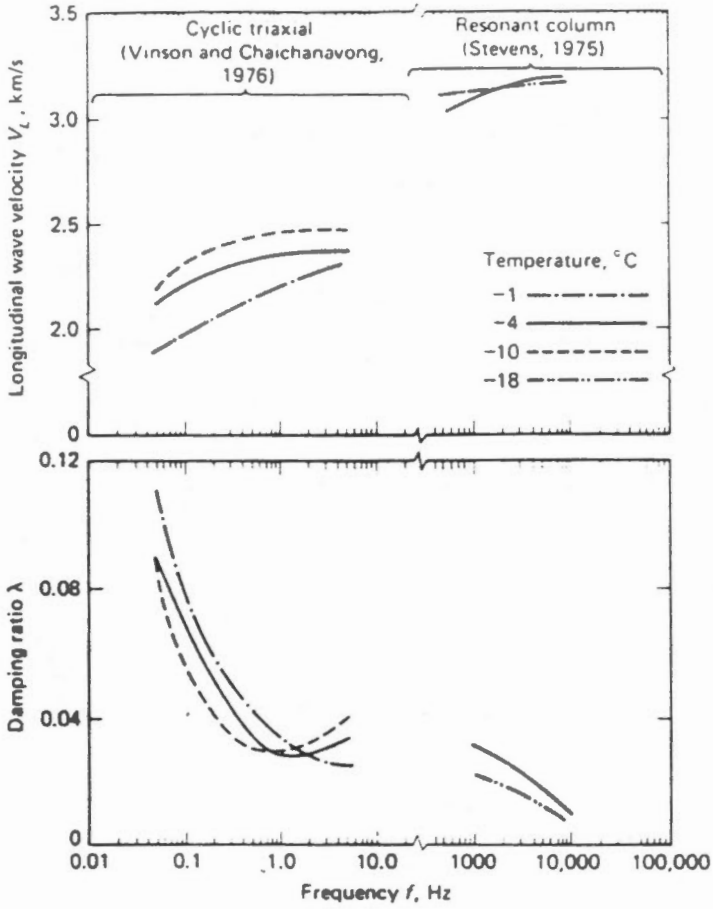

The effect of frequency on the dynamic properties of ice (Vinson, 1978).

FIGURE 11.13

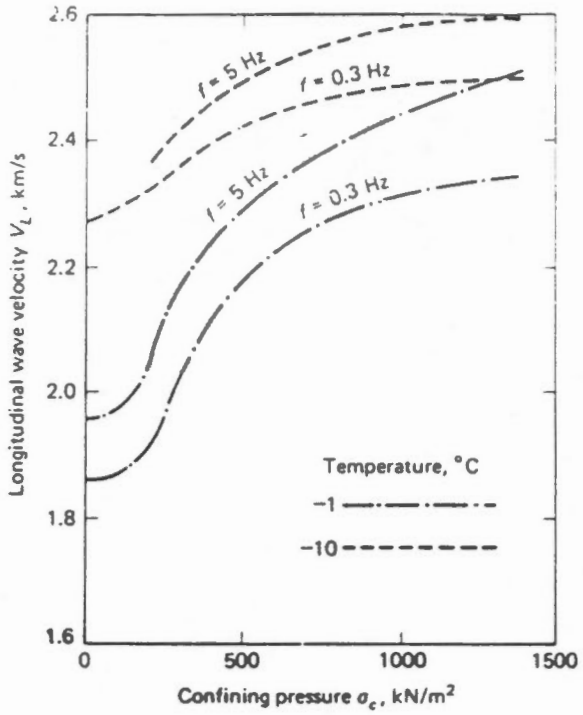

The effect of confining pressure on the longitudinal wave velocity of ice (Vinson, 1978).

FIGURE 11.14

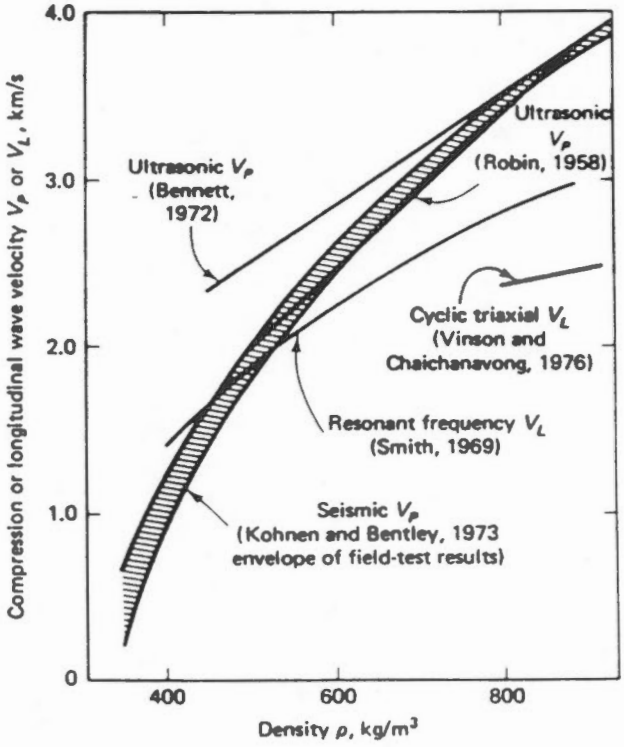

The effect of density on the wave velocity of ice (Vinson, 1978).

FIGURE 11.15

Soil type	Locality	Compression-wave velocity, km/s		Estimated ground temperature, C	Ref
		Frozen	Unfrozen		
Coarse-grained					
Floodplain alluvium	Fairbanks area, Alas.	2.4-4.3	1.9-2.1	-1	Barnes (1963)
Gravel	Fairbanks area, Alas.	4.0-4.6	1.8-2.3	-1	Barnes (1963)
Glacier moraine	Delta Junction, Alas.	2.3-4.0		-2	Barnes (1963)
Aeolian sand	Tetlin Junction, Alas.	2.4		-3	Barnes (1963)
Outwash gravel	Tanacross, Alas.	2.3-3.0		-3	Barnes (1963)
Glacier outwash	Thule, Greenland	4.5-4.7		-11	Roethlisberger (1961)
Glacier till	Thule, Greenland	4.7-4.8		-11	Roethlisberger (1961)
	McMurdo Sound, Antarctica	3.0-4.3	0.5-1.5	-20	Bell (1966)
Till	Norman Wells, N.W.T.	2.2-3.6	...	...	King et al. (1974)
Frozen ground	Lake Fryxell, Lake Vanda, Lake Bonney, Antartica	3.8-4.5	...	...	McGinnis et al. (1973)
Sand and clay	Norman Wells, N.W.T.	3.1-3.4	...	...	King et al. (1974)
Saturated sand	...	3.2-4.0	...	...	Hunter (1973)
Water-saturated gravel	...	3.6-4.0	...	...	Hunter (1973)
Gravel	Klondike area, Yukon	5.5	...	...	Hobson (1966)
Outwash with relatively thick ice lenses	Lake Vida, Antartica	5.7-5.9	...	...	McGinnis et al. (1973)
Outwash	Meirs Valley, Antarctica	3.6-4.0	...	...	Bell (1966)
Fine-grained:					
Silt and gravel	Fairbanks area, Alas.	2.3-3.0	...	-1	Barnes (1963)
Silt and organic matter	Fairbanks area, Alas.	1.5-3.0	0.6-1.2	-1	Barnes (1963)
Silt with ice lenses	Eielson Airforce Base, Alas.	2.0-2.8	...	-1.5	Blouin (1976)
Alluvial clay	Northway, Alas.	2.4	...	-2	Barnes (1963)
Silt	Glen Creek valley, Alas.	2.7-3.3	...	-4.2	Hunter (1974)
Tundra silts, sands, and peats:					
Gubik Formation, probably saline	Barrow area NPR-4, Alas.	2.4-2.7	...	-9	Woolson (1963)
	Skull Cliff area, NPR-4, Alas.	2.3-2.7	...	-9	Woolson (1963)
Gubik Formation, less saline	Topagoruk area, NPR-4, Alas.	2.4-3.7	...	-9	Woolson (1963)
Unclassified sediments	Isachsen, N.W.T.	2.7	...	-10	Hobson (1962)
Silt and Clay	Norman Wells, N.W.T.	3.1	...	...	King et al. (1974)
Clay	...	1.5-2.1	...	...	Hunter (1973)
	Norman Wells, N.W.T.	2.5-2.8	...	...	King et al. (1974)
Ice-saturated silts	...	1.8-3.1	...	...	Hunter (1973)
Silt and Clay	Beaufort Sea, N.W.T.	1.4-2.1	...	-1	Kurfurst and Pullan (1985)

† Cylindrical in situ test result.
‡ Northern Petroleum Reserve.

Compression-wave velocities of frozen soil from seismic surveys (Vinson, 1978).

Soil name	Unified Soil Classification group symbol	Coefficient of uniformity C_u	Coefficient of curvature C_c	Atterberg limits w_L w_p I_p	Sp gr	Soil legend[f]	Degree of ice saturation S_i, %	Void ratio e	Test frequency, Hz	Strain amplitude ϵ_a, %	Poisson's ratio μ	Density, kg/m³	Confining pressure kN/m²	Source[a]
Coarse-grained														
Peabody gravelly sand	SP	10 7	0 7	Nonplastic	2.72	PGS	83[b]	0 48[b]	7100	...	0 28	2100	0	1
McNamara concrete sand	SP	5 4	0 8	Nonplastic	2.72	MCS	85[b]	0.48[b]	6300	...	0 23	2110	0	1
East Boston till	SC	220	5 9	21 14 7	2.76	EBT	80[b]	0 34[b]	5700	...	0.28	2260	0	1
Mixture McNamara concrete sand and East Boston till	SM	220	5 9	Nonplastic	2.72	CEB	99[b]	0.37[b]	6200[b]	...	0.36	2250	0	1
Mixture Manchester fine sand and East Boston till	SM	57	9 6	Nonplastic	2.72	MEB	87[b]	0 45[b]	6500[b]	...	0 31	2140	0	1
20/30 Ottawa sand	SP	1 1	1 1	Nonplastic	2.65	OS	100	0.38	10^{6}	...	0 25	2190	0	2
							99[b]	0 54[b]	5000	$2^{b} \times 10^{-3}$	0 30[b]	2070	0	3
							100	0 49	0.3	10^{-2}	...	2000	345	4
						OSL	100	3 73	0.3	10^{-2}	...	1290	345	4
Thetford till	SW	25 8	1 0	Nonplastic	2.64	TT	93	0 80[b]	5000	4×10^{-3}	...	1880	0	
Fine-grained														
Alaska silt	ML	[c]	[c]	Nonplastic	2.70	AS	100	0 59	0.3	10^{-2}	...	2090	345	5
New Hampshire silt	CL-ML	[c]	[c]	26 21 5	2.70	NHS	93[b]	1 05[b]	5400[b]	...	0 28	1790	0	1
Yukon silt	CL-ML	[c]	[c]	28 19 9	2.73	YS	99[b]	0 60[b]	5100	...	0 39	2080	0	1
Boston blue clay	CL	[c]	[c]	47 20 27	2.81	BBC	96[b]	1 87[b]	4800[b]	...	0 44	1600	0	1
Fargo clay	CH	[c]	[c]	68 22 46	2.76	FC	92[b]	1 13[b]	2700[b]	...	0.38	1780	0	1
Fairbanks silt	ML-OL	[c]	[c]	28 24 4	2.69	FS	99[b]	0 68[b]	5500[b]	...	0 28	2000	0	1
Hanover silt	ML	[c]	[c]	Nonplastic	2.74	HS					0 18[d]			
							100	1.10	10^{6}	...	0 28[e]	1830	0	2
							100	0 60	0.3	10^{-2}	...	2030	345	3
											0.15[e]			
Gosnold clay	CL	[c]	[c]	41 23 18	2.82	GC	100	1.28	10^{6}	...	0.28[e]	1810	0	2
							97	0 83	5000	$1^{b} \times 10^{-6}$	0.39	1980	0	3
Manchester silt	ML	[c]	[c]	Nonplastic	2.73	MS	96	0.73	5000	$3^{b} \times 10^{-5}$	0.27	1980	0	3
Suffield clay	CL	[c]	[c]	45 24 21	2.69	SC	100	0 51	5000	$1^{b} \times 10^{-6}$	...	2120	0	3
Ontonagon clay	CH	[c]	[c]	61 24 37	2.74	OC	100	1 50	0 3	10^{-2}	...	1620	345	6
Mixture Ontonagon and sodium montmorillonite clay	CH	[c]	[c]	98 37 61	2.74	OMC	100	1.56	0 3	10^{-2}	...	1660	345	6

[a] 1 = Kaplar (1969); 2 = Nakano, Martin, and Smith, (1972); 3 = Stevens (1975); 4 = Vinson, Czaikowski, and Li, (1977); 5 = Czaikowski (1977); 6 = Chaichanavong (1976).

[b] Average value

[c] Not applicable

[d] At - 2°C.

[e] At - 4 to - 14°C.

[f] Letter appended to soil legend in Figs. 8.15 to 8.19 and 8.22 indicates source (K = source 1, N = source 2, S = source 3, V = sources 4–6).

Summary of soil characteristics of frozen soil samples tested in the laboratory (Vinson, 1978).

THURBER

FIGURE 11.17

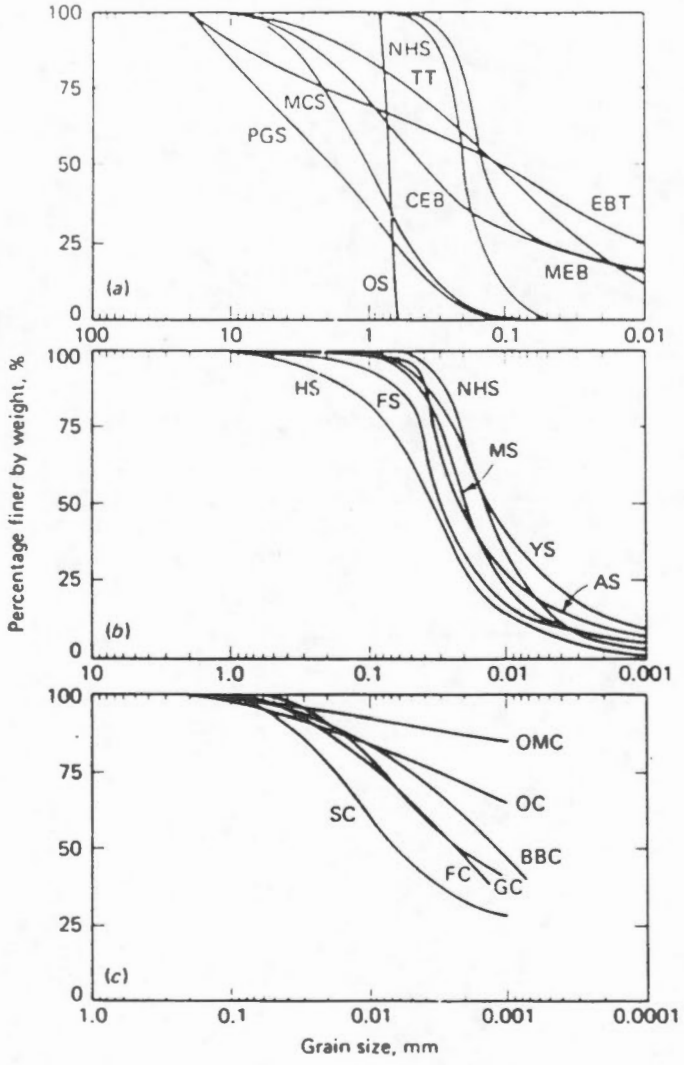

Summary of gradations of frozen soil samples tested in the laboratory (Vinson, 1978).

THURBER

FIGURE 11.18

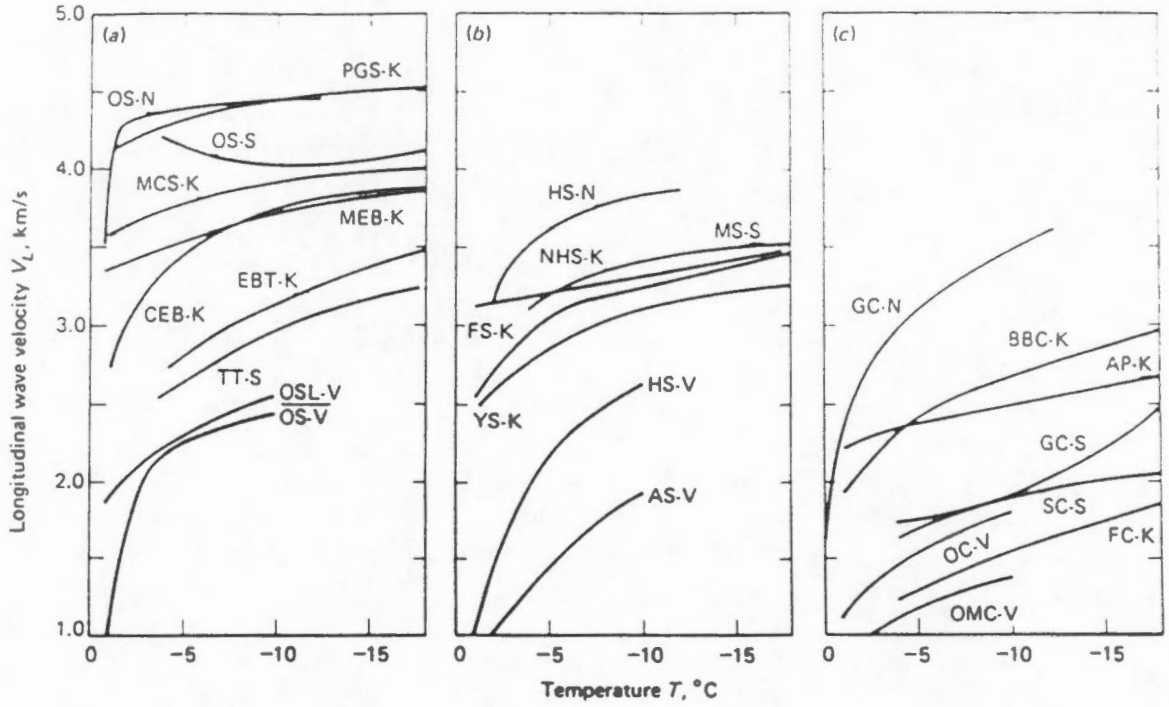

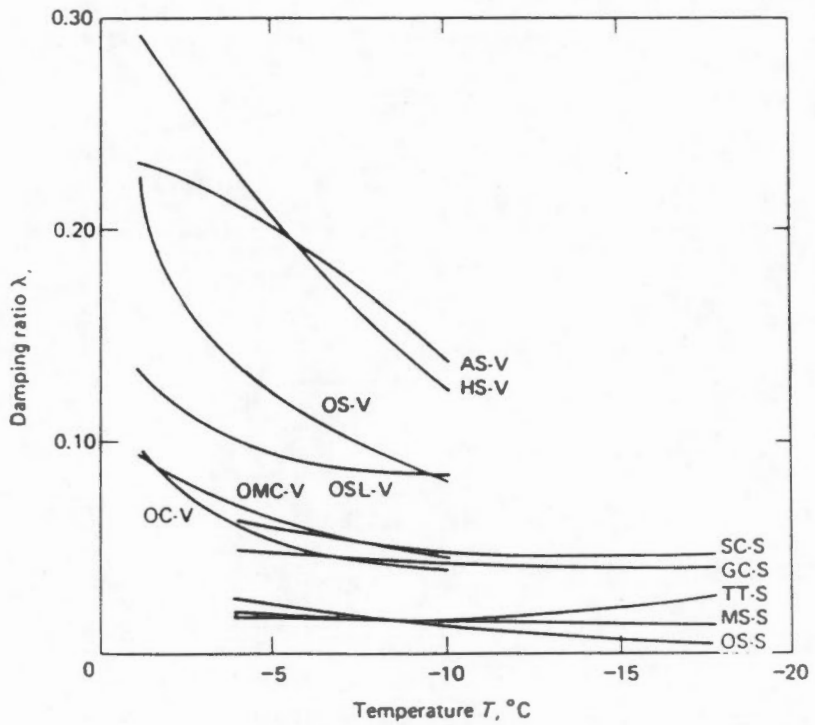

The effect of temperature on the dynamic properties of frozen soil (Vinson, 1978).

THURBER

FIGURE 11.19

Table V. Poisson's ratio for several soils.

Frequency, Hz	Temperature +25°F	+15°F	0°F
20-30 Ottawa sand			
σ_d = 0.1 psi			
1000	0.25	0.34	0.28
5000	0.28	0.38	0.26
10000	0.33	0.33	0.28
σ_d = 1.0 psi			
1000	0.25	0.34	0.28
5000	0.28	0.37	0.25
10000	0.32	0.36	0.35
σ_d = 5.0 psi			
1000	0.28	0.30	0.27
5000	0.29	0.38	0.25
10000	0.27	0.34	0.24
Manchester silt			
σ_d = 0.1 psi			
1000	0.25	0.27	0.25
5000	0.27	0.26	0.22
10000	0.30	0.29	0.26
σ_d = 1.0 psi			
1000	0.25	0.28	0.25
5000	0.29	0.27	0.24
10000	0.30	0.29	0.22
σ_d = 5.0 psi			
1000	0.26	0.29	0.24
5000	0.30	0.31	0.23
10000	0.30	0.29	0.21
Goodrich clay			
σ_d = 0.1 psi			
1000	0.72	0.35	0.51
5000	0.54	0.38	0.36
10000	0.52	0.40	0.32
σ_d = 1.0 psi			
1000	0.59	0.37	0.47
5000	0.52	0.40	0.34
10000	0.47	0.41	0.32
σ_d = 5.0 psi			
1000	0.58	0.40	0.46
5000	0.47	0.42	0.32
10000	0.42	0.43	0.32

Summary of Poisson's Ratio for several soils under various loading conditions (Stevens, 1975).

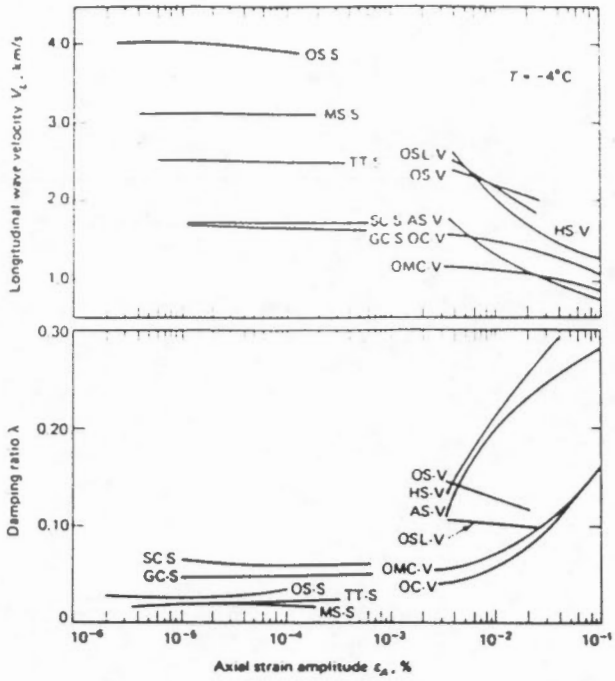

The effect of strain amplitude on the dynamic properties of frozen soil (Vinson, 1978).

FIGURE 11.21

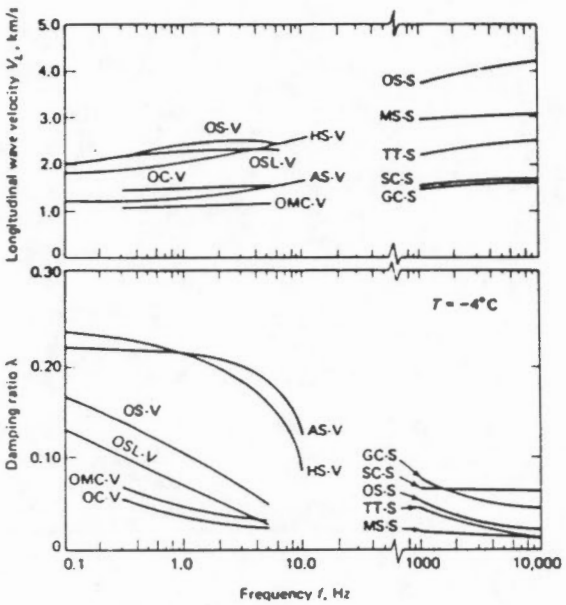

The effect of frequency on the dynamic properties of frozen soil (Vinson, 1978).

FIGURE 11.22

THURBER

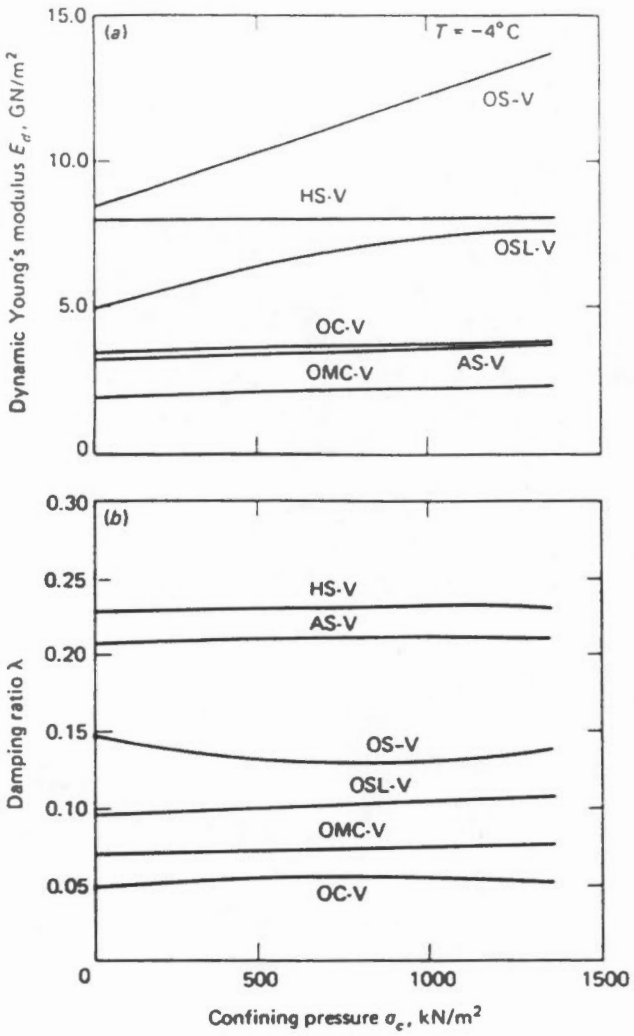

The effect of confining pressure on the dynamic properties of frozen soil (Vinson, 1978).

FIGURE 11.23

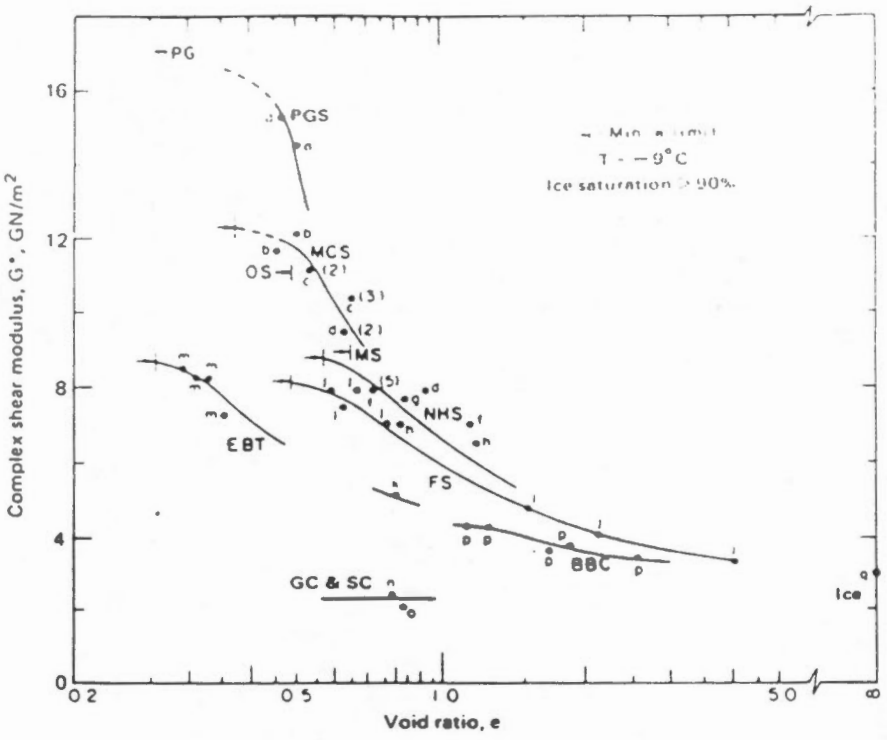

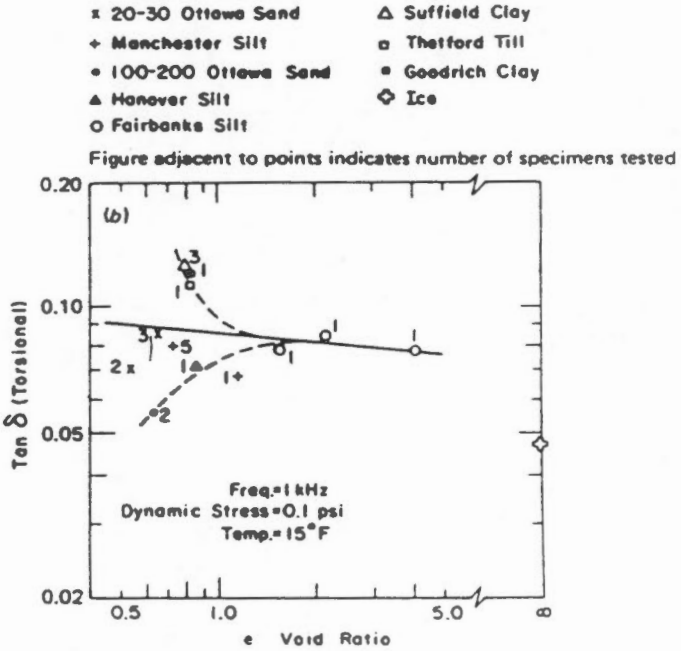

The effect of void ratio on the dynamic properties of frozen soil (Vinson, 1978).

FIGURE 11.24

Curve	Frozen soils	f kHz	Temp °F
A	Suffield clay	1	15
B	Manchester silt	1	25
C	20-30 Ottawa sand	1000	14

Point	Non-frozen soils σ_0 = 5 psi	Water content	e
A′	Suffield clay	12.7	0.94
B′	Manchester silt	18.3	0.80
C′	20-30 Ottawa sand	Dry	0.50

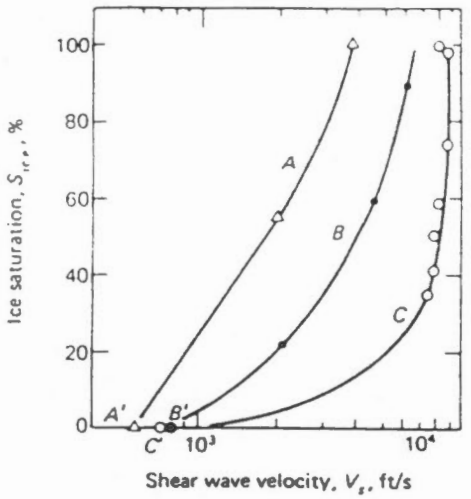

The effect of ice saturation on the shear wave velocity of frozen soil (Vinson, 1978; after Stevens, 1975).

FIGURE 11.25

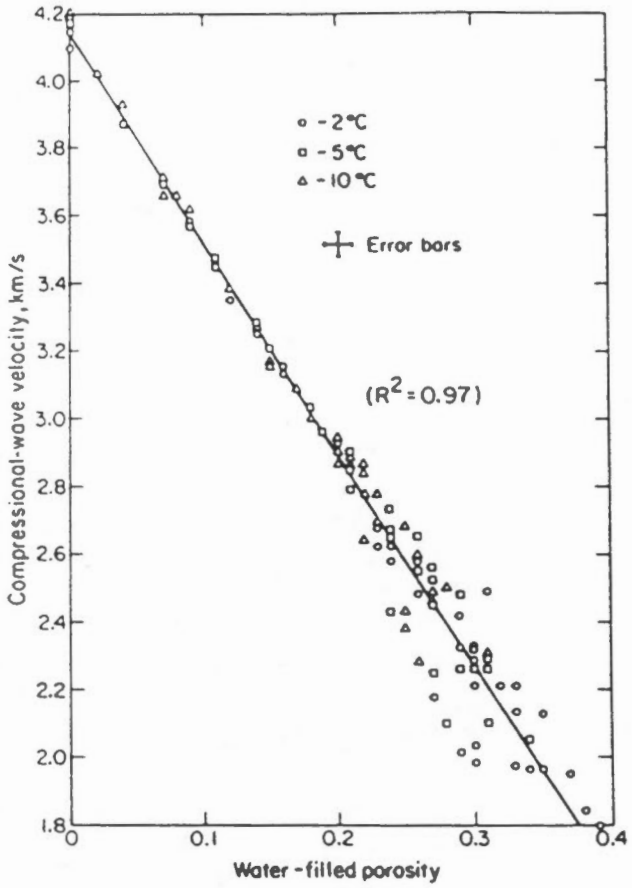

The effect of water-filled porosity on the compressional wave velocity of frozen soil (King, 1984).

FIGURE 11.26

THURBER

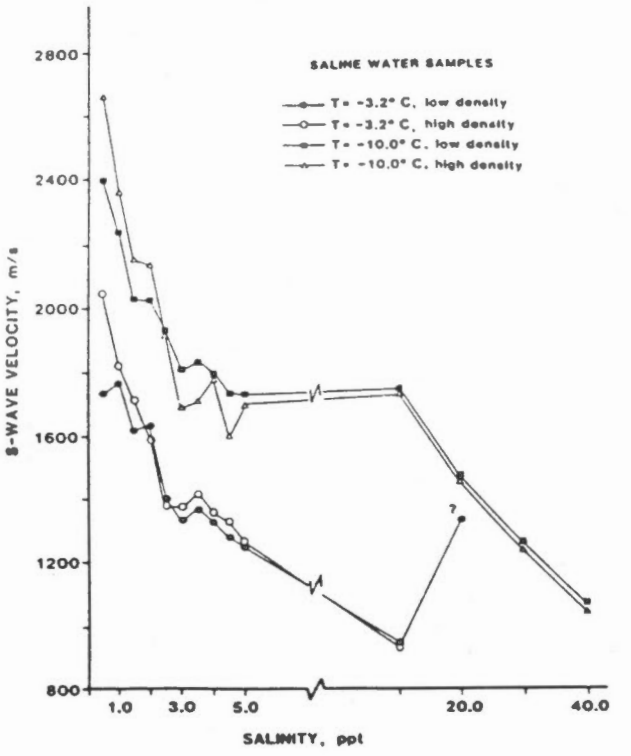

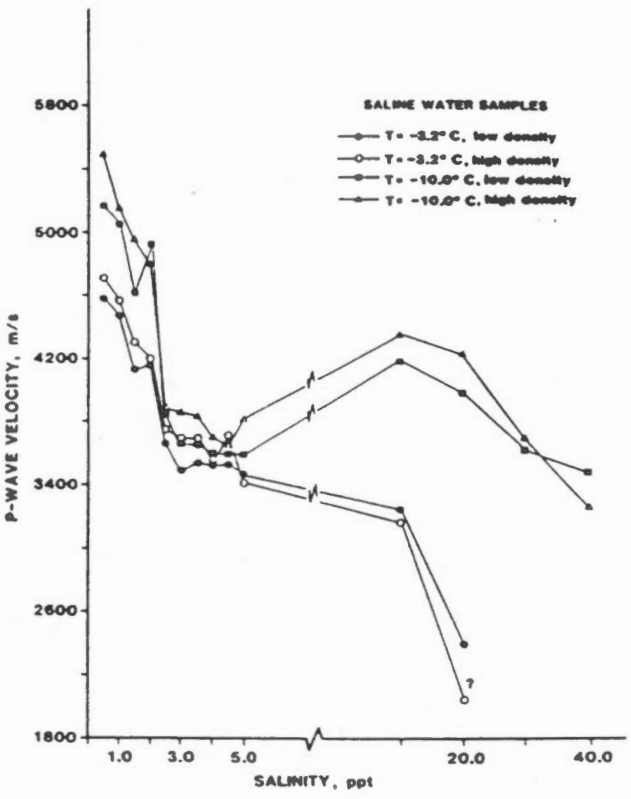

The effect of salinity on the wave velocities of frozen soil (Baker and Kurfurst, 1985).

THURBER

FIGURE 11.27

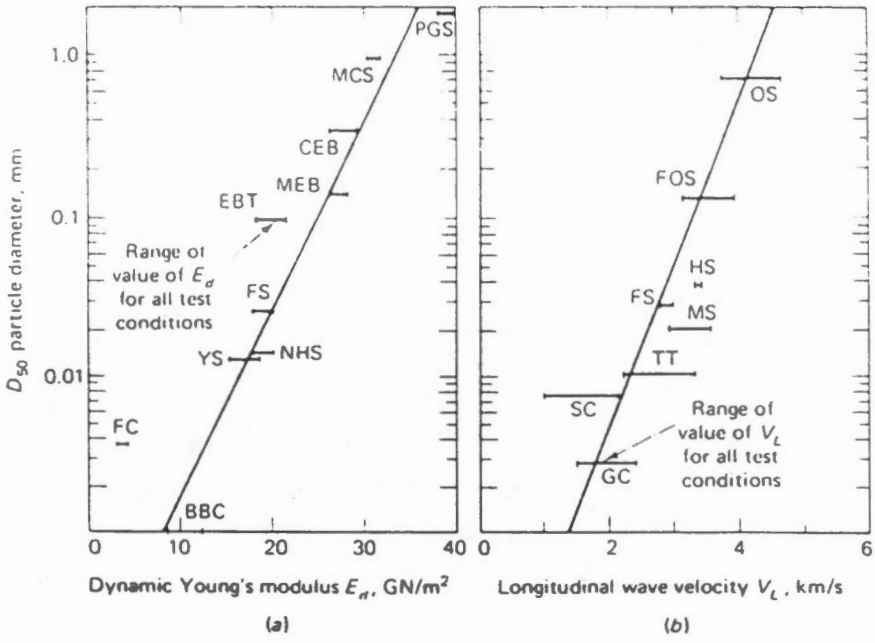

The effect of D_{50} on the dynamic stress-strain properties of frozen soil (Vinson, 1978; after Kaplar, 1969 and Stevens, 1975).

FIGURE 11.28

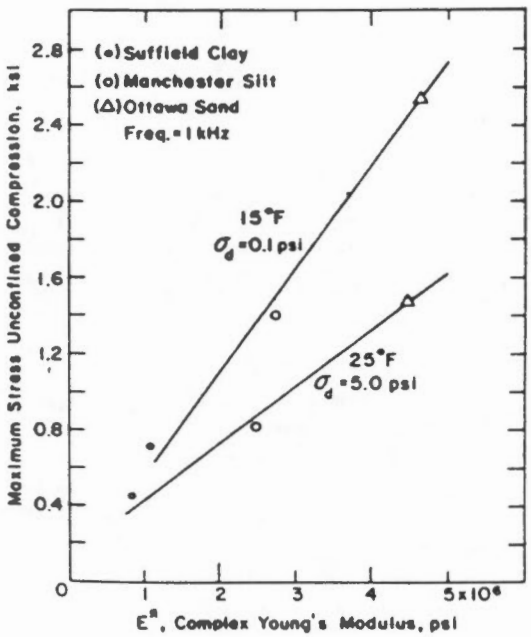

The effect of unconfined compressive strength on the complex Young's Modulus of frozen soil (Stevens, 1975).

FIGURE 11.29

	Dynamic stress-strain properties	Energy-absorbing properties	Fig.
Material parameters:			
Material type and composition	Very important; dynamic stress-strain properties for coarse-grained soils can be nearly an order of magnitude greater than for fine-grained soils	Very important; energy-absorbing properties can differ by an order of magnitude or greater for different soil types	8.15, 8.16, 8.24
Material density or void ratio (for fully saturated soils)	Important; over a range of void ratios from 0.3 to ice, dynamic stress-strain properties can decrease by a factor of 5; over the range of void ratios associated with a given soil type the influence of dynamic stress-strain properties will not be as great; dynamic stress-strain properties of ice decrease substantially with decreasing density	Probably unimportant; there may be a slight decrease in damping ratio with decreasing density over the range associated with the given soil type	8.20, 8.21
Ice content or degree of ice saturation per unfrozen water content	Very important; however, occurrence of coarse-grained soils with 90% ice saturation is rare in nature; degree of ice saturation for fine-grained soils is related to unfrozen water content and the influence in this case is reflected by temperature	Important; see comments under Dynamic stress-strain properties	8.22
Field- and/or test-condition parameters:			
Temperature	Very important for frozen soils, particularly in the range 0 to $-5°C$	Very important for frozen soils in the range 0 to $-5°C$; relatively unimportant in the range -5 to $-20°C$	8.15, 8.16
Strain (or stress) amplitude of loading	Unimportant for axial strain amplitudes less than $10^{-3}\%$ for frozen soils and ice; important for axial strain amplitudes between 10^{-3} and $10^{-1}\%$ for frozen soils	Unimportant for axial strain amplitudes less than $10^{-3}\%$; important for axial strain amplitudes between 10^{-3} and $10^{-1}\%$ for most frozen soils	8.17
Frequency of loading	Relatively unimportant	Probably important	8.18
Confining pressure	Important for coarse-grained soils and ice; unimportant for fine-grained soils	Unimportant	8.19

Relative importance of material and field-and/or test-condition parameters on the dynamic properties of frozen soils (Vinson, 1978).

FIGURE 11.30

SECTION 12

ELECTRICAL PROPERTIES

SECTION 12

ELECTRICAL PROPERTIES

12.1 General

McNeill (1980) presents a general review of the electrical properties of soils and rocks, including effects of permafrost. A doctoral thesis by Olhoeft (1975) presents a detailed description of the electrical properties of permafrost and a discussion of the physical processes involved as based on natural and synthetically prepared samples of permafrost materials. Keller and Frischnecht (1970) have published an excellent text describing the application of electrical methods to geophysical prospecting. This section of the report summarizes important aspects common to the above and other pertinent discussions to illustrate the electrical properties of ice and frozen soil.

A knowledge of the electrical properties of permafrost is essential to the successful employment of electrical geophysical methods to delineate frozen and unfrozen rock and soil. Typical mapping objectives in permafrost terrain include:

1) groundwater supply studies, where the presence of large volumes of unfrozen granular subsurface materials may identify aquifers,

2) transportation corridor selection, where potentially thermally unstable or liquefiable materials may be located and further investigated by drilling,

3) general site investigations, for which the distribution of different soil types, the location of selective borrow, and depth to and type of bedrock may need be determined in the presence of permafrost, and

4) investigations of the active layer.

In addition, a knowledge of the electrical properties of permafrost is required for the design of electrical grounding and lightning protection of power and communication facilities, and cathodic protection of buried metallic utilities such as pipelines or cable sheaths.

THURBER

The most important electrical properties of interest include:

1) resistivity
2) dielectric constant
3) loss tangent

The resistivity is the resistance to current flow of the material under an applied voltage.

The dielectric constant is the ratio of the capacity of a material to store charge when an electric field is applied, as compared to that of free space.

The loss tangent is the ratio of the real conductivity (measured at low frequencies) to the complex conductivity (which is measured at high frequencies).

Other electrical properties include magnetic permeability, and natural electrical potential. These properties are of only secondary interest in permafrost soils and will not be discussed further in this report.

12.2 Methods of Measurement

There are a wide variety of geophysical methods and techniques employed to study the resistivity structure of the earth. They vary in many respects including frequency range of operation, effective exploration depth constraints, and whether they measure the electric field or the magnetic field, or both. Scott et. al. (1978) provides a review of geophysical methods for permafrost mapping purposes. Keller and Frischnecht (1970) and Sunde (1968) provide details of the operating principles for many of the common methods. Figure 12.1 lists some electrical geophysical methods that have been used to investigate permafrost, and their respective frequency ranges of operation.

The effective depth of exploration of any of the methods shown on Figure 12.1 can be controlled, to some extent, depending upon the geophysical method, by the following factors:

1) resistivity structure (lateral and vertical) of the ground,

2) effective frequency range of operation,

3) measurement array geometry, and

4) energizing power levels.

For electrical methods operating at higher frequencies, the depth of exploration is predominantly controlled by signal strength attenuation. The attenuation is usually described in terms of the electromagnetic skin depth (depth to which the energizing field falls to about 37 percent of its value at source level). The skin depth (Z_s) in metres can be estimated (Telford et.al., 1976) from:

$$Z_s = 500 \sqrt{\rho} / f$$

where ρ is the resistivity (ohm-m), and

f is the frequency (hertz).

For radar operating at 20 Mhz in 1000 ohm-m ground, the skin depth would then be about 3.5 metres. Similarly, for very low frequency (VLF) systems operating at 16 Khz in 1000 ohm-m ground, the skin depth would be about 125 metres.

The resistivity in permafrost terrain is generally high enough so that electrical resistivity, Frequency Electro Magnetic (FEM) and Horizontal Loop Electro Magnetic (HLEM) techniques are not skin depth limited. For electrical resistivity methods (essentially direct current) the depth of exploration constraints are generally controlled by array geometry, signal power and the depth to the first thick high resistivity strata encountered (often the permafrost table). For frequency electro magnetic and horizontal loop electro magnetic methods (at low induction number) the depth of exploration constraints are generally controlled by array geometry and depth to the first appreciably low resistivity strata encountered (often the base of the permafrost).

Investigations of permafrost to shallow depth (less than 30 metres) have often been performed using frequency electromagnetic and electrical resistivity methods (e.g. Sellman et. al., 1985, Sartorelli and French, 1982). Electrical resistivity methods can be complicated by the inability to ground current and electrode probes in highly resistive ground. FEM and HLEM methods do not require grounding, and exhibit a better ratio of array length to depth of exploration than do electrical resistivity methods. Each is essentially a low frequency method with the measured

THURBER

apparent resistivity being considered as a function of spacing. Investigations of permafrost at moderate to large depth are generally conducted using transient electromagnetic, magnetotelluric or other suitable techniques (e.g.Rozenberg, et.al., 1985). Investigations to very shallow depth can be accomplished using ground probing radar. Radar appears to have the ability to image ice wedges and other shallow features (e.g. Pilon et. al., 1985, and Kovacs et. al., 1985).

The measured electrical properties of permafrost will be a function of the following variables:

1) applied frequency,
2) unfrozen water content,
3) soil type,
4) temperature,
5) confining pressure, and
6) applied electric field strength.

12.3 Frequency

The electrical properties of permafrost earth materials exhibit a complex dependence on the frequency of the applied voltage (or current). The behaviour is discussed by Olhoeft (1975), and results from polarization and relaxation effects of contained water and ice. Olhoeft (1975) suggests that conduction effects predominate below energizing frequencies of one kilohertz and that dielectric (capacitive) effects predominate above the megahertz level. Between the kilohertz and megahertz levels both conduction and dielectric effects are important.

At low frequencies, the electrical resistivity will be equal to the inverse of the electrical conductivity. At higher excitation frequencies the dielectric constant and loss tangent become more important and real resistivity need not necessarily be the inverse of real conductivity.

Olhoeft adopts a silicate-water-ice model to effectively describe the physical processes governing the variation in electric properties as functions of temperature, water content and resistivity, uniaxial confining load, and excitation frequency and field strength. The model assumes simplified pore structure and applicable double layer theory of electrochemical solid-liquid boundaries.

Figure 12.2 (Olhoeft, 1975) shows the real resistivity and loss tangent for natural clay permafrost over a frequency spectrum from 10^{-3} to 10^{8} hertz. As indicated

THURBER

these properties were measured at two field strengths (.0022 and 22 Volts per cm) and two temperatures -10.1°C and -27°C).

Figure 12.3 shows similar plots for a natural ice sample. There is little dependence of resistivity on field strength but a strong dependence on temperature. The resistivity of water is seen to be about 50 ohm-metre. The loss tangent in Figure 12.3 shows a definite peak at about 20 kHz. This is due to relaxation of Bjerrum defects in the ice (Alignment of two oxygen and two hydrogen atoms in the ice lattice rather than hydrogen-oxygen orientation). A variety of models describing relaxation effects on the electrical properties of permafrost at high frequency are discussed in Olhoeft (1975).

Keller and Frischnecht (1970) state that the dielectric constant of water is frequency dependent and arises due to molecular polarization in the presence of an electric field. At low frequency the dielectric constant is about 81.5 while at frequencies in the order of 30 megahertz it is about 4. The difference arises due to the time required to complete molecular polarization. Thus at high frequencies water is not readily polarizable.

Figure 12.4 (Keller and Frischnecht, 1970) shows the dielectric constant of ice versus temperature and frequency. The lattice structure of ice inhibits molecular polarization especially at high frequency and low temperature. Figure 12.5 (Olhoeft, 1975) shows a similar situation for a synthetic Kaolinite permafrost sample.

12.4 Unfrozen Water Content

Most soil and rock forming minerals are electrical insulators of high resistivity as compared to the resistivity of aqueous solutions contained in pores and voids (McNeill, 1980). The resistivity of ice is in the order of that of the mineral constituents (Keller and Frischnecht, 1970). As a result, the electrical properties of earth materials are essentially electrolytic and are strongly influenced by the unfrozen water content.

For fully saturated and clay free soils or rocks Archies law is an empirical relation for bulk material resistivity (ρ), pore water resistivity (ρ_w) and fractional porosity, (n), (Keller and Frischnecht, 1970).

$$\rho = a \rho_w n^{-m} \qquad (1)$$

THURBER

where a and m are parameters derived from the fit with a set of measurements. The parameter, m is usually in the order of 2.

12.5 Soil Type

The typical ranges of electrical resistivity at low frequencies for a variety of unfrozen soil types are shown in Figure 12.6. It is apparent that resistivity decreases as the fine-grained fraction increases. The overlap in the ranges of resistivity values indicates that identification of a particular soil type with a particular resistivity value requires site specific correlation with other geologic information. This is particularly so if the contained pore water is strongly electrolytic.

The difference in resistivity between coarse-grained and clayey soil types arises mainly from the differences in grain surface area per unit mass (specific surface area), which is very much higher for clays. The higher specific surface areaof clays results in a large capacity for ion exchange with adsorbed water films (McNeill, 1980).

12.6 Temperature

Figure 12.7 (McNeill, 1980) indicates that in permafrost terrain frozen and unfrozen materials of the same type may have substantially different values of electrical resistivity. The increase in resistivity accompanying the temperature decrease is due primarily to the difference in the frozen and unfrozen resistivity of the pore water, and to a varying extent upon constituent mineralogy, porosity and unfrozen moisture content. For this reason no unique relation exists between electrical resistivity and volumetric ice content.

Hoekstra (1969) states that current flow in response to an electrical gradient in frozen soils occurs almost entirely through unfrozen water films. Olhoeft (1975) gives a relation for unfrozen water content (W_u, gm H_2O/gm soil), specific surface area (S, m^2/gm) and temperature ($\emptyset$, °C) below zero.

$$\ln W_u = 0.2618 + 0.5519 \ln S - 1.449\, S^{-0.264} \ln \emptyset$$

In the range from 0 to -6°C Olhoeft expects that the formation of ice crystals in pore volumes is accompanied by an increase in concentration of impurities in the unfrozen water which depresses the freezing point. Below -6°C a somewhat stable layer remains near pore walls. Some unfrozen water is likely to be present until temperatures go below -60°C.

THURBER

At essentially direct current levels the resistivity of synthetically produced permafrost samples below 0°C is controlled by unfrozen water content and water resistivity.

12.7 Confining Pressure

The effect of confining pressure is to further depress the pore water freezing point (Hoekstra, 1969). Olhoeft's investigations show that for ice cores and permafrost samples characterized by specific surface areas less than 25 m^2/gm there is little dependence of electrical properties on uniaxial load. For samples characterized by high specific surface area a strong dependence on uniaxial load occurs as indicated on Figure 12.8 (Olhoeft, 1975).

12.8 Field Strength

The measured electrical properties can vary depending on the strength of the applied voltage. This is illustrated in Figure 12.2. The resistivity of the natural clay is seen to be lower, at frequencies of less than about 1 kHz, as the applied voltage is increased. As shown on Figure 12.3, the resistivity and loss tangent of natural ice is not affected significantly by the applied voltage.

12.9 Other Factors

Freezing rate can be expected to have an affect on resistivity since formation of pore ice over prolonged periods will more completely exude ions to unfrozen pore water (Olhoeft, 1975). Organic materials contained in soils may have enhanced cation exchange capacity and thereby affect measured electrical properties (McNeill, 1980).

12.10 Summary

The electrical properties of permafrost result from a number of complex interactions between the pore water, ice, and the mineral matrix. In the low frequency limit, for which permafrost can be considered a simple conductor, the main property of interest is resistivity. Resistivity is found to be dependent upon soil type, pore water resistivity, water-ice content, temperature, and in the case of high specific surface area (colloidal) soils on confining pressure and electric field strength. At higher energizing frequencies, dielectric loss mechanisms are predominate and the dielectric properties of the water, ice and boundary zones become important. The real resistivity generally exhibits a decrease with increasing frequency.

THURBER

A major engineering consideration in permafrost regions is the determination of the volumetric ice content of frozen soils. Due to the complexity of factors affecting permafrost electrical properties, in situ measurements using electrical geophysical techniques have not been shown to be able to accurately predict ice contents.

The main application of electrical geophysical methods to permafrost studies have been to map the presence or absence of frozen ground, to delineate its vertical and lateral extent, and to estimate the distribution of different soil types in the presence of permafrost. Methods have been devised for operation in both on and off shore environments. Research regarding the application of electrical geophysical methods in support of a host of terrain mapping objectives in permafrost regions is in progress on many fronts. The objective requiring the most research effort is expected to be the determination of ice content using geophysical methods.

The presence of permafrost presents some interesting challenges to the design of power and communication facilities involving earth return grounds, and lightning protection. Henry (1987) describes major problems to be the general high resistivity of permafrost and the resistivity variation with season. Both Henry and Sunde (1968) present methods of designing effective grounding resistances in the presence of terrain of arbitrary resistivity. The physical basis for electrolytic corrosion and methods of protection for buried metallic facilities is described in detail by Sunde (1968). Exhaustive research in support of these design considerations in permafrost terrain may be best undertaken on a project by project basis.

ELECTRICAL PROPERTIES

LIST OF REFERNECES

Committee on Permafrost, Polar Research Board, Exploration Geophysics, in Workshop on Permafrost Geophysics, Appendix B., (1985). CRREL Special Report 85-5.

Henry, K., (1987). Electrical Grounding in Cold Regions. CRREL Cold Regions Technical Digest No. 87-1.

Hoekstra, P., (1969). The Physics and Chemistry of Frozen soils, in Effects of Temperatures and Heat on Engineering Behaviour of Soils, Highways Research Board Special Report 103. Washington, D.C., USA.

Keller, G.V., and Frischnecht, F.C., (1970). Electrical methods in Geophysical Prospecting. Pergamon Press, New York, N.Y., USA.

Kovacs, A., and Morey, R.M., (91985). Impulse Radar Sounding of Frozen Ground, in Workshop on Permafrost Geophysics, pp. 28-40. CRREL Special Report 85-5.

McNeill, J.D., (1980). Electrical Conductivity of Soils and Rocks, Geonics Limited Technical Note TN-6. Mississauga, Ontario, Canada.

Olhoeft, G.R., (1975). The Electrical Properties of Permafrost. Ph.D. Thesis, University of Toronto.

Pilon, J.A., Annan, A.P., and Davis, J.L., (1985). Monitoring Permafrost Ground conditions with Ground Probing Radar (GPR) in Workshop on Permafrost Geophysics, pp. 71-73. CRREL Special Report 85-5.

Rozenberg, G., Henderson, J.D., and Sartorelli, A.N., (1985). Some Aspects of Transient Electromagnetic Soundings for Permafrost Delineation, in Workshop on Permafrost Geophysics, pp. 74-90. CRREL Special Report 85-5.

Sartorelli, A.N., and French, R.B., (1982). Electromagnetic Induction Methods for Mapping Permafrost Along Northern Pipeline Corridors. Proceedings of Fourth Canadian Permafrost conference, Calgary, Alberta, March, 1981, pp. 283-295.

THURBER

LIST OF REFERENCES
(continued)

Scott, W.J., Sellmann, P.V., and Hunter, J.A., (1978). Geophysics in the Study of Permafrost. In Proceedings, Third International Conference on Permafrost, Edmonton, July, Vol.2, pp. 93-116.

Sheriff, R.E., 91973). Encyclopedic dictionary of exploration geophysics. Society of Exploration Geophysicists, Tulsa, Ok., USA.

Sunde, E.D., (1968). Earth conduction effects. Dover Publications Inc., New York, N.Y., USA.

Telford, W.M., Gedart, L.P., Sheriff, R.E. and Keys, D.A., (1976). Applied geophysics. Cambridge University Press, New York, N.Y., USA.

THURBER

ELECTRICAL PROPERTIES

LIST OF FIGURES

THURBER

1. Active Source Methods	Frequency Range
Electrical Resistivity	0.1 hz to 4 hz
Induced Polarization (IP)	0.1 hz to 4 hz
Complex Resistivity	0.1 hz to 50 kHz
Transient Electromagnetic (TEM)	0.3 hz to 100 kHz
Very Low Frequency (VLF)	10 kHz to 30 kHz
Radar	1 Mhz to 500 Mhz
Audio Frequency Electromagnetic - Horizontal Loop (HLEM) (Max-Min) Turam Frequency electromagnetic (FEM) Controlled Source Audio Magnetotelluric (CSAMT)	15 hz to 20 kHz

2. Natural Source Methods	
Magnetotelluric (MT)	10^{-3} hz to 100 hz
Audiomegnetictelluric (AMT)	10^{-1} hz to 10 hz

Electrical Geophysical Methods and Frequency Range

Figure 12.1

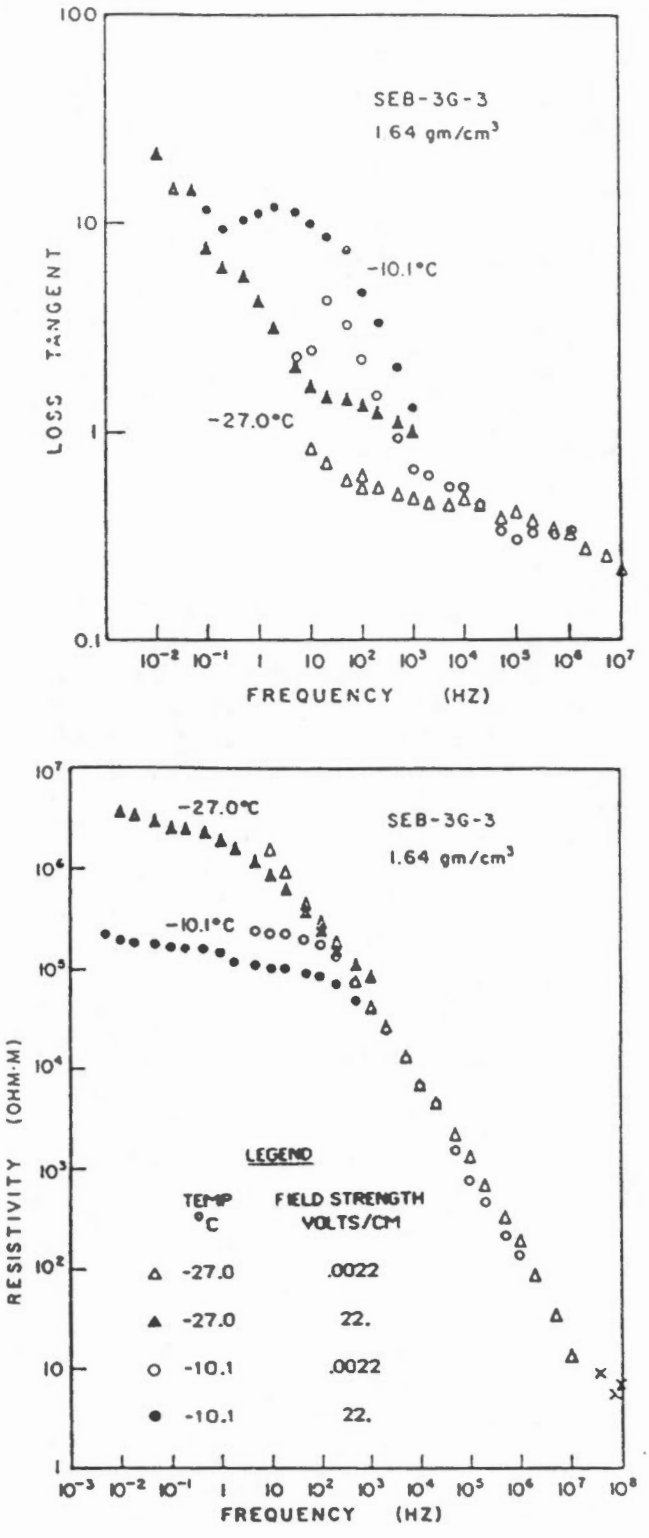

Frequency dependence of real electrical resistivity and loss tangent for frozen natural clay (Olhoeft, 1975).

THURBER

FIGURE 12.2

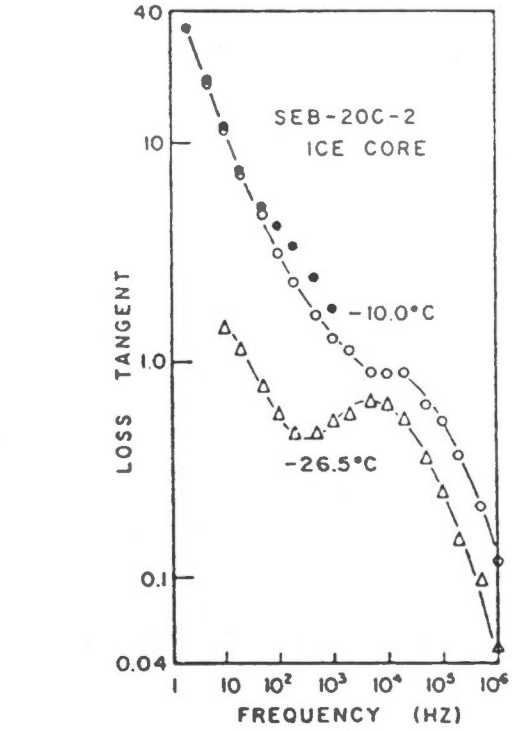

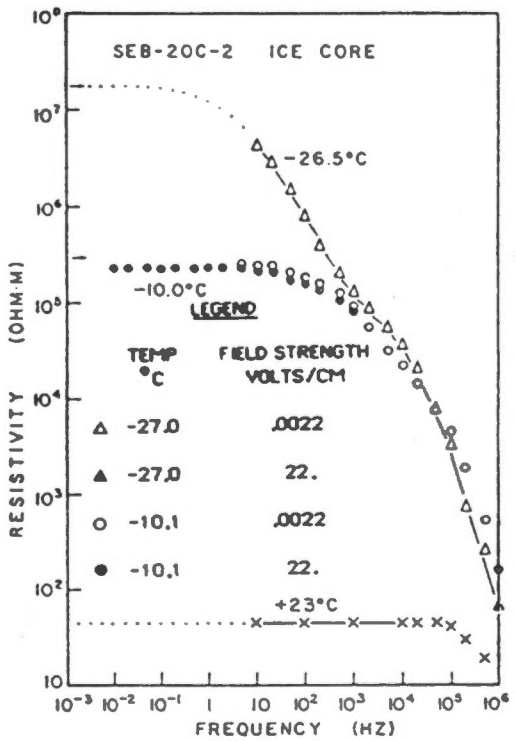

Frequency dependence of real electrical resistivity and loss tangent for natural ice (Olhoeft, 1975).

THURBER

FIGURE 12.3

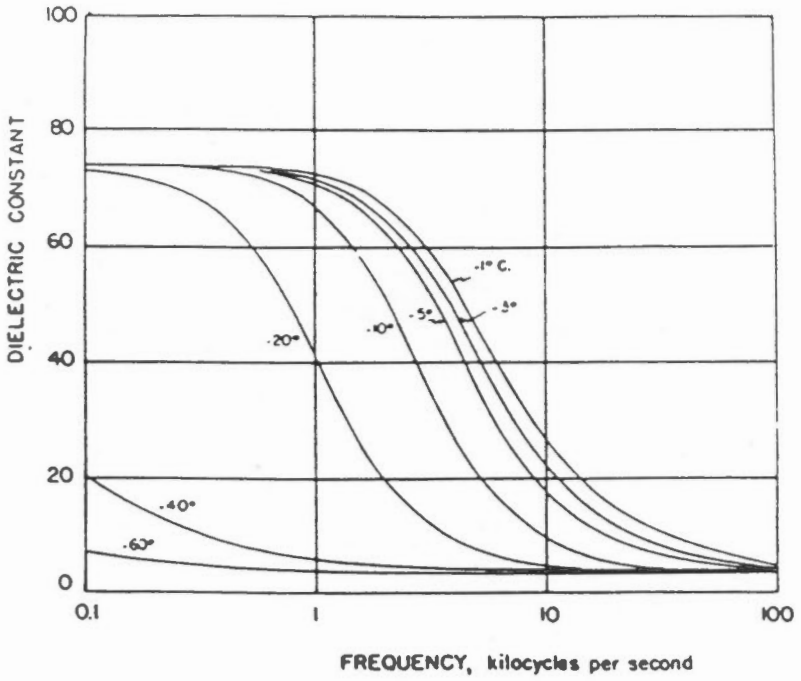

The effect of frequency and temperature on the dielectric constant of ice (Keller and Frischnecht, 1970).

THURBER

FIGURE 12.4

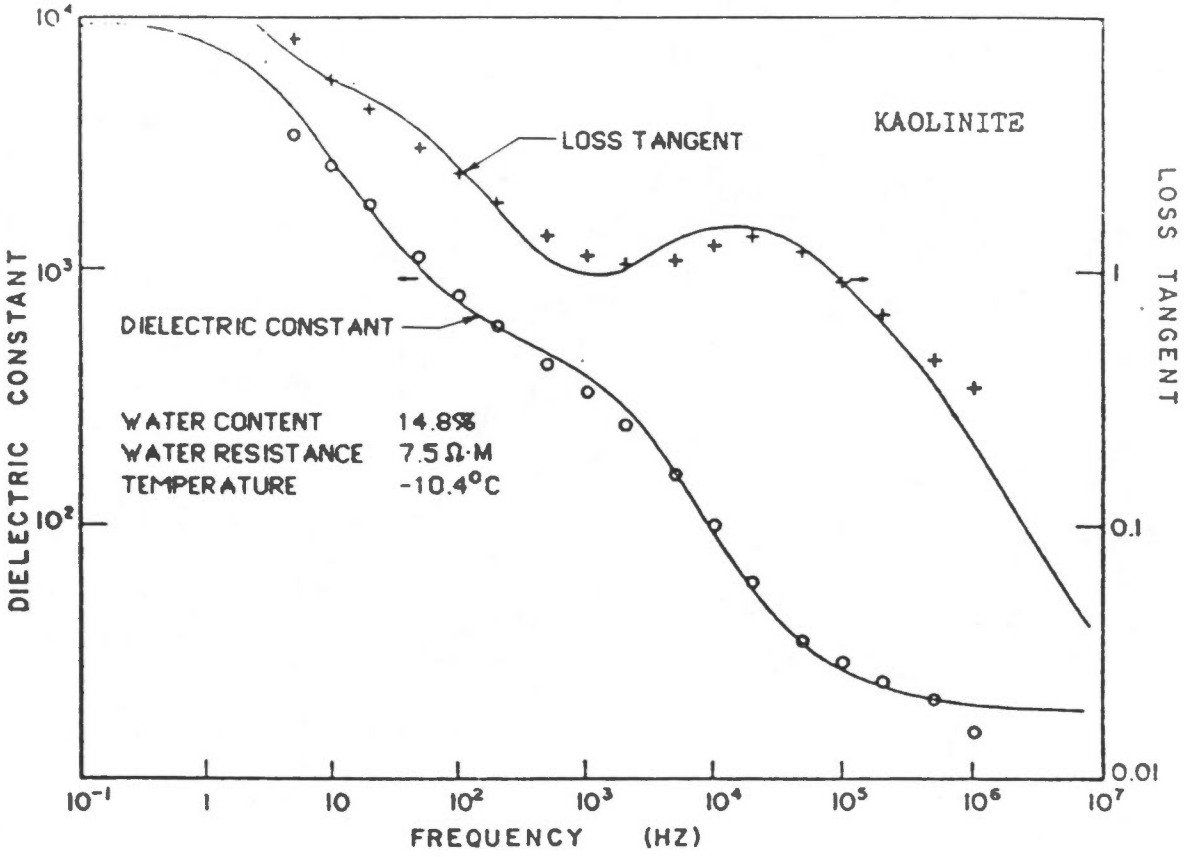

Frequency dependence of the dielectric constant and loss tangent of kaolinite (Olhoeft, 1975).

THURBER

FIGURE 12.5

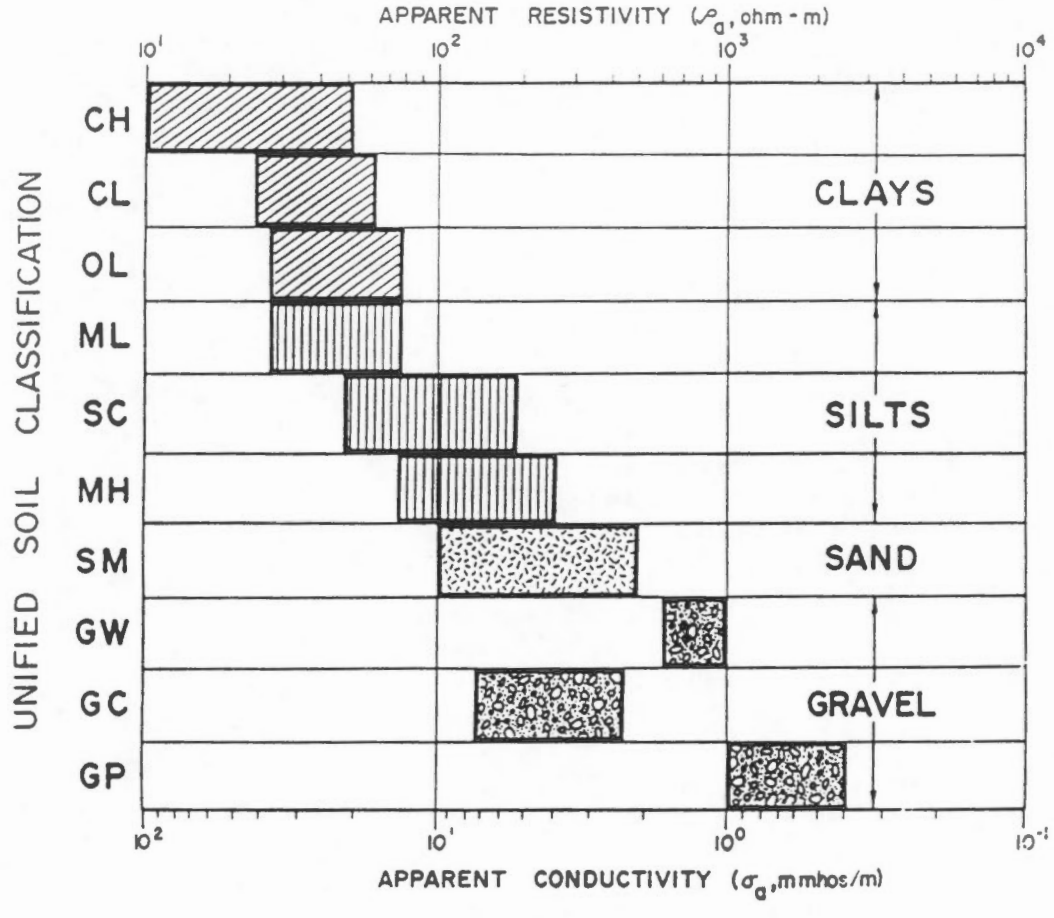

Electrical resistivity as a function of soil type at low frequencies.

FIGURE 12.6

THURBER

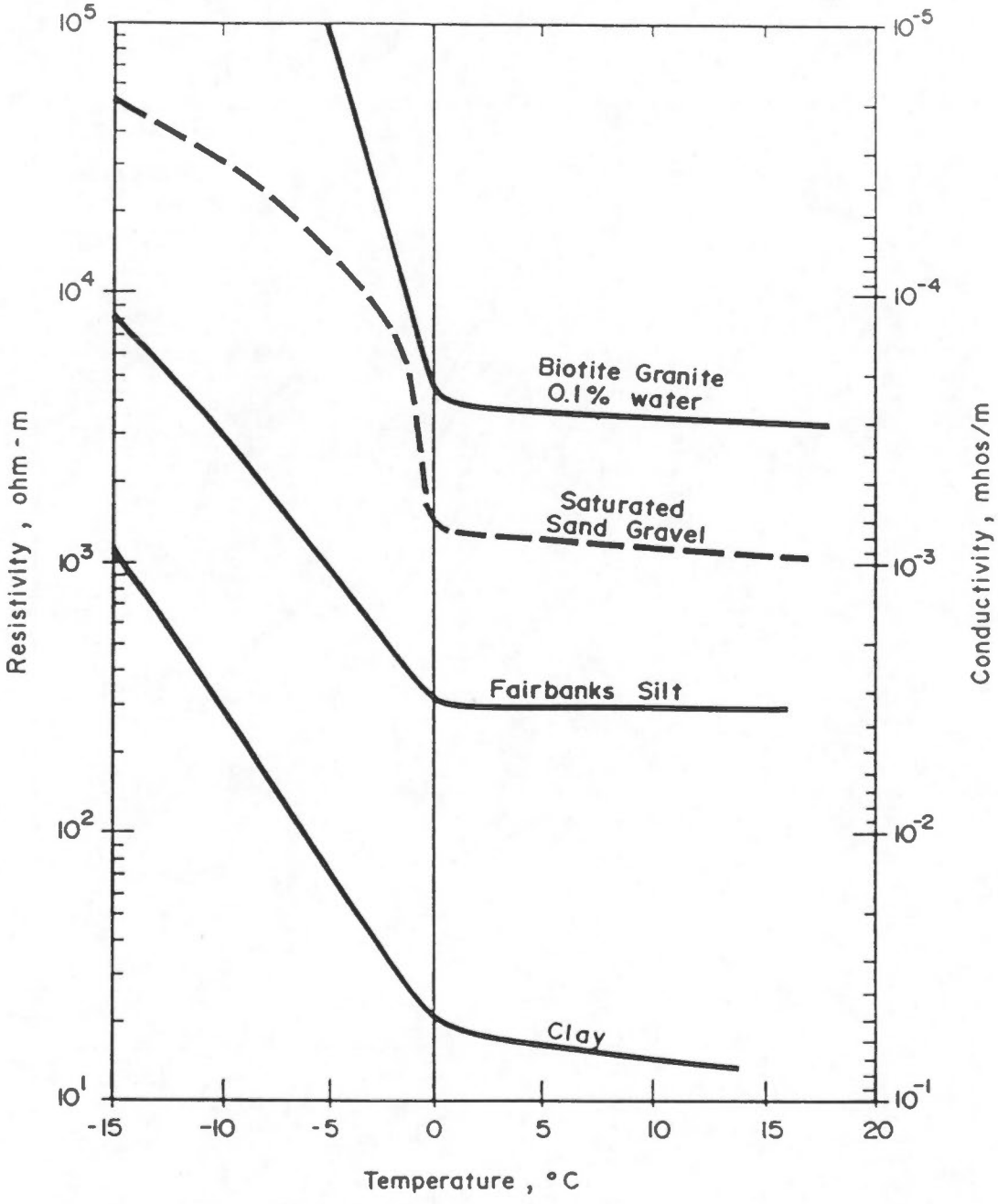

Electrical resistivity as a function of soil type and temperature at low frequencies (McNeill, 1980).

THURBER

FIGURE 12.7

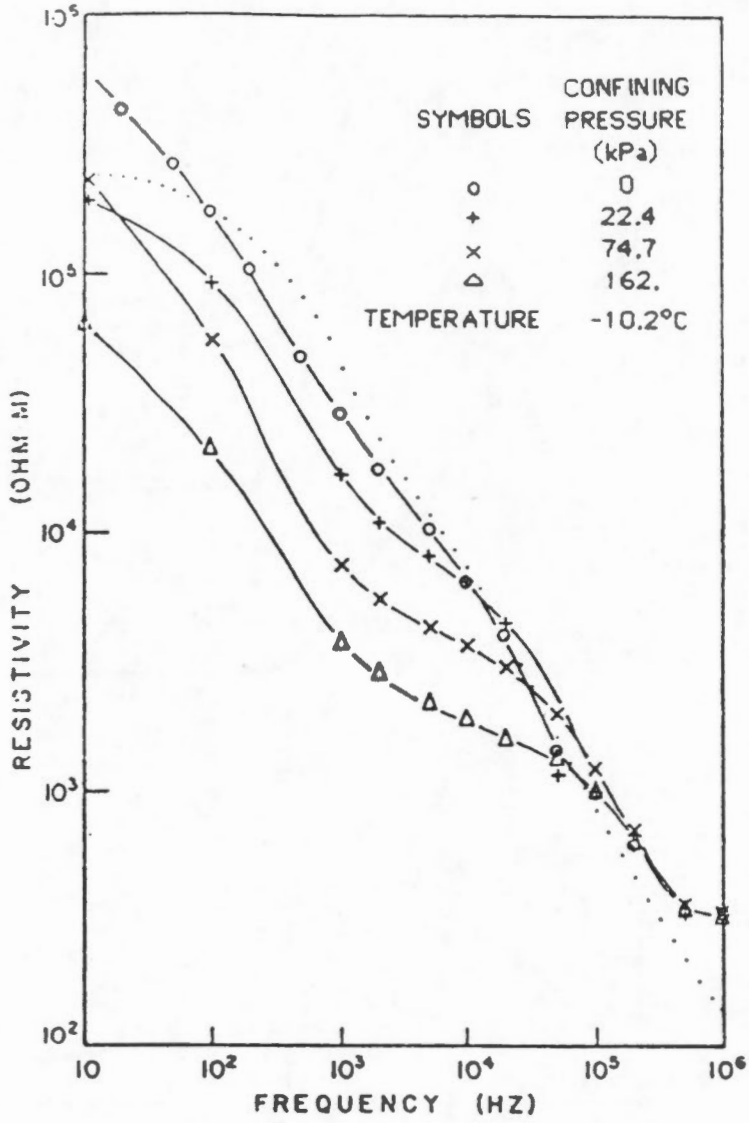

Electrical resistivity as a function of frequency and confining pressure for clay (Olhoeft, 1975).

FIGURE 12.8